TESIS DE LA UNIVERSIDAD DE ZARAGOZA

2024 232

Javier Granado Fornas

Aprendizaje profundo aplicado al procesado de señales de faltas en redes eléctricas

Director/es
Herrero Jaraba, José Elías
Llombart Estopiñán, Andrés

ISSN 2254-7606

Prensas de la Universidad Universidad Zaragoza

Universidad de Zaragoza
Servicio de Publicaciones

ISSN 2254-7606

Universidad Zaragoza
1542

Tesis Doctoral

APRENDIZAJE PROFUNDO APLICADO AL PROCESADO DE SEÑALES DE FALTAS EN REDES ELÉCTRICAS

Autor

Javier Granado Fornas

Director/es

Herrero Jaraba, José Elías
Llombart Estopiñán, Andrés

UNIVERSIDAD DE ZARAGOZA
Escuela de Doctorado

Programa de Doctorado en Ingeniería Electrónica

2024

UNIVERSIDAD DE ZARAGOZA

APRENDIZAJE PROFUNDO APLICADO AL PROCESADO DE SEÑALES DE FALTAS EN REDES ELÉCTRICAS

Tesis doctoral presentada por Javier Granado Fornás

dentro del Programa de Doctorado en Ingeniería Electrónica

Dirigida por Dr. Elías Herrero Jaraba

y Dr. Andrés Llombart Estopiñán

UNIVERSIDAD DE ZARAGOZA

APRENDIZAJE PROFUNDO APLICADO AL PROCESADO DE SEÑALES DE FALTAS EN REDES ELÉCTRICAS

Tesis doctoral presentada por Javier Granado Fornás
dentro del Programa de Doctorado en Ingeniería Electrónica
Dirigida por Dr. Elías Herrero Jaraba
y Dr. Andrés Llombart Estopiñán

El doctorando | El director | El director

Zaragoza, Septiembre de 2023

A mi mujer Rosa.

Por estar siempre a mi lado y apoyarme en todo lo que hago.

A mis hijos Marcos y Raquel.

Por ser los mejores hijos que un padre pueda desear

“No soy feliz ni falta que me hace”

Albert Einstein.

Publicaciones

Declaro que esta Tesis Doctoral titulada “Aprendizaje Profundo Aplicado al Procesado de Señales de Faltas en Redes Eléctricas“ es una presentación de trabajo original y representa mi propio esfuerzo personal. Este trabajo no ha sido presentado previamente para su examen en esta universidad ni en ninguna otra institución académica.

La interpretación presentada se basa en mi propia lectura y comprensión, y no ha sido tomada de otras fuentes, salvo cuando se indique específicamente. Todos los recursos utilizados se han citado adecuadamente dentro del texto como referencias.

Además, confirmo que soy uno de los principales autores del trabajo utilizado en esta Tesis. A continuación, se listan las cinco referencias bibliográficas seleccionadas para poder defender la tesis doctoral en la modalidad de compendio de publicaciones:

1. J. G. Fornás, E. H. Jaraba, H. Bludszuweit, D. C. García and A. L. Estopiñan, ”Modeling and Simulation of Time Domain Reflectometry Signals on a Real Network for Use in Fault Classification and Location,ïn IEEE Access, vol. 11, pp. 23596-23619, 2023, doi: 10.1109/ACCESS.2023.3253772
   Q2 en Engineering, Electrical & Electronic. Factor de impacto 3,9 (2022).
2. J. G. Fornás, E. H. Jaraba, A. L. Estopiñan and J. Saldana, ”Detection and Classification of Fault Types in Distribution Lines by Applying Contrastive Learning to GAN Encoded Time-Series of Pulse Reflectometry Signals,ïn IEEE Access, vol. 10, pp. 110521-110536, 2022, doi: 10.1109/ACCESS.2022.3214994
   Q2 en Engineering, Electrical & Electronic. Factor de impacto 3,9 (2022).

3. J. G. Fornas, E. H. Jaraba and A. L. Estopinan “Generation of Synthetic Examples Using Generative Adversarial Networks (GAN) to Extend the Database of Fault Signals on Power Distribution Lines” CIRED - international conference on electricity distribution / Rome (2023)
4. J. G. Fornas, E. H. Jaraba and A. L. Estopinan TransSiamese: “A Transformer-Based Siamese Network for Anomaly Detection in Time Series as Approach for Fault Location in Distribution Grids” IEEE Access, 2023, doi: 10.1109/ACCESS.2023.3316600 *Q2 en Engineering, Electrical & Electronic. Factor de impacto 3,9 (2022).*
5. J. Granado, D. Cervero, M. Mañana, R. Cimadevilla, J. Ivan Rodriguez y A. Gonzalez “Experiencia Piloto de Localización de Faltas en Red de Media Tensión Mediante la Técnica de la Reflectometría en el Dominio del Tiempo (TDR)e en el Proyecto H2020 -FLEXIGRID” Futured / Congreso de redes Inteligentes (2022)

Agradecimientos

Esta Tesis es la culminación de un desafío personal que comenzó en el año 2008.

Me gustaría expresar mi agradecimiento a mis directores de Tesis. En primer lugar a Elías Herrero Jaraba, que ha sido una fuente de inspiración permanente en el desarrollo de esta Tesis. Con él he pasado momentos difíciles en los que parecía que la cosa no iba a salir adelante, pero la firmeza y la determinación de Elías siempre me guió por el camino correcto. Mención aparte merece su implicación en todos los artículos en los que ha participado activamente y en los que ha sido determinante sus conocimientos, así como su capacidad de trabajo y de apoyo. Mi más sincero agradecimiento Elías.

En segundo lugar, me gustaría agradecer a Andrés Llombart Estopiñán, director del Centro Tecnológico CIRCE, donde trabajo actualmente. Sin su apoyo a través de la integración de la Tesis dentro de uno de los proyectos Europeos desarrollados en CIRCE, así como su implicación y apoyo personal, no hubiera sido posible esta Tesis. Cuando me cambié de trabajo para venir a CIRCE, buscaba entre otras cosas una empresa con adn de investigación donde intentar encajar mi Tesis que, hasta el momento, había pasado por varias fases pero estaba en punto muerto. No me equivoqué, y CIRCE me brindó esa oportunidad. Gracias Andrés.

Hubo que esperar 2 años de baja voluntaria en la Tesis hasta que culminé ese cambio de trabajo y pude hacer realidad el encaje en un proyecto Europeo dentro de CIRCE. Tras abrirse esa nueva posibilidad, contacte de nuevo con Elías para hablarle de la posibilidad de retomar la Tesis, esta vez con apoyo financiero y con un objetivo definido dentro del marco de un proyecto Europeo y Elías mostró predisposición desde el inicio. Aún recuerdo las palabras de respuesta de Elías al whatsapp que le mandé, después de llevar 2 años de baja voluntaria

en la Tesis y prácticamente sin haber hablado “Ya sabes que conmigo tienes siempre un apoyo...”. Lo demás ya es historia.

Nací en el año 1968, es decir, actualmente tengo 55 años. Acabé mi carrera de Ingeniería Electrónica en el año 1994. Desde entonces y hasta el año 2008 estuve trabajando en I+D en distintas empresas desarrollando proyectos de electrónica. Pero en el año 2008 me hice la pregunta de si sería capaz de sacarme el doctorado teniendo en cuenta que tenía ya 40 años, dos hijos pequeños, que había dejado de estudiar hacía 14 años, que trabajaba a tiempo completo y que tenía que cursar antes un máster que me diera acceso al doctorado.

Todas las personas a las que les comenté la idea me respondieron lo mismo, “vaya locura, nunca lo conseguirás”. Todas menos una, mi mujer Rosa, que siempre me ha dicho que podría hacer lo que me propusiera. Así que decidí intentarlo, y después de empezar el máster de Ingeniería Biomédica, cambiarme al año siguiente al nuevo máster de Ingeniería Electrónica, que me ofrecía la posibilidad de la especialidad de “Ambientes Inteligentes” y era más afín a mis anteriores estudios, estar un año entero desarrollando el TFM, de 8 años de tesis contando con dos años de baja voluntaria, y de haberme incluso cambiado de empresa para poder compatibilizar la Tesis con mi trabajo, aquí estoy, a punto de defender mi tesis doctoral y conseguir contestar a la pregunta que me hice con un “SI”, si he podido hacerlo. A todos aquellos que me desanimasteis en la persecución de este sueño, gracias, vuestro desanimo me animo aún más en mi propósito.

Siempre he sido una persona inconformista, sobre todo conmigo mismo. Necesito constantemente desafíos personales que me hagan sentir que puedo superarlos. Esto hace que normalmente mi estado habitual sea una mezcla de frustración, infelicidad, ansia por acabar algo, enfado por no poder hacerlo, etc... Esto normalmente suele ser algo que la gente que lo sufre intenta evitar, pero en mi caso lo busco, porque no sé vivir en un estado cercano a la sensación de que ya está todo hecho. A mi, el estado cercano a la felicidad en el que todo parece que está bien

y que ya no hay mucho que hacer para mejorar no solo no me gusta sino que me da miedo. Por eso la frase “No soy feliz ni falta que me hace”, me representa totalmente y por eso la he querido incluir en esta Tesis. Es una frase que para mi representa la necesidad de estar siempre buscando, preguntando y superando desafíos y, esto, obviamente no te hace feliz, pero como dice la frase, ni falta que me hace.

Quiero tener un recuerdo especial para mi padre, que murió cuando yo tenía apenas 8 años y que estoy seguro que se sentiría muy orgulloso de ver hasta donde había llegado su hijo. También para ti, mamá, que aunque hace mucho tiempo que no entiendes nada de “esas cosas raras que tu haces”, gracias a ti estoy aquí y te debo lo más importante del mundo, la vida.

Quiero dejar para el final la parte más importante de los agradecimientos. En primer lugar para ti, Rosa, que llevas a mi lado 34 años y me conoces mejor que nadie . Has sido todo para mi, mi pareja, mi amiga y la madre de mis hijos. Siempre has confiado en mi, siempre me has animado en todos y cada una de mis desafíos, incluso cuando en muchos de ellos, ta ha tocado ocuparte de nuestros hijos mientras yo estaba en clase después de salir de trabajar, o incluso, cuando he tenido que perder innumerables días y noches con reuniones, escribiendo artículos, yendo a congresos, etc... Siempre te estaré agradecido por ese apoyo incondicional y que a ti, personalmente, solo te ha traído problemas. Gracias por aguantar los interminables rollos que te he soltado durante estos años y que has escuchado estoicamente sin desfallecer. Gracias también por decirme a veces las cosas como son, y por hacerme ver a veces, que había cuestiones familiares que no debía descuidar por mi obsesión con los estudios. Gracias a todo ese apoyo en la sombra, esta Tesis ha llegado a ver la luz. Te quiero.

Por último, quiero hacer un mención especial a mis hijos Marcos y Raquel. Ellos están empezando ahora su aventura universitaria y no puedo estar más orgulloso de ellos. En primer lugar porque son unas buenas personas. Unas personas inteligentes y que representan lo mejor de

la juventud de hoy en día. En ellos veo una ilusión que me recuerda cuando yo tenía su edad. Espero que podáis conseguir todo lo que os propongáis en esta vida y en cualquier caso, que disfrutéis intentándolo. A veces me preguntáis por qué sigo estudiando si no lo necesito. La realidad es que lo necesito para no “acabar siendo feliz”. Os quiero mucho.

Índice general

Abstract

The automatic detection, classification, and localization of faults (short circuits, ground faults, or breakdowns) in electrical lines are a crucial process in the electric power distribution industry. From a system operation perspective, electric power distribution companies (DSO's) are particularly concerned with reducing service interruption times. Commercially, during these periods, an indeterminate number of customers lose their electrical supply, and some power generation plants cease to provide energy, especially distributed generation (GD) plants that can be affected. Therefore, the proper detection, classification, and localization of faults in electrical distribution networks are effective methods to reduce the duration of downtime, as most interruptions are caused by these reasons [1] [2] [3]. If maintenance teams can identify the problem more quickly using these techniques, the fault can be repaired sooner, significantly enhancing the user experience.

This doctoral thesis has focused on utilizing the Time Domain Reflectometry (TDR) technique as a physical principle (a technique where pulses are injected into the network and reflected back with information about its condition) and the adaptation of various neural network (NN) models to enhance some phases of fault detection, classification, and localization:

– **Modeling and simulation of a real network:** Given the randomness of faults and the extensive distribution network, it is challenging to have a database of faults for training AI systems. This study models a real network for simulating faults and, through the TDR technique, obtains response signals from the network, thereby creating a simulated signal database. Though limited to 200 examples, these simulated signals closely resemble real ones. However, simulating all necessary phenomena for training NN would be time-consuming.

- **Database augmentation:** Starting from the simulation-obtained database, expansion (DA) is undertaken. A Generative Adversarial Network (GAN), once trained with the simulated signal database, generates synthetic examples. These synthetic examples provide a sufficient database for training the DNNs responsible for fault detection, classification, and localization.
- **Fault detection and classification:** With the expanded database of 10,000 examples, the first step involves the detection and classification of various fault types using Siamese Neural Networks (SNN). For training, the synthetic database (10,000 examples) is used as training data, while the original simulated signal database (200 examples) is used as the test set. This study validates the synthetic database generated in the previous study and addresses the challenge of fault detection and classification.
- **Time to Fault detection (TtoF):** This study analyzes the fault signal to determine the temporal point at which the fault occurred. Transformers, a type of neural network, are used for this purpose. Detecting the temporal point at which the fault occurred allows us to estimate the time taken for the injected pulse to travel from the injector to the fault and back. This time can be used to extrapolate a distance from the injector to the fault (DtoF), but the actual fault localization can only be achieved by incorporating information about the branch of the electrical network where the fault occurred.
- **Pilot experience:** A pilot experience of a physical system developed in the European H2020 FLEXIGRID project is presented. This system is designed to inject pulses and record the network's response using the TDR technique. The system is installed in the same network used for obtaining the simulated signal database. The goal is for the system to record real fault signals for a year to compare the results with those obtained from simulation. Additionally, the aim is to obtain a real-world database

for training the previously used models and comparing their responses with new signals. As a final objective, this study aims to contribute to the understanding of this solution and, in future projects, take a step closer to the industrialization of a system meeting these criteria that can be commercialized.

Resumen

La detección, clasificación y localización automática de faltas (cortocircuitos, faltas a tierra o averías) en líneas eléctricas es un proceso crucial en la industria de la distribución de energía eléctrica. Desde el punto de vista de la operación del sistema, las compañías distribuidoras de energía eléctrica (DSO's por sus siglas en Inglés) se preocupan especialmente por reducir los tiempos de interrupción del servicio. Desde el punto de vista comercial, durante estos períodos un número indeterminado de clientes pierden su suministro eléctrico, y algunas plantas de generación de energía dejan de suministrar energía, especialmente las plantas de generación distribuida (GD) pueden verse afectadas. Por lo tanto, la adecuada detección, clasificación y localización de faltas en las redes de distribución eléctrica son métodos efectivos para reducir la duración de los tiempos de inactividad, ya que la mayoría de las interrupciones son causadas por este motivo [1] [2] [3]. Si los equipos de mantenimiento pueden encontrar el problema más rápido gracias a estas técnicas, la falta puede ser reparada antes y, por lo tanto, la experiencia del usuario mejora considerablemente.

La presente tesis doctoral se ha centrado en la utilización de la técnica de la reflectometría en el dominio del tiempo (TDR por sus siglas en Inglés) como principio físico (técnica mediante la cual se inyectan pulsos en la red y vuelven reflejados con información del estado de esta) y en la utilización y adaptación de varios modelos de redes neuronales (NN por sus siglas en Inglés) para la mejora de alguna de las fases de la detección, clasificación y localización de las faltas:

– **Modelado y simulación de una red real:** Dada la aleatoriedad de las faltas y la gran extensión de la red de distribución es muy difícil disponer de una base de datos de faltas con las que entrenar sistemas de IA. En este estudio se modela una red real con la que poder simular faltas y, mediante la técnica TDR, obtener las

señales de respuesta de la red para disponer así de una base de datos de señales simuladas que, aunque limitado a 200 ejemplos, son de gran calidad en cuanto a su semejanza con las reales. Sin embargo, simular todos los fenómenos necesarios para entrenar NN sería muy costoso en tiempo.

- **Ampliación de la base de datos:** Partiendo de la base de datos obtenida mediante simulación, se acomete la ampliación de esta (DA por sus siglas en Inglés). Para ello se utiliza una red generativa adversaria (GAN por sus siglas en Inglés) que, una vez entrenada con la base de datos de señales simuladas, es capaz de generar ejemplos sintéticos con los que poder disponer de una base de datos suficiente para el entrenamiento de las NN encargadas de la detección y clasificación de faltas y las encargadas de localizarlas.
- **Detección y clasificación de faltas:** Con la base de datos ampliada a 10.000 ejemplos, se acomete como primer paso la detección y clasificación de los distintos tipos de faltas mediante la utilización de Redes Neuronales Siamesas (SNN por sus siglas en Inglés). Para entrenar estas redes, se utiliza la base de datos sintética (10.000 ejemplos) como entrenamiento y la base de datos de señales simuladas (200 ejemplos) como test. Con este estudio se ha validado la base de datos sintética generada en el anterior estudio, a la vez que se acomete la problemática de la detección y clasificación de la falta.
- **Detección del tiempo a la Falta (TtoF):** En este estudio se analiza la señal de la falta para detectar el punto temporal a partir del cual se ha producido la falta. Para ello, se utilizan un tipo de redes neuronales llamadas Transformers. Detectar el punto temporal a partir del cual se ha producido la falta, significa que podemos estimar el tiempo que ha tardado el pulso inyectado en ir y volver desde el inyector a la falta y viceversa. Con este tiempo se puede extrapolar una distancia desde el inyector a la falta (DtoF), pero la localización de la falta *per se*, solo puede hacerse si además, se

incorpora la información de la rama de la red eléctrica donde se ha producido la falta.

– **Experiencia piloto:** A continuación se presenta la experiencia piloto de un sistema físico desarrollado en el proyecto Europeo H2020 FLEXIGRID en el que se ha diseñado y construido un equipo capaz de inyectar pulsos y registrar la respuesta de la red a estos mediante la técnica TDR. Este equipo se ha instalado en la misma red que se ha modelado para la obtención de las señales de la base de señales simuladas. El objetivo es que el equipo esté durante un año registrando señales reales de falta para comparar los resultados con los obtenidos mediante la simulación. También se pretende obtener una base de datos real con la que poder entrenar los modelos anteriormente usados y comparar la respuesta con las nuevas señales.

  Como objetivo final, se pretende que este estudio pueda servir para aumentar el conocimiento acerca de este tipo de solución y, en futuros proyectos, poder dar un paso más hacia la industrialización de un equipo que cumpla con estas características y pueda ser comercializado.

Índice general

Índice de figuras

Índice de tablas

ACRÓNIMOS

GD	Generación Distribuida
DA	Data Augmentation
IT	Isolé-Terre
BT	Baja Tensión
MT	Media Tensión
CE	Comisión Europea
DERs	Distributed Energy Resources
EMC	Compatibilidad Electro-Magnética
EEG	Electro Encefalografía
LV	Low Voltage
TDR	Time Domain Reflectrometry
DtoF	Distance to Fault
TtoF	Time to Fault
DSO's	Distribution System Operators
TRL	Technology Readiness Level
VE	Vehículo Eléctrico
NN	Neural Network
ANN	Artificial Neural Network
GAN	Generative Adversarial Network
CGAN	Convolucional Generative Adversarial Network
cGAN	Conditional Generative Adversarial Network
cDCGAN	Conditional Deep Convolutional Generative Adversarial Network
SNN	Siamese Neural Network
IA	Inteligencia Artificial
DWT	Discrete Wavelet Transform
ST	Stockwell Transform
MLP	Multilayer Perceptron
SWM	Support Vector Machine
CNN	Convolutional Neural Network
GCT	Graph Convolutional Transformer
AGRU	Attention-Based Gated Recurrent Units
GRT	Gate Recurrent Transformer
MHA	Multi Head Attention

PAA	Piecewise Aggregate Approximation
GASF	Gramian Angular Summation Field
GAF	Gramian Angular Field
FF	Feed Forward
GPS	Global System Position
GADF	Gramian Angular Difference Field

ACRÓNIMOS

Capítulo 1

Introducción

Resumen: En esta tesis se exploran varios enfoques destinados a mejorar la detección, clasificación y localización de las faltas en líneas de distribución eléctrica basados en técnicas de aprendizaje profundo, en concreto redes neuronales NN. En primer lugar, se acomete la generación de las señales de falta necesarias para desarrollar las técnicas de detección, clasificación y localización objeto de la tesis. Para ello, se ha modelado una red real en la que se han simulado faltas de distinta naturaleza y a distintas distancias del punto de detección, obteniendo de este modo una base de señales simuladas de falta. En segundo lugar, se hace una ampliación de la base de señales simuladas (200 ejemplos) mediante el uso de GAN para poder obtener una base ampliada de ejemplos sintéticos (10.000) con los que poder entrenar la NN. En tercer lugar, se implementa la detección y clasificación mediante el uso de SNN. En cuarto lugar, se desarrolla una técnica de detección de anomalías en series temporales basada en un tipo de red neuronal denominada Transformer. Con esta técnica se determina el tiempo transcurrido TtoF desde que la señal que sale del inyector se encuentra con el punto donde se ha producido la falta, rebota debido al cambio de impedancia y vuelve de nuevo al detector. Utilizando este valor temporal se puede estimar la distancia a la falta DtoF. En último lugar, se hace referencia mediante la inclusión en esta tesis del congreso presentado en FUTURED, a la experiencia piloto llevada a cabo dentro del proyecto Europeo H2020

FLEXIGRID en la que se ha diseñado y construido un equipo con las mismas características que el equipo modelado y se ha instalado en esa misma red. Con esta experiencia se pretende registrar las señales de falta naturales que se produzcan a lo largo de un año de funcionamiento, para poder comprobar la validez de los modelos desarrollados en esta tesis con señales reales y seguir avanzando en la mejora de los mismos.

1.1 Motivación y objetivos

Inyectando pulsos en una red eléctrica...

¿Podemos clasificar y localizar las faltas, extrayendo la información de la respuesta a estos pulsos?

Esta es la **pregunta** que inicialmente se formuló un grupo de investigación de CIRCE y sobre ella han girado las investigaciones que se han llevado a cabo en los últimos años dentro de este grupo en relación a la localización de faltas. Por eso esta pregunta constituye también **el eje central** de esta tesis. Se pretende avanzar en la problemática de la detección, clasificación y localización automática de faltas en las líneas de distribución eléctrica, haciendo una aportación al estado del arte mediante la incorporación de algoritmos de **Aprendizaje Profundo** en las distintas fases del proceso.

El grupo de investigación ha venido desarrollado algoritmos para la localización automática de faltas en líneas eléctricas aproximadamente desde el año 2012 [4] basándose en la técnica de la **Reflectometría en el Dominio del Tiempo** (Técnica basada en la inyección periódica de pulsos en la red eléctrica, TDR por sus siglas en Inglés). Esta técnica se basa en inyectar pulsos periódicamente mientras la red eléctrica está operando con normalidad. Cada vez que se inyecta un nuevo pulso, se compara la señal de respuesta de la red eléctrica a ese pulso con la anterior. Si se detecta que ha habido una falta, se procede a comparar esas dos señales para obtener la distancia a la falta. (DtoF).

Detectar en qué punto de esa señal de respuesta registrada se ha producido una **diferencia** con respecto a la señal de la red en el estado normal es, saber cuánto le ha costado al pulso rebotado ir hasta ese punto y volver al inyector. Con esto, se puede saber la "**distancia**" a la que se encuentra la falta del punto de inyección, aunque se necesita información redundante para localizar esta en una de las bifurcaciones de la red.

Antes de entrar en los aspectos puramente técnicos y físicos de las faltas, hay toda una serie de consecuencias sociales y económicas que conviene tener presente para hacerse una idea de la repercusión de la problemática abordada, y que afecta al

corazón mismo de nuestra sociedad. Nos referimos al suministro eléctrico (o más bien a su carencia, en este caso) y la total **dependencia** de la sociedad actual del mismo.

Las faltas en una línea eléctrica generan una serie de impactos significativos en el suministro eléctrico, los usuarios y la infraestructura. Uno de los principales efectos es la **interrupción** del suministro, lo que puede causar inconvenientes y perturbaciones en la vida diaria de las personas, como ocurrió durante el apagón de Nueva York el 14 de julio del año 2019 (Figura 1.1).

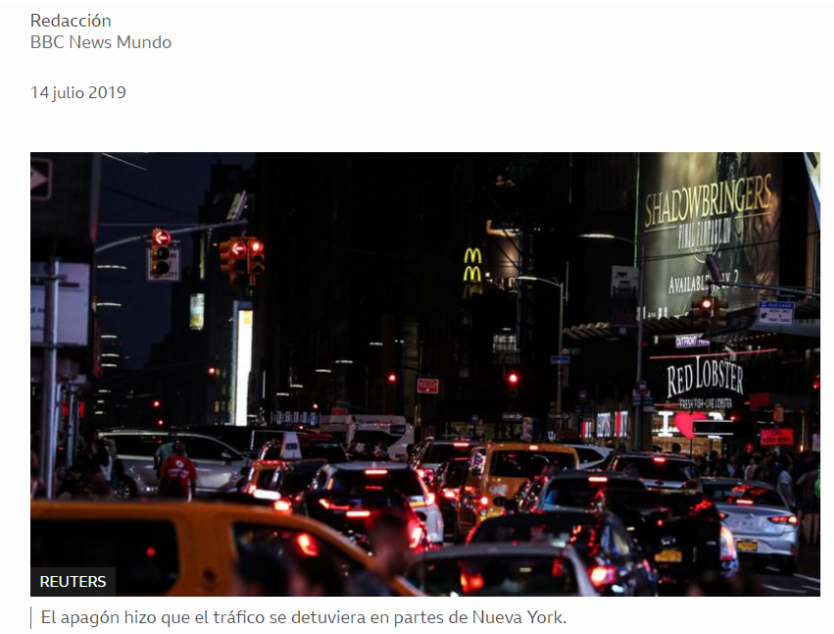

Figura 1.1: Apagón en Nueva York en el año 2019 debido a un fallo originado en una subestación

Además, las faltas pueden ocasionar **daños** en los equipos conectados a la red eléctrica. Los picos de tensión, las fluctuaciones y las sobrecargas eléctricas generadas durante una falta pueden dañar electrodomésticos, dispositivos electrónicos y maquinarias industriales. Esto no solo implica costes de reparación o reemplazo, sino también la posibilidad de pérdida de datos y documentos importantes.

Otro riesgo asociado a las faltas es el peligro de incendios y explosiones. Cuando ocurre una falta grave o un cortocircuito, se pueden generar altas temperaturas, chispas y arcos eléctricos.

Las faltas pueden ser ocasionadas por múltiples factores como el impacto de un ave, la caída de rayos, arboles que tocan las líneas eléctricas, etc...(Figura 1.2)

Figura 1.2: Árboles caidos sobre una línea eléctrica

La inestabilidad en la red eléctrica es otro problema derivado de las faltas ya que estos eventos, pueden causar desequilibrios en la tensión y corriente eléctrica, fluctuaciones en la frecuencia de la red e incluso transitorios eléctricos.

Estas perturbaciones pueden tener un efecto en cascada, afectando a otros componentes de la red y causando apagones generalizados o daños adicionales. Por eso, las empresas distribuidoras se afanan en aumentar el grado de automatización con el fin de minimizar estos problemas (Figura 1.3).

Mediante la **automatización** de la red, se logra aumentar la capacidad de realizar aperturas y cierres de interruptores de forma remota utilizando telemandos cuando se producen incidencias o averías en una línea. Además, se permite el trasvase de tramos de red de una línea a otra, lo que posibilita una **recuperación** más rápida del suministro para los clientes.

Durante el año 2020, se llevaron a cabo instalaciones de 180 interruptores telecomandados en líneas de media tensión y centros de distribución (media tensión/baja tensión) en Mallorca, Ibiza y Menorca. Esta iniciativa representó una **inversión** total de más de 3,6 millones de euros. Todos estos esfuerzos tienen como objetivo

Endesa instalará 381 nuevos interruptores para intervenir de manera remota en líneas en caso de avería

20M EP / NOTICIA / 29.03.2021 - 12:16H

E-distribución, la empresa de distribución de Endesa, con la voluntad de preparar la red eléctrica para el futuro, continúa su plan de automatización de la red de mediana tensión en Baleares, con la instalación de 381 interruptores para intervenir de manera remota en las líneas y facilitar la recuperación del servicio en caso de avería.

Endesa instalará 381 nuevos interruptores para intervenir de manera remota en líneas en caso de avería. / ENDESA

Figura 1.3: Sistemas de interruptores de protección en un C.T.

mejorar la calidad del servicio en términos de minimizar el tiempo sin suministro tras una falta.

La **calidad en el suministro**, en función de las interrupciones sufridas por los abonados se mide con dos parámetros, el **SAIFI** (System Average Interruption Frecuency Index), que es un indicador de la frecuencia de interrupción media por usuario, y que nos permite conocer cual es la cantidad de cortes de suministro por usuario en un periodo de tiempo determinado. El SAIFI se mide en [interrupciones / usuario-semestre]. Por otro lado, tenemos el **SAIDI** (System Average Interruption Duration Index), que es un indicador de la duración de interrupción media por usuario, que permite conocer cual es la duración media de un corte de suministro y se mide en [horas o minutos / usuario-semestre].

En la Figura 1.4 se puede ver una gráfica de los valores SAIDI de Europa entre los periodos 2002-2016.

Todas estas medidas encaminadas a la automatización de las redes eléctricas

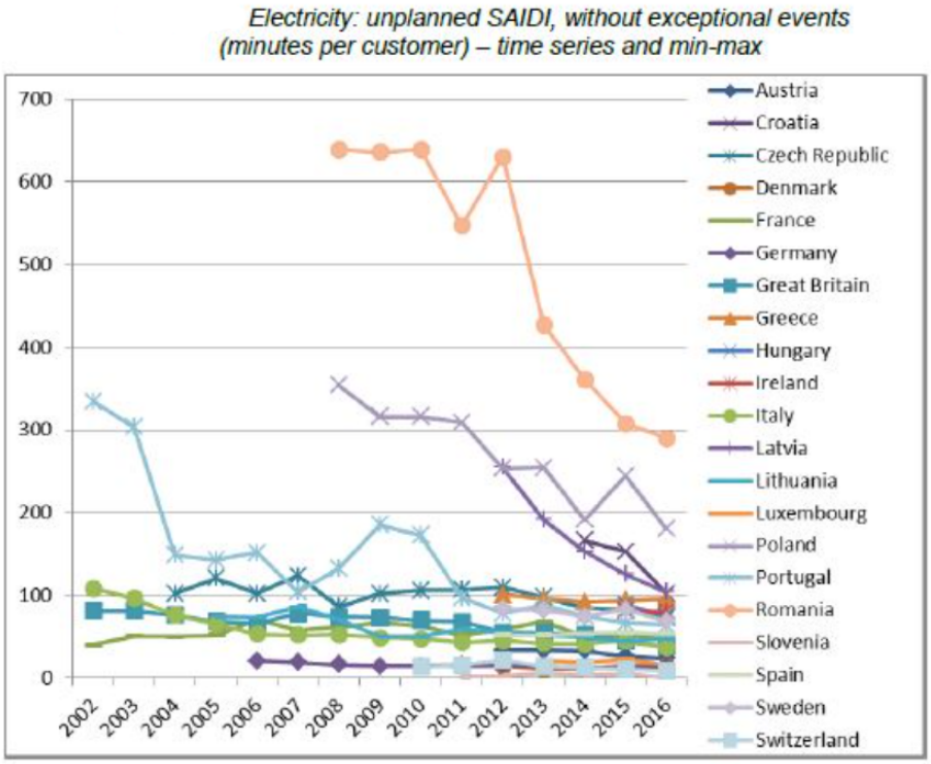

Figura 1.4: Valores SAIDI de Europa (2002-2016) – Fuente: Council of European Energy Regulators

(**Smart Grids**), tienden a alcanzar el cumplimiento de los objetivos de reducción de los tiempos de interrupción.

En la Figura 1.5 se pueden ver los objetivos de **reducción** de tiempos de interrupción en un escenario Smart Grid previstos hasta 2030.

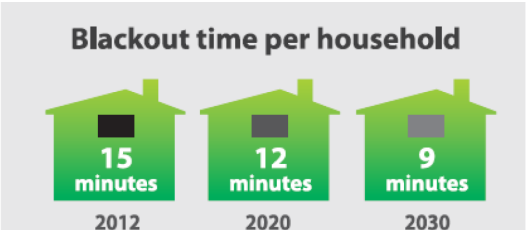

Figura 1.5: Objetivos de reducción de tiempos de interrupción en un escenario Smart Grid / Fuente: Korea Smart Grid Institute, "Korea´s Smart Grid Roadmap 2030." 2010.

Finalmente, las faltas también generan **costes** operativos y de mantenimiento

para los operadores del sistema eléctrico. La detección y reparación de las faltas requieren la movilización de personal especializado, equipos de diagnóstico y materiales necesarios. Además, durante el proceso de reparación, puede ser necesario interrumpir el suministro eléctrico en determinadas áreas, lo que conlleva costes adicionales y una interrupción en la actividad económica. Estos costes aumentan si la inversión en las infraestructuras eléctricas no se adecúa a la demanda.

Por ejemplo, en Estados Unidos, incluso con la creciente demanda, ha habido una crónica **falta de inversión** en expandir la infraestructura de transmisión y distribución de energía, lo que limita la eficiencia y confiabilidad de la red. Aunque hay cientos de miles de líneas de transmisión de alta tensión que se extienden por todo Estados Unidos, desde el año 2000 solo se han construido 668 millas adicionales de transmisión interestatal. Como resultado, las restricciones del sistema empeoran en un momento en el que los cortes de suministro y los **problemas de calidad** de energía se estima que cuestan a las empresas estadounidenses más de **$100 mil millones** en promedio cada año. (*Fuente: The Smart Grid: an introduction, US Department of Energy, 2008*)

Una vez presentada la faceta socio-económica del problema, que da idea de la importancia de aportar a la sociedad cualquier mejora que represente un avance en este área de investigación, y que, sin duda, representa una motivación suficiente para tratar esta temática dentro de una tesis, hay que decir que también ha sido una motivación muy importante en esta tesis la **necesidad** del grupo de investigación de CIRCE de avanzar hacia el desarrollo de un **localizador de faltas automático** que pueda ser instalado y validado en una red real para, posteriormente, ser **transferido a la industria**. Para ello, con esta tesis, se pretende realizar una contribución de nuevos métodos para avanzar en el procesamiento automático de las señales de falta en las líneas eléctricas.

En esta tesis se propone el uso de técnicas novedosas basadas en **Aprendizaje Profundo** para la detección, clasificación y la detección de la DtoF de faltas en líneas eléctricas.

El grupo de investigación de CIRCE planteó la utilización del principio físico de la Reflectometría en el Dominio del Tiempo (**TDR**), que presenta la ventaja de ser un método **agnóstico** del tipo de red eléctrica. Esto supone la no necesidad de

tener un conocimiento previo de la red, además de necesitar un único dispositivo para realizar el proceso completo (la inyección y el registro de la respuesta se realiza en el mismo equipo aprovechando la reflexión de los pulsos).

Antes de esta tesis, CIRCE realizó algunas investigaciones utilizando técnicas y algoritmos basados en el cálculo de impedancia, la Transformada Discreta de Fourier (DFT), algoritmo de ecuaciones diferenciales (DEA), así como en la transformada Wavelet [4][83]. Los resultados del grupo no fueron suficientemente satisfactorios debido, en parte a que se trabajaba con la señal resultante de la diferencia entre la señal de prefalta y la de falta.

En teoría, las dos señales son identicas antes del punto de la falta y divergen a partir de este. En la realidad, la señal resultante presenta unos niveles de amplitud muy pequeños respecto a las señales simuladas, debido a ser una señal diferencia entre ambas. Esto hace que la relación señal/ruido se vea muy empeorada. Esto, unido al hecho de que en las señales hay una atenuación debida a la distancia y al rudio añadido hacian que solamente se obtuvieran resultados satisfactorios en la localización en aquellas señales provenientes de simulaciones de faltas francas a corta distancia.

En esta tesis, se propuso la posibilidad de enmarcar la investigación en técnicas de Aprendizaje Profundo. Al principio, se estableció como objetivo atacar el problema de la localización de las faltas directamente, sin embargo, una primera etapa de estudio de la naturaleza del problema y los **problemas iniciales** que se encontraron, reveló que una mejor estrategia, podía ser, dividir el problema en etapas que nos hiciera avanzar solucionando los distintos problemas que fueran apareciendo.

El primer problema que apareció fue el de la **escasez de señales**. Para poder entrenar una NN, se necesitan típicamente miles de ejemplos. Las faltas son, **cortocircuitos** que se producen en la red eléctrica entre una o varias de sus fases y/o tierra. Estas faltas son eventos fortuitos y a menudo catastróficos (caída de árboles en la línea, rayos, impacto de un ave contra la línea, etc...). Por su propia naturaleza, es muy difícil obtener estas señales mediante la medición en campo. Su carácter caótico y estocástico hacen prácticamente **imposible predecir** su aparición.

Como primera aproximación a la solución del problema se planteó modelar un tramo de una red real. Esto permitía poder lanzar **simulaciones** de faltas con las que obtener señales de faltas que se necesitaban para realizar los estudios posteriores.

Se modeló una red junto con el resto de elementos del sistema de detección (acopladores, inyector, cables, etc...), y se hicieron una serie de pruebas de laboratorio para comprobar que las simulaciones y las señales experimentales eran similares.

Una vez modelada la red apareció el enorme hándicap de los costes computacionales, por ejemplo la simulación de 10.000 señales de faltas diferentes tomaban el tiempo aproximado de un año. Esto era inviable, máxime cuando la parametrización de cada una de las faltas hay que hacerla maualmente indicando el tipo (entre una fase y tierra, entre dos fases y tierra, etc...), la impedancia, la posición dentro de la red, etc... La primera decisión fue la de simular solo 200 ejemplos de faltas. Con estas señales el reto era conseguir 10.000 señales más. Se decidió codificar las 200 señales temporales como **imágenes** ya que en el estado del arte, las CNN han dado muy buen resultado en tareas de clasificación, que era el siguiente problema a enfrentar. Para **aumentar la base de datos** de 200 a 10.000 ejemplos **se repasaron el estado del arte** de las técnicas habituales de DA. Sin embargo se concluyó que no podían ser aplicadas a nuestro caso ya que, las rotaciones, traslaciones y otra serie de pasos intermedios relacionados con estas técnicas podían afectar a la información temporal embebida en las imágenes.

Para esta ampliación se ha utilizado un tipo de **NN** llamada **GAN**, que una vez entrenada es capaz de sintetizar imágenes de la misma naturaleza partiendo única y exclusivamente de ruido. Se realizaron numerosas pruebas con distintos tipos de GAN (GAN Lineales, Convolucionales (CGAN), GAN condicionales (cGAN), e incluso con GAN condicionales profundamente convolucionales (cDCGAN)) hasta que se concluyó que las GAN que mejor trabajaban para el objetivo deseado eran las más sencillas, las GAN lineales.

Con la base de datos **ampliada** a 10.000 ejemplos gracias a la utilización de los GAN, se probó a clasificar los tipos de falta con distintos modelos de NN conocidos en el estado del arte obteniendose resultados muy pobres (ver apartado 2.3). Al final se obtuvieron **muy buenos resultados** (como se verá en los trabajos que se presentan posteriormente en la tesis) gracias al uso de las **SNN**. En este tipo de redes, se presentan parejas de ejemplos de clases similares y clases diferentes y gracias a la incorporación de la función de pérdida Contrastiva, se acentuan aún más el aprendizaje de esas diferencias entre diferentes clases.

Una vez abordado con éxito la tarea de la clasificación, se comenzó con la localización, que implica determinar **donde** se ha producido la falta, es decir, en que momento la señal de falta difiere de la de prefalta. La localización implica tratar un problema de regresión lineal (predecir una variable continua). Al tratarse de un problema temporal la base de datos ampliada en forma de imágenes utilizada para solucionar el problema de clasifciación no se podía utilizar y tampoco se pudo entrenar una red GAN. Por lo tanto, para abordar este problema solo se disponía de la base de datos de señales simuladas.

Repasando en el estado del arte se encontraron los **Transformers**, NN muy utilizadas para problemas de análisis de series temporales. El aprovechamiento de los Transformers resulta altamente ventajoso en escenarios donde hay **escasez de muestras** etiquetadas como es nuestro caso. Los Transformers son capaces de **aprender los patrones secuenciales** dentro de datos de series temporales y predecir la evolución de la señal. Para lograr la localización los Transformer se han entrenado mediante una arquitectura de red siamesa que introduce una función de perdida Contrastiva que maximiza las diferencias entre ejemplos distintos. Con este modelo al que hemos llamado **TransSiamese**, hemos obtenido unos **resultados bastante buenos** en la detección de la distancia a la falta DtoF y una línea prometedora sobre la que avanzar en futuros trabajos hacia el objetivo final de la localización, que precisa adicionalmente, entre otras cosas, de información sobre la topología de la red.

Derivado de lo descrito anteriormente, los **objetivos específicos** abordados durante la investigación se resumen en la tabla 1.1. En ella, se numera cada uno de ellos con el fin de relacionar estos con los **artículos publicados** durante la investigación en apartados posteriores.

Tabla 1.1: Objetivos específicos de la tesis.

Objetivo 1	Modelado y simulación de una red electrica real mediante el software PSCAD utilizando la técnica TDR para obtener una base de datos de faltas originales de la tesis
Objetivo 2	Ampliación de la base de datos original (DA) mediante el uso de GAN para tener una cantidad de señales suficiente para ser usadas en el entrenamiento de redes neuronales (NN por sus siglas en Inglés) para la clasificación.
Objetivo 3	Detección y clasificación de faltas mediante el uso de SNN.
Objetivo 4	Aproximación a la DtoF usando Transformers mediante la detección de anomalías en series temporales
Objetivo 5	Diseño, fabricación e instalación de un equipo prototipo en la red real modelada para recopilar señales reales de prefaltas y faltas durante un año, y poder seguir avanzando en la mejora de los métodos empleados en esta tesis.

1.2 Cronología de la Tesis

La cronología de la tesis refleja los problemas que se han tenido y que han sido comentados en el anterior capítulo.

Al principio, se pensó en atacar el problema de la localización de las faltas directamente, sin embargo, un análisis inicial, mostró que una mejor estrategia, podía ser, dividir el problema en etapas que nos hiciera avanzar solucionando los distintos problemas que fueran apareciendo.

En el inicio de la tesis se enfrentó el problema de la escasez de ejemplos naturales y de la imposibilidad de generar los suficientes incluso simulándolos en una red modelada a tal efecto. Después de aumentar la base de datos de señales simuladas (200), mediante la generación de ejemplos sintéticos (10.000) usando GAN, y alcanzar el objetivo de la clasificación, hubo que volver a la base de datos inicial (200), al tratarse en este caso de un problema de regresión lineal a diferencia del de clasificación. En este caso se tuvo que buscar una NN que pudiera tratar este tipo de datos de series temporales y que funcionara con pocos ejemplos disponibles, como el caso de los Transformers, que se utilizaron en esta tesis.

La figura 1.6 muestra como dato curioso el hecho de que, el modelado y simulación de las señales de faltas de una red eléctrica real [5], que es la primera tarea que se desarrolló en la tesis, no dio lugar a la primera publicación, debido, como se explica a continuación, a los problemas que se han enfrentado en esta tesis.

Inicialmente, se partió del modelado de una red real en la que se modeló tanto el inyector, como los acopladores. De ahí, se paso a simular una serie de señales que fueran manejables en cuanto al tiempo de computo (200 señales). Este conjunto de señales de falta, contiene solamente una señal de prefalta. Esta señal de prefalta, corresponde a la respuesta de la red eléctrica al pulso inyectado en condiciones de funcionamiento normal.

En condiciones teóricas ideales, esto arrojaría una diferencia apreciable entre las dos señales a partir del punto temporal de ocurrencia de la falta, mientras que durante el tiempo anterior a la falta, la diferencia entre las dos señales sería muy pequeña. Al trabajar con la señal diferencia entre los estados de prefalta y falta, el estado de la red antes de ocurrir la falta puede ser cualquiera ya que, al inyectar pul-

sos de manera periódica, el estado de la red en prefalta y en falta será virtualmente el mismo.

Además, simular el mismo número de prefaltas y faltas supone, duplicar el tiempo de simulación. En este contexto, se desarrollaron los algoritmos en los que vino trabajando CIRCE. Sin embargo, para abordar la tesis desde el punto de vista de las NN, se necesitan una gran cantidad de ejemplos de todos los tipos (también de la prefalta).

Ante este escenario, se decidió dar un enfoque distinto a la tesis e intentar primero abordar la clasificación de los tipos de falta antes de acometer la detección de la DtoF. En este caso, se planteó la posibilidad de que la información del tipo de falta podría estar embebida en cada una de las señales de falta. Si esto fuera así, no se necesitaría tener la señal diferencia entre prefalta y falta, lo cual, reportaría dos beneficios. Uno era el de no necesitar la señal de prefalta, con lo cual se solucionaba el problema de no tener más que una señal. El otro, era el hecho de que se trabajaba con la señal original y no con una señal diferencia, la cual tenia mucha menos amplitud y cuya relación señal a ruido era considerablemente peor que la original.

Con esta decisión, se planteó resolver el primer gran desafío de la tesis. Este fue el de encontrar un método para ampliar la base de datos inicial. Para este cometido, se utilizaron los GAN. Se probaron múltiples tipos de GAN y se lidió con problemas relativos al "colapso de modo" o el "Desvanecimiento del Gradiente" y a la dificultad intrínseca que tienen este tipo de redes para converger.

Al final se consiguió entrenar un GAN lineal para cada una de las etiquetas (tipos de falta), con el que se consiguió generar una base de datos extendida de 10.000 ejemplos.

Tras este "éxito" parcial, se probaron a entrenar varios modelos de NN y se encontró que la combinación de una SNN con función de pérdida Contrastiva ofrecía unos resultados muy buenos en clasificación de los tipos de falta.

Una vez obtenidos unos resultados satisfactorios en la clasificación, se publicó el artículo. Tras la aceptación del artículo, parecía que por fin la tesis cogía fuerza y se vió que se podía seguir avanzando en la confianza de que el trabajo realizado estaba dando su fruto en forma de reconocimiento por parte de la comunidad científica.

Tras conseguir la primera publicación relativa a la clasificación de faltas, y antes de acometer el objetivo de la detección de la DtoF, se pensó que ya se podía explicar la parte física en la que estaban apoyadas estas señales (su naturaleza, el modelado, simulación, etc...).

Por este motivo, la publicación de la detección y clasificación de faltas usando SNN [6], es la primera en cuanto a fecha de publicación. De otro modo, si no hubiera habido éxito en la clasificación, el artículo acerca de las señales físicas y su modelado y simulación, no hubiera tenido sentido.

La obtención de señales sintéticas mediante el uso de GAN [7], fue el siguiente artículo redactado, y se envió en el año 2022, en forma de congreso internacional (CIRED - Roma). Aunque por los tiempos del congreso, la propia presentación y publicación del artículo en el congreso no tuvo lugar hasta un año después (en junio de 2023).

Durante este periodo de redacción del artículo sobre el modelado y simulación de señales basadas en la TDR y el congreso sobre el uso de GAN, se reflexionó sobre como acometer el objetivo de la localización.

Como ya se ha explicado, debido a la problemática "intrínseca" de las múltiples bifurcaciones de una red eléctrica, el objetivo de la localización pasó a ser el objetivo de la detección de la distancia a la falta (DtoF). En este caso tuvimos que contar, como ya se ha dicho, con la base de señales original. Mediante la aplicación de Transformers, y mediante la detección de la anomalía entre la señal de falta y la de prefalta, se consiguió detectar el (TtoF) y de manera indirecta, estimar la (DtoF). En el año 2023 se instalo un prototipo en la red real modelada y se presentó un congreso nacional que trataba del desarrollo de este prototipo y todo lo concerniente a su diseño e instalación [8]. Tras la publicación y aceptación del último artículo sobre la detección de la distancia a la falta usando Transformers [9], se dio por concluida esta etapa de investigación y se redactó esta tesis por compendio que recoge todos estos trabajos.

Cada uno de ellos, ha llevado a esta tesis por caminos a veces inesperados, a veces infructuosos, otras veces sorprendentes. Pero todos han representado un aprendizaje no solo a nivel técnico sino sobre todo a nivel de crecimiento personal en cuanto al esfuerzo y sacrificio que hay en todos y cada uno de ellos.

La Figura 1.6, resume de una manera gráfica todo ese esfuerzo, donde se muestra además, la cronología de los trabajos y el hilo conductor desde los inicios, donde solo había señales físicas que "rebotaban" por la red eléctrica, hasta el artículo final en el que la capacidad de abstracción del Aprendizaje Profundo ha obrado el milagro de extraer una información de las señales eléctricas, que de otro modo, probablemente hubiera permanecido ahí oculta. También se puede ver en la Figura 1.6 la relación de cada artículo con los objetivos planteados en la sección anterior.

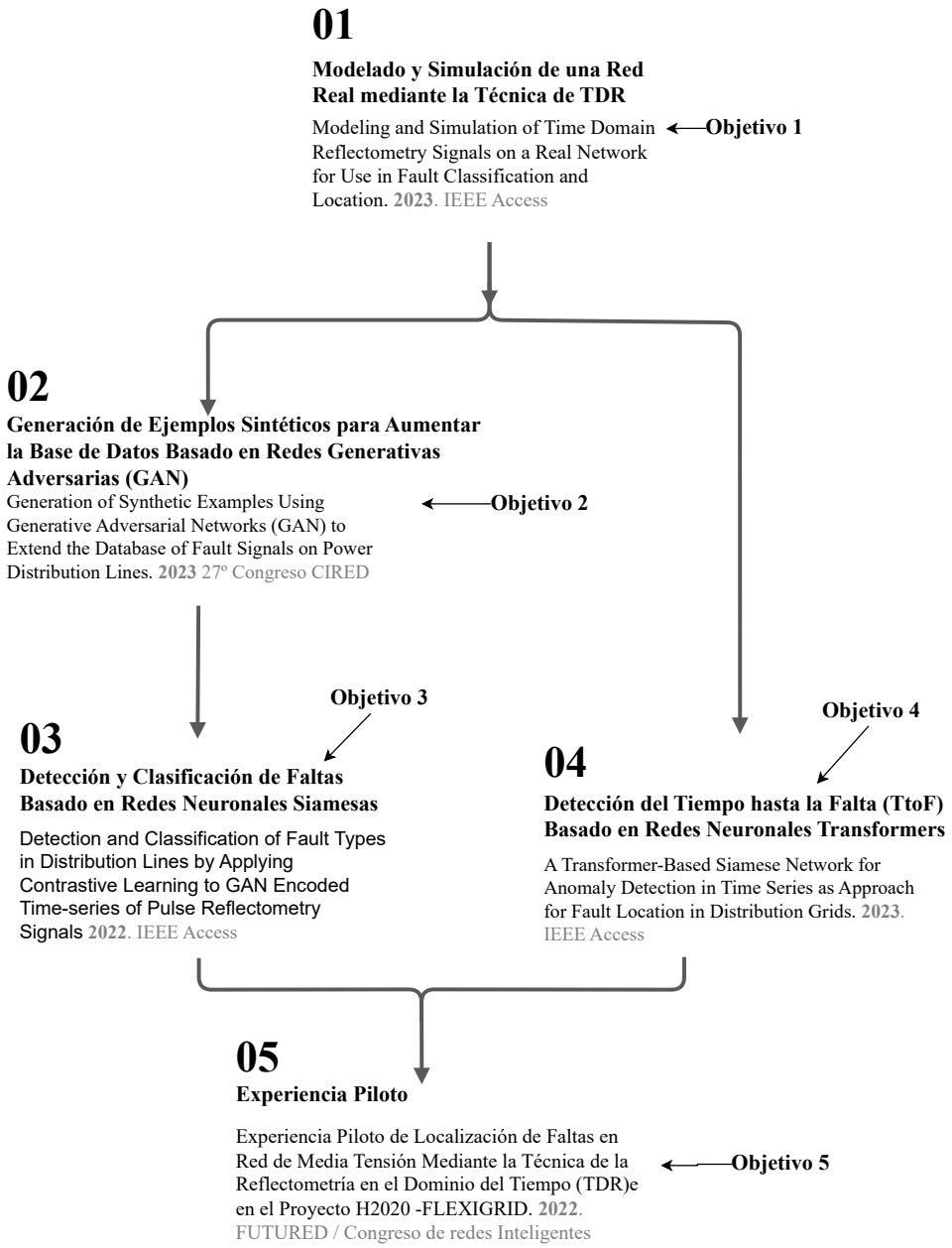

Figura 1.6: Unidad temática entre los artículos que componen la tesis. Se indica también la relación entre cada artículo y el objetivo (ver Tabla 1.1) que satisface.

1.3 Revisión Bibliográfica

1.3.1 Antecedentes

La importancia de la detección, clasificación y localización automática de faltas radica en varios aspectos:

- **Mantenimiento eficiente:** Permite a las compañías eléctricas conocer la ubicación exacta de un problema en la línea, lo que reduce el tiempo necesario para enviar técnicos y reparar la falta. Esto mejora la eficiencia del mantenimiento y reduce los costos operativos.
- **Tiempo de respuesta más rápido:** Ofrece una respuesta más rápida ante interrupciones en el suministro eléctrico, ya que las compañías eléctricas pueden tomar medidas inmediatas para restaurar la energía en las áreas afectadas y minimizar las interrupciones en el servicio.
- **Mejora de la confiabilidad:** La detección y localización temprana de faltas en líneas eléctricas contribuye a mejorar la confiabilidad del sistema eléctrico en general, ya que se reducen los apagones prolongados y se evita que las faltas se propaguen a otras partes del sistema.
- **Seguridad:** También juega un papel importante en la seguridad del personal y los usuarios al poder tomar medidas para evitar accidentes eléctricos y minimizar los riesgos para la vida y la propiedad.
- **Optimización de la red eléctrica:** Al recopilar datos sobre las faltas y su ubicación, las compañías eléctricas pueden analizar patrones y tendencias para mejorar el diseño y la planificación de la red eléctrica. Esto permite optimizar la infraestructura y tomar decisiones informadas sobre mejoras y expansiones futuras.

En resumen, la detección, clasificación y localización automática de faltas en líneas eléctricas es esencial para mantener la confiabilidad, eficiencia y seguridad del sistema eléctrico. Proporciona una detección temprana de problemas, acelera la respuesta y mejora la calidad del servicio eléctrico en general.

Por otro lado, las técnicas de localización de faltas ya se utilizan ampliamente en las líneas de transporte, donde cada línea se monitoriza por separado. Sin

embargo, las redes de distribución en entornos reales suelen tener una topología radial, en anillo o en malla, con muchos nodos y ramificaciones [10] [11] [12], lo que hace inviable utilizar estos sistemas tan costosos en cada tramo. Por lo tanto, los métodos de localización necesitan un enfoque diferente para obtener un sistema rentable que pueda monitorizar toda la red o una sección importante de la misma.

Además, también es importante considerar otras características específicas de los sistemas de distribución, como la presencia de cargas desequilibradas, laterales y diferentes tipos de cables/conductores. Estas características afectan negativamente a los métodos de localización, lo que reduce su rendimiento.

Vale la pena mencionar un par de casos significativos:

- **Las redes IT(*Isolé-Terre*):** O también llamadas redes de neutro aislado, son comunes en los sistemas de distribución y representan un desafío adicional para la localización [13], ya que los métodos clásicos basados en la impedancia presentan errores sustanciales.
- **Las redes de distribución de baja tensión (LV):** Carecen especialmente de estudios sobre técnicas de localización de faltas [14]. Estas últimas redes tienen como diferencias importantes en comparación con las redes de alta y media tensión que, las líneas subterráneas suelen estar compuestas por cables blindados y que los puntos finales del sistema son las cargas de los clientes, por lo que hay una variabilidad en el valor de su impedancia. Por ejemplo, las faltas en serie [15] son causadas por cables rotos y aumentan la impedancia de las líneas afectadas. A su vez, las faltas se pueden clasificar según el número de fases defectuosas y la implicación de la tierra:
  - Una fase a tierra
  - Entre dos fases
  - Doble fase a tierra
  - Entre Tres fases
  - Tres fases a tierra

Cada tipo de falta provoca diferentes respuestas eléctricas y puede generar efectos menos o más peligrosos. Por lo tanto, un método completo de diagnóstico de faltas debe ser capaz de determinar no solo la localización del punto de falta, sino también

el tipo de falta encontrada en la red de distribución [16]. Existen diversas técnicas sobre las que se basa la detección, clasificación y localización de faltas:

- **Análisis de ondas viajeras:** Las ondas viajeras son señales electromagnéticas generadas cuando ocurre una falta en una línea eléctrica. Al analizar las características de estas ondas, como la amplitud y el tiempo de propagación, es posible determinar la ubicación de la falta [17] [18].
- **Método de la impedancia:** Esta técnica se basa en la medición de la impedancia de la línea eléctrica. La impedancia varía en función de la distancia desde el punto de medición hasta la falta. Al analizar los cambios en la impedancia, se puede determinar la ubicación de la falta [13].
- **Técnica de la reflectometría en el dominio del tiempo TDR:** En esta técnica, se envían pulsos de alta frecuencia a través de la línea eléctrica y se monitoriza la señal reflejada. Cuando ocurre una falta, se producen cambios en la señal reflejada que pueden utilizarse para localizar la falta [19].
- **Utilización de algoritmos de procesamiento de señales:** Se pueden aplicar algoritmos de procesamiento de señales para analizar los datos recopilados de la línea eléctrica y detectar patrones asociados con las faltas. Estos algoritmos pueden utilizar técnicas como la transformada de Fourier, el análisis de componentes principales o técnicas basadas en Deep Learning, entre otras [20] [21].
- **Sistemas de localización basados en GPS:** Algunos sistemas de localización automática de faltas utilizan tecnología de posicionamiento global (GPS) para determinar la ubicación exacta de la falta. Se colocan sensores equipados con receptores GPS a lo largo de la línea eléctrica para detectar y localizar las faltas.

  Es importante destacar que estas técnicas se pueden utilizar de manera individual o en combinación, dependiendo de las características de la línea eléctrica y de los requerimientos específicos del sistema de distribución de energía. Además, el avance tecnológico continúa mejorando y desarrollando nuevas técnicas de detección, clasificación y localización automática de faltas para hacer que los procesos sean más precisos y eficientes. En esta tesis, se combina la técnica TDR como principio físico con el que se obtienen las señales

de faltas y prefaltas que, posteriormente son procesadas mediante distintas redes neuronales para acometer cada uno de los objetivos planteados en ella.

1.3.2 Revisión Bibliográfica de la reflectometría en el dominio del tiempo (TDR)

En el anális del estado del arte de este artículo se pueden diferenciar tres partes.

La primera, relativa a la necesidad de crear escenarios más realistas para realizar simulaciones de faltas con las que se obtengan señales más cercanas a la realidad. En este sentido, se justifica la necesidad de migrar desde modelos de red tipo *Benchmark Test Feeder*, como el IEEE 13 [22] (modelos teóricos), hacia modelos como el presentado en esta tesis que estan basados en redes eléctricas reales. Existen múltiples publicaciones que usan esta red IEEE 13 para desarrollar y comparar distintos algoritmos de clasificación y localización de faltas [23] [24] [25]. Esta red puede ser muy útil para hacer comparaciones entre distintos algoritmos pero, al no tener una correspondencia con una red real, los resultados no pueden ser verificados.

La segunda parte es la relativa a la técnica TDR. En el estado del arte encontramos referencias del uso de la TDR aplicado a la localización de faltas mediante algoritmos de inteligencia artificial (IA) [26] [27]. Tambien se encuentran referencias al uso de la TDR en otros campos, como la aviación y la automoción, entre otros [28] [29] [30] [31]. En general, la técnica de la reflectometría de pulsos está presente en el estado del arte para la localización de faltas, aunque en esta tesis presenta la peculiaridad de inyectar pulsos de manera continua para aprovechar la diferencia en la respuesta en el estado de prefalta y falta para determinar, por un lado la ocurrencia de esta, y por otro utilizar esas dos señales para determinar la DtoF.

La tercera parte es la relativa a las técnicas de clasificación y localización. Básicamente en el estado del arte encontramos técnicas basadas en la medida de los cambios de impedancia en la red para determinar la falta [32] [13], mediante la medida de la onda viajera producida por el transitorio de la propia falta [17] [33], y mediante la inyección de pulsos de alta frecuencia y la medida de la señal reflejada en los cambios de impedancia de la red (TDR) [19] [18] [34]. En esta tesis,

se utiliza esta última técnica (TDR), pero con la peculliaridad de que inyectamos pulsos continuamente y cuando se detecta que la señal de respuesta es diferente de la anterior, se determina que ha habido una falta y se procede a su localización procesando el cambio producido en la respuesta de la red. En el estado del arte también encontramos referencias a la aplicación de la IA unida a distintas técnicas como las ya mencionadas [20] [21] [23].

1.3.3 Revisión Bibliográfica de la Generación de ejemplos sintéticos mediante el uso de Redes Generativas Adversarias (GAN)

Las NN estan dando buenos resultados en el campo de la detección, clasificación y localización de faltas [35] [36]. Durante el proceso de entrenamiento de una NN se le muestran ejemplos de eventos, y de este modo aprende a reconocer ejemplos nunca vistos antes. En las redes eléctricas, es muy complicado obtener señales de faltas reales, debido a la naturaleza del evento. Modelar la red y simular las faltas es prácticamente imposible debido a la cantidad de tiempo de computación necesario. En este trabajo se propone la utilización de la técnica (DA) para aumentar la base de datos. De este modo, se parte de un número de señales (unos cientos), simuladas sobre una red real modelada y posteriormente se procede a ampliar esa base de datos. En nuestro caso, no podemos aplicar técnicas de DA clásicas como rotaciones, escalado, simetrías, etc..., que se utilizan habitualmente con imágenes ya que en nuestro caso, las imágenes son señales temporales transformadas [37].

En el estado del arte, existen referencias a la generación de ejemplos sintéticos en imágenes mediante el uso de GAN [38]. Algunas de las aplicaciones más usadas con GAN son el aumento de resolución en imágenes, la modificación de la apariencia de una imagen o la generación de imágenes sintéticas [39] [40] [41] [42] [43].

Existen varios tipos de GAN: GAN Lineales, Convolucionales (CGAN), GAN condicionales (cGAN), incluso GAN condicionales profundamente convolucionales (cDCGAN) [43] [44] [45] [46]. En nuestro caso, intentamos utilizar GAN condicionales inicialmente, ya que ellas permiten incluir en la infromación de entrada el tipo de falta, con lo que se hace el entrenamiento una sola vez para todos los tipos. Sin embargo, uno de los problemas que tienen los GAN es su dificultad a

la hora de estabilizar el entrenamiento ya que sufren de problemas propios de su aruitectura comoo el colapso de modo etc.. que hacen que solo aprendan un tipo de ejemplos y no puedan generalizar el resto. De la misma forma los GAN convolucionales, específicos para tratamiento de imágenes representaron un problema a la hora de entrenar nuestros ejemplos que, por su naturaleza no hacian que los GAN tuvieran una convergencia en su entrenamiento. Al final, resolvimos el problema entrenando cada uno de los 5 tipos de falta con un GAN lineal que por su simplicidad conseguimos una convergencia y entrenamiento adecuados para la posterior generación de ejemplos. Con la aplicación de este tipo de GAN lineales a nuestros ejemplos estamos utilizando unas NN existentes en el estado del arte pero usándolas de una manera novedosa para resolver nuestro problema concreto de falta de ejemplos.

1.3.4 Revisión Bibliográfica de la Detección y clasificación de faltas mediante la aplicación de Contrastive Learning en Redes Siamesas

Como se puede ver, en el estado del arte existen varias técnicas utilizadas en la detección y clasificación de faltas. A continuación, se hace un resumen de las distintas técnicas encontradas en el estdo del arte, junto con algunas referencias que han servido de base para el desarrollo de esta etapa de la tesis, en la que se ha abordado la clasificación de las faltas.

Los tres grupos de técnicas principales encontrados son [47]:

- **Técnicas Destacadas:** Dentro de este grupo nos encontramos con varias técnicas, como la Transformada Wavelet Discreta (DWT por sus siglas en Inglés) [48]. Dentro de este grupo encontramos también las técnicas basadas en Redes Neuronales Artificiales (ANN por sus siglas en Inglés) [49]. También se han hecho intentos utilizando Lógica Difusa [50]
- **Técnicas Híbridas:** Las técnicas híbridas pretenden combinar varias técnicas para intentar abordar mejor el problema. Aquí encontramos la unión de la transformación Stockwell (ST por sus siglas en Inglés) junto con el Perceptron Multicapa (MLP por sus siglas en Inglés) [22] [24] testados en IEEE-13 test feeder. También encontramos aquí la combinación de DWT y ANN [51]

– **Técnicas Modernas:** Las técnicas modernas incluyen las maquinas de vector soporte (SWM por sus siglas en Inglés). Esta técnica se utiliza para aprender a separar funciones en tareas de clasificación [52]. En este grupo se encuentran también los algoritmos genéticos [53]

Centrándonos en las NN, que es la técnica que usamos, hemos encontrado algunos artículos adicionales que tienen relevancia especial para el trabajo desarrollado en este artículo: Algunos estudios han utilizado redes neuronales para procesar señales de voltaje y corriente de líneas de energía para clasificar faltas [54] [55] [56] [57] [58]. Los voltajes y corrientes se digitalizaron para formar la entrada de la red neuronal.

También se han realizado trabajos para la detección y localización de secciones de cables envejecidos en líneas subterráneas [59]. En este caso, la función de transferencia del cable se utiliza como entrada de la CNN.

También se han realizado estudios sobre detección de faltas, intentando extrapolar los valores de voltaje de varias redes de energía simuladas. Estos valores se utilizaron para entrenar una red neuronal para detectar faltas en una red eléctrica real [60]. Hemos encontrado algunos estudios en los que se utilizaron redes neuronales convolucionales (CNN) para procesar series temporales. Las señales de falta son señales de series temporales, por lo que este tipo de trabajo es muy relevante para nosotros. En particular, se ha utilizado EEGNet, una CNN compacta para la clasificación e interpretación de señales de Electroencefalografía (EEG), para clasificar este tipo de señal [61].

Otro trabajo interesante es el procesamiento de señales temporales de fenómenos de descarga parcial en redes eléctricas utilizando transformaciones de imagen (escalograma) [62]), en el que la naturaleza de las señales es muy similar a la nuestra. La transformación de este tipo de señal en imágenes permite que sea procesada por redes neuronales convolucionales (CNN). Este tipo de red neuronal proporciona excelentes resultados en el procesamiento de imágenes.

Como se puede ver, en la literatura, existen varias publicaciones que proponen el uso de Redes Neuronales para la detección de faltas y otros fenómenos de naturaleza similar en redes de distribución eléctrica.

En esta tesis, se ha apostado por la utilización de NN. Tras intentar clasificar el tipo de falta utilizando diferentes modelos de NN existentes en el estado del arte sin obtener buenos resultados, se ha seguido investigando hasta encontrar una combinación de SNN y función de perdida Contrastiva, que ha llevado a obtener muy buenos resultados en la detección y clasificación de los tipos de falta.

1.3.5 Revisión Bibliográfica de la detección de anomalías en las señales de falta mediante el uso de Transformers

En este caso, estamos frente a un problema de regresión lineal y a diferencia de la clasificación de faltas, no es posible entrenar un GAN para generar ejemplos sintéticos con la DtoF "etiquetada" correctamente. A partir de este nuevo escenario, se exploran otras NN y nos encontramos con la posibilidad de utilizar un modelo de aprendizaje automático que se ha vuelto muy popular en el procesamiento del lenguaje natural (NLP, por sus siglas en inglés), llamado Transformer. Los Transformers son especialmente conocidos por su aplicación en tareas como la traducción automática y la generación de texto.

La arquitectura del Transformer, tiene en cuenta las interacciones entre los diferentes instantes temporales de una secuencia de entrada. A diferencia de las arquitecturas recurrentes tradicionales, como las redes neuronales recurrentes (RNN), los Transformers no requieren de una estructura secuencial para procesar la información. En cambio, utilizan mecanismos de atención para capturar las relaciones entre todas las posiciones de la secuencia de entrada en paralelo.

La arquitectura del Transformer ha demostrado ser muy exitosa en múltiples desafíos de procesamiento del lenguaje natural, y su introducción ha sido un avance significativo en el campo de las redes neuronales y el aprendizaje automático aplicado al procesamiento del lenguaje.

Este tipo de NN aparecieron por primera vez en un artículo llamado "Attention is all you need" [63] publicado en 2017, que introdujo por primera vez una arquitectura de encoder-decoder basada en capas de "atención". Los autores lo llamaron "Transformer". La detección de anomalías en series temporales han sido implementadas con exito mediante modelos basados en Transformers [64] [65] por su

habilidad para modelar dependencias temporales. Ese es nuestro caso, en el que los eventos del pasado tienen influencia en los eventos del futuro.

Varios modelos basados en Transformers han mostrado resultados prometedores para detección de anomalías en series temporales. Entre estos modelos se encuentran los Gated Recurrent Transformers (GRT por sus siglas en Inglés)[66], Multi-Head Attention Networks (MHA por sus siglas en Inglés) [67] [68] [69] [70], Deep Transformers [71] [72], Graph Convolutional Transformers (GCT por sus siglas en Inglés) [73] [74] [75], and Attention-based Gated Recurrent Units (AGRU por sus siglas en Inglés) [76] [77] [78].

Nuestra primera inspiración ha sido el artículo [65], en el que el autor propone el *Anomaly Transformer* en el que se introduce un termino en la función de pérdida que captura las dependencias temporales y contextuales en las señales. Nuestra segunda fuente de inspiración es el artículo (*TranAD*) [79] que propone un mecanismo de *focus Scoring* y *Adversarial Training* con el que se pueden detectar pequeñas diferencias como las que tenemos entre nuestras señales de prefalta y falta. La tercera inspiración son las SNN [80] [81] [82] [83]. Esta arquitectura usada en la tesis, de red siamesa basada en Transformer ($TransSiames$), está inspirada en el modelo *TranAD*, que incorpora autocodificación basada en puntajes de enfoque y un proceso de entrenamiento adversario. Este Transformer ha sido modificado para ser entrenado de manera siamesa.

Aprovechar los Transformers resulta altamente ventajoso en escenarios donde los ejemplos etiquetados son escasos como en nuestro caso. Los Transformers son capaces de aprender los patrones secuenciales dentro de los datos de series temporales y predecir la evolución de la señal. De esta forma, somos capaces de determinar en que punto la señal de falta se diferencia de la de prefalta. El punto en el que el Transformer no es capaz de predecir la evolución de la señal, es el punto en el que se ha producido la falta, ya que es ahí donde las señales empiezan a divergir.

1.4 Estructura de la Tesis

A partír de este punto, la tesis se estructura del siguiente modo:

El Capítulo 2 se centra en la discusión general de cada uno de los artículos presentados como compendio en esta tesis y que se van a denominar como **Estudios**.

En este capítulo se exponen las contribuciones clave de cada uno de los estudios realizados en el marco de esta tesis. Esto proporciona una visión panorámica de la contribución de esta investigación al campo de estudio en el que se enmarca, así como al avance del estado del arte en el sector. En cada uno de ellos, la discusión se centra en explicar de una manera sintetizada, las cuestiones más relevantes para la tesis y de qué forma han contribuido a los objetivos de esta.

En el Capítulo 3 se presenta el compendio de todos los artículos presentados en esta tesis. En cada uno de ellos se hace una pequeña introducción y a continuación se incluye el artículo íntegramente tal y como ha sido publicado para facilitar la labor de su revisión por parte del tribunal evaluador.

Finalmente, en el Capítulo 4 se presentan las conclusiones y las futuras líneas de trabajo. En este capítulo, el objetivo es resumir las aportaciones de la tesis en la temática del procesado de señales de faltas aportando información sobre el grado de consecución de los objetivos planteados.

Asimismo, se hace una reflexión acerca de as futuras líneas de investigación que se abren, derivadas de objetivos no cumplidos en su totalidad y de oportunidades de seguir avanzando en nuevas líneas que han surgido a raíz de la realización de esta tesis.

Posteriormente se incluye la bibliografía utilizada en la redacción de esta tesis. Esta bibliografía es solo una parte de la bibliografía total comprendida entre todos los artículos, pero, sirve como muestra de las referencias más relevantes en las que se ha apoyado esta tesis. En el Anexo A, se presenta la lista de publicaciones, desglosada en artículos de revistas científicas y congresos.

Capítulo 2

Discusión general y principales contribuciones

RESUMEN: En este capítulo se presentan las principales aportaciones de cada uno de los estudios realizados al conjunto de la tesis. De este modo, se ofrece una visión global de la contribución de esta tesis al ámbito de estudio en el que se engloba y al progreso del estado del arte del sector.

2.1 Contribución del Estudio 1 al modelado y simulación de señales de faltas para la generación de una base de datos

La Figura 2.1 muestra el Test Feeder IEEE 13 bus [22]. Este Test Feeder, es un sistema específico de distribución eléctrica de tamaño reducido que sigue el estándar IEEE 13, utilizado para testar sistemas de distribución. Existen múltiples publicaciones que emplean la red IEEE 13 para desarrollar algoritmos de localización o clasificación de faltas [20]-[23]. Si bien esta red puede ser adecuada para realizar comparaciones de diferentes técnicas o algoritmos, dado que se trata de una red simulada que carece de correspondencia con una red real, las simulaciones no pueden ser verificadas.

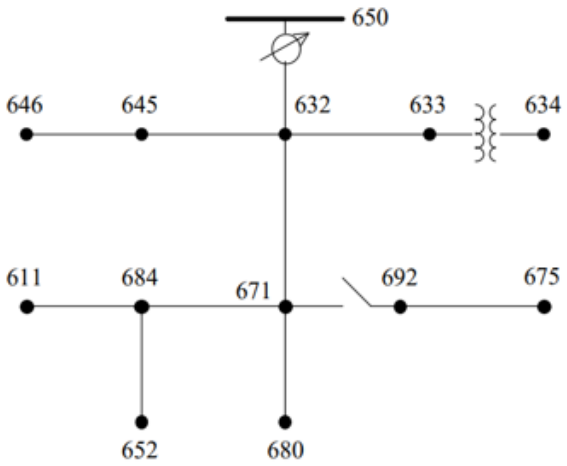

Figura 2.1: Diagrama de línea simple IEEE 13 (13 nodos)

Este primer Estudio de la tesis, describe la metodología para crear un modelo de una red de distribución compleja existente en la realidad y, a partir de ahí, generar una base de datos de señales de faltas mediante simulación. Ambos objetivos se enmarcan en la técnica de la reflectometría de pulsos en el dominio del tiempo (TDR) (Figura2.2). De esta manera, se crea una base de datos a partir de los resultados de simulaciones de una red de distribución real y compleja, modelada mediante el software $PSCAD^{TM}$, los cuales han sido validados con mediciones

obtenidas de un montaje experimental. Esta base de datos se va a compartir con la comunidad científica.

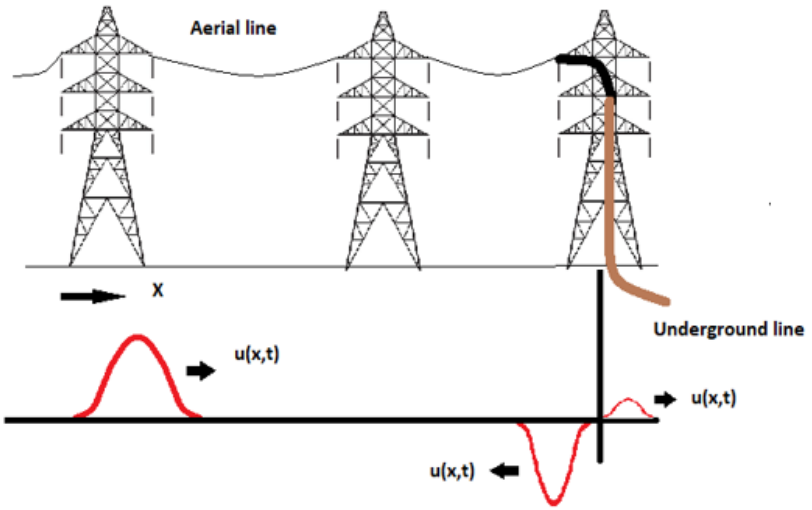

Figura 2.2: Onda incidente, reflejada y transmitida debido al cambio de impedancia en la técnica TDR

Las validaciones experimentales realizadas en laboratorio en un montaje con una bobina de cable de 2.250 m, los acopladores y el inyector, han demostrado que la combinación de la técnica TDR con el modelado de una red real (que incluye tanto el inyector real como el filtro de acoplamiento de la red del prototipo) proporciona señales de alta calidad que son muy similares a las reales.

La Figura 2.3 muestra la metodología seguida en este estudio hasta obtener la base de datos de señales de falta de esta tesis.

Figura 2.3: Diagrama de la metodología seguida

Por lo tanto, basándonos en lo expuesto anteriormente, la contribución de este artículo se sustenta en los siguientes puntos:

- Demostrar la metodología para modelar no solo una red de distribución real, si no también el dispositivo inyector (ya que es el componente central en nuestra línea actual de investigación), y finalmente, el dispositivo de acoplamiento (para proteger y aislar el inyector).

- Simular el estado de la red eléctrica previo a la falta (prefalta) y posterior a la falta, y obtener las señales de respuesta de la red en ambos escenarios.

- Verificar la calidad suficiente de las señales obtenidas para su utilización en el procesado posterior, con el fin de detectar y clasificar faltas en primera instancia y, posteriormente, determinar el Tiempo hasta la Falta (TtoF) como aproximación a la localización de faltas.

- Por último, crear y compartir una base de datos de señales simuladas provenientes de una red real, lista para ser utilizada en futuros estudios por parte de otros investigadores.

2.2 Contribución del Estudio 2 a la ampliación de la base datos de las señales de falta

El uso de redes neuronales (NN) ha demostrado buenos resultados en la detección, clasificación y localización de faltas en líneas de distribución. Durante el proceso de entrenamiento, se presentan ejemplos de señales etiquetadas a la Red Neuronal, que aprende ciertas características para reconocer nuevos ejemplos. Para un entrenamiento adecuado y evitar el sobre entrenamiento (*overfitting*), se requiere, una gran cantidad de ejemplos de entrenamiento.

Sin embargo, en el contexto de líneas de distribución eléctricas y los eventos de faltas, obtener una base de datos extensa de señales reales resulta altamente complejo. Las faltas suelen ser eventos caóticos y catastróficos, como la caída de árboles o los rayos, lo que dificulta su reproducción, predicción, recolección y etiquetado. Si bien se podría modelar la línea de distribución real utilizando software adecuado y simular las faltas, simular esta cantidad necesaria (típicamente decenas de miles) de señales, se convierte en una tarea prácticamente inviable debido a la variedad de causas que generan estos eventos y a la gran cantidad de tiempo de procesado necesario (en nuestro caso, las estimaciones arrojaron alrededor de un año para simular 10.000 señales de falta). Además, seleccionar manualmente todas las posibles situaciones para reproducir los distintos eventos es una tarea casi imposible de realizar.

Frente a estos desafíos, una solución planteada implica aumentar artificialmente la cantidad de ejemplos disponibles a través de la síntesis de las señales simuladas. En el campo de las técnicas de aumento de datos DA, se pueden identificar dos enfoques fundamentales: uno implica añadir versiones ligeramente modificadas de los ejemplos ya existentes, mientras que el otro se basa en la generación de ejemplos sintéticos a partir de los datos previamente disponibles, utilizando para ello Redes Generativas Adversarias (GAN). El primer enfoque se basa en aplicar cambios como rotaciones, simetrías o escalado a los ejemplos existentes. Sin embargo, en el caso de señales temporales, como las utilizadas en este estudio, la aplicación de técnicas clásicas de aumento de datos resulta impredecible y afecta la información contenida en la señal.

Para abordar este desafío, se propone una solución que consiste en obtener una base de datos reducida de señales de gran calidad, simuladas a partir del modelado de una red eléctrica real y, posteriormente, extender esta base de datos mediante el uso de Redes Generativas Adversarias (GAN). Esta técnica simplifica el proceso de obtención de la base de datos de señales de falta.

Las (GAN) (Figura 2.4), son un tipo de sistema de aprendizaje automático descubierto en 2014. En las GAN, dos redes neuronales compiten entre sí: un generador y un discriminador. El generador se entrena para generar nuevos datos con características similares a los datos de entrenamiento existentes, mientras que el discriminador se entrena para distinguir entre datos generados y datos reales. Cuando el discriminador no es capaz de distinguir entre una señal real o generada, el entrenamiento se para y a partir de aquí, se puede utilizar el generador para producir tantos ejemplos sintéticos como se necesiten. Estos ejemplos serán distintos entre si, ya que han sido generados a partir de una señal aleatoria (ruido), pero, contendrán las características "esenciales" del tipo al que pertenecen ya que el GAN, ha sido capaz durante el entrenamiento, de extraer esas características.

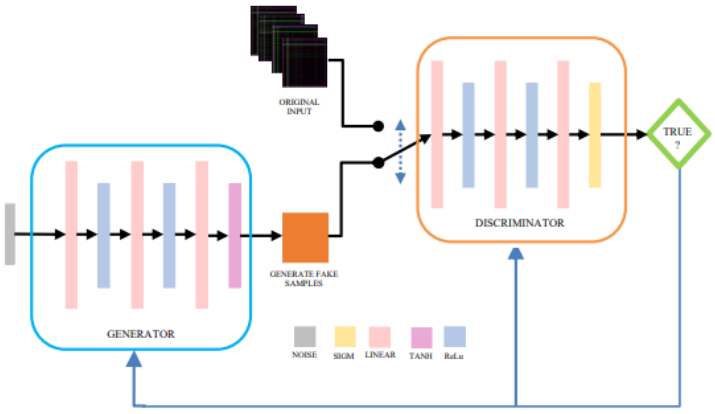

Figura 2.4: Arquitectura de una red neuronal GAN

Las señales temporales originales se transforman en imágenes para facilitar el procesamiento de datos por medio de redes neuronales convolucionales (CNN). La transformación utilizada es el GAF (Gramian Angular Field). En la transformación GAF, la señal temporal se representa en un sistema de coordenadas polares. La

amplitud de la señal se codifica como el coseno angular, y el instante de tiempo como el radio. Esta información se recopila en forma de matriz en la cual se pueden identificar las relaciones entre los diferentes instantes de tiempo. En esta matriz, cada elemento es el coseno de la suma de los ángulos (GASF) o el seno de la diferencia de los ángulos (GADF). La transformación GASF tiene la ventaja sobre la transformación GADF de que la señal de tiempo se puede reconstruir a partir de la imagen. Esta propiedad permite comparar las señales originales con las transformadas (Figura 2.5). En el proceso de transformación de series de tiempo a imágenes, también podemos reducir la dimensionalidad de las imágenes. El algoritmo utilizado se llama PAA (Piecewise Aggregate Approximation). Con PAA, intentamos reducir la dimensionalidad tanto como sea posible para mejorar los procesos de entrenamiento posteriores.

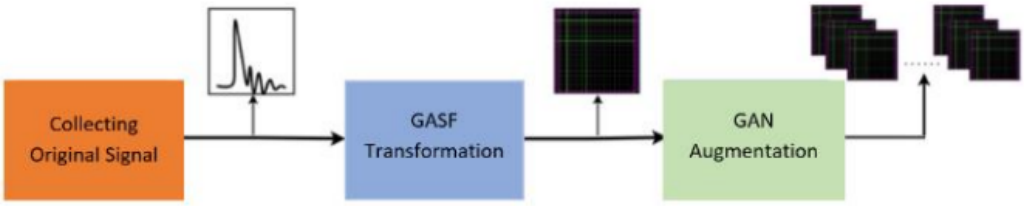

Figura 2.5: Diagrama del proceso de aumento de ejemplos mediante GAN

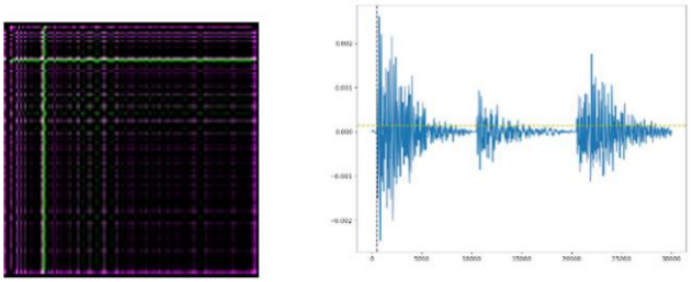

Figura 2.6: Señal transformada (Izda) y señal original (Dcha)

En este caso, hemos procesado las imágenes a partir de su dimensionalidad inicial (4000x4000x3) y las hemos reducido progresivamente a una dimensionalidad

de 128x128x3. Con esta reducción, hemos logrado disminuir el tiempo de entrenamiento de la GAN, así como el procesamiento posterior por parte de las redes neuronales, sin reducir la precisión en la clasificación de las diferentes clases.

En conclusión, la obtención de una base de datos extensa de señales de falta en el contexto de las líneas de distribución es un desafío complejo debido a la naturaleza caótica y catastrófica de estos eventos. La propuesta presentada en este artículo, consiste en combinar el modelo de una red eléctrica real y las simulaciones de las señales de falta, con el uso de (GAN) para generar datos sintéticos adicionales. Esta metodología permite superar las limitaciones de obtener señales reales en cantidades suficientes y simplifica el proceso de obtención de la base de datos de señales de falta. Como ya se ha mencionado, obtener señales reales de faltas suficientes como para entrenar una NN es inviable debido a que son fenómenos naturales y se necesitan típicamente decenas de miles de ejemplos. Simular decenas de miles de ejemplos, supondría alrededor de un año de tiempo de simulación. Por otro lado, con el modelado de esta red real y el entrenamiento de la red GAN para la generación de ejemplos sintéticos, se puede entrenar NN para generalizar a partir de estas señales cualquier otra señal proveniente de otra red eléctrica, ya que se procesa la diferencia entre las señales de falta y prefalta.

2.3 Contribución del Estudio 3 a la detección y clasificación de faltas

La tesis introduce un método innovador para detectar y clasificar defectos en líneas de distribución eléctrica (Figura 2.7). Las señales se transforman en imágenes y tras una reducción de dimensionalidad, se procesan con redes neuronales convolucionales (CNN, por sus siglas en inglés).

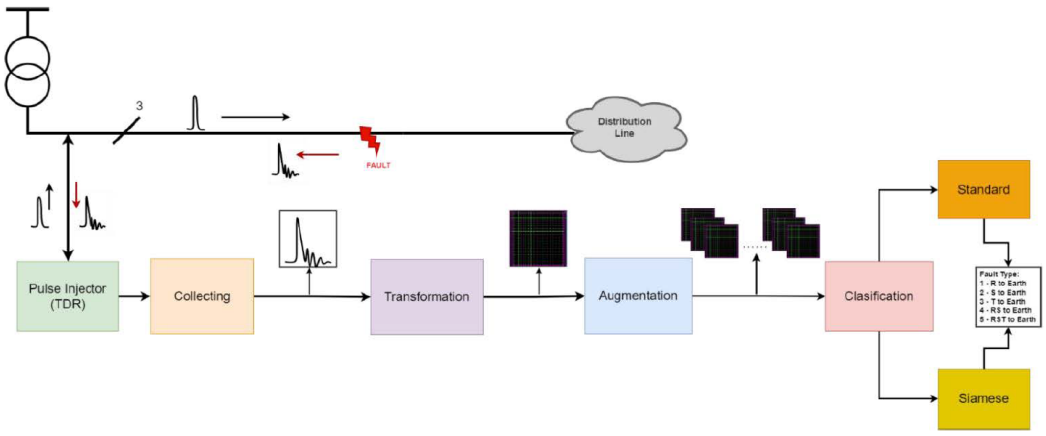

Figura 2.7: Diagrama del proceso de clasificación

El proceso involucra la creación de una base de datos de señales generadas por el software ($PSCAD^{TM}$). Las señales inyectadas se muestrean a 100 Msps y se digitalizan para su entrada en la red neuronal. Luego, se convierten en imágenes utilizando la técnica GASF, que representa las series temporales en coordenadas polares. En la tercera etapa, se amplía la base de datos mediante el uso de GAN. El resultado es una base de datos de 200 señales simuladas convertidas en imágenes GASF para pruebas, y una base de datos de 10.000 señales sintéticas generadas por GAN para el entrenamiento del sistema.

El primer reto a considerar reside en la estrategia de clasificación de los diversas tipos de faltas (Falta entre una de las fases y tierra, entre dos fases y tierra, entre las tres fases y tierra). Dentro del contexto de las redes de distribución de media tensión, cuyos umbrales exceden los 20 kV, se establece como común la presencia de dispositivos de salvaguardia, como los relés de desconexión ante fallos. Estos

dispositivos ostentan la capacidad de emitir una notificación al equipo de protección, induciendo la desconexión de la línea para circunscribir la porción afectada de la red, hasta tanto se logre subsanar el problema. Es de destacar que estos relés monitorizan de manera constante tanto la corriente como la tensión. Tal información asume relevancia fundamental para un equipo que aspira a la localización de la falta en una porción específica tras confirmarse su existencia. No obstante, en las redes de distribución de baja tensión, cuyo umbral es inferior a 1 kV, no es frecuente hallar la presencia de estos relés. En esta coyuntura se concibió el enfoque de clasificar en primer término los tipos de faltas, para emplear dicha clasificación como un método previo a la localización cuando no se cuente con esta información.

Como primer paso, verificamos los resultados obtenidos utilizando NN existentes en el estado del arte. Desde la más simple hasta la más compleja, se utilizaron LeNet, AlexNet y ResNet18 en este trabajo. Con estos clasificadores, los resultados fueron muy pobres. El modelo puede obtener valores de precisión en la clasificación cercanos al 100 % después de algunas pocas épocas, tanto en entrenamiento como en validación (con datos sintéticos). Sin embargo, en la etapa de prueba, con los ejemplos originales, la precisión es baja, lo que significa que el modelo no puede generalizar bien. Esto significa que estos modelos elegidos no pueden aprender a generalizar correctamente cuando se entrenan con una base de datos con una cantidad muy grande de ejemplos sintéticos. Estos resultados concuerdan con lo que se encuentra en la literatura en cuanto a la necesidad de entrenar utilizando un número limitado de ejemplos. Al entrenar estas redes con ejemplos sintéticos, estos modelos solo aprenden los ejemplos de entrenamiento (generados), pero no logran trabajar adecuadamente con muestras originales.

Para intentar obtener mejores resultados se hizo una búsqueda de RRNN que pudieran entrenarse solamente con datos sintéticos. Se encontraron las redes convolucionales Siamesas (SNN). Como se muestra en la Figura 2.8, las Siamesas son redes gemelas que comparten los mismos pesos. En este caso, la característica principal es que pueden entrenarse para aprender un espacio en el que las características de las diferentes clases sean muy cercanas entre sí, gracias al entrenamiento contrastivo. Este es también nuestro escenario, en el que las imágenes GASF de las diferentes faltas son muy similares.

Esto se logró exponiendo la red a un par de observaciones similares y disímiles en cada entrenamiento. Al introducir dos ejemplos del mismo tipo, se tiende a que el entrenamiento de la red minimice la diferencia entre ellos y si se introducen dos ejemplos diferentes, se tiende a que el entrenamiento de la red aumente la diferencia entre ellos. De este modo se consigue entrenar la red para que, al introducir un ejemplo nuevo nunca visto, obtengamos la mayor probabilidad de que se parezca a uno de los tipos mostrados durante el entrenamiento (5 tipos de faltas), haciendo de este modo posible la clasificación del tipo de falta y de manera indirecta, la detección de la falta.

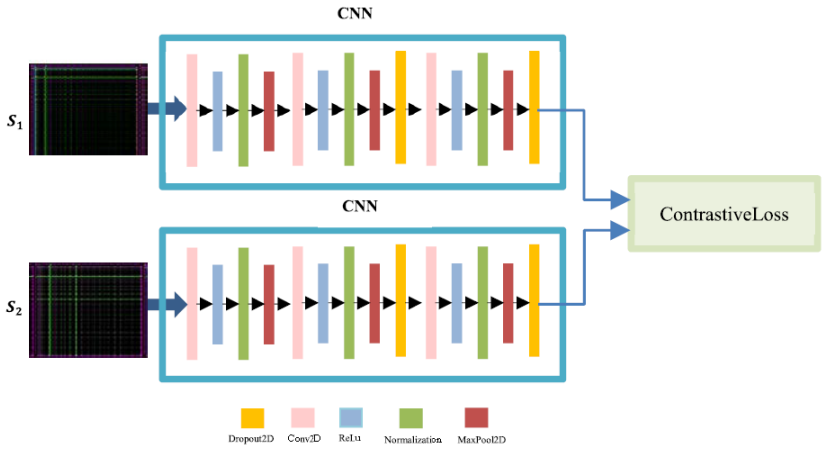

Figura 2.8: Arquitectura de las redes neuronales convolucionales siamesas unidas por la función de perdida Contrastiva

La red minimiza la distancia euclidea entre pares similares y maximiza la distancia entre pares disímiles ($L = pérdida\ Contrastiva$).

En las ecuaciones siguientes, se puede ver que s_1 y s_2 son dos muestras (imágenes GASF), y es un booleano que denota si las dos muestras pertenecen a la misma clase, α y β son dos constantes, y m es el margen.

$$L(s_1; s_2; y) = \alpha(1-y)D^2\omega + \beta y max(0, m - D_\omega)^2 \quad (1)$$

$$D_w = \|f(s_1; w_1) - f(s_2; w_2)\|^2 \quad (2)$$

Basado en lo anterior, la contribución del presente artículo es doble:

- Se ha demostrado que la información del tipo de falta está presente en las señales reflejadas por la red como resultado de los pulsos inyectados (TDR). Se obtuvieron resultados muy buenos al realizar una reducción de dimensionalidad aplicando la técnica PAA. Esto revela que la información del ToF se encuentra en las frecuencias bajas de la señal y se puede prescindir, al menos en este estudio, de las frecuencias más altas.
- Se ha logrado entrenar una red Siamesa (SNN) (con función de perdida Contrastiva) únicamente con ejemplos sintetizados y testearla con ejemplos originales, obteniendo una precisión muy alta. Este nuevo método facilita el entrenamiento de redes neuronales con este tipo de señal, para las cuales hay pocos ejemplos disponibles debido a su naturaleza.

2.4 Contribución del Estudio 4 a la detección del Tiempo hasta la Falta (TtoF)

La localización de faltas en redes de distribución representa un aspecto crucial para lograr el concepto de redes inteligentes dentro de las redes eléctricas. A pesar de la existencia de diversos enfoques para abordar este problema, sigue siendo un tema abierto y desafiante en situaciones reales y, por lo tanto, en redes complejas. En este artículo, proponemos un enfoque novedoso para abordar el problema de extraer información del tiempo a la falta (TtoF) y de manera indirecta de la distancia a la falta (DtoF) a partir de señales de TDR. Nuestro enfoque se basa en el empleo de una red tipo Transformer para la detección de anomalías.

La detección de anomalías no supervisada en series temporales sigue siendo un problema desafiante, especialmente cuando se trata de series temporales que exhiben dinámicas complejas. Si bien algunos métodos anteriores han intentado abordar este desafío a través de representaciones punto a punto o aprendizaje de asociaciones por pares, estos no funcionan bien en este tipo de contextos, en parte debido a la rareza de las anomalías, que dificulta la construcción de asociaciones entre puntos anormales y el resto de la serie. Recientemente, los Transformers han surgido como un enfoque poderoso para modelar estas anomalías en series temporales.

Los sistemas del mundo real a menudo funcionan de manera continua, generando mediciones sucesivas monitorizadas por sensores. En nuestro caso, las mediciones provienen de la respuesta de la red a los pulsos de inyección (TDR). Esas señales son reflexiones sucesivas causadas por cambios de impedancia en toda la red. Detectar cualquier anomalía entre dos señales consecutivas (antes de la falta y después de la falta) se reduce a detectar puntos anormales dentro de las dos series temporales. Sin embargo, las anomalías suelen ser procesos muy raros y están ocultas entre una gran cantidad de puntos normales dentro de la serie temporal.

En el caso de la localización de faltas, obtener etiquetas para la distancia a la falta (el momento en que ocurre la primera anomalía entre ambas series temporales) es muy difícil, ya que los ejemplos reales son eventos caóticos que no se pueden reproducir ni medir fácilmente en el campo debido a su naturaleza. La simulación de estos fenómenos también es compleja, ya que los tiempos de simulación hacen que sea inviable tener un número suficientemente grande de ejemplos para entrenar

un sistema supervisado. Debido a todas estas razones, nos centraremos en detectar anomalías en series temporales bajo la premisa de un entrenamiento no supervisado.

Concretamente, en este estudio, hemos utilizado una arquitectura de red siamesa basada en Transformer (abreviada como $TransSiames$), que está inspirada en el modelo *TranAD*, que incorpora auto-condicionamiento basado en puntuación de enfoque y un proceso de entrenamiento adversario.

Cuando se habla de un Transformer que incorpora auto-condicionamiento basado en puntuación de enfoque, significa que el modelo se entrena para aprender a autogenerar una secuencia de salida a partir de una secuencia de entrada dada. La puntuación de enfoque se refiere a una medida de relevancia o importancia asignada a cada elemento de la secuencia de entrada mientras se genera la salida. En este caso, el modelo utiliza la puntuación de enfoque para enfocarse en partes específicas de la secuencia de entrada y generar una salida que esté condicionada o influenciada por estas partes relevantes. Esto permite al modelo aprender a autoregularse y mejorar la coherencia y relevancia de la salida generada.

El proceso de entrenamiento adversario implica la incorporación de un componente adicional en el entrenamiento del modelo llamado "adversario". El adversario tiene como objetivo mejorar el rendimiento y la capacidad del modelo al desafiarlo con ejemplos difíciles o engañosos. El adversario puede proporcionar retroalimentación negativa al modelo, lo que obliga al modelo a mejorar su capacidad de respuesta y adaptación.

En resumen, un Transformer que incorpora auto-condicionamiento basado en puntuación de enfoque y un proceso de entrenamiento adversario se entrena para generar secuencias de salida coherentes y relevantes, al tiempo que se desafía y se mejora continuamente mediante la retroalimentación adversaria. Esto ayuda al modelo a capturar relaciones a largo plazo en las secuencias y a mejorar su capacidad de respuesta y adaptación en diversas tareas de procesamiento de datos secuenciales.

Este Transformer está basado en una arquitectura siamesa con función de pérdida contrastiva. Esta arquitectura siamesa implica tener dos ramas idénticas de la red, que comparten los mismos pesos y parámetros.

En este caso, el Transformer se utiliza para extraer características y representaciones de las señales de entrada, que son las señales de falta y prefalta de nuestra base de datos. Cada rama del Transformer procesa uno de los datos de entrada y genera una representación de alta dimensionalidad.

La función de pérdida Contrastiva se utiliza para medir la similitud o diferencia entre las representaciones generadas por las dos ramas del Transformer. Esta función penaliza las diferencias entre representaciones de pares de datos que deberían ser similares y recompensa las similitudes entre representaciones de pares de datos que deberían ser diferentes.

El proceso de entrenamiento implica presentar al Transformer pares de datos de entrada junto con etiquetas que indican si los datos son similares o diferentes. El Transformer procesa cada dato de entrada y genera su representación correspondiente. Luego, se calcula la pérdida Contrastiva comparando las representaciones de los pares de datos y ajustando los pesos y parámetros del modelo para minimizar la pérdida.

En la inferencia, el Transformer puede utilizarse para comparar cualquier par de datos nuevos y calcular una medida de similitud o diferencia basada en las representaciones generadas.

En resumen, un Transformer basado en una arquitectura de red siamesa con una función de pérdida Contrastiva se utiliza para extraer características y realizar comparaciones entre pares de datos. Esto permite medir la similitud o diferencia entre los datos y entrenar el modelo para aprender a generar representaciones que capturen adecuadamente las relaciones y características de los datos de entrada. El aprovechamiento de los Transformers resulta altamente ventajoso en escenarios donde los ejemplos etiquetados son escasos, como ocurre en nuestro caso. A continuación, en la Figura 2.9 se muestra la metodología seguida en este artículo y se hace una discusión general del mismo.

En este trabajo, como hemos dicho, utilizamos un modelo Transformer con auto-condicionamiento basado en puntuación de enfoque ($FocusScore$) (Figura 2.10). El Transformer requiere dos entradas, la primera utilizada por el Codificador y la segunda por el Decodificador. El Codificador supervisa la información temporal a corto plazo (Historic Signal, HS), y el Decodificador se encarga de combinar la información histórica con la señal actual en proceso (Signal S). Cabe destacar

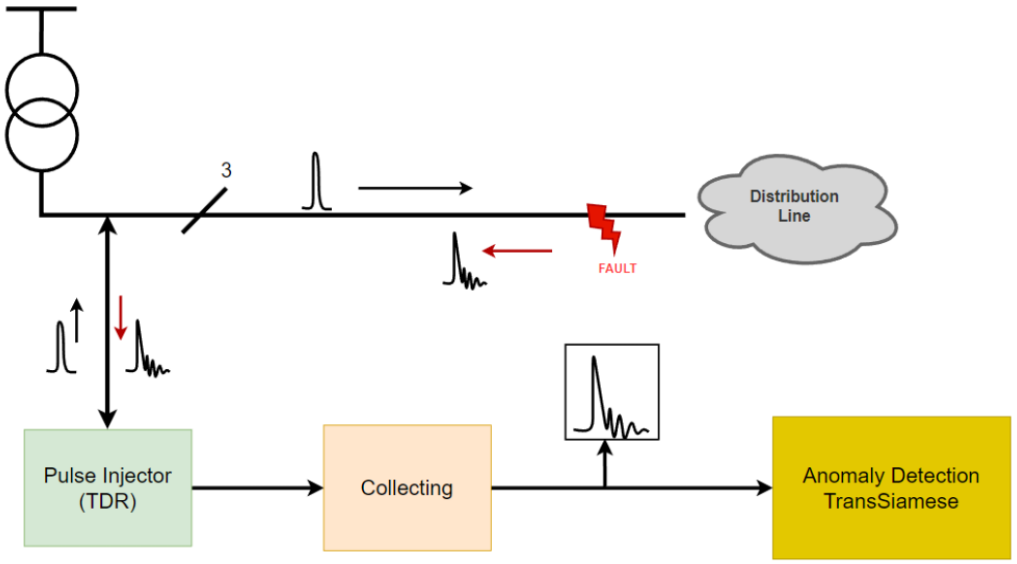

Figura 2.9: Diagrama de la metodología.

que HS se construye uniéndola a las D señales anteriores a la actual (en nuestras pruebas, el parámetro D se estableció en el valor entero de 10, ya que una variación del mismo no causó cambios significativos en el rendimiento del sistema en general). Por lo tanto, en un estado inicial, el historial de la señal HS se concatena con un vector de ceros y se presenta al Codificador para obtener una primera aproximación de la señal de entrada. A continuación, la desviación observada de esta

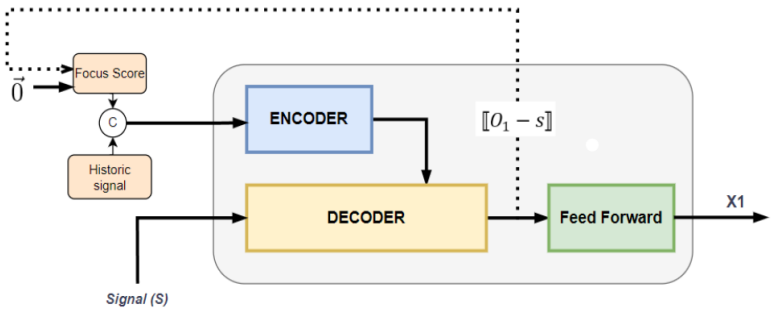

Figura 2.10: Transformer auto-condicionado con puntuación basada en el enfoque

primera reconstrucción, denominada puntuación de enfoque, sirve para facilitar la atención de la red dentro del Codificador del Transformer en una segunda iteración. Este mecanismo de atención se encarga de extraer tendencias temporales al enfo-

carse en secuencias con altas desviaciones. Posteriormente, en esta nueva iteración conocida como auto-condicionamiento (línea de puntos), la puntuación de enfoque derivada de la primera iteración indica las disparidades entre la salida reconstruida y la entrada proporcionada. Esta modificación propuesta tiene como objetivo extraer tendencias temporales a corto plazo, al permitir una mayor activación de la red neuronal para subsecuencias de entrada específicas. Finalmente, la observación O_1 devuelta por el Decodificador en la segunda fase se procesa mediante una única red de retroalimentación ($FeedForward$)(FF por sus siglas en Inglés), a partir de la cual se obtiene la representación de la señal de entrada S (X_1).

La principal característica de la arquitectura $TransSiames$ es su capacidad para capturar y modelar eficientemente relaciones complejas entre pares de secuencias de entrada. Es por eso que se utilizan dos copias idénticas de la arquitectura Transformer, conocidas como "ramas Siamesas". Cada rama toma una pareja diferente de entradas y las procesa de forma independiente. Las representaciones obtenidas de ambas ramas se comparan luego para realizar tareas como comparación de similitud, clasificación de pares o extracción de características. Además, la arquitectura Siamesa permite el aprendizaje conjunto y el intercambio de conocimientos entre las ramas, lo que puede mejorar la eficiencia y generalización del modelo.

En nuestro caso, como se muestra en la Figura 2.11, los dos Transformers (Fase 1 y Fase 2) comparten los mismos pesos en un modelo Siamés único. Este último está diseñado y utilizado teniendo en cuenta las características de nuestros datos. Al final, nuestras anomalías en las señales no ocurren de manera puntual en el tiempo. Ambos tipos de señales (Pre-falta y falta) son muy similares hasta el punto en que ocurre la falta, después de lo cual las señales continúan siendo diferentes. Por lo tanto, necesitamos pensar en una solución que maximice las diferencias en ambos tipos de señales en su conjunto, en lugar de en puntos específicos en el tiempo.

Esta característica surge del uso de la función de pérdida Contrastiva (3). Esta adaptación mejora el proceso de entrenamiento del modelo y contribuye a su rendimiento general. La pérdida Contrastiva tiene como objetivo minimizar la distancia euclidea entre pares de instancias similares (señales de Pre-falta) y, al mismo tiempo, maximizar la distancia entre pares de instancias diferentes (señales de Pre-falta vs. falta).

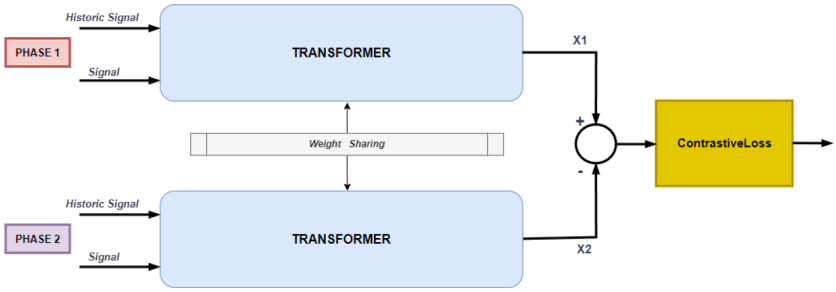

Figura 2.11: Entrenamiento del modelo TransSiames

De esta manera, favorece que el modelo discrimine de manera efectiva entre diferentes clases o categorías. Esto promueve una mejor separación y agrupación de los datos y entrena al Transformer de manera más efectiva para predecir series temporales similares, como faltas y Pre-faltas, y lograr una mejor detección de anomalías. En resumen, el Transformer es capaz de utilizar la pérdida proporcionada por el método contrastivo para resaltar las diferencias después de cada falta. De hecho, es la forma más rápida e intuitiva de querer alejar un patrón de una señal de otro tipo diferente.

Finalmente, en la siguiente ecuación se muestra lo comentado anteriormente en esta sección.

$$L = (1 - y) \cdot \|PF - F'\|^2 + y \cdot (M - \|PF' - F'\|^2) \tag{3}$$

Donde, si y es 1 (clases diferentes), el término de la izquierda desaparece y tratamos de maximizar la distancia entre ejemplos hasta algún límite M. Por otro lado, si y es 0 (clases iguales), el término de la derecha desaparece y tratamos de minimizar la distancia entre ejemplos. Basado en lo anterior, la contribución de este estudio es:

- Proponer un enfoque novedoso basado en Transformers, llamado $TransSiames$, que ha demostrado su capacidad para funcionar como detector de anomalías, e incluso como un enfoque viable y potencial para el problema de la determinación del TtoF y la DtoF.
- Se ha utilizado un esquema de red Siamesa potenciando así las características de este Transformer para resaltar las diferencias mínimas entre dos señales

que se van a comparar (gracias al aprendizaje contrastivo utilizado).

– Con este método, también se ha contribuido a superar el problema inherente de la escasez de ejemplos del mundo real en este tipo de problemas de regresión lineal, donde ni las técnicas de aumento de datos tradicionales ni las basadas en GAN, son factibles debido a la naturaleza de la señal.
– Finalmente, en el modo de inferencia, proponemos una función de puntuación de anomalía basada en energía ponderada, que potencia el rendimiento de la red Siamesa.

2.5 Contribución del Estudio 5 a la verificación de los estudios realizados mediante la instalación de un piloto en una red real

Dentro del proyecto FLEXIGRID, la localización de faltas pretende desarrollar el primer demostrador en una instalación real de un localizador de faltas basado en la técnica ya mencionada de la Inyección de pulsos de alta frecuencia (TDR). En el proyecto se pretende colocar el prototipo (en una primera fase), en una red de Viesgo en la que se producirán faltas con un generador de faltas que se dispondrá a tal efecto. Una vez verificado el funcionamiento correcto y reajustado el algoritmo de localización, se instalará en otra red de la empresa distribuidora VIESGO, donde se producen faltas "naturales" con relativa frecuencia. De este modo se pretende comprobar la precisión en la localización del prototipo desarrollado. Con toda la información recopilada durante el proyecto y los datos de campo se podrá seguir mejorando el sistema de cara a conseguir diseñar un equipo que pueda ser industrializado al menor coste posible. Esquemáticamente, el sistema se puede representar tal como se aprecia en la Figura 2.12.

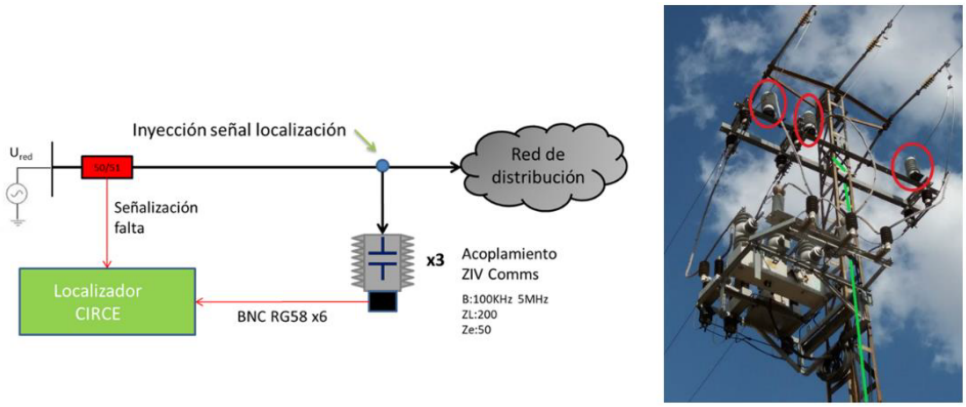

Figura 2.12: Esquema del TDR

El sistema consta del localizador propiamente dicho, el cual genera los pulsos de alta frecuencia que se inyectan en la red y también digitaliza la señal de respuesta de la red para poder ser almacenada y procesada posteriormente. El Localizador se conecta a la red de media tensión (DA) a través de un acoplamiento desarrollado

por la empresa ZIV. Este acoplamiento es en esencia una capacidad y una inductancia que sirve para aislar el localizador de la tensión de red (12kV) al bloquear las bajas frecuencias (50 Hz) de la misma. Asimismo, permite que los pulsos de alta frecuencia generados por el localizador atraviesen el acoplamiento y se inyecten en la red. También se cuenta con un relé de señalización de falta que avisa al localizador cuando se produce una falta. De este modo el localizador sabe cuándo realizar la inyección en falta.

En la Figura 2.13 se aprecia como el sistema comercial utilizado es un CompactRIO de National Instruments, que dispone además de 4 conversores A/D para digitalizar las señales de respuesta de la red, así como 4 canales I/O con el que se generan los pulsos de alta frecuencia para inyectar en la red. Las señales de salida (pulsos) se adaptan en tensión y corriente para poder inyectar la energía necesaria a la red. Esto se consigue mediante una tarjeta electrónica desarrollada *ad-hoc* por CIRCE. Asimismo CIRCE ha desarrollado una tarjeta de adaptación de las señales de respuesta para adaptarlas en nivel de tensión a los requisitos de entrada del conversor A/D. En la Figura 5 se puede apreciar también los acoplamientos aportados por ZIV (uno por cada fase R-S-T) para conectar el localizador a la red.

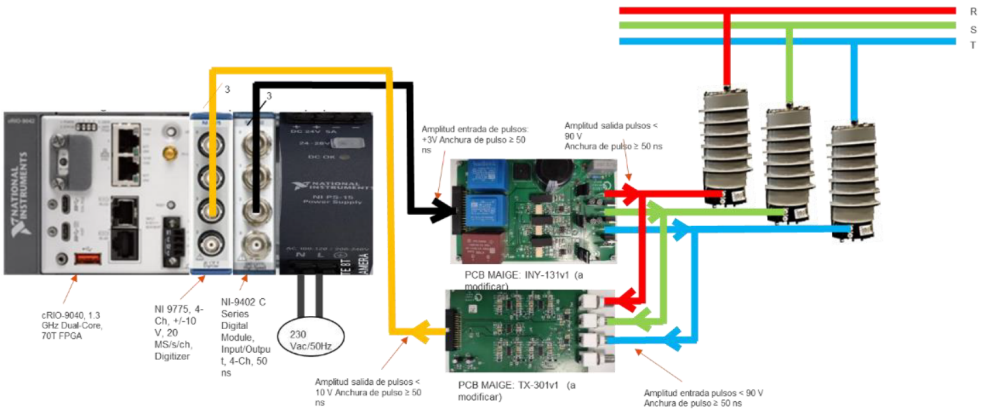

Figura 2.13: Hardware del TDR

Tras su instalación, el prototipo ha estado durante 2 meses funcionando de manera ininterrumpida cumpliendo así uno de los requisitos del proyecto en cuanto a robustez del sistema. Por otro lado, las señales de respuesta de la red real tienen unas características muy similares a las simuladas y sobre todo a las inyectadas

Figura 2.14: Instalación del TDR

en el laboratorio. La siguiente fase del piloto es registrar faltas durante un periodo de tiempo de aproximadamente un año. Con estas señales se pretende verificar los modelos de redes neuronales presentados en estos estudios, así como avanzar en la mejora de los mismos y en el avance de esta línea de investigación.

Capítulo 3

Publicaciones

RESUMEN: En esta sección se muestran las publicaciones que forman parte del compendio de esta tesis.

3.1 Estudio 1: Modeling and Simulation of Time Domain Reflectometry Signals on a Real Network for Use in Fault Classification and Location

RESUMEN: En la actualidad, la clasificación y ubicación de fallas en redes eléctricas es un tema de interés. Las fallas representan un problema debido al tiempo y costos necesarios para detectar, ubicar y repararlas. Para reducir estos tiempos y costos, la clasificación y ubicación automáticas de fallas están ganando relevancia. Este artículo describe una metodología para crear una base de datos y un modelo de una red de distribución compleja utilizando el principio de reflectometría de pulso en el dominio del tiempo (TDR). Esta técnica permite monitorizar grandes distancias con un solo dispositivo. Se utiliza una base de datos creada a partir de simulaciones en el software PSCAD y validada con pruebas experimentales. La combinación del TDR con el modelado de una red real ha demostrado proporcionar señales de alta calidad. El objetivo es utilizar este modelo como base para técnicas de vanguardia y ofrecer una alternativa adaptada a grupos no familiarizados con el mundo eléctrico, pero especializados en el procesamiento de datos.

IEEE Access
Multidisciplinary ⋮ Rapid Review ⋮ Open Access Journal

Received 17 February 2023, accepted 5 March 2023, date of publication 6 March 2023, date of current version 13 March 2023.

Digital Object Identifier 10.1109/ACCESS.2023.3253772

RESEARCH ARTICLE

Modeling and Simulation of Time Domain Reflectometry Signals on a Real Network for Use in Fault Classification and Location

JAVIER GRANADO FORNÁS[1], ELÍAS HERRERO JARABA[2], (Member, IEEE), HANS BLUDSZUWEIT[1], DAVID CERVERO GARCÍA[1], AND ANDRÉS LLOMBART ESTOPIÑAN[1], (Member, IEEE)

[1]CIRCE Foundation Parque Empresarial Dinamiza, 50018 Zaragoza, Spain
[2]Department of Electronic Engineering and Communications, University of Zaragoza, 50018 Zaragoza, Spain

Corresponding author: Javier Granado Fornás (jgranado@fcirce.es)

This work was supported by the FLEXIGRID Project from the European Union's Horizon 2020 Research and Innovation Programme under Agreement No 864579.

ABSTRACT Today, the classification and location of faults in electrical networks remains a topic of great interest. Faults are a major issue, mainly due to the time spent to detect, locate, and repair the cause of the fault. To reduce time and associated costs, automatic fault classification and location is gaining great interest. State-of-the-art techniques to classify and locate faults are mainly based on line-impedance measurements or the detection of the traveling wave produced by the event caused by the fault itself. In contrast, this paper describes the methodology for creating a database and a model for a complex distribution network. Both objectives are covered under the paradigm of the time-domain pulse reflectometry (TDR) principle. By using this technique, large distances can be monitored on a line with a single device. Thus, in this way a database is shared and created from the results of simulations of a real and complex distribution network modeled in the PSCAD^{TM} software, which have been validated with measurements from an experimental test setup. Experimental validations have shown that the combination of the TDR technique with the modeling of a real network (including the real injector and the network coupling filter from the prototype) provides high-quality signals that are very similar and reliable to the real ones. In this sense, it is intended firstly that this model and its corresponding data will serve as a basis for further processing by any of the existing state-of-the-art techniques. And secondly, to become a valid alternative to the already well-known Test Feeders but adapted to work groups not used to the electrical world but to the environment of pure data processing.

INDEX TERMS Fault classification, fault location, transmission lines, time-domain pulse reflectometry, modelling networks, distribution networks.

I. INTRODUCTION

From a maintenance cost point of view, distribution system operators (DSOs) are specially concerned with reducing outage times. In a collateral way, from a commercial point of view, an indeterminate number of clients lose their power supply during these periods, and some power stations (specially distributed generation, DG) may also be affected thereby. Therefore, the location of electrical faults in distribution networks and their identification are an effective method to reduce the duration of downtime, considering that most outages are caused by faults in the distribution network [1], [2], [3]. When maintenance crews can find the problem faster due to location and identification techniques, the fault can be fixed earlier and therefore the user experience is greatly improved.

On the other hand, fault location techniques are widely used in transmission systems where each line is monitored separately. But distribution networks in real environments usually have a radial, ring, or mesh topology, with many

The associate editor coordinating the review of this manuscript and approving it for publication was Yizhang Jiang.

nodes and branches [4], [5], [6], [7], [8]. Therefore, location methods need a different approach to obtain a cost-effective system that can monitor the entire grid or an important section of it.

Additionally, it is also important to consider other specific characteristics of distribution systems, such as the presence of unbalanced loads, laterals, and different types of cables/conductors. These features affect several assumptions of location methods, reducing their performance.

It is worth mentioning a couple of significant cases: 1) IT (Isolé-Terre) networks, which are common in distribution systems. In which, location is more challenging [9] since classical impedance-based methods have substantial errors. And 2), low voltage (LV) distribution grids, which especially lack studies of fault location techniques [10]. These last networks have two important differences regarding high- and medium-voltage grids:

- Underground lines are commonly made up of unshielded wires.
- The system end points are the customer loads, so there is a variability in their impedance value.

For example, series faults [11] are caused by broken wires and increase the impedance of the affected lines. Or shunt faults [12] consisting of a contact among one phase and the ground and/or other phase/s. Distribution networks suffer mainly from shunt faults [13] and, in turn, can be classified considering the number of faulty phases and the involvement of the ground:

- Single line to ground.
- Double line.
- Double line to ground.
- Three phases.
- Three-phase to ground.

Each kind of fault causes different electrical responses and may produce less or more hazardous effects. Thus, a complete fault diagnosis method should be able to resolve not only the location of the fault point but also the kind of fault found in the distribution network [14].

In conclusion, more research is needed to find more suitable fault location techniques adapted to the special characteristics of real distribution networks, and on the other hand, more realistic scenarios and data must be created and shared. In this sense, the complexity of these scenarios must be accompanied by a comprehensive set of data where several electrical faults can be found.

So, based on the above, the contribution of the present paper is built over the next points:

1) To demonstrate the methodology to model not only a real distribution network but also the injector device (as it is the central device in our current line of research), and finally, the coupling device (to protect and isolate the injector).
2) Simulate the pre-fault and fault state of the network and obtain the network response signals.
3) Certify the sufficient quality of signals obtained to be used in post-processing to detect, locate, and classify faults.
4) And finally, creating and sharing a database of simulated signals from a real network ready to be used for future studies and by many other researchers.

II. ENVIRONMENT

Today, electrification has become one of the paradigms of our society. The technological progress that humanity is undergoing generates an unprecedented dependence on electricity.

In this context, distribution networks play a fundamental role, as a service failure can have catastrophic consequences. Examples include the dependence of telecommunications, aviation, the medical industry (which is becoming more and more technologically advanced), the arms industry and, of course, the dependence of today's society on artificial lighting.

As already mentioned, the physical principle used in this work is the TDR [15], [16]. This technique was first used in 1952 by the Japanese company Tohoku, which designed a TDR-based locator (D type - by pulse injection) for a 154 kV power grid [17].

The injected pulses propagate through the network, bounces (at each impedance change) and returns to the locator, bringing information about the state of the network.

In our case, it basically consists of performing periodic injections of pulses into the line in each of the phases of the network (R-S-T). In this way, the electrical response of the network is always updated and data-ready for further faults since if a new fault occurs, the response signal is different from the signal received when the network was operating normally.

This reflection of the pulses makes it possible to record at the injection point all the signals that ''come back'' after ''bouncing'' through the different bifurcations of the network. These signals are digitized in the injector itself so that they can be further processed.

With this method, the network responses are obtained before and just after a fault occurs. Periodic injection during normal network operation provides a ''snapshot'' of the updated network status. When the fault occurs, it is injected once more to obtain the response of the network in the fault state.

So, with the perspective of what has been said so far, we address the task of modelling a real complex distribution network in order to, subsequently, by means of simulation, be able to generate network response signals to the pulses injected into the network.

With these data, a representative database [18](which is provided for other groups to investigate with) is obtained to be further processed with different fault location algorithms [19]

In the TDR technique, high-frequency pulses are injected into the network. To do that and receive the response from the network, we use an injector and coupler devices [19].

Injectors are basically voltage sources whose output can be switched for a certain time to obtain the required pulse width.

Between the injector and the network, the coupler is placed. The coupler is basically a filter that lets high-frequency pulses through in one direction and blocks the low-frequency (50 Hz) of the mains in the other direction [21], [22].

In this work, we have modelled the injector and the real coupler used in the prototype installed in the field.

We have used PSCAD^{TM} software to model the real electrical network selected. PSCAD^{TM} is a general-purpose tool to address design and simulation tasks in the areas of power electronics, power quality analysis, protections, and electrical system planning studies.

There are other software tools that are also useful for this purpose, such as DIgSILENT^{TM}-PowerFactory^{TM}, Matlab^{TM}-Simulink^{TM}. PSCAD^{TM} has been used in the research group for years, and it was decided to use this experience in the modelling of the network of this work.

In addition to modelling a complex real network, this work has the advantage of having a prototype injector placed in it. This fact will allow us to obtain a signal database that can be used in the future to compare and validate the signals obtained by simulation.

It will also allow for validating algorithms that are developed based on the signals obtained by simulation and that can be tested with real faults occurring in the network to validate its correct operation.

III. STATE OF THE ART

Due to the nature of this article, the state of the art has been broken down into three main sections. The first section discusses the need to create more realistic environments that bring future theoretical studies closer to the real existing problems. Therefore, a change of scenario from IEEE 13 simulations to a real network is shown. However, since our data and research are deeply linked to the TDR principle, previous work related to injectors and couplers will be discussed. Finally, since our joint aim is to provide a basis for experimentation in the task of locating and classifying electrical faults, we will review the main methods used to date.

A. CHANGE OF SCENARIO: FROM BENCHMARK TEST FEEDERS TO REAL NETWORK MODELING

The IEEE 13 bus feeder [22] is a small system that is used to test distribution systems. It operates at 4.16kV, using just one source, a sin regulator, a number of short unbalanced transmission lines, and finally, shunt capacitors. Fig. 1 shows the one-line diagram of the test system.

There are multiple publications that use the IEEE 13 network to develop fault location or classification algorithms [20], [21], [22], [23]

This network may be suitable for making comparisons of different techniques or algorithms, but since it is a simulated network that does not have some correspondence with a real network, the simulations cannot be verified.

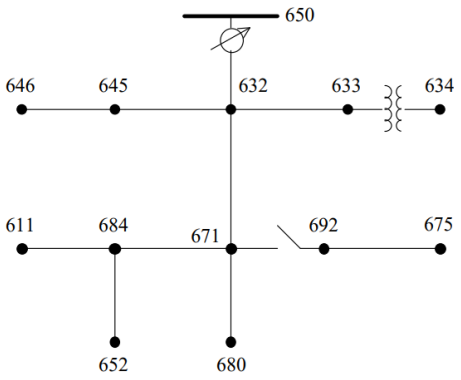

FIGURE 1. One line diagram of the IEEE 13 bus power system.

It is a very useful network for theoretical studies, where a more complex network would make it difficult to obtain clear and concise results. Frequency domain studies for harmonic minimization [24] stub line compensation [25] or studies with unbalanced loads [29]

There is a paper where the history and evolution of Test Feeders used since the 1990s is faithfully summarized [26]. Briefly, we highlight the original Test Feeder that was created in 1991, where transformers of various configurations, three-phase lines, and unbalanced loads were represented. In 1992 other models were presented at the 2000 PES Summer Meeting that were intended to become experimental platforms for unbalanced three-phase radial systems. The 13-bus Feeder [30] discussed above was published at this time along with others such as the 34-bus Feeder [30] the 37-bus Feeder [27] or the 123-bus Feeder [30]

It was not until 2010 that the 8500-Node Test Feeder was published, which aimed to scale these models to larger problems with 2500 primary buses, 4800 in total including secondary buses and loads, with a total of 8500 nodes.

In the same year, the Neutral-Earth-Voltage (NEV) Test Feeder was presented with the intention of representing very detailed models of a distribution system. It was based on a real system and contains, among other things, a line segment with 4 circuits sharing a common neutral.

For further details and study, the reader is recommended to refer to [27]

B. TDR TECHNIQUE

This work has relied heavily on the TDR technique when studying and modelling the power grid, so we see fit to review the state of the art of it by presenting works in different fields.

As stated, this technique was first used in 1952 by the Japanese company Tohoku [19]. This was the first time that an attempt was made to locate a fault in the power grid by periodic pulse injection.

In the state of the art, we find other references of TDR applied to power line fault location. In these cases, the use of this physical principle (TDR) is accompanied by another

part of the signal processing obtained through the response to these pulses. Typically, this processing consists of algorithms based on artificial intelligence [28], [29].

Also, within this same field, multiple faults have been attempted simultaneously relying on the use of this technique [30]. More recently, in the literature we can find references to the use of the TDR technique versus FDR (Frequency Domain Reflectometry), not only for the localization of faults in power lines but also in antenna cables. [31].

The popularity of this technique has led to its use in demanding fields such as automotive [32] or aviation [33], where it has been shown to increase safety in the use of these transport systems by monitoring their electrical systems.

We can even find uses for this technique in the rail sector applied to the detection of faults in railway electrical systems. For example, in [34]. The design of a portable device that uses TDR to detect short circuits or open circuits in train data cables is presented.

Even in electronic design, in [35] an analytical method is developed to check and correct the impedance based on TDR in the lines, of application in the development of printed circuit boards (PCBs).

C. LOCALIZATION AND CLASSIFICATION TECHNIQUES

Multiple techniques have been proposed to address the fault location problem. However, all methods can be grouped in three main categories: impedance measurement, travelling waves, and artificial intelligence.

1) IMPEDANCE MEASUREMENT

This methodology consists of measuring the apparent impedance at the rated frequency from a single point within the electrical network. The impedance measurement changes between a healthy and a faulty line. Moreover, the impedance variation is related to the fault distance. Therefore, if the apparent impedance is monitored during a fault occurrence, it is possible to determine the location of the fault.

The main advantage of this method is to work with steady-state values. Thus, the required acquisition device can be relatively inexpensive and simple. However, distribution networks have inherent characteristics that introduce substantial errors in this technique [9], [36], [37]:

- Nonuniformity of the lines.
- High-impedance faults, especially in IT grids.
- Radial topology leading to the multipoint location problem.
- Unbalanced loads among phases.

Furthermore, the presence of distributed generation becomes more challenging using impedance-based methods [38]. Consequently, this methodology does not seem to be the most suitable solution for location in the new paradigm of power distribution networks.

2) TRAVELLING WAVES

The well-known propagation of electromagnetic waves through transmission lines is the basis of this location method. Mainly, telegraph equations describe this phenomenon, where two important properties allow locating faults in power systems:

- Waves travel at a certain speed depending on the properties of the wire.
- Any impedance change along the line produces a partial reflection of the electromagnetic waves.

There are two main approaches to this technique:

- Measurement of the transient signal produced by the fault. This approach is widely used in transmission systems [39] where lines are monitored separately. However, in distribution networks, those transient waves experience multiple reflections due to the topology. Therefore, the signal intensity may be too low when it arrives at the locator, making it difficult to locate the origin of the fault. Many alternatives have been proposed to solve this challenge [8], [13], [37], [40], [41], [42], [43]. On the one hand, some of them require the installation of many complex and synchronised devices, thus the solution is not cost-effective. On the other hand, the single-device approaches rely on either complex mathematical transformation or grid simulations. Both solutions require offline calculation, and the latter is model-dependent.
- Injecting a high-frequency signal and measuring the reflected wavefronts. This technique is commonly named TDR. However, distribution networks have many forks where the travelling wave is reflected, hence the electrical response of the grid is complex. Several solutions [41], [42], [43] have been proposed to overcome this problem, but all require difficult boundary conditions or have not been proven to solve the problem in a real network yet.

In summary, TDR has shown good results in distribution systems, both in medium voltage (MV) and LV networks [43], but further research is needed in order to obtain a generalised and cost-effective method.

3) ARTIFICIAL INTELLIGENCE

There are several approaches within this discipline. Regarding fuzzy logic, it is still not clear what number of fuzzy functions are necessary to define the problem. Genetic algorithms introduce unacceptable uncertainties considering this application. While support vector machines and artificial neural networks seem to fit for fault location. Thus, many works can be found about applying these two methods to locate or classify faults in distribution networks, usually combined with other techniques [13], [20], [44].

However, these approaches always have the same problem: it is difficult to achieve an adequate database to train the algorithms due to the needed amount of data and the lack of measured waveforms from faulty lines. Therefore, nowadays each training is based on simulations and every proposed method strongly relies upon the grid model, requiring a retraining when any characteristic of the electrical grid changes [2], [10]. Furthermore, further investigations are

needed to increase the precision of these methods in fault location [44].

IV. THEORY

A. TELEGRAPHER'S EQUATIONS

For the study of transmission lines, the model used consists of a temporal discretization of the lines, that is, an infinitesimal analysis of the line is performed to understand the temporal and spatial evolution of both voltage and current.

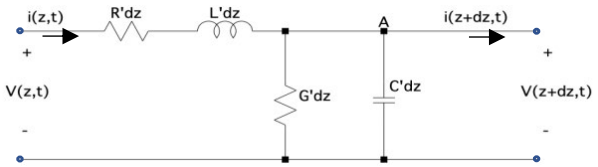

FIGURE 2. Infinitesimal portion of a transmission line.

For this purpose, the line is modelled as shown in Fig. 2, and the differential equations obtained are called the telegrapher's equations (the complete process of this model can be studied in [45].

$$\frac{\partial i\,(z,\,t)}{\partial z} + G' \cdot v\,(z,\,t) + C' \cdot \frac{\partial v\,(z,\,t)}{\partial t} = 0 \qquad (1)$$

$$\frac{\partial v\,(z,\,t)}{\partial z} + R' \cdot i\,(z,\,t) + L' \cdot \frac{\partial i\,(z,\,t)}{\partial t} = 0 \qquad (2)$$

The most general solution to the above equations for voltage and current is as follows:

$$v\,(z,\,t) = V^{+} \cdot e^{(jwt-\gamma z)} + V^{-} \cdot e^{(jwt+\gamma z)} \qquad (3)$$

$$i\,(z,\,t) = I^{+} \cdot e^{(jwt-\gamma z)} + I^{-} \cdot e^{(jwt+\gamma z)} \qquad (4)$$

where V^{+}, V^{-}, I^{+}, and I^{-} represent the amplitudes of the corresponding waves.

Equations (3) and (4) show that at any point on the transmission line, z, and at any instant, t, the measured voltage and current are the sum of the values of the two corresponding waves (progressive and regressive).

Thus, all the points on the transmission line experience the same variation as a function of time, the factor $j\omega t$, but with a delay due to the position, the factor γz, which will be greater the greater the distance from the origin on the z-axis. For more details, please refer to the corresponding theoretical content in [46]

B. MORPHOLOGY AND CONFIGURATION OF INJECTED SIGNALS

Taking advantage of the behavior showed in the previous section, in which the nature of the emission of a signal on a transmission line produces a return signal, we can use the latter as a "tracking" signal in search of possible disturbances in the distribution network.

In this way, electrical pulses (24 V) will be injected into the network itself, giving us updated information on the status of the network. In other words, a pulse sent to the grid in its normal state will return a series of different return signals than those that would be received when the pulse is sent when the grid is at fault.

The state of the distribution network prior to the time of the fault (with the network in its normal state) will be called the *pre-fault state*. And consequently, we will call it the *fault state* to the state of the network once the fault has occurred.

In other works, such as [44], pulses are proposed into the grid at zero crossings of the grid voltage waveform. Therefore, this imposes important restrictions on the number of pulses to be injected, mainly because the time available to inject the pulses is limited to the interval between the detection of the fault and the subsequent opening of the line breaker.

In our approach, we suppress the dependence of the injection on zero crossings and allow them to be generated at any time.

The parameters used in the implementation proposed in this article are the following:

Sampling frequency: The proposed three-phase prototype, having no limitation on the number of pulses to be injected, reconstructs the system response from the injection of four pulses, which allows one to obtain a reconstructed signal with a frequency of 100 MHz.

Injected pulse width: There is a blind zone, defined as the distance below which the proposed system is unable to locate any faults accurately. During this period of time, the system is unable to detect any disturbances or changes occurring in the power grid, which corresponds to the blind zone of the system. Therefore, to reduce the blind zone, the width of the injected pulse was reduced to 10 ns.

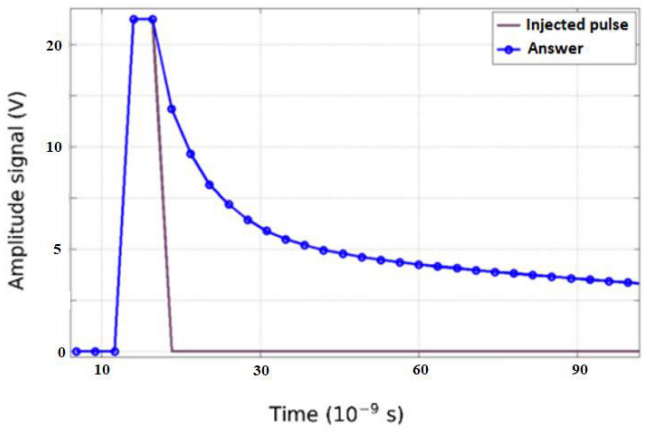

FIGURE 3. Pulse width 10 ns and response to that pulse (sampling frequency 100 MHz).

Fig. 3 shows a pulse width of 10 ns, sampled at a frequency of 100 MHz. It shows how the system response diverges at sample n=2 (taking n=0 as the instant where the pulse starts). The blind zone is calculated from the sampling frequency of the equipment (fs) and the propagation velocity of the pulse

on the line (v) according to:

$$d = n \cdot \frac{v}{2 \cdot f_s} \tag{5}$$

where n is the number of samples where the response diverges.

Therefore, consider a pulse propagation velocity of $1,65 \cdot 10^8$ m/s, and at the sampling frequency of 100 MHz, the blind zone for such a pulse is 1,65 m. However, for a pulse width of 2.5 ns, and taking the same sampling frequency and propagation speed, the first variation in the response will be seen in sample n=5, which is equivalent to 4,125 m of blind zone.

Equipment input impedance: An important addition that has been considered in our approach is the modification of the input impedance of the system. This prevents the reflected pulse from being reflected at the system connection point. In addition, to achieve a greater range when detecting or locating faults, a high impedance has been set at the input of the system.

C. NETWORK RESPONSE TO INJECTED SIGNALS

At the moment when the waveform appears, a voltage originates at the power line input, the propagation of which continues until a point of discontinuity is reached, where a change of characteristic impedance occurs, as shown in Fig. 4.

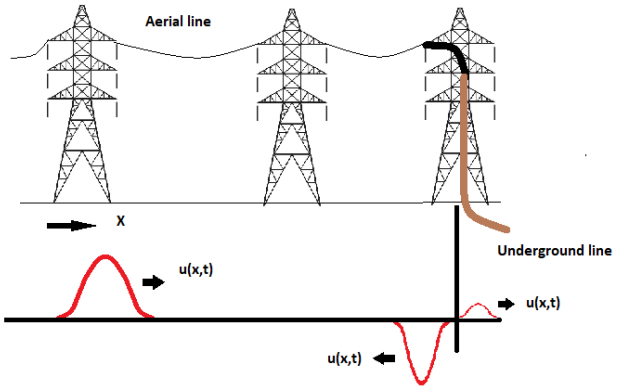

FIGURE 4. Incident, reflected, and transmitted waves at a discontinuity due to a change in impedance.

Through the characteristic impedance line Z_{0L} of the diagram in Fig. 4 an incident voltage wave u^+, and hence a current wave given by:

$$i^+(x,t) = \frac{u^+(x,t)}{Z_{0L}} \tag{6}$$

When u^+ reaches the point of discontinuity, a reflected wave u^- originates and propagates to the left, superimposing itself on the incident wave. Also, part of the incident wave is transmitted into the new medium, giving rise to a wave u^t. The continuity of the electric potential is complied with:

$$u^+(x,t) + u^-(x,t) = u^t(x,t) \tag{7}$$

Similarly, the continuity condition for the current is fulfilled at the point of discontinuity:

$$i^+(x,t) + i^-(x,t) = i^t(x,t) \tag{8}$$

Therefore:

$$\frac{u^+(x,t)}{Z_{0L}} - \frac{u^-(x,t)}{Z_{0L}} = \frac{u^t(x,t)}{Z_{0C}} \tag{9}$$

We can therefore define the reflection coefficient at the point of discontinuity as follows.

$$\zeta = \frac{u^-(x,t)}{u^+(x,t)} = \frac{Z_{0C} - Z_{0L}}{Z_{0C} + Z_{0L}} \tag{10}$$

In a zero-loss power line, these characteristic impedances do not depend on the frequency, and therefore, after transformation to the frequency domain, the reflection coefficient remains the same.

On the other hand, it follows from (10) that when the impedances of both power lines are equal, $\zeta = 0$, i.e., there is no reflected wave, and the lines are said to be matched. In the case of a short-circuit in the line, the impedance Z_{0C} can be considered as 0, so $\zeta = -1$, or in other words, $u^-(x,t) = -u^+(x,t)$, i.e. at the point where the short-circuit has occurred the entire incident wave is reflected. In the same way, it follows that, in the case of an open line $Z_{oc} = \infty$, the reflection coefficient is equal to unity, the reflected wave being twice the incident wave.

To derive equation (10), the load impedance or the characteristic impedance Z_{0C} has been considered purely resistive. However, when this impedance is reactive, the reflection coefficient in the time domain becomes a function of time and, therefore, the reflected wave $u^-(x,t)$ is defined as the convolution product between the incident wave $u^+(x,t)$ and the reflection coefficient $\zeta(x,t)$:

$$u^-(x,t) = u^+(x,t) * \zeta(x,t) \tag{11}$$

Finally, another parameter to consider would be the transmission coefficient τ, which would be defined as the relationship between transmitted and reflected waves:

$$\tau = \frac{u^t(x,t)}{u^+(x,t)} = \frac{2 \cdot Z_{0C}}{Z_{0C} + Z_{0L}} \tag{12}$$

Whose relationship with the reflection coefficient would be:

$$\tau = 1 + \zeta \tag{13}$$

V. METHODOLOGY

This section describes the methodology used to obtain response signals from an electrical network using the TDR principle. We will start by explaining our proposed system from the basic building elements (which need to be modelled accordingly), continue with the modelling of the electrical network itself, and finally, the relevant simulation process will be explained. Therefore, the following three sections will be explained in detail:

- Blocks modeling.
- Network modeling.
- Simulation process.

FIGURE 5. Methodology block diagram.

A. BLOCKS MODELING

This first section describes the basic blocks modelled (Fig. 5). It contains a generic connection to the grid, cables, loads, filters, and the pulse injector.

1) GRID CONNECTION MODEL

The system includes the CT (transformer) connection and also the MV connection, modeled with an ideal source and an R-L impedance that reflects both the Scc and the R/X ratio of the network upstream of the transformer.

Scc is the short-circuit power of the upstream MV network without CT, from which the LV model hangs and where pulses are injected.

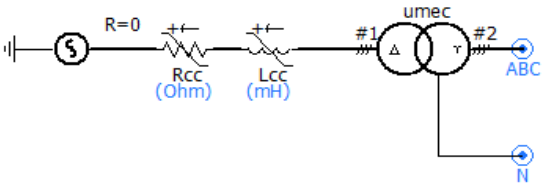

FIGURE 6. Change in impedance.

The LV network grid connection has been modelled with an adjustable RL-based equivalent load together with a transformer, as shown in Fig. 6.

The parameters of the model are:

- Short-circuit power (MVA): 20
- X/R ratio: 10
- High voltage (kV): 15
- Low voltage (kV): 0.4
- Transformer power (MVA): 0.5

The RL equivalent parameters Rcc and Lcc are calculated from the short-circuit power and the X/R ratio.

Several tests have been carried out to evaluate the impact of a variation of the R-L equivalent of the upstream MV network. The system response was tested for values of Scc = 5, 10 and 20 MVA and X/R = 10, 5 and 1. For all combinations, almost identical results were observed. Only the nominal power of the LV transformer has been found to be relevant only for the short-circuit transient, which is attenuated less with a 50 kVA transformer than with 500 kVA. Therefore, typical values have been chosen for the experiment setup.

2) LOAD MODELS

Loads are very critical in a LV network configuration, as they behave similar to faults. Load variations will cause different reflection pattern, which means that the obtained reflected signal will be very noisy. In this sense, four different load models have been implemented:

- No load (1 GΩ).
- Single-phase load.
- Symmetric 3-phase load.
- Asymmetric 3-phase load (several single-phase loads on the same bus).

The loads in the model have been derived from historical data from the active and reactive power smart meters. Average values have been converted to R and L, assuming nominal voltage. 3-phase meters were implemented as symmetric 3-phase loads. Single-phase meters are modeled as such, but on occasions, several clients are connected to the same bus. In this case, all loads are aggregated and modeled as an unbalanced 3-phase load.

3) CABLE MODELS

The grid model contains detailed models of the cables, including five different types. In LV networks, cables are not shielded, which means that HF signals travel partly outside the insulator and may have some interference with neighboring conductors. This is a fundamental difference compared to medium voltage (MV) networks, where cables are typically shielded. Geometrical cable parameters are the following:

- Number of conductors
- Conductor radius
- Insulator radius (measured from conductor center)
- Conductor distance from ground
- Conductor distances relative to each other
- Cable type: aerial or underground

All cables are considered to have 4 conductors, where the neutral wire may have a different diameter.

Apart from the geometric parameters, the frequency-dependent model has another set of parameters. The adopted values shown in table 1 have been adjusted during model

TABLE 1. Options of the frequency-dependent cable model.

Model option	Value
Travel Time Interpolation	On
Curve Fitting Starting Frequency	0.1 Hz
Curve Fitting End Frequency	1 GHz
Total Number of Frequency increments	500
Maximum Order of Fitting for Yc	20
Maximum Fitting Error for Yc	0.1 %
Max. Order per Delay Grp. for Prop. Func.	20
Maximum Fitting Error for Prop. Func.	0.1 %
DC correction	Functional Form
Passivity Checking	Disabled

testing. The fitting accuracy needed to be increased compared to the default values, in order to avoid numerical oscillations. Namely, starting frequency was reduced from 0.5 Hz to 0.1 Hz and end frequency increased from 1 MHz to 1 GHz. Frequency increments were increased from 100 to 500 and fitting errors were reduced from 0.2% to 0.1%. Finally, DC correction was modified from "Disabled" to "Functional Form".

4) PULSE INJECTOR DEVICE MODEL

The injector device mainly consists of an HF pulse generator and data acquisition with very high time resolution, which permits registration of oscillations in the nanosecond range. The pulse is created by a switch and triggered by a pulse controller. The pulse amplitude was fixed at 24 V.

Within the simulation, this controller generates one trigger before the fault event, creating the reference response, and another one after the fault event. It may be mentioned here that one trigger event consists of three triggers (one for each phase), with a time delay of 0.5 ms between them. This time delay is necessary to obtain the necessary attenuation of the pulse response, because oscillations are induced in all 3 phases.

For the pulse generator, two different options were implemented, to study the differences in response. One option was a sinusoidal signal of one period, and the other one was a rectangular pulse of half-period duration. With a pulse frequency of 1 MHz, this means that the pulse has a duration of 500 ns.

Simulation tests revealed that an ideal rectangular pulse was not suitable. Due to the detailed time-domain model, infinite ramps create singularities, and the model did not converge. Therefore, a more realistic pulse was implemented where the switch is modelled as a controllable resistance with a defined pulse.

"on" resistance (R_{on} fixed at 10 mΩ) and "off" resistance R_{off}. A ramp rate defines how fast the transition between Ron and R_{off} will occur. In the model (Fig. 7), this realistic switch model received two parameters:

- R_{off}: 1 MΩ ("off" resistance of the switch)
- ramp rate (200 ns from low to high)

These two parameters have been adjusted together with the network filter (see next section), in order to minimize oscillations induced by the switch.

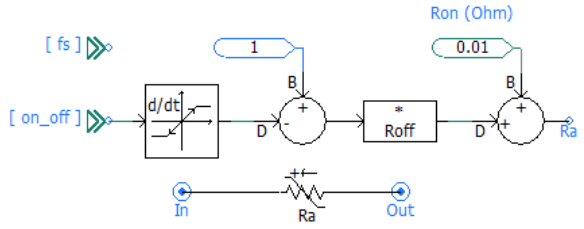

FIGURE 7. Realistic switch model with controlled switch ramps.

5) COUPLER DEVICE MODEL

The injector device is connected to the network through a filter called "Coupler" which aims to remove the grid frequency (50 or 60 Hz) and harmonics. A simple high-pass L-C filter has been used for this purpose in the model (Fig. 8). The desired design frequency of 100 kHz can be obtained from many possible combinations of L and C. Tests have shown that many combinations, especially with a large capacitance, cause oscillations when the 1-MHz pulse signals are injected.

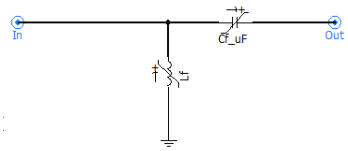

FIGURE 8. Realistic L-C network filter.

Oscillations could be reduced to an acceptable level by designing the high-pass filter with L-C values of 25.3 μH and 100 nF respectively. Note that these values are only valid together with the ramp parameters of the switch. Therefore, in a real device, filter design will be very critical. Figure 9 shows the Bode plot response diagram of the filter.

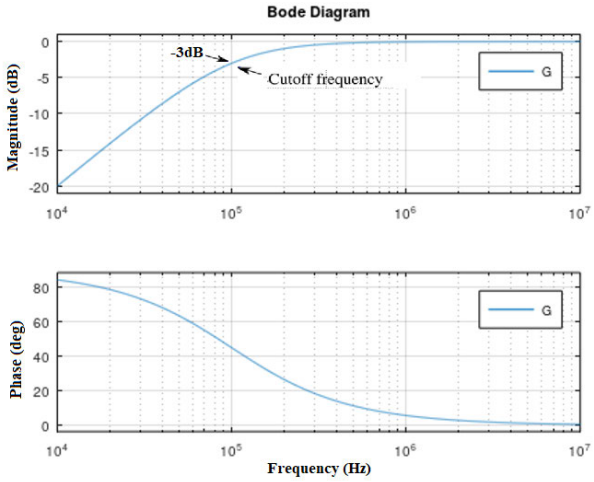

FIGURE 9. Filter-Bode plot response diagram.

B. NETWORK MODELING

This section describes the network modelled. It contains the relations between the basic blocks of the previous section. A diagram of the real network modeled is shown in Fig. 10.

Subsequently, each of the elements that have been modeled in this schematic are described one by one, allowing a simulation of the real network. This elements including the locator, which contains the pulse injector, the network coupling filter, the modeling of the network cables (with the real parameterization of each cable so that they behave like the real one), the modeling of the faults, the modeling of the loads, etc. All these elements make it possible to subsequently

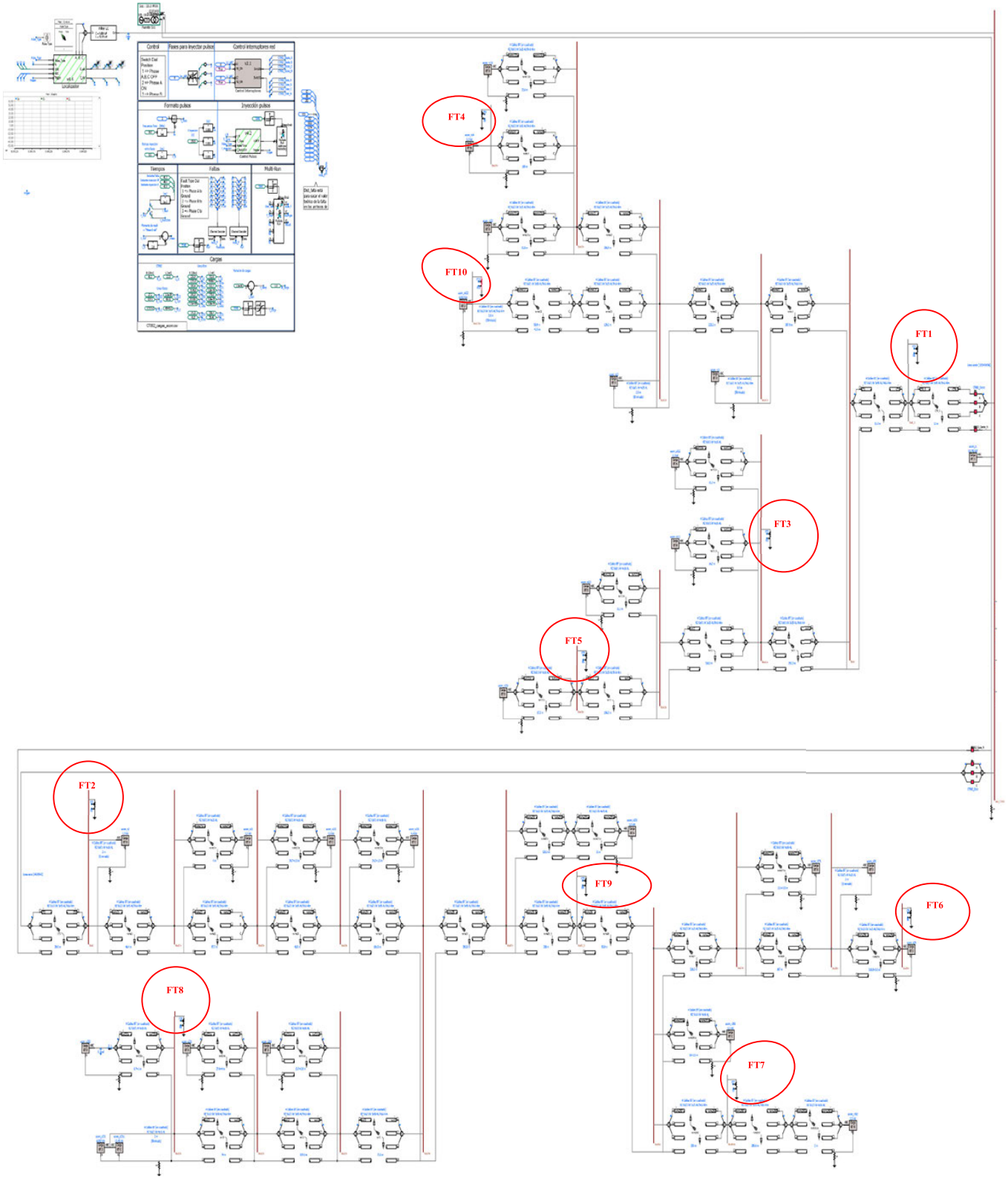

FIGURE 10. Diagram of the real network modeled.

launch simulations that allow obtaining signals very similar to these of the real network.

As we were simulating a real network, very short line segments were present in the model (below 1 m). These segments had to be eliminated or increased to a minimum length of 3 m, which was found to be a good compromise of model accuracy and simulation time. Another issue was the numerical stability of the model, depending on the grounding

resistance of the neutral. A minimum resistance of 5 Ohm was found to lead to a stable simulation.

The diagram shows the following elements:

1) FAULT LOCATOR

This is the element that injects the pulses and subsequently digitizes the network response signals (Fig. 11). These signals return after bouncing in all impedance changes (loads, bifurcations, cable type changes, faults, etc…).

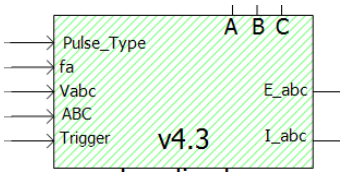

FIGURE 11. Fault locator.

Inside this block (Fig. 12), you can see the pulse injector circuit for phase A, with continuous source Va (pulse), and phase selection (switch A). The "pulse A" signal triggers the injection and comes from the "trigger" input.

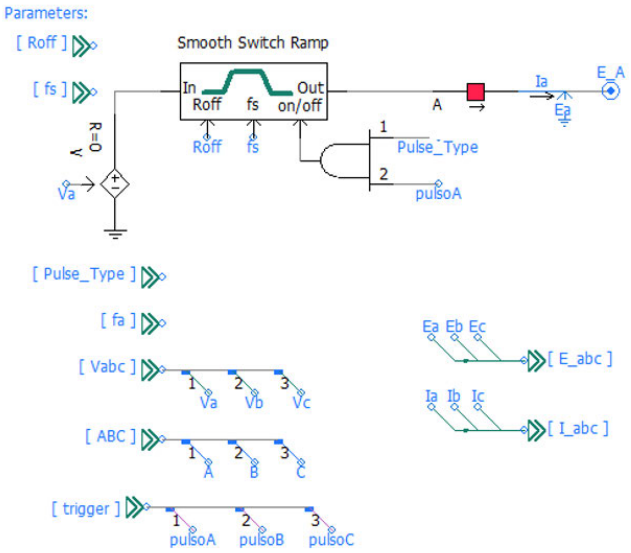

FIGURE 12. Inner fault locator.

The Fig. 7 shows the inner of the smooth-switch Ramp block.

PSCAD models the electronics (transistors, IGBTs, etc.) as ideal switches (no ramping). It has been observed that this introduces extreme transients in the model, especially when a pulse is injected. The mains LC filter has been identified as the cause, which has some sensitivity to high dU/dt ramps. Adjusting the L and C values of this filter, the effect can be minimized, but not eliminated.

To solve this problem, a new module called "Smooth Switch" has been created as an element to connect and disconnect the source to inject the pulse. This element is intended to create a more realistic pulse with controlled edges to avoid extreme ramps.

2) L-C NETWORK FILTER

The element shown in Fig. 13 represents a decoupler device (see previous section) that is placed between the injector and the mains as an insulator against the mains voltage. It is a filter for the mains frequency (50 or 60 Hz) but allows high-frequency pulses to pass in both directions.

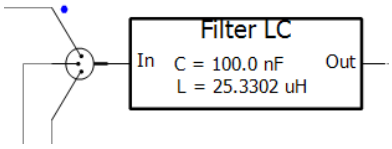

FIGURE 13. L-C network filter.

3) DETAIL OF THE NETWORK SECTION (FEEDERS)

The bifurcation, the distance of the section, the type of cable used, and the type of load at the end of the feeder are shown in Fig. 14, including the cable model and the load model. In our actual modelled grid, we have 38 feeders as it can be seen in Figure 10.

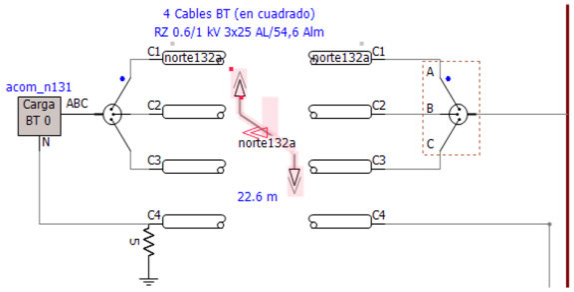

FIGURE 14. Detail of the network section.

4) DEFINITION OF FAULTS

The faults can be placed at any point on the network. Their impedance value and type can also be defined. Fig. 15 shows

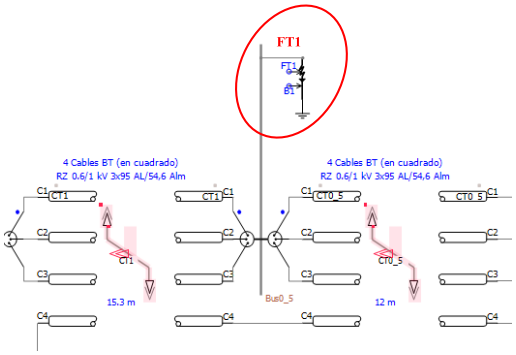

FIGURE 15. Fault FT1 in the middle of a cable run.

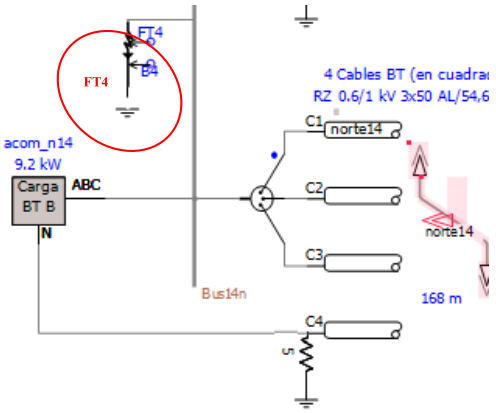

FIGURE 16. FT4 failure at the end of the run and before the load.

a fault (FT1), placed in the middle of a cable run, and Fig. 16 shows a fault (FT4), placed at the end of the run before the load.

C. SIMULATION PROCESS

1) SIMULATION PARAMETERS

This section explains all the parameters that can be set when performing a multi-run simulation.

Types of faults: Up to 10 different fault types can be defined in the simulation (Table 2):

TABLE 2. Combinations of the fault types.

Fault Type Dial Position
1 => Phase A to Ground
2 => Phase B to Ground
3 => Phase C to Ground
4 => Phase A,B to Ground
5 => Phase A,C to Ground
6 => Phase B,C to Ground
7 => Phase A,B,C to GRD
8 => Phase A,B
9 => Phase A,C
10=> Phase B,C

Position of the fault: The faults can be placed at any point on the network. In our case, we have placed 10 faults at different distances from the injector (Table 3):

Impedance of the fault: Different types of impedance can be associated with each of the defined faults. In our case, we have defined four impedance values (Table 4), ranging from a very low impedance fault or short circuit (0.01Ω) to a high impedance fault (1000 Ω):

Load values: Each of the network loads can be modeled as a resistance plus an inductance. In our case, since it is a real network, the actual data of the existing loads have been used (Fig. 17).

Injected pulse values: The injected pulse can be parameterized by varying its width, amplitude, and time delay between phases (Fig. 18).

Injection time values: The pulses can be parameterized to be injected at the most convenient time in each case. The fault event time can also be fixed(Fig. 19).

TABLE 3. Location of the faults in the simulation network.

Number of Fault	Name of bus	Distance from TDR (m)
1 (FT1, B1)	Bus0_5	12
2 (FT2, B2)	Bus2	40
3 (FT3, B3)	Bus11s	283
4 (FT4, B4)	Bus14n	933
5 (FT5, B5)	Bus13s	757
6 (FT6, B6)	Bus29n	1833
7 (FT7, B7)	Bus261n	1274
8 (FT8, B8)	Bus23s	594
9 (FT9, B9)	Bus25_5n	968
10 (FT10, B10)	Bus122n	520

TABLE 4. Impedance values.

1	0.01 Ω
2	80 Ω
3	150 Ω
4	1000 Ω

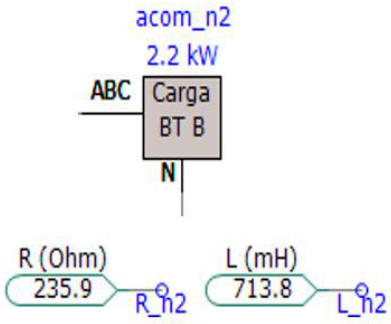

FIGURE 17. R and L are the load n2 values.

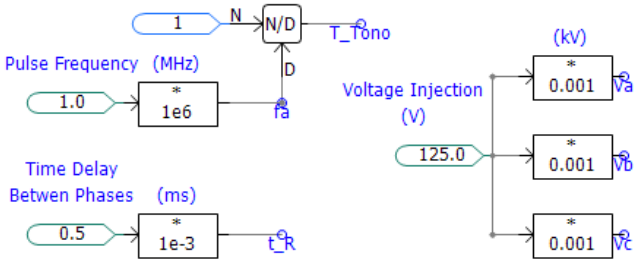

FIGURE 18. Voltage (V) and pulse rate (MHz).

Miscellaneous simulation time considerations: The simulation process starts with a waiting time of about 0.04s to reach the steady state. This process is necessary because the simulator starts the process by abruptly imposing the defined voltage on the line.

Once the steady state has been reached, a pulse is injected into each phase (R-S-T) at defined width and amplitude.

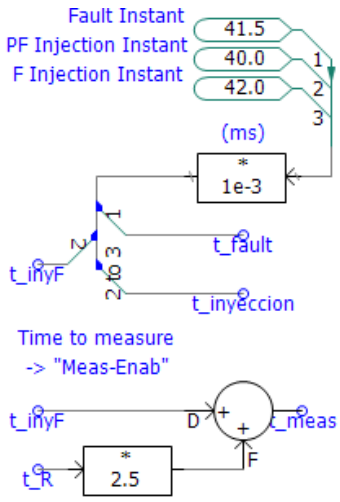

FIGURE 19. Injection time parameters.

Pulses injected in one phase can be induced in adjacent phases. To avoid this problem, it is necessary to wait until the pulse in one phase is extinguished before injecting it in the next phase. This time depends on several factors such as pulse voltage, pulse width, and the line response itself. This value is adjusted by trial and error with only one simulation case before launching all final simulations.

The simulation of each case needs about 160 s of execution time (running in Intel Core i7 7th gen).

This time is for the specific case of the real network simulated in this work.

The more complex the network, the more runtime each simulation needs.

The total number of simulated faults and the total time required for the simulation can be calculated as follows:

- Having 14 fault locations in the network. These locations have been chosen to have a wide range of distances to the injector and at various bifurcations.
- with 10 different types of fault.
- and 6 possible types of injection that arise from the combination of the number of phases in which we inject: Inject in all three phases, two by two or one by one.
- and finally, a range of fault impedances from 0.01Ω to 1000Ω. Making 5Ω steps, we have 200 values for each fault.

According to (14), as shown at the bottom of the page, with all these data, if we wanted to simulate all combinations, the complete simulation to obtain 168,000 examples would cost almost a year. It is a major problem with respect to simulating a real network. This is especially true for those classification or localization techniques based on neural networks because

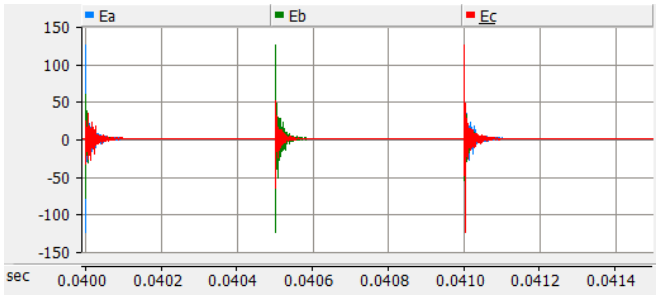

FIGURE 20. Snapshot of the pre-fault reference pulse response.

these types of technique require a large number of examples for training.

D. RESULTS OF SIMULATION RUNS

With the model set up and all design values adjusted, a multirun simulation plan was developed to create a number of different scenarios that can be feasibly simulated in a reasonable amount of time.

Bearing in mind that it must be possible to repeat the simulation in order to modify any of the parameters, we decided to select the following.

- 10 different fault locations within the network, covering cases of faults at different distances.
- 4 fault resistances: 0.01, 80, 150 and 1000 Ω
- 5 types of failures:
  - Phase-to-ground (R) -Type 1
  - Phase-to-ground (S) - Type 2
  - 2 phases-to-ground (S-T) -Type 3
  - 3-phase-to-ground (R-S-T) -Type 4
  - 2 phases-to-ground (R-S) -Type 5

All combinations were simulated, obtaining a total of 200 results.

Considering that each simulation costs about 160s, the 200 simulations take about 9 hours. This gives us a reasonable margin to run different simulations until we get the one that best suits our needs.

The simulation time step was 10 ns, and results were saved at a sample rate of 50 ns. Before starting the multiple run, the pre-fault references are obtained from a separate simulation.

A snapshot (data acquisition) with a duration of 1.51 ms is saved after 40 ms, when stationary conditions are reached. A reference response is obtained for each type of pulse.

The figures 20 and 21 show the result of one of the 200 simulations carried out (Node 1, Fault R to Ground and R_fault = 0.01 Ω) on the real simulated network. Figure 20 shows how the response to a network pulse is simulated first

$$\frac{14\,(nodes)\times 10\,(fault\ types)\times 200\,(impedance\ values)\times 6\,(Injection\ types)\times 160s}{3,600s\times 24h}=\frac{168,000\,(samples)\times 160s}{3,600s\times 24h}=311\ days \tag{14}$$

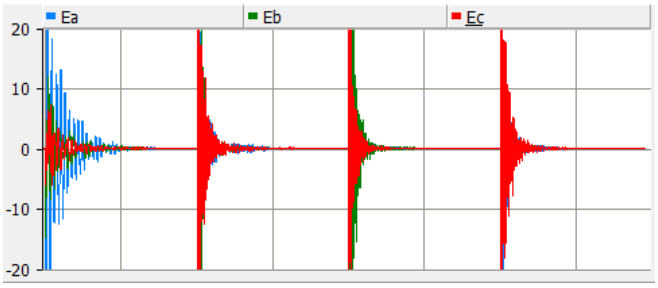

FIGURE 21. Example of pulse responses after a fault event (x: 250 μs/div, y: 10 V/div). Snapshot of the pre-fault reference pulse response.

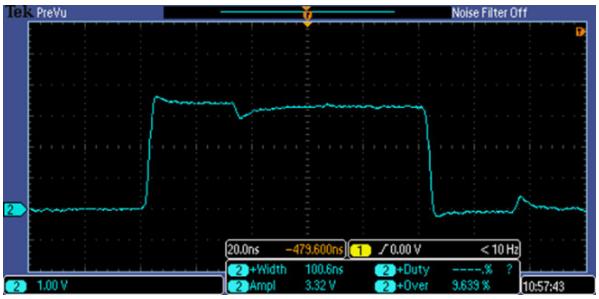

FIGURE 22. Injection pulse width = 100 ns.

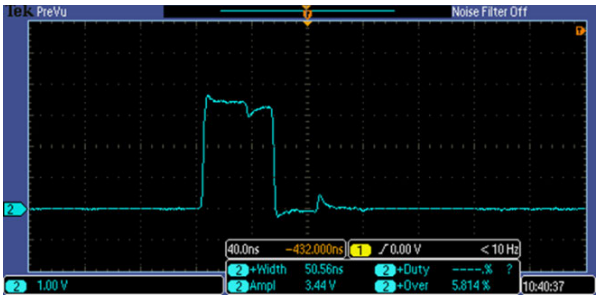

FIGURE 23. Injection pulse width = 30 ns.

before the fault occurs. It can be seen how it is injected each time in one of the phases (R-S-T labelled as Ea-Eb-Ec in the simulation software) and waits for the response to be extinguished, since the signals are normally induced in the other phases. In this way, the pulse is injected, its response is recorded, it waits for it to die out and is injected in the next phase, until completing the three injections (one of each phase). Each of the responses is concatenated to have a single network response signal before the fault (which is what is seen in the figure). Similarly, in Figure 21, the same process is seen, but before injecting, the occurrence of a fault is simulated. This signal is the first one seen in the figure and is the result of the spike that appear on the line at the moment the fault occurs. After waiting for the effects of the fault to die out, the three pulses (one in each phase) are injected in the same way as before the fault.

Finally, from the 200 simulation runs snapshots are created with a slightly longer time interval (2.01 ms), since the fault event itself is also included..

Each snapshot was saved in csv text format, and all snapshots together formed the basis for creating the database of fault signals.

VI. RESULTS

As we have no real and significant signals of faults, since we have to wait for them to occur naturally, we are going to carry out some experiments to check the validity of the work done.

The results of these experiments will be structured in four sections.

First, we are going to study the real signals available to us. On the one hand, we will compare a signal on a real single line measured with the oscilloscope against a simulated signal (section A and B). We will also compare a signal injected into the real network in normal operating state (no fault) against a simulated signal under the same conditions (section C).

Subsequently we will perform studies on simulated signals. First, we will see the behavior of the signal in a simple line without bifurcations and we will do another test in the presence of simple bifurcations in a line and putting a fault in the line to see its response (sections D and E).

We also want to see how the response of the network varies with different parameters of the simulation (fault impedance and pulse width) (sections F and G).

Finally, we will make a temporal and frequential study on the set of 200 simulated signals over the entire simulated network to draw conclusions about the information that can be extracted from them (section H).

A. STUDY OF REAL SIGNALS INJECTED IN A SINGLE SECTION WITHOUT BIFURCATIONS

The purpose of this experiment is to test the performance and validity of the injector model in a simple environment such as a single line without bifurcations.

This validation is done with a visual study of the dynamics of the response of this simple infrastructure. This similarity can be seen between the group of figures 22 to 24, and figure 26. To do this, we have performed several tests injecting pulses into a simple line formed by a coaxial cable connecting the signal injector with the oscilloscope.

The injector has an output impedance of 50 Ω, while the oscilloscope has an input impedance of 1 MΩ.

According to theory, since there is an impedance mismatch between the injector and the impedance of the oscilloscope (which here plays the role of an open line end with impedance), part of the injected signal must bounce back and return to the injector.

Fig. 22, 23 and 24 show how, after injection of a positive signal edge, a signal appears after a time according with the distance of the wire length connecting the injector and the oscilloscope. This is due to the bounce of the signal against the oscilloscope input impedance change. This property is very useful for the task of fault localization.

This signal is of opposite sign to the injected signal and of much lower amplitude. The time in which it appears is in

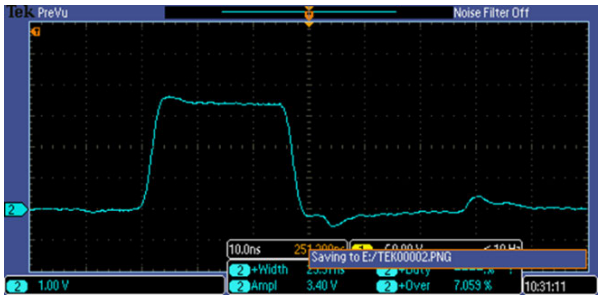

FIGURE 24. Injection pulse width = 50 ns.

FIGURE 25. Simulation of a simple line 2.5 m long.

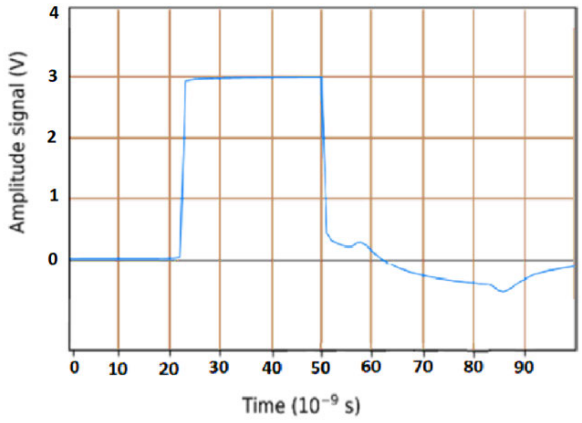

FIGURE 26. Line response to a 30 ns pulse.

accordance with the distance of the cable between the injector and the oscilloscope.

It is also observed that there is a signal bounce for each edge. One bounce is a consequence of the injection of the positive edge of the signal and another as a consequence of the negative edge.

In Fig. 24 even shows that, if the pulse width is sufficiently small, the two bounces appear once the pulse has finished, and each bounce appears approximately 35 ns from the signal that originated it. This reflection time changes according to the distance of the cable used.

In our case for a cable length of 2.5 m, considering that the propagation speed of electric current in such a cable is 0.7 c (where c is the speed of light) and that the pulse has to travel three times the length of the cable (pulse going to the oscilloscope, bouncing to the injector and bouncing to the oscilloscope again) to be "seen" by the oscilloscope. According to (15), the length L of the cable would be 2.5 m.

$$L = \frac{t_p \cdot 0.7c_0}{N} = \frac{35 \cdot 10^{-9}[s] \cdot 0.7 \cdot 3 \cdot 10^8[\frac{m}{s}]}{3} = 2.45m \tag{15}$$

B. STUDY OF SIMULATED SIGNALS IN A SINGLE SECTION WITHOUT BIFURCATIONS

In this experiment, we try to reproduce the pulse bounce phenomenon to check whether our simulation is correct.

Fig. 26 shows how in the simulation we have injected a pulse of 30 ns width and 3v amplitude. The two bounces appear once the pulse has finished approximately 35 ns later.

It can be seen that the signal is similar to the one in Fig. 24. The differences are due to the different behavior of the cable and the simulated generator with respect to the real one.

C. COMPARATIVE STUDY BETWEEN SIMULATED AND MEASURED SIGNALS

This section shows a comparison between the response to an injected pulse (in its normal state without fault) in the modeled network and the real network (Fig. 27 and Fig. 28) where the prototype injector has been installed.

The injector is placed at the same point in the network. It can be seen that the signals have a similar appearance in the time domain.

In the frequency domain, it can be observed that the real signal contains a spectrum richer in frequencies, in any case the simulation shows a good approximation to the real network.

However, the discrepancies between the two signals are expected since the modeled network is in a given state with the impedances (loads) in that state during the pulse injection.

In the real network response, the network is, in general, in a different state from that of the simulation. For this reason, in this TDR technique, pulses are constantly injected into the pre-fault state. Thus, the "picture" of the current state of the network is obtained. When the fault occurs, a pulse is injected again, and that response is processed together with the pre-fault one. In both cases, the state of the network is the same and, in variations, will be the information of the type and the distance to the fault.

This information can be extracted by the appropriate algorithms. Fig. 29 shows the actual field-assembled.

prototype with which the real signals have been injected. Fig. 30 and Fig. 31 shows the real installation on field.

The prototype will be in operation collecting signals for one year. During this period, it will record both the signals of the network in its fault-free operating state, as well as the faults that occur in the network. While these signals are being recorded, a fault location algorithm will be developed based on the database of 200 signals obtained in this work and the 10,000 synthesized signals obtained from these 200 that have been published [47] and whose database has been shared [18]. These results will be published and will also contain the error between the simulated, synthesized, and real signals obtained in the real network.

This prototype is a work of the CIRCE research group and will be presented at a congress that is in the process of being developed.

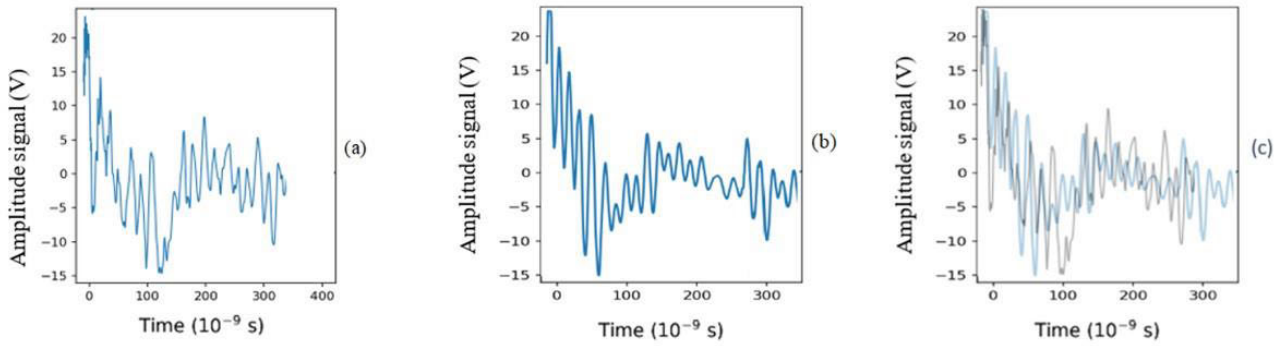

FIGURE 27. Time-domain network response to an injected pulse (a) real, (b) modelled and (c) superimposed signals.

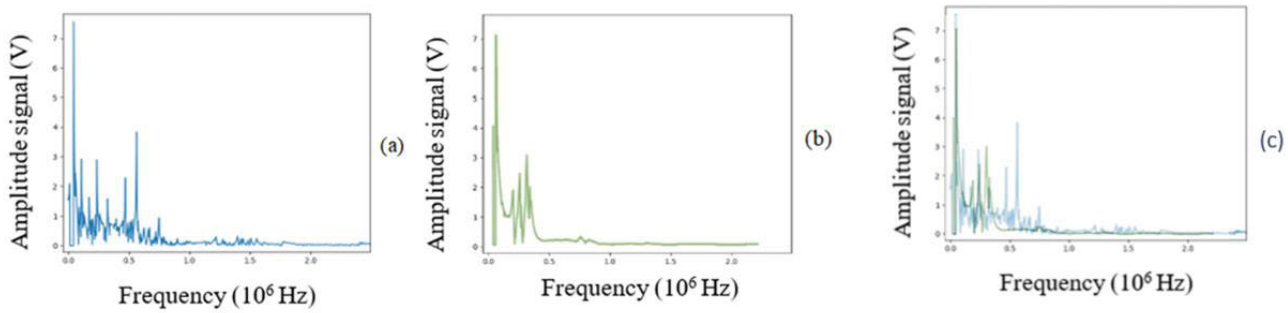

FIGURE 28. FFT network response to a pulse injected. (a) real, (b) modelled and (c) superimposed signals.

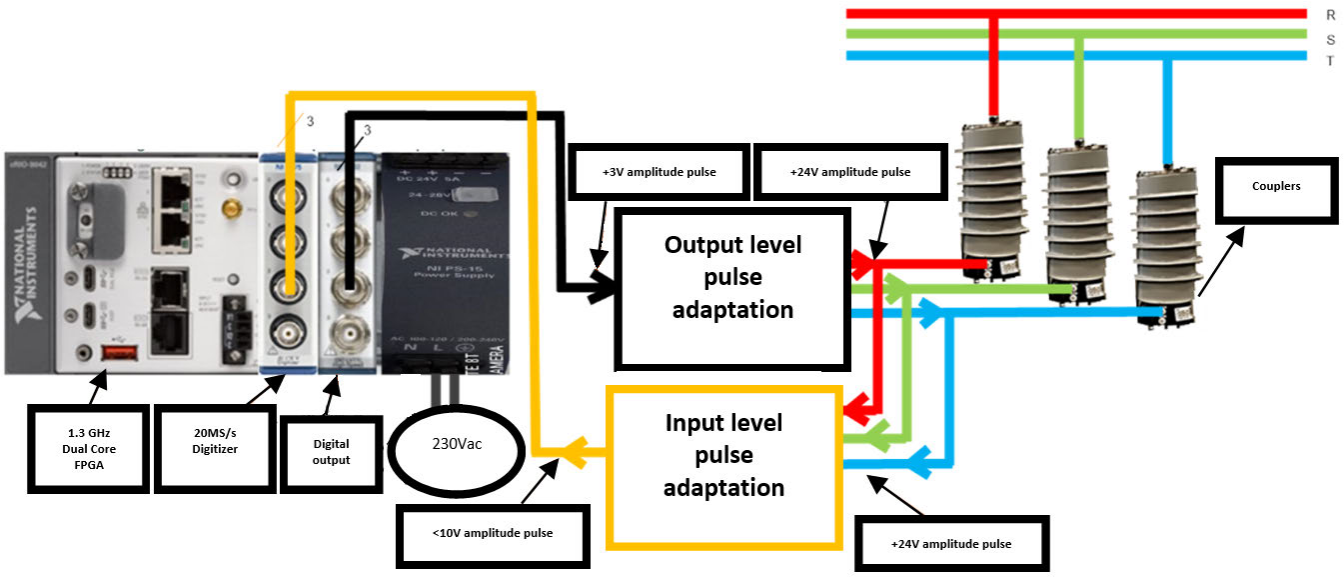

FIGURE 29. Schematic of the real prototype installed.

D. STUDY OF SIMULATED SIGNALS IN A 300 m LONG SIMPLE SECTION WITHOUT BIFURCATIONS

In this experiment, we try to reproduce the pulse bounce phenomenon to check whether our simulation is correct.

Fig. 32 shows how in the simulation we have injected a pulse of 250 ns ($5\times50\cdot10^{-9}[s]$) width and 24v amplitude, and a propagation speed in this case of 0.63 c. After about 3150 ns ($63\times50\cdot10^{-9}[s]$), the pulse bounce appears at the end of the line.

According to (16), the distance to the end of the line L is:

$$L=\frac{63\times50\cdot10^{-9}[s]\cdot0.63\cdot3\cdot10^{8}[\frac{m}{s}]}{2}=297m \quad (16)$$

which is consistent with the length of the simulated line.

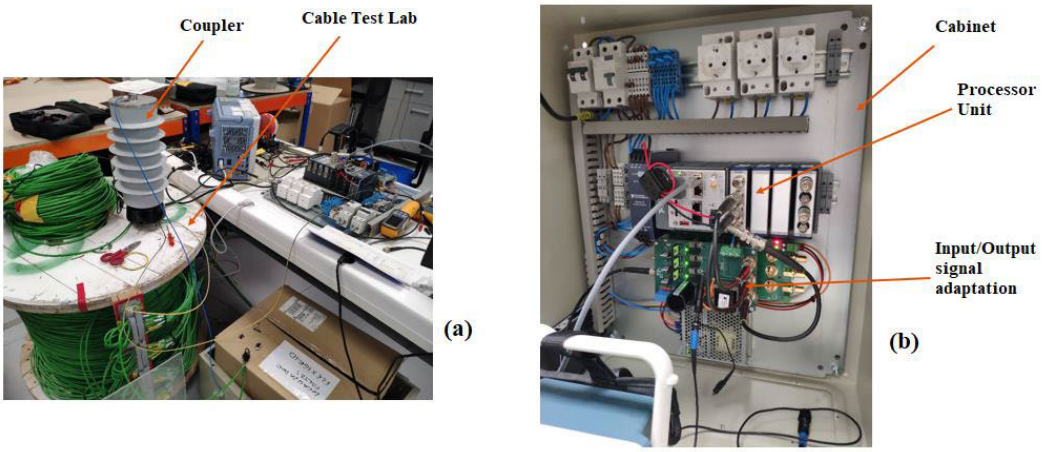

FIGURE 30. Test in lab of the prototype over single cable line (a). Fig. 1. Prototype elements in the final cabinet ready to install in field (b).

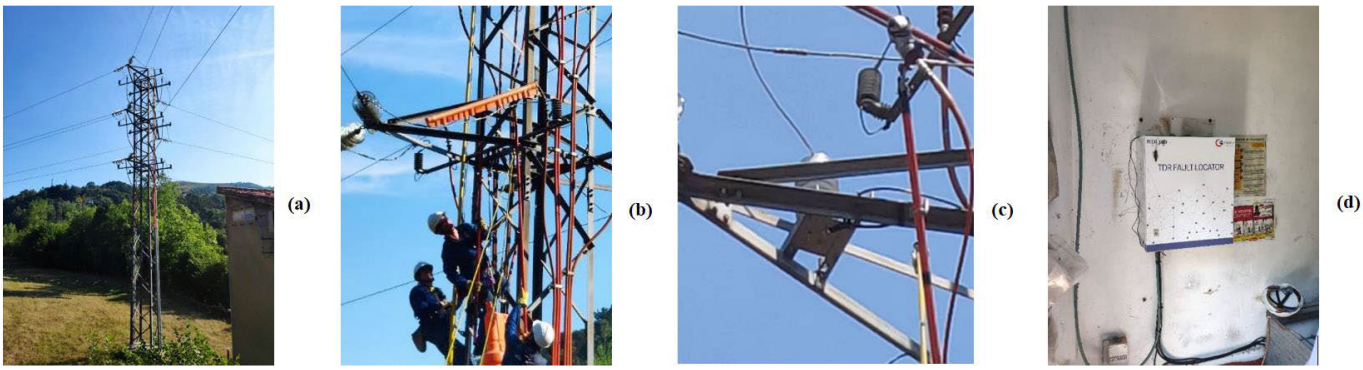

FIGURE 31. Pictures of the installation. Post where the pulses will be injected (a). Preliminary works for live installation (b). Installation of the couplers (c). Prototype cabinet installed inside the transformer station near to the post(d).

FIGURE 32. Simulation of a simple line 300m long.

E. STUDY OF SIMULATED SIGNALS IN A SECTION WITH BIFURCATIONS

This section shows (Fig. 35) the response of a bifurcated network (Fig. 34).

A fault has occurred on this line at 1100 m. The upper part of the figure shows the response of the network without fault, in which it is possible to distinguish perfectly the rebound generated at the bifurcation and the one coming from the end of the line. The lower half of the figure shows the presence of a negative sign rebound, which starts around 1100 m, the distance at which the fault occurred.

In Figure 35 (a), we can see the impedance changes that the injected pulse undergoes. first there is the bifurcation, in which part of the injected signal continues and part is reflected. Then, there is the end of line in which the signal bounces depending on the impedance of the end of line. In Figure 35 (b), we can see the same response as the previous one (with the bifurcation and the end of line), but this time, in addition, we can see how in the middle, there is another impedance change due to the fault occurred at that point (with a certain value of Z), which makes part of the signal is reflected and part continues to the end of line. The response of the section after the fault is not the same as in the previous one (a), because the signal traveling from the fault to the end of line is not the same as in the previous case, where there was no fault and the signal after the bifurcation did not suffer any impedance change.

F. IMPEDANCE INFLUENCE IN THE RESPONSE TO THE INJECTED

Fig. 31 shows the response of a single line without bifurcations to the cases of open-circuit and short-circuit line end.

In the open circuit case, the pulse reaches the end of the line and the bounce generated is of the same sign as the incident signal. In contrast, in the case where the end of the line is short-circuited, the reflected signal has the opposite

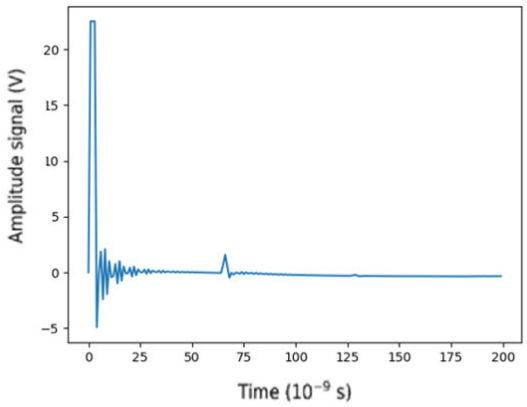

FIGURE 33. Line response to a pulse.

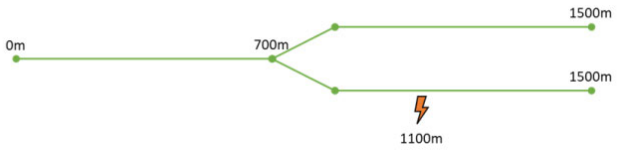

FIGURE 34. Simulation of bifurcation line.

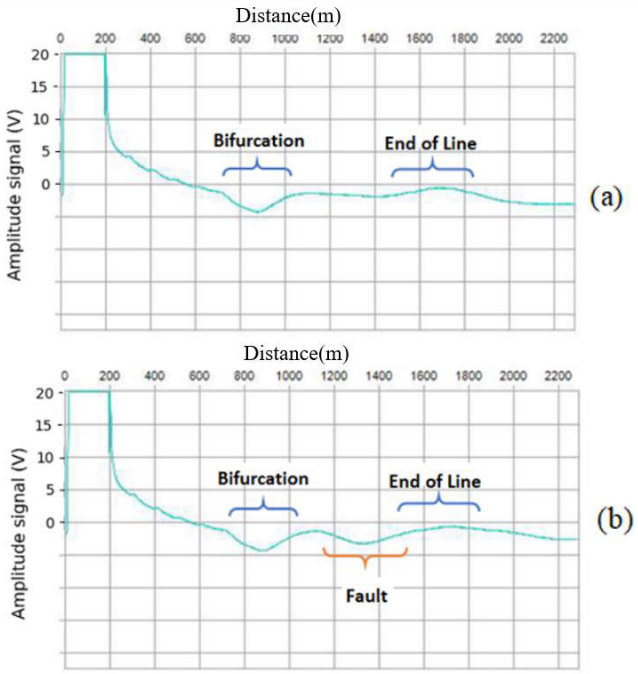

FIGURE 35. Pulse response of bifurcation line (a) without fault and (b) with fault.

sign to the incident signal, and the injector registers a negative pulse. These results confirm the theory of refraction of signals generated in line impedance changes.

G. INFLUENCE OF PULSE WITH

As already explained, the proposed localization technique is based on the reflectometry phenomenon and uses the

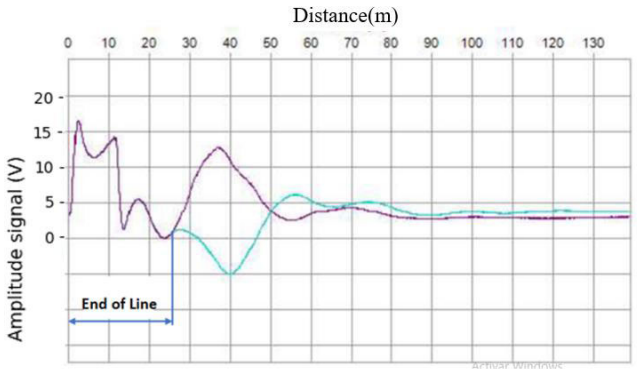

FIGURE 36. Influence of end-line impedance value.

comparison of the network response to a given signal during the pre-fault (PF) and fault (F) states. To evaluate this difference, the "error signal" (E) is defined as the arithmetic difference, sample to sample, between the two signals, both being synchronized at the instant of injection of their respective signals.

The graphs in Fig. 37 show the error signal of the three phases (R-S-T) superimposed. the response after the fault occurs. It can be seen how at the beginning, the error signal is practically null (or of a very small value), since up to the point where the fault has occurred, the signals bounced before the fault and after the fault are practically identical and begin to differ from the point where the fault has occurred.

For the determination of the pulse width, simulations of low-impedance faults have been performed at different locations in the network.

Fig. 37 shows the comparison of four simulations employing different pulse widths while keeping all other conditions constant. As can be seen in the image, the amplitude of the received signal increases with pulse width, so that a longer time on high of the injected pulse will amplify the received signal, facilitating the measurement of more distant faults.

This amplification occurs up to a certain point, since if the pulse width is increased too much, its characteristic frequency will approach the cutoff frequency of the network filter and will be attenuated by it. In this case, it has been detected that the maximum received amplitude occurs for a pulse width of 2 μs (Fig. 37 (c)).

H. TEMPORAL AND FRECUENCIAL STUDY OF THE SIMULATED SIGNALS

Finally, we analyse the simulated signals to determine whether fault information is present in the signals and can be amenable to extraction. Next, we will explain the content of each figure and the process we have followed with the injected signals.

Each figure consists of three parts. The subfigure (a) is the complete time response of the network to the injection of a pulse. At the top is the R phase, in the middle is the S phase and at the bottom is the T phase.

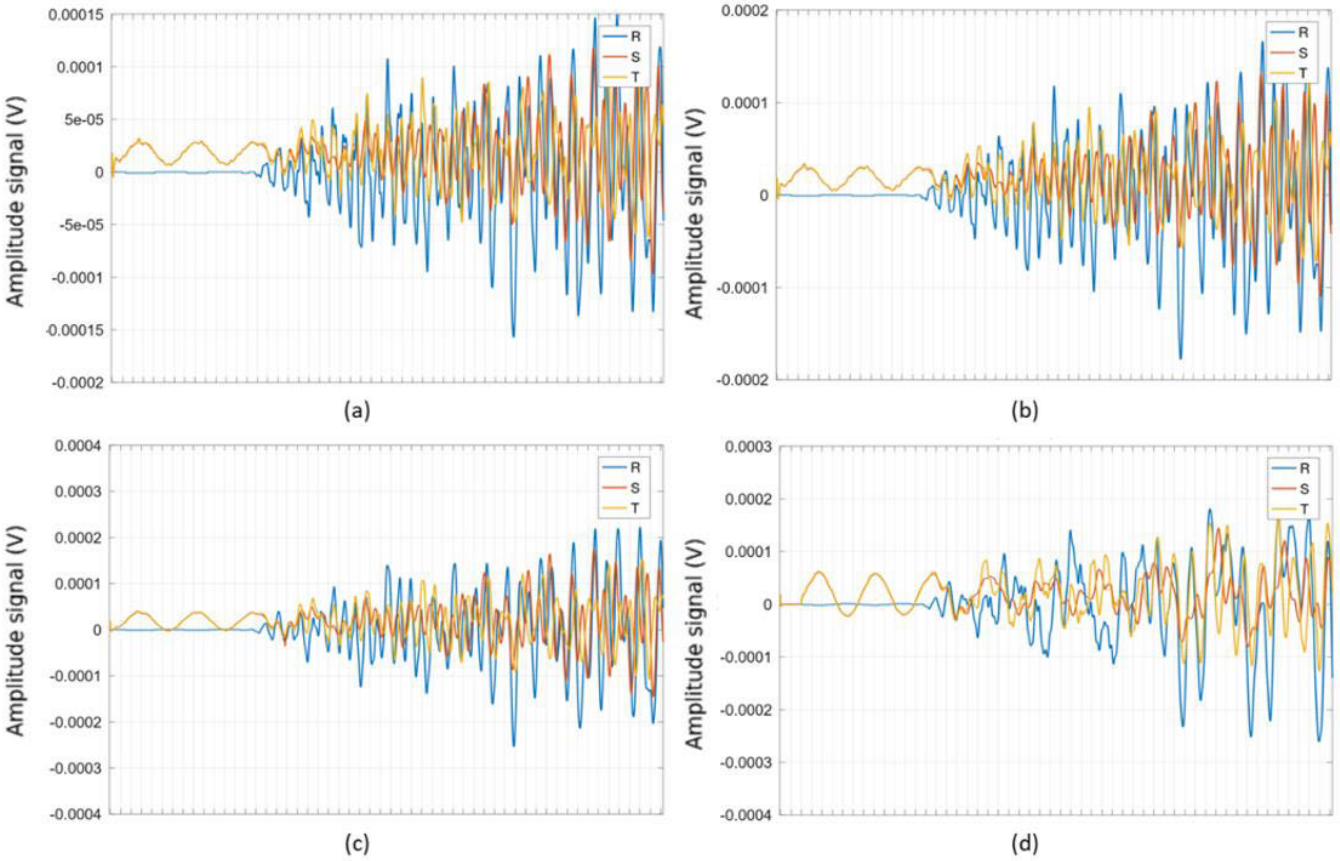

FIGURE 37. Error signal in phases R, S and T, for a low impedance fault located at a distance of 594 m in the network model for a pulse width of: (a) 0.5 μs, (b) 1 μs, (c) 2 μs, (d) 10 μs.

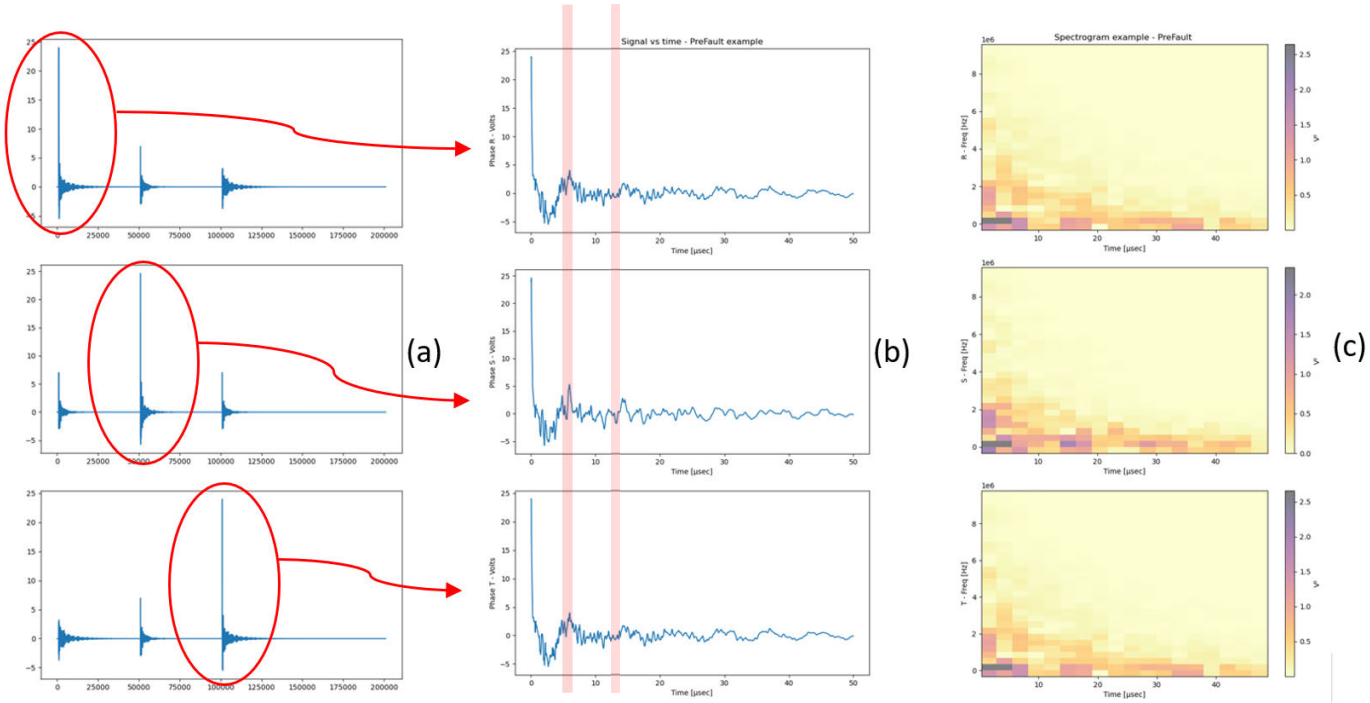

FIGURE 38. Pre-Fault signal (Top-Phase R / Middle-Phase S / Bottom-Phase T). (a) Complete Injection, (b) Phase Injection, (c) Spectrogram.

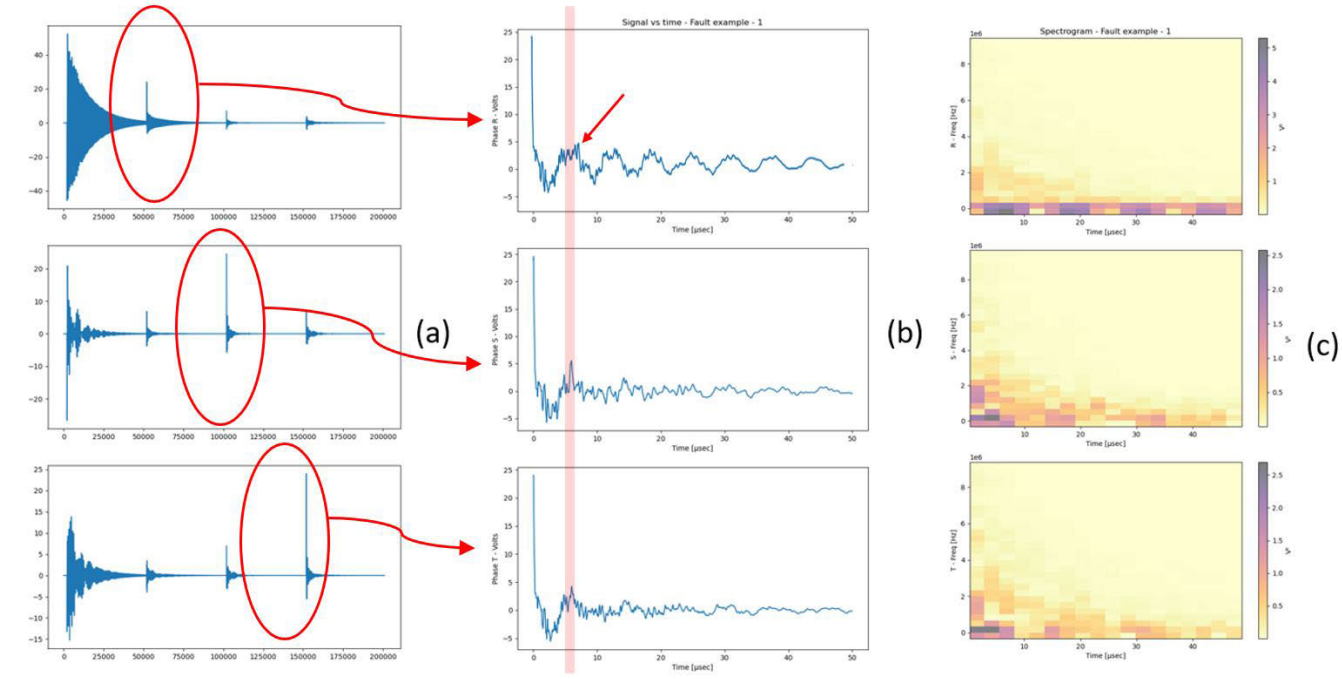

FIGURE 39. Fault signal Type 1 (Top-Phase R / Middle-Phase S / Bottom-Phase T). (a) Complete Injection, (b) Phase Injection, (c) Spectrogram.

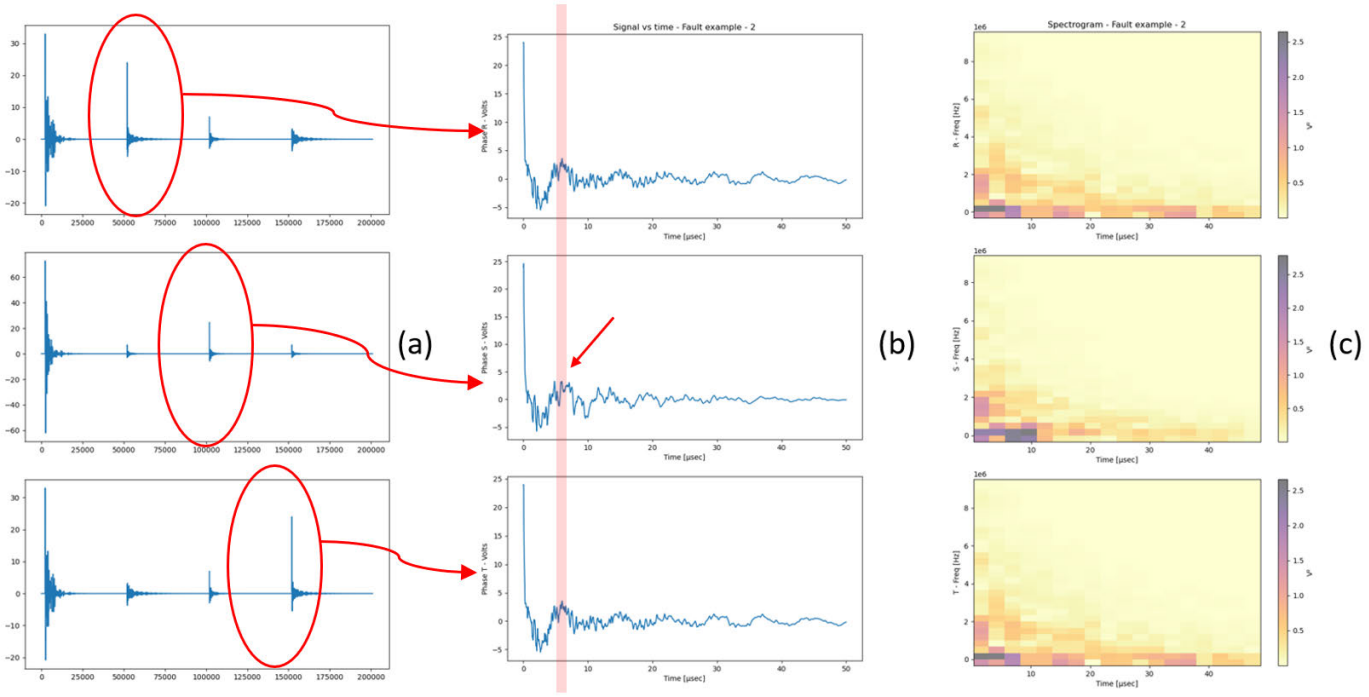

FIGURE 40. Fault signal Type 2 (Top-Phase R / Middle-Phase S / Bottom-Phase T). (a) Complete Injection, (b) Phase Injection, (c) Spectrogram.

In figures (39, 40, 41, 41, 42 and 43), it can be seen how the first signal that appears is the fault event itself. This means that the simulator simulates the short-circuit of the phase(s) to ground and a ''spike'' is produced as a consequence of the short-circuit. Then, a necessary time is waited for the event to extinguish. This is necessary to avoid injecting when traces of the fault spike signal are still present in the network. This would cause our injected pulse to have noise and give us erroneous information about the state of the network. Obviously, in Figure 38, there is no such signal from the fault event since that is the case where we inject a pulse into the network without a fault.

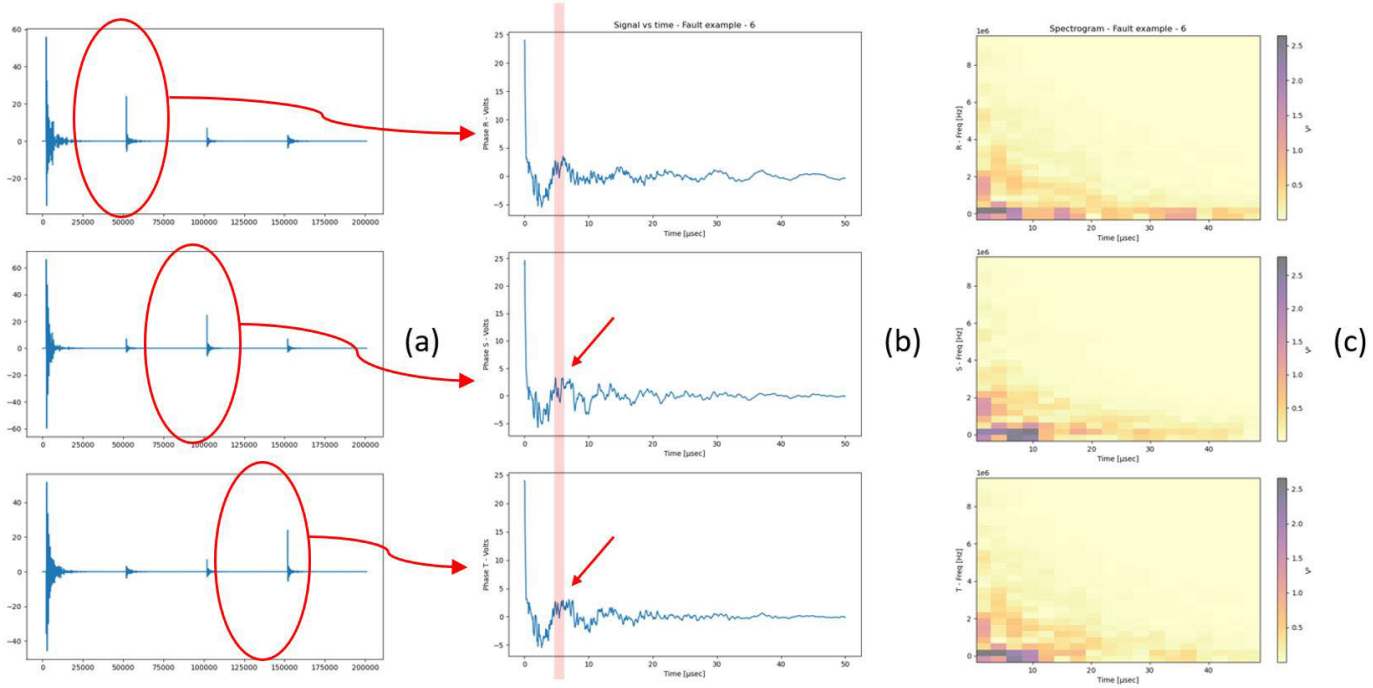

FIGURE 41. Fault signal Type 3 (Top-Phase R / Middle-Phase S / Bottom-Phase T). (a) Complete Injection, (b) Phase Injection, (c) Spectrogram.

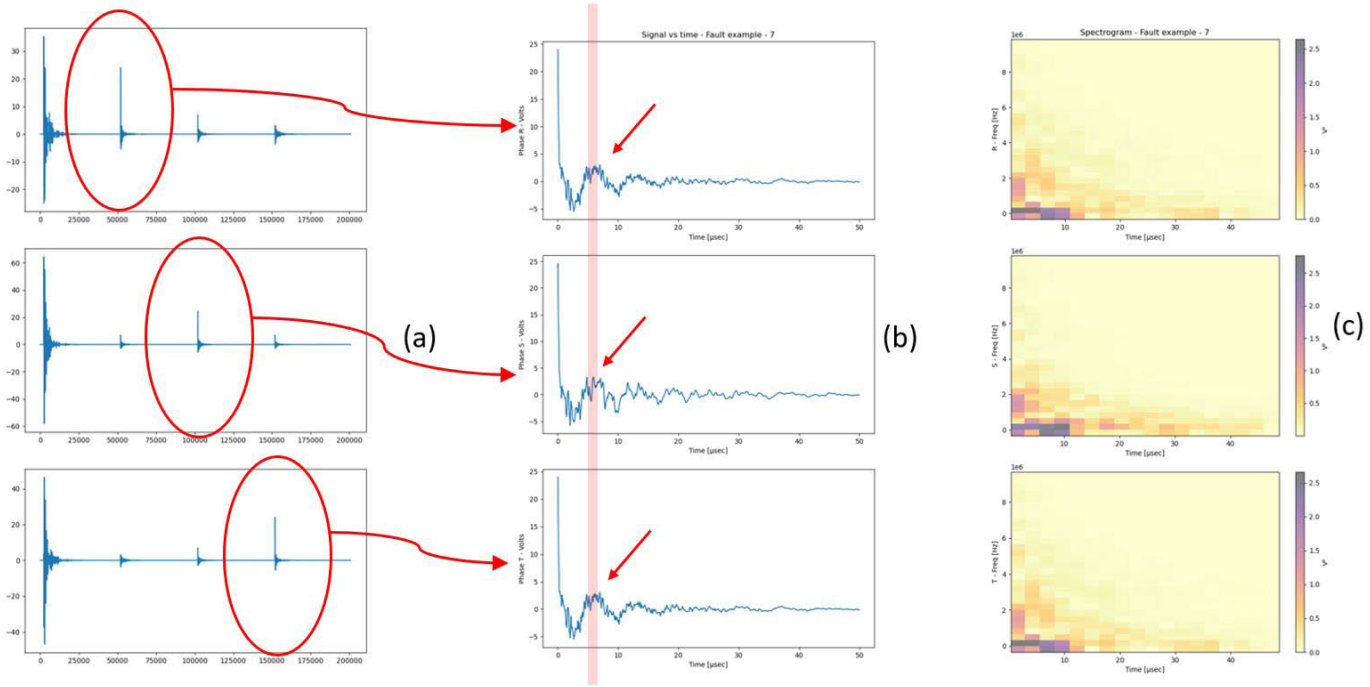

FIGURE 42. Fault signal Type 4 (Top-Phase R / Middle-Phase S / Bottom-Phase T). (a) Complete Injection, (b) Phase Injection, (c) Spectrogram.

In each one of the phases, the injected pulse is marked with a red circle. The injection process is as follows. A first pulse is injected in the S phase (red circle in the upper signal). This pulse is also induced in the other two phases (S and T). After waiting a certain time for the injected pulse to die out, another pulse is injected, but this time in the S phase (red circle in the middle signal). Which is also induced in the other two phases (R-T). Finally, another pulse is injected in the T phase (red circle in the bottom signal).

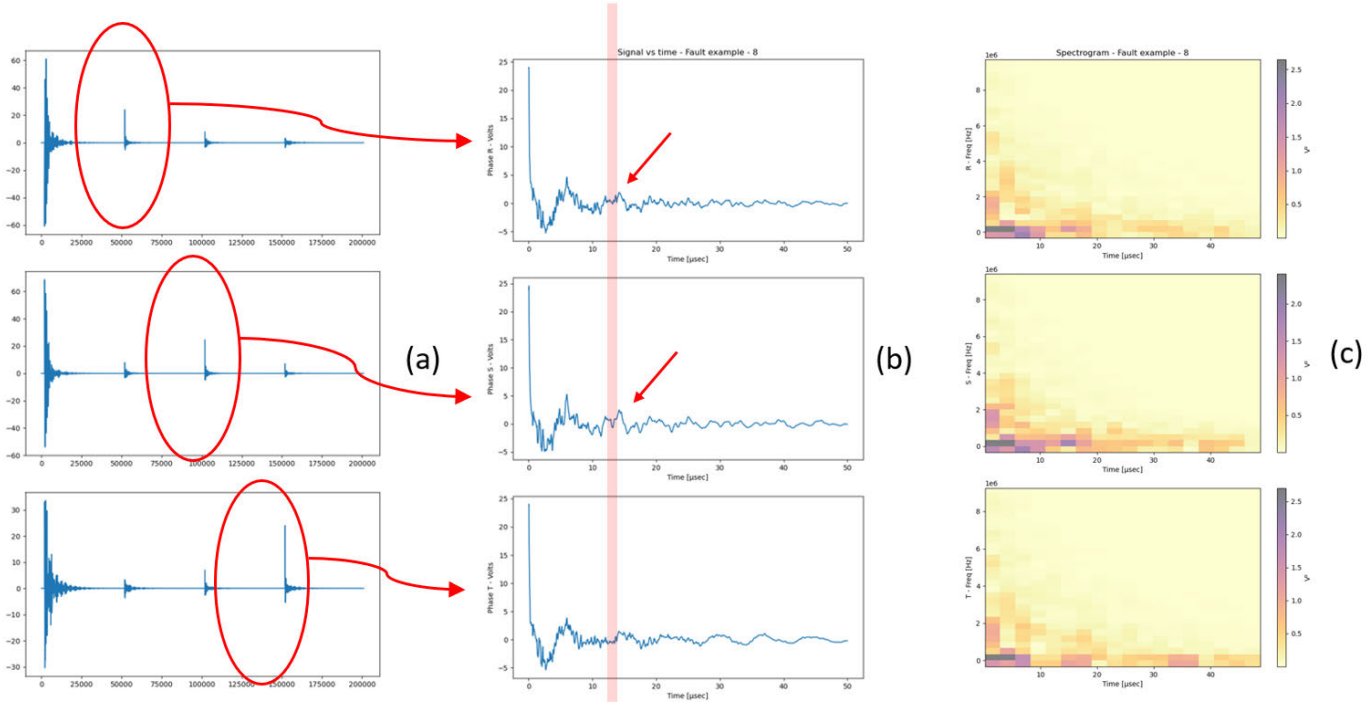

FIGURE 43. Fault signal Type 5 (Top-Phase R / Middle-Phase S / Bottom-Phase T). (a) Complete Injection, (b) Phase Injection, (c) Spectrogram.

This injection sequence is intended to avoid mixing the injected signals with those induced from the other phases, which would lead to erroneous signals.

In this process, each time a pulse is injected, the response of the signal bounced by the network is sampled (at the same injection point). In this way, at the end of the three injections, we will have 3 buffers with the response signal of each of the phases, thus discarding the rest of the induced signals that contain redundant information, as well the ''spike'' signal of the fault event.

In subfigure (b) we can see the three signals obtained from the previous process. In each of the figures, we have marked with a red stripe the time at which the rebound of the fault occurs and with a red arrow, the phase(s) in which the fault has occurred.

The first figure (Fig. 38) shows the response to the injected pulse of the modelled real network in its normal state (without any fault produced).

In the examples shown below, we have chosen the FT4 fault, which is located at about 933m and whose rebound should arrive at 6 μs after injection. The pulse travels about 300m/us, but it has to go to the fault and bounce back to the injection point, so it has to travel the distance to the fault twice so, the fault bounce should show some peculiar characteristic at about 6 μs.

Each of the other figures (Fig. 39, 40, 41, and 42), the response of each type of fault is shown. Thus, we should find in the vicinity of those 6 μs differences between the responses of each type of fault and that of the pre-fault. Moreover, these differences should be consistent with the type of fault, i.e., the differences should appear in those phases in which the fault occurred and not in the rest.

In Fig. 41, we have chosen the fault FT6, which is at about 1833m, to have another example at a different distance. In this case, the rebound should arrive at about 12 μs, so we should see some difference with the pre-fault signal around that time.

As can be seen in the figures, around the distance to the fault, a ''subtle'' difference between the pre-fault and fault signals can be appreciated. Moreover, as we expected, this difference occurs only in those phases in which the foul has occurred, while in the rest, the fault and pre-fault signals are practically identical.

It can be seen how the differences between the signals have a very small amplitude, which is mixed with the rest of the ''peaks'' that appear over time, and which correspond to each impedance change that the injected signal encounters on its way. Thus, as already explained, the fault is one more impedance variation in the line.

In the spectrogram, we can see how around the zone where the fault occurs (6 us), we have signals of several frequencies with the highest amplitudes to decay with time. This agrees with the time signal and with the theory since, at the beginning, the bounced signal still has enough energy. This energy disappears over time due to the attenuation of the signal as it travels along the line.

We can also observe in the spectrogram, as there is a relatively low frequency (KHz) that is present and that is due to the resonance of the coupler to the pulse injection. This signal plays the role of ''carrier'' on which is ''mounted'' the information of the ''bounces'' of the injected pulse. As it

does not contain information on the network status, this low frequency signal can be eliminated in the post-processing.

As a conclusion, as we have already mentioned, we can say that these variations are not at all obvious and reflect the complexity of extracting the classification of the type of fault, as well as its precise location. For the location accuracy to be less than 15 m, we would have to make a location error of less than 0.1 μs (the time it takes for a pulse to travel the distance of 30 m (15 m out and 15 m back). As can be seen, an error of 0.1 μs in 6 μs equals approximately 1.6%.

With this study of the signals, we can conclude that the information of interest is embedded in the response of the network to the pulse injection. With these simulated signals from a real network, we can, therefore, develop algorithms that allow us to classify and/or locate the faults. Later in the future, we can verify them when the real faults occur in the selected network where the pulse injector has been installed.

VII. CONCLUSION

As mentioned above, there are data from different power grids of varying complexity and age, most of them supported by the IEEE Power & Energy Society. Even though all of them provide a very good test bed for experiments with power failures, we believe that new techniques and scenarios require more complex data and there have been great advances in this line of research because of this initiative.

Therefore, we are confident that the new proposal based on the TDR principle can offer new insights, and additionally, creating and providing ready-made data for processing by researchers not directly linked to the electrical field can provide a strong boost to advances in this sector.

On the other hand, the shared data have been obtained with a simulation software, PSCAD^{TM}, with great potential and capacity to perform highly complex studies. We think it is a very good alternative at the moment when no real power failure signals are available, because fortunately no such incidents have occurred in an in-service network. But high-quality signals are available thanks to this software, very similar to those expected when such incidents occur in the future.

Finally, since this is purely experimental research, a couple of applications have been carried out in which the know-how obtained has been put into practice. On the one hand, a prototype has been installed (as shown in Fig. 29, Fig. 30 and Fig. 31) inside an existing installation, and on the other hand, the simulated data obtained have been processed for the classification of electrical faults [47] using the latest techniques of pattern recognition and deep learning.

In summary, the main points of our study are as follows:

- Simulate a real electrical network in PSCAD to obtain a database of 200 simulated fault signals.
- Install a prototype pulse injector (TDR) in that modeled real installation to be able to record real signals.
- And a real system ready to collect real data of electrical incidents. In this way, it is possible to populate and compare the results obtained in the immediate future from simulated signals with responses to future real signals.

VIII. FUTURE WORK

In the short-term work, the expectations from this work are:

- Possibility to compare in the future the signals obtained by simulation and synthesis with the signals recorded in the field.
- Verify if the detection and classification performed with these synthesized signals is able to train the system to be able to detect and classify the real signals recorded in the field.
- Populate with more examples that are consistent and of the same complexity as the original ones. In this way, and in the previous referenced work, a system for synthesized data generation is proposed, which is a suitable complement to the original data. All of these data is intended to be included in the same shared repository.

Talking about our future medium-term work, it will be focused on the TDR technique and on trying to explore and improve the limits that this phenomenon can provide us when identifying, and subsequently locating, faults with a higher impedance.

Together with the objective mentioned above, we want to focus on the problem of the presence of distributed generations in different distribution networks. Also, in applications where detection/localization is required in greater distance ranges, playing with different injection frequencies, or even considering multipoint injection systems.

On the other hand, and with our own experience gained from our previous works, the objective of obtaining a target fault location system, and with the highest possible accuracy, becomes indispensable. This objective could not be achieved without the progress we are currently making in the definition and formalization of simulation systems. These systems provide us with the seed with which to produce training data that will provide us with the minimum capacity to meet the localization challenge.

REFERENCES

[1] L. Peretto, R. Tinarelli, A. Bauer, and S. Pugliese, "Fault location in underground power networks: A case study," in *Proc. ISGT*, 2011, pp. 1–6, Accessed: Mar. 30, 2022. [Online]. Available: https://ieeexplore-ieee-org.cuarzo.unizar.es:9443/document/5759198/

[2] A. Bahmanyar, S. Jamali, A. Estebsari, and E. Bompard, "A comparison framework for distribution system outage and fault location methods," *Electric Power Syst. Res.*, vol. 145, pp. 19–34, Apr. 2017.

[3] J.-H. Teng, W.-H. Huang, and S.-W. Luan, "Automatic and fast faulted line-section location method for distribution systems based on fault indicators," *IEEE Trans. Power Syst.*, vol. 29, no. 4, pp. 1653–1662, Jul. 2014, doi: 10.1109/TPWRS.2013.2294338.

[4] M. A. López, "Algoritmos de localización de faltas en redes eléctricas," Doctoral dissertation, 2016.

[5] S. Robson, A. Haddad, and H. Griffiths, "Fault location on branched networks using a multiended approach," *IEEE Trans. Power Del.*, vol. 29, no. 4, pp. 1955–1963, Aug. 2014, doi: 10.1109/TPWRD.2014.2302137.

[6] K. Sun, Q. Chen, and Z. Gao, "An automatic faulted line section location method for electric power distribution systems based on multisource information," *IEEE Trans. Power Del.*, vol. 31, no. 4, pp. 1542–1551, Aug. 2016, doi: 10.1109/TPWRD.2015.2473681.

[7] S. Lotfifard, M. Kezunovic, and M. J. Mousavi, "A systematic approach for ranking distribution systems fault location algorithms and eliminating false estimates," *IEEE Trans. Power Del.*, vol. 28, no. 1, pp. 285–293, Jan. 2013, doi: 10.1109/TPWRD.2012.2213616.

[8] R. J. Hamidi and H. Livani, "Traveling-wave-based fault-location algorithm for hybrid multiterminal circuits," *IEEE Trans. Power Del.*, vol. 32, no. 1, pp. 135–144, Feb. 2017, doi: 10.1109/TPWRD.2016.2589265.

[9] A. Farughian, L. Kumpulainen, and K. Kauhaniemi, "Review of methodologies for earth fault indication and location in compensated and unearthed MV distribution networks," *Electric Power Syst. Res.*, vol. 154, pp. 373–380, Jan. 2018, doi: 10.1016/j.epsr.2017.09.006.

[10] P. Stefanidou-Voziki, N. Sapountzoglou, B. Raison, and J. L. Dominguez-Garcia, "A review of fault location and classification methods in distribution grids," *Electric Power Syst. Res.*, vol. 209, Aug. 2022, Art. no. 108031, doi: 10.1016/j.epsr.2022.108031.

[11] K. Yang, R. Zhang, J. Yang, Y. Chen, and S. Chen, "Research on low-voltage series arc fault detection method based on least squares support vector machine," *Open Electr. Electron. Eng. J.*, vol. 9, no. 1, pp. 408–421, Sep. 2015, doi: 10.2174/1874129001509010408.

[12] D. Bisht and A. Bhandakkar, "Shunt faults detection on transmission line: A review," *Int. J. Elect. Electron. Res.*, vol. 3, no. 4, 2015, Accessed: Feb. 16, 2023. [Online]. Available: https://www.researchpublish.com/papers/shunt-faults-detection-on-transmission-line-a-review

[13] S. S. Gururajapathy, H. Mokhlis, and H. A. Illias, "Fault location and detection techniques in power distribution systems with distributed generation: A review," *Renew. Sustain. Energy Rev.*, vol. 74, pp. 949–958, Jul. 2017, doi: 10.1016/j.rser.2017.03.021.

[14] Y. Q. Chen, O. Fink, and G. Sansavini, "Combined fault location and classification for power transmission lines fault diagnosis with integrated feature extraction," *IEEE Trans. Ind. Electron.*, vol. 65, no. 1, pp. 561–569, Jan. 2018, doi: 10.1109/TIE.2017.2721922.

[15] J. Oasa, M. Yamanaka, S. Higashiyama, Y. Inaoka, T. Hisakado, O. Wada, T. Matsushima, T. Hirayama, and K. Yamaoka, "Verification of fault location by TDR measurement on an actual line including multiple ground-mounted equipment," in *Proc. 26th Int. Conf. Exhib. Electr. Distrib.*, 2021, pp. 1274–1278.

[16] R. Lacoste, *Robert Lacoste's The Darker Side: Practical Applications for Electronic Design Concepts From Circuit Cellar*. 2010, pp. 33–47, doi: 10.1016/B978-1-85617-762-7.00003-4.

[17] Y. Miyoshi and S. Saba, "Some features and performances of type C transmission-line fault locators," *Trans. Amer. Inst. Electr. Eng. III, Power App. Syst.*, vol. 76, no. 3, pp. 445–451, Apr. 1957, doi: 10.1109/AIEEPAS.1957.4499585.

[18] E. Herrero, J. Granado, and A. Llombart, "CVLAB-UNIZAR/CIRCE_fault_database: Initial release," Tech. Rep., Nov. 2022, doi: 10.5281/ZENODO.7316010.

[19] F. J. L. Padua and R. De Oliveira, "Allocation of PLC devices in a low-voltage grid," in *Proc. IEEE PES Innov. Smart Grid Technol. Conf.-Latin Amer.*, Sep. 2019, pp. 1–4, doi: 10.1109/ISGT-LA.2019.8895457.

[20] R. Dashti, S. Salehizadeh, H. Shaker, and M. Tahavori, "Fault location in double circuit medium power distribution networks using an impedance-based method," *Appl. Sci.*, vol. 8, no. 7, p. 1034, Jun. 2018, doi: 10.3390/app8071034.

[21] M. Shafiullah and M. A. Abido, "S-transform based FFNN approach for distribution grids fault detection and classification," *IEEE Access*, vol. 6, pp. 8080–8088, 2018, doi: 10.1109/ACCESS.2018.2809045.

[22] A. Aljohani, A. Aljurbua, M. Shafiullah, and M. A. Abido, "Smart fault detection and classification for distribution grid hybridizing ST and MLP-NN," in *Proc. 15th Int. Multi-Conference Syst., Signals Devices (SSD)*, Mar. 2018, pp. 94–98, doi: 10.1109/SSD.2018.8570582.

[23] A. Ekka and A. Yadav, "Fault identification using fuzzy in renewable energy interfaced IEEE 13 bus system," in *Proc. Int. Conf. Intell. Controller Comput. Smart Power*, 2022, pp. 1–6, doi: 10.1109/ICICCSP53532.2022.9862498.

[24] G. R. Kumar. *Estimation and Minimization of Harmonics in IEEE 13 Bus Distribution System*. Accessed: Nov. 23, 2022. [Online]. Available: www.ijert.org

[25] B. Ahmed, A. Abdelgadir, N. A. Saied, and A. A. Karrar, "A compensated distributed-parameter line decoupling approach for real time applications," *IEEE Trans. Smart Grid*, vol. 12, no. 2, pp. 1761–1771, Mar. 2021, doi: 10.1109/TSG.2020.3033145.

[26] K. P. Schneider, B. A. Mather, B. C. Pal, C. W. Ten, G. J. Shirek, H. Zhu, J. C. Fuller, J. L. R. Pereira, L. F. Ochoa, L. R. de Araujo, and R. C. Dugan, "Analytic considerations and design basis for the IEEE distribution test feeders," *IEEE Trans. Power Syst.*, vol. 33, no. 3, pp. 3181–3188, Oct. 2017, doi: 10.1109/TPWRS.2017.2760011.

[27] W. H. Kersting, "Radial distribution test feeders distribution system analysis subcommittee report," in *Proc. IEEE Power Eng. Soc. Winter Meeting*, Feb. 2001, pp. 908–912, Accessed: Nov. 23, 2022. [Online]. Available: http://ewh.ieee.org/soc/pes/dsacom/testfeeders.html

[28] M. Scarpetta, M. Spadavecchia, G. Andria, M. A. Ragolia, and N. Giaquinto, "Analysis of TDR signals with convolutional neural networks," in *Proc. IEEE Int. Instrum. Meas. Technol. Conf. (IMTC)*, May 2021, pp. 1–6, doi: 10.1109/I2MTC50364.2021.9460009.

[29] D. Nagata, S. Fujioka, T. Matshushima, H. Kawano, and Y. Fukumoto, "Detection of fault location in branching power distribution network using deep learning algorithm," in *Proc. Int. Symp. Electromagn. Compat.*, Sep. 2022, pp. 655–660, doi: 10.1109/EMCEUROPE51680.2022.9901205.

[30] D. Haddad, A. Y. Kallel, N. E. B. Amara, and O. Kanoun, "Multiple faults detection and location in bus-shaped cable networks by distributed time-domain reflectometry," *IEEE Sensors Lett.*, vol. 6, no. 5, pp. 1–4, May 2022, doi: 10.1109/LSENS.2022.3170645.

[31] S. Thomas, "Antenna system measurements using frequency domain reflectometry vs. time domain reflectometry," in *Proc. IEEE Autotestcon*, Sep. 2006, pp. 230–236, doi: 10.1109/AUTEST.2006.283643.

[32] A. Tengg and P. Hank, "Reflectometry based fault localization in automotive bus systems," in *Proc. IEEE Int. Instrum. Meas. Technol. Conf.*, Mar. 2012, pp. 397–402, doi: 10.1109/I2MTC.2012.6229648.

[33] X. Gu, "On-line test and fault location of aviation general-purpose cables based on TDR," in *Proc. 3rd Int. Conf. Comput. Vis., Image Deep Learn. Int. Conf. Comput. Eng. Appl.*, May 2022, pp. 294–297, doi: 10.1109/CVIDLICCEA56201.2022.9825377.

[34] M. Ziwei and W. Xueye, "A portable railway signal cable fault detector," in *Proc. 5th Int. Conf. Inf. Sci., Comput. Technol. Transp. (ISCTT)*, Nov. 2020, pp. 69–72, doi: 10.1109/ISCTT51595.2020.00021.

[35] M. Hampe, M. Tetzlaff, and T. Müller, "Analytical method to check and correct the TDR impedance profile of low-loss transmission lines," in *Proc. Int. Symp. Electromagn. Comput.*, Sep. 2022, pp. 740–743, doi: 10.1109/EMCEUROPE51680.2022.9901087.

[36] J. Mora-Flòrez, J. Meléndez, and G. Carrillo-Caicedo, "Comparison of impedance based fault location methods for power distribution systems," *Electr. Power Syst. Res.*, vol. 78, no. 4, pp. 657–666, Apr. 2008, doi: 10.1016/j.epsr.2007.05.010.

[37] C. Galvez and A. Abur, "Fault location in active distribution networks containing distributed energy resources (DERs)," *IEEE Trans. Power Del.*, vol. 36, no. 5, pp. 3128–3139, Oct. 2021, doi: 10.1109/TPWRD.2020.3034179.

[38] H. Mirshekali, R. Dashti, A. Keshavarz, A. J. Torabi, and H. R. Shaker, "A novel fault location methodology for smart distribution networks," *IEEE Trans. Smart Grid*, vol. 12, no. 2, pp. 1277–1288, Mar. 2021, doi: 10.1109/TSG.2020.3031400.

[39] X. Lin, F. Zhao, G. Wu, Z. Li, and H. Weng, "Universal wavefront positioning correction method on traveling-wave-based fault-location algorithms," *IEEE Trans. Power Del.*, vol. 27, no. 3, pp. 1601–1610, Jul. 2012, doi: 10.1109/TPWRD.2012.2190108.

[40] C.-C. Zhou, Q. Shu, and X.-Y. Han, "A single-phase earth fault location scheme for distribution feeder on the basis of the difference of zero mode traveling waves," *Int. Trans. Electr. Energy Syst.*, vol. 27, no. 5, p. e2298, May 2017, doi: 10.1002/ETEP.2298.

[41] W. Chonglin, W. Yangyang, L. Rui, and S. Gang, "Fault location for single-phase-to-earth faults based on transient traveling wave method and artificial pulse signal injection method," in *Proc. Int. Conf. Electr. Control Eng.*, Jun. 2010, pp. 3737–3741. [Online]. Available: https://ieeexplore-ieee-org.cuarzo.unizar.es:9443/document/5629889/

[42] M. Abad, S. Borroy, D. Lopez, and M. Garciagracia, "New fault location method for up-to-date and upcoming distribution networks," in *Proc. CIRED*, 2015, pp. 15–18.

[43] J. Livie, P. Gale, and A. Wang, "Experience with on-line low voltage cable fault location techniques in Scottish power," in *Proc. 19th Int. Conf. Electr. Distrib.*, 2007, pp. 1–4.

[44] M. A. Aftab, S. M. S. Hussain, I. Ali, and T. S. Ustun, "Dynamic protection of power systems with high penetration of renewables: A review of the traveling wave based fault location techniques," *Int. J. Electr. Power Energy Syst.*, vol. 114, Jan. 2020, Art. no. 105410, doi: 10.1016/j.ijepes.2019.105410.

[45] R. Benato and A. Paolucci, "Operating capability of long AC EHV transmission cables," *Electric Power Syst. Res.*, vol. 75, no. 1, pp. 17–27, Jul. 2005, doi: 10.1016/J.EPSR.2004.11.011.

[46] C. A. Nucci, F. Rachidi, and M. Rubinstein, "Derivation of telegrapher's equations and field-to-transmission line interaction," *WIT Trans. State Art Sci. Eng.*, vol. 29, pp. 1755–8336, Jan. 2008, doi: 10.2495/978-1-84564-063-7/01.

[47] J. G. Fornas, E. H. Jaraba, A. L. Estopinan, and J. Saldana, "Detection and classification of fault types in distribution lines by applying contrastive learning to GAN encoded time-series of pulse reflectometry signals," *IEEE Access*, vol. 10, pp. 110521–110536, 2022, doi: 10.1109/ACCESS.2022.3214994.

JAVIER GRANADO FORNÁS received the B.Sc. degree in industrial engineering (specialized in industrial electronics) and the M.Sc. degree in electronics engineering (intelligent environments specialization) from the University of Zaragoza, Spain, in 1994 and 2014, respectively. He is currently pursuing the Ph.D. degree in deep learning around the classification and localization of faults in distribution lines. Since 2009, he has been a Senior Researcher with the Electronics Systems Group, CIRCE Technology Center. His main research interests include electronic design control projects around deep learning and algorithms for fault detection.

ELÍAS HERRERO JARABA (Member, IEEE) received the Ph.D. degree in engineering from the University of Zaragoza, in June 2005.

He has been a Professor with the University of Zaragoza, since 2002. In 1999, he worked in the automotive field with the Production Department, Opel Spain, for four years. Within the university, he has developed his research in the area of computer vision, and since 2012, he has been focused his interest on the field of neural networks, and more recently, in deep learning. In the meantime, he held the position of coordinator of the Smart Vehicle Initiative with the Aragon Institute for Engineering Research (I3A). He currently holds a European patent and has led to more than six projects funded in public competitions, more than 20 projects with companies, 12 indexed publications, and more than 50 contributions to international conferences. He is currently developing his research career within the research group "Human OpenWare Research Lab (Howlab)." His teaching work has focused on electronics, from its basics to power electronics, including embedded systems.

Dr. Jaraba received the 3M Award for his research in the CvLAB Research Group.

HANS BLUDSZUWEIT was born in Jena, Germany, in 1974. He received the Dipl.-Ing. degree in electrical engineering from the Technical University of Ilmenau, Germany, in 2001, and the Ph.D. degree (European Doctorate) in electrical engineering from the University of Zaragoza, Spain, in 2009. He worked as a Field Test Engineer on the sector of solar PV module production with First Solar, for one year. Since 2009, he has been a Researcher in the field of electrical systems with CIRCE, where he is currently a Technological Expert with the Smart Grid Operation Group. His activity is focused on smart grids (optimization of distributed resources, including storage and statistical analysis of Smart Meter data) and grid integration of electric vehicles, including dynamic wireless charging (e-roads).

DAVID CERVERO GARCÍA received the B.Sc. degree in industrial engineering (specializing in electric systems) and the M.Sc. degree in renewable energies and energy efficiency from the University of Zaragoza, in 2009 and 2011, respectively.

Currently, he is a Project Manager with the Electronic Systems Group, CIRCE Technology Centre. He has a deep expertise in power quality (PQ) assessment in electrical systems, data acquisition, especially in digital signal processing, developing dedicated software for measuring PQ in electrical distribution networks and the performance of renewable energy sources. His research interests include fault location and power systems monitoring, with an application in predictive maintenance. Currently, his main research field is focused on designing resonant converters for high-voltage applications.

ANDRÉS LLOMBART ESTOPIÑAN (Member, IEEE) received the industrial engineering degree from the University of Zaragoza, in 1994, and the Ph.D. degree in electrical engineering from the University of Zaragoza, in 2000.

He has been the General Director of CIRCE, since April 2016, and the former Executive Director, since January 2011. He was also a Lecturer with the Electrical Department, University of Zaragoza, from June 2003 to May 2018. In November 2011, he was designated by the Science and Innovation Ministry as the Expert of the Energy Area Committee of the7th Funding Program of the European Union, being in charge of the coordination of electricity grid topics. In CIRCE, he is in charge of the Innovation and Promotion Unit, created by himself, in May 2009. From March 2007 to March 2009, he was the Subdirector of the Institutional Relations of the Superior Polytechnic Centre, University of Zaragoza. Later, he researched the impact reduction of power electronic source grids using passive filters in the kilowatt range. From December 1994 to May 2001, he was an Associate Professor with the Electrical Engineering Department, University of Zaragoza, where he performed the following teaching activities: electric circuit theory, industrial actuation, wind energy, and renewable energy integration. He participated in more than 35 R&D+i projects; in 16 of them, he was the primary researcher. He has authored ten articles in indexed journals and more than 50 contributions to international congresses. His active participation in forums, associations, and platforms is linked to activity lines. He holds eight patents, of which seven are being exploited.

3.2 Estudio 2: Generation of Synthetic Examples Using Generative Adversarial Networks (GAN) to Extend a Database of Fault Signals on Power Distribution Lines

RESUMEN: Este estudio propone un método para obtener una base de datos extendida de señales de falla y utilizar redes neuronales para procesarlas. Debido a la dificultad de obtener suficientes señales reales, se utiliza la simulación de una red eléctrica para ampliar la base de datos mediante el uso de GAN. Esta técnica simplifica el proceso de obtención de la base de datos de señales de falla.

GENERATION OF SYNTHETIC EXAMPLES USING GENERATIVE ADVERSARIAL NETWORKS (GAN) TO EXTEND A DATABASE OF FAULT SIGNALS ON POWER DISTRIBUTION LINES

Javier GRANADO
Circe – Spain
jgranado@fcirce.es

Elías HERRERO
University of Zaragoza – Spain
jelias@unizar.es

Andrés LLOMBART
Circe – Spain
allombart@fcirce.es

ABSTRACT

The detection and classification of the type of fault is an essential technique for the improvement of electricity grids due to its potential to improve the reliability of supply and, therefore, its quality. This paper reports a method to obtain an extended database of fault signals in order to use Neural Networks (NN) to process them. The need of a large database for the training process is an inherent need for the right working of a NN. In this type of chaotic nature signals, it is impossible to record enough real ones and, even simulating is near unfeasible task due to the variety of the causes that produces faults events. The proposed solution is to obtain a short database of simulated signals from a real modelled electrical grid and extend this database by means of GAN. This technique simplifies the process to obtain the database of fault signals.

Keywords: GAN, Fault Signals, Distribution Lines.

1 INTRODUCTION

The use of neural networks are giving good results in the field of detection, classification, and localization of faults in distribution lines [1]–[4].

During the corresponding training process, a series of examples of labelled signals are shown to the Neural Network (NN). Then, NN learns certain features in order to recognize a new example shown to it. This training process typically requires tens of thousands of examples to correctly train the NN and avoid the well-known phenomenon of overfitting. When this last happens, the NN learns the few examples shown and is unable to generalise.

In distribution lines, in fault classification and location problems, obtaining a large database of real signals is a very complex process. The fault is usually a catastrophic and chaotic event (tree fall, lightning, etc.), so it is difficult to reproduce, predict, collect, and label.

Model the real distribution line with appropriate software and simulate the faults could be an option. However, obtaining tens of thousands of examples is practically unfeasible because it takes a lot of time. In addition, selecting all the different situations by hand to reproduce all possible events is an almost impossible task.

These are the main reason because data augmentation is intended to increase the number of examples. There are two basic techniques among others, by adding slightly modified versions of existing examples, or by adding synthetic examples created from existing ones. Modifying existing examples is based on applying changes such as rotations, symmetries, scaling, etc. In case of example synthesis, new examples are obtained by using generative adversarial networks (GAN).

Unlike other problems related to image classification (animal detection in photos, etc.) here, the images (Fig. 1) are a transformation [5] of temporal signals[6](Fig. 2). Classical data augmentation techniques cannot be applied since the effects over the information contained in the temporal signal would be unpredictable.

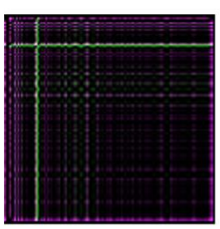

Figure 1. Original signal transformed into image.

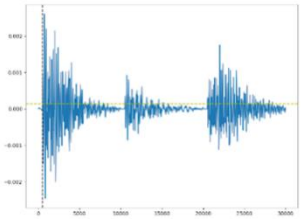

Figure 2. Original time signals

Generative Adversarial Network (GAN) is a branch of machine learning systems discovered in 2014 [7]. In GAN, two neural networks compete against each other.

For an existing database, the GAN will be trained to generate new data with the same characteristics as the training data. For example, a GAN trained with images of people can generate new images that look real to humans, with many lifelike attributes. GAN is composed of two neural networks (Fig.3), a generator and a discriminator.

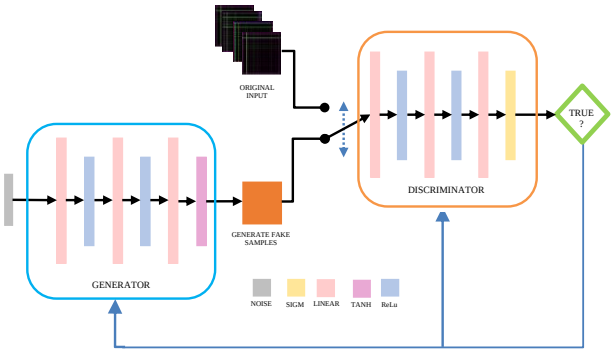

Figure 3. Architecture of the GAN

The generator produces examples while the discriminator evaluates them. Training continues until the discriminator is no longer able to determine whether the displayed example is real or generated. The training objective of the generator is to decrease the discriminator's error (i.e., to "fool" the discriminating system by creating new examples that the discriminator believes to be real).
A set of real data examples serves as a reference for the discriminator. Generally, the generator generates the examples from random information. The examples generated are then evaluated by the discriminator. Backpropagation is applied in both systems. While the discriminator becomes progressively more adept at detecting fake images, the generator system becomes progressively more adept at generating better images.
Some of the most useful applications of GANs are enhancing the resolution of images [8], modifying the appearance of an image [9][10], or generating images synthetically [11][12].
Here we find several types of GAN: Linear GAN, Convolutional GAN (CGAN) [13], Conditional GAN (cGAN) [13], even Conditional Deep Convolutional GAN (cDCGAN)[14].
In this paper, we intend to address data augmentation using GAN[15][16]. In this way, we want to introduce versatile examples. Here, it is the GAN itself during its training, which manages to extract the hidden information, and by generating each new example from noise, the GAN adds variability without losing the essence that characterizes each class (type of fault).

2 PROPOSED SOLUTION

This section explains the complete process (Fig. 4). It is divided into two parts: transformation of time signals to images and generation of examples using GAN.
In our case, we start from time signals. These signals come from the response of the electrical network to pulse injection (TDR technique). For each example, we have three signals (coming from each of the R-S-T phases of the electrical network). After digitization, we have 12,000 samples (4,000 x 3). Then, signals are transformed into images for better and easier data processing by convolutional neural networks.
The transformation used is *GAF* (Gramian Angular Field). In the GAF transformation, the time series is represented in a polar coordinate system. The amplitude of the signal is encoded as the angular cosine, and the time stamp as the radius. This information is collected in the form of a matrix in which the relationships between the different time instants can be identified. In this matrix, each element is either the cosine of the sum of the angles (GASF) or the sine of the difference of the angles (GADF). The GASF transform has the advantage over the GADF transform that the time signal can be reconstructed from the image. This property makes it possible to compare the original signals with the transformed ones.
In the process of transformation from time series to images, we can also reduce the dimensionality of the images. The algorithm used is called *PAA* (Piecewise Aggregate Approximation). With PAA, we try to reduce the dimensionality as much as possible to improve the subsequent training processes.
We have processed the images starting from their initial dimensionality (4000x4000x3) and we have progressively reduced it to a dimensionality of 128x128x3. With this reduction we have been able to reduce the training time of the GAN, as well as the subsequent processing by NN without reducing the accuracy in the classification of the different classes.

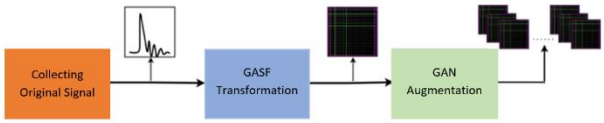

Figure 4. Process block diagram

At the end, GAN has been used to generate the extended database.
GANs are difficult neural networks to training and suffer from some inherent problems in their structure [15][16]. One of them is mode collapse. In this case, the generator learns to generate a few examples from the data distribution but fails to learn many others. In the worst case, the generator simply produces a single example.
Another typical problem with GANs is the vanishing gradient problem. This occurs when training these GANs and the gradient becomes infinitely small. This, in the worst case, can cause the neural network to stop training and evolving to the minimum.
On the other hand, and as already explained, GANs are successfully used in applications where it is required to generate examples of a very high quality, which are practically indistinguishable from the real ones. To achieve this, we would need to train GANs with complex structures (cGAN, cDCGAN, etc...).
Having said that, and having the chance to choose different alternatives, the GAN tested in this work are based on:

- Linear GAN,
- Conditional GAN (cGAN)
- Convolutional GAN (CGAN)
- Conditional Deep Convolutional GAN (cDCGAN)

In general, CGANs are more powerful for image training than linear GANs, although this power also has a trade-off in training time and parameterization difficulty.
On the other hand, Conditional GANs (cGAN and cDCGAN) have the advantage that all classes can be trained at the same time. This is done by introducing the class type as additional information to the generator.
This, a priori, is an advantage, but this type of GAN has a greater tendency to present mode collapse. In our case, we had to train a linear GAN by training each class separately.

4 RESULTS

First, we tried to implement a Conditional Deep Convolutional Generative Adversarial Networks (cDCGAN) to try to train all classes at once.
We tried first it with some known state-of-the-art database such as MNIST. With this database, the GAN converges correctly.
However, with our database, we had the problem of mode collapse. Mode collapse manifests itself because although the input of the generator is random, the generated images are always the same, i.e. the generator specializes in generating the same image of each class.
We tried to apply some of the existing techniques to avoid mode collapse[17], [18]. We try for example to adjust the learning rate of the GAN, since, as a general rule, lowering the learning rate can make the problem disappear.
Another method we tried was known as label smoothing, i.e., assigning a value of "0.9" to real labels instead of a "1". This usually makes the discriminator not too confident in its classification, which sometimes avoids mode collapse.
Another way to try to avoid the mode collapse is to implement the Wasserstein GAN, or WGAN[19], [20]. This is an extension of the GAN that seeks an alternative way to train the generator model. The modification over the GAN basically boils down to using a linear activation function in the output layer of the discriminator. Also, it uses the Wasserstein loss (RMSProp) to train the discriminator and generator instead of ADAM and SDG respectively and updating the discriminator more times than the generator.
But when applying these techniques, either the cDCGAN did not converge correctly (Fig. 5), or it converged but mode collapse occurred and generated the same image for each class.

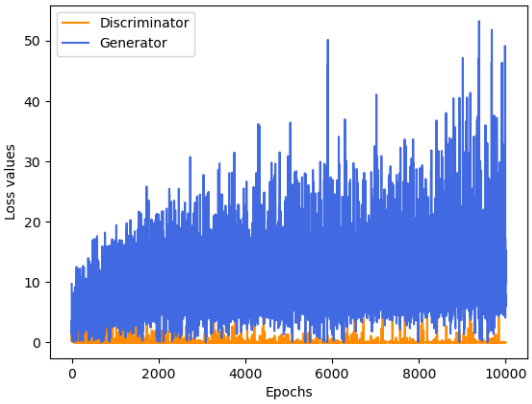

Figura.5 Training cDCGAN

We also tried to train a cGAN, i.e., a convolutional but not conditional GAN. The result was not good either. We still had mode collapse. We tried to train the cGAN without dimensionality reduction, i.e. with 4000x4000 images, to see if the problem was the loss of information in the dimensionality reduction. The problem was that GAN training with high dimensionalities is state of the art and they have convergence problems, so this didn't work either. The conclusion is that our images have little variability as they are transformed images of temporal signals very similar to each other.
In the end, we tried to train an independent linear GAN for each class with images of 128x128 dimensionality.
This finally made it possible to train all classes and generate a database of 2000 examples of each class different from each other.
For our data augmentation objective, we need to have sufficient variability to have distinct examples and we also need to be able to generate many examples in a robust way (without mode collapse). Also, it is desirable that does not require a large amount of computational cost. Thus, it has been decided to use a GAN formed by linear layers (Fig. 3) and apply a dimensionality reduction of the images that allows us to continue to successfully classify the different types of faults (128 x 128 x 3). Figure 6 shows the training of the linear GAN in which it can be seen that after the epoch 1000, the discriminator loss is around 0.5, while the generator is around 1.5. These values are typical of a correct GAN training.

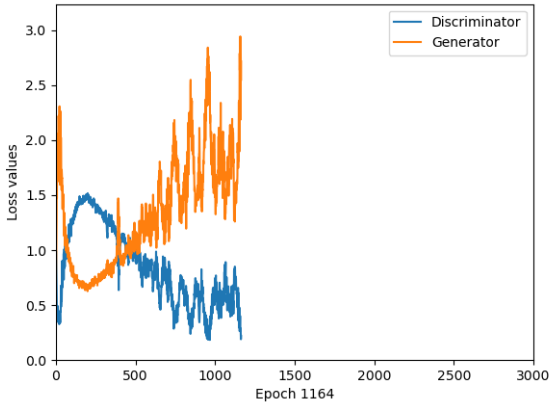

Figura.6 Training Linear GAN

The following figures show four examples of signals (images) from the original database (Fig. 7) and synthetic examples generated by the GAN (Fig. 8).

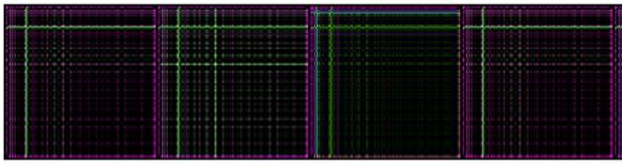

Figure 7. Original examples

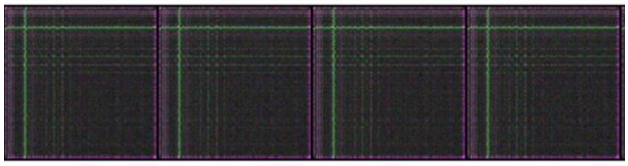

Figure 8. Synthesized examples generated by the GAN

Thus, with the generation of data augmentation by GAN, we are able to introduce versatility of examples, while maintaining the essence that characterizes each class (type of fault). In this case, it is the GAN itself during its training, which manages to extract the hidden information. We have also demonstrated that the dimensionality of the original signals can be reduced and that a very simple version of GAN (linear GAN) can be trained, avoiding the inherent problems of mode collapse in this type of neural networks.

In the literature, there are several metrics used to measure the quality with which GANs generate synthetic images. The parameters that are usually measured are:

- Creativity: non-duplication of the actual images.
- Consistency: the generated images must have the same style.
- Diversity: the generated images are different from each other.

The main parameter is called *Likeness Score* (*LS*), wich is (based on Euclidean distance) to analyse how two classes of data are mixed together.

In our case, the LS metric yields values very low, which is to be expected since, as we have said, the generated images have a very high variability respect to the original ones, which results in a low "quality" from the point of view of the LS metric.

In our experiment, we have used as metric the distance based on the *Contrastive Learning*. This metric is based on the percentage of success obtained in the classification of the different types of faults between the original images and those synthetically generated by the GAN.

We have a database of 200 original examples classified in 5 classes (0, 1, 2, 3, 4), with 40 examples of each class. In addition, a database of synthetic examples generated by our linear GAN is also available. These last are 10,000 examples also classified in 5 classes (0, 1, 2, 3, 4), with 2,000 examples for each class.

The tables below show the percentage of success in determining whether a class belongs to the class to which it is being compared. The first table (Table I) compares synthetic examples generated by GAN. Each class is compared with 384 different images from its own class and with 96 images from each of the other classes. The second table (Table II) compares original examples with synthetic examples generated by GAN. Each class is compared with 28 examples from its own class, and with 8 examples from each of the other classes.

CONCLUSIONS

Data augmentation is a widely used tool, with excellent results, in the field of machine learning. Being able to have a strongly extended training set of examples leads to more robust and better performing learning processes.

	0	1	2	3	4
0	99,73%	100%	100%	100%	100%
1	100%	99,73%	100%	100%	100%
2	100%	100%	99,73%	100%	100%
3	100%	100%	100%	100%	100%
4	100%	100%	100%	100%	100%

Table I. Comparison of synthetic examples vs synthetic examples

	0	1	2	3	4
0	96,43%	100%	100%	100%	100%
1	100%	100%	100%	100%	100%
2	100%	100%	100%	100%	100%
3	100%	100%	100%	100%	100%
4	100%	100%	100%	100%	100%

Table II. Comparison of original examples vs synthetic examples

Normally standard techniques such as rotations, scaling, etc. can be used, which unfortunately in some other cases is not possible. Therefore, GANs are becoming a very feasible option to generate these new examples, and to extend the number of training examples.

In conclusion, we can say that the proposed method manages to increase the signal database in an efficient way and solves the problem of this type of signals due to the difficulty to obtain them in field, or even simulating them by means of a model of the electrical grid.

In this article we start from a very small database of 200 examples, and finally get a set of 10,000 new examples with sufficient variability. Finally, all of this is backed up by a classification process with excellent results.

REFERENCES

[1] M. M. A. K. E. M. and H. H. M. M. Irzaei, "(PDF) Review of fault location methods for distribution power system." https://www.researchgate.net/publication/234682955_Review_of_fault_location_methods_for_distribution_power_system (accessed Jan. 05, 2023).

[2] R. J. Hamidi and H. Livani, "Traveling-Wave-Based Fault-Location Algorithm for Hybrid Multiterminal Circuits," *IEEE Transactions on Power Delivery*, vol. 32, no. 1, pp. 135–144, Feb. 2017, doi: 10.1109/TPWRD.2016.2589265.

[3] S. Wei, G. Yanfeng, and L. Yan, "Traveling-wave-based fault location algorithm for star-connected hybrid multi-terminal HVDC system," *2017 IEEE Conference on Energy Internet and Energy System Integration, EI2 2017 - Proceedings*, vol. 2018-January, pp. 1–5, Jun. 2017, doi: 10.1109/EI2.2017.8245645.

[4] L. Xie *et al.*, "A novel fault location method for

hybrid lines based on traveling wave," *International Journal of Electrical Power & Energy Systems*, vol. 141, p. 108102, Oct. 2022, doi: 10.1016/J.IJEPES.2022.108102.

[5] Z. Wang and T. Oates, "Imaging Time-Series to Improve Classification and Imputation," *IJCAI International Joint Conference on Artificial Intelligence*, vol. 2015-January, pp. 3939–3945, Jun. 2015, doi: 10.48550/arxiv.1506.00327.

[6] J. G. Fornas, E. H. Jaraba, A. L. Estopinan, and J. Saldana, "Detection and Classification of Fault Types in Distribution Lines by Applying Contrastive Learning to GAN Encoded Time-series of Pulse Reflectometry Signals.," *IEEE Access*, 2022, doi: 10.1109/ACCESS.2022.3214994.

[7] D. M. de Silva and G. Poravi, "A Review on Generative Adversarial Networks," *2021 6th International Conference for Convergence in Technology, I2CT 2021*, Apr. 2021, doi: 10.1109/I2CT51068.2021.9417942.

[8] C. Ledig *et al.*, "Photo-Realistic Single Image Super-Resolution Using a Generative Adversarial Network," *Proceedings - 30th IEEE Conference on Computer Vision and Pattern Recognition, CVPR 2017*, vol. 2017-January, pp. 105–114, Sep. 2016, doi: 10.48550/arxiv.1609.04802.

[9] J. Y. Zhu, T. Park, P. Isola, and A. A. Efros, "Unpaired Image-to-Image Translation using Cycle-Consistent Adversarial Networks," *Proceedings of the IEEE International Conference on Computer Vision*, vol. 2017-October, pp. 2242–2251, Mar. 2017, doi: 10.48550/arxiv.1703.10593.

[10] W. Chen and J. Hays, "SketchyGAN: Towards Diverse and Realistic Sketch to Image Synthesis," *Proceedings of the IEEE Computer Society Conference on Computer Vision and Pattern Recognition*, pp. 9416–9425, Jan. 2018, doi: 10.48550/arxiv.1801.02753.

[11] F. H. Kiyoiti, S. Tanaka, C. Aranha, W. S. Lee, and T. Suzuki, "Data Augmentation Using GANs," *Proc Mach Learn Res*, vol. XXX, pp. 1–16, Apr. 2019, doi: 10.48550/arxiv.1904.09135.

[12] E. Mansfield, J. Wang, J. Russell, J. Li, and C. Adams, "Data Augmentation Generative Adversarial Networks," Nov. 2017, doi: 10.48550/arxiv.1711.04340.

[13] M. Li, J. Lin, Y. Ding, Z. Liu, J.-Y. Zhu, and S. Han, "GAN Compression: Efficient Architectures for Interactive Conditional GANs," *IEEE Trans Pattern Anal Mach Intell*, vol. 44, no. 12, pp. 9331–9346, Nov. 2022, doi: 10.1109/TPAMI.2021.3126742.

[14] F. Zhu, M. He, and Z. Zheng, "Data augmentation using improved cDCGAN for plant vigor rating," *Comput Electron Agric*, vol. 175, p. 105603, Aug. 2020, doi: 10.1016/J.COMPAG.2020.105603.

[15] T. Salimans *et al.*, "Improved Techniques for Training GANs," *Adv Neural Inf Process Syst*, vol. 29, 2016, Accessed: Jan. 06, 2023. [Online]. Available: https://github.com/openai/improved-gan.

[16] A. Srivastava, L. Valkov, C. Russell, M. U. Gutmann, and C. Sutton, "VEEGAN: Reducing Mode Collapse in GANs using Implicit Variational Learning," *Adv Neural Inf Process Syst*, vol. 2017-December, pp. 3309–3319, May 2017, doi: 10.48550/arxiv.1705.07761.

[17] M. Heusel, H. Ramsauer, T. Unterthiner, B. Nessler, and S. Hochreiter, "GANs Trained by a Two Time-Scale Update Rule Converge to a Local Nash Equilibrium," *Adv Neural Inf Process Syst*, vol. 2017-December, pp. 6627–6638, Jun. 2017, doi: 10.48550/arxiv.1706.08500.

[18] Y. Qin, N. Mitra, and P. Wonka, "How does Lipschitz Regularization Influence GAN Training?," *Lecture Notes in Computer Science (including subseries Lecture Notes in Artificial Intelligence and Lecture Notes in Bioinformatics)*, vol. 12361 LNCS, pp. 310–326, Nov. 2018, doi: 10.48550/arxiv.1811.09567.

[19] T. Miyato, T. Kataoka, M. Koyama, and Y. Yoshida, "Spectral Normalization for Generative Adversarial Networks," *6th International Conference on Learning Representations, ICLR 2018 - Conference Track Proceedings*, Feb. 2018, doi: 10.48550/arxiv.1802.05957.

[20] A. Karnewar and O. Wang, "MSG-GAN: Multi-Scale Gradients for Generative Adversarial Networks," *Proceedings of the IEEE Computer Society Conference on Computer Vision and Pattern Recognition*, pp. 7796–7805, Mar. 2019, doi: 10.48550/arxiv.1903.06048.

3.3 Estudio 3: Detection and Classification of Fault Types in Distribution Lines by Applying Contrastive Learning to GAN Encoded Time-series of Pulse Reflectometry Signals

RESUMEN: Este estudio propone un nuevo método para detectar y clasificar faltas en líneas de distribución utilizando reflectrometría de pulso en el dominio del tiempo (TDR). Se inyectan pulsos de alta frecuencia en la línea y se analizan las señales reflejadas para determinar el estado de la línea. Se utiliza una base de datos inicial obtenida mediante simulaciones en PSCAD y se procesa utilizando redes neuronales convolucionales (CNN). Para superar la falta de ejemplos originales, se utilizan redes neuronales generativas adversarias (GAN) para sintetizar nuevos ejemplos y ampliar la base de datos. La combinación de redes Siamesas y GAN permite la clasificación de las señales de falta utilizando ejemplos sintéticos para entrenar y validar, y ejemplos originales para probar la red. Esto resuelve el problema de la escasez de ejemplos originales en señales de fenómenos naturales difíciles de obtener y simular.

IEEE Access
Multidisciplinary ⋮ Rapid Review ⋮ Open Access Journal

Received 29 September 2022, accepted 12 October 2022, date of publication 14 October 2022, date of current version 21 October 2022.

Digital Object Identifier 10.1109/ACCESS.2022.3214994

RESEARCH ARTICLE

Detection and Classification of Fault Types in Distribution Lines by Applying Contrastive Learning to GAN Encoded Time-Series of Pulse Reflectometry Signals

JAVIER GRANADO FORNÁS[1], ELÍAS HERRERO JARABA[2], (Member, IEEE), ANDRÉS LLOMBART ESTOPIÑAN[1], (Member, IEEE), AND JOSE SALDANA[1], (Senior Member, IEEE)

[1]CIRCE Technology Center, 50018 Zaragoza, Spain
[2]Department of Electronic Engineering and Communications, University of Zaragoza, 50018 Zaragoza, Spain

Corresponding author: Javier Granado Fornás (jgranado@fcirce.es)

This work was supported by the Interoperable solutions for implementing holistic FLEXIbility services in the distribution GRID (FLEXIGRID) Project from the European Union's Horizon 2020 Research and Innovation Programme under Grant 864579.

ABSTRACT This study proposes a new method for detecting and classifying faults in distribution lines. The physical principle of classification is based on time-domain pulse reflectometry (TDR). These high-frequency pulses are injected into the line, propagate through all of its bifurcations, and are reflected back to the injection point. According to the impedances encountered along the way, these signals carry information regarding the state of the line. In the present work, an initial signal database was obtained using the TDR technique, simulating a real distribution line using (PSCAD^{TM}). By transforming these signals into images and reducing their dimensionality, these signals are processed using convolutional neural networks (CNN). In particular, in this study, contrastive learning in Siamese networks was used for the classification of different types of faults (ToF). In addition, to avoid the problem of overfitting owing to the scarcity of examples, generative adversarial neural networks (GAN) have been used to synthesise new examples, enlarging the initial database. The combination of Siamese neural networks and GAN allows the classification of this type of signal using only synthesised examples to train and validate and only the original examples to test the network. This solves the problem of the lack of original examples in this type of signal of natural phenomena which are difficult to obtain and simulate.

INDEX TERMS Artificial Neural Networks (ANNs), deep learning, siamese networks, generative adversarial neural networks (GAN's), fault classification, fault detection, transmission lines.

I. INTRODUCTION

The automatic detection and classification of short circuits (faults) in distribution lines (especially in low-voltage installations) is a hot research topic with significant challenges ahead. Several techniques are available for the detection and classification of the type of fault (hereinafter referred to as ToF) [1], [2]. One is the analysis of the event signal (high-frequency spike) that appears when a fault occurs somewhere in the network [3], [4], [5]. Owing to the catastrophic and chaotic nature of these events (faults), the acquisition, simulation, and analysis of these types of signals represent a very difficult problem.

Another way to detect and classify the ToF is to analyse the response to the injection of high-frequency pulses into the power grid. The different responses of the grid to these injected signals, owing to the different types, makes it possible to classify these faults.

This study presents an analysis of these signals using neural networks. The objective was to solve the main problem

The associate editor coordinating the review of this manuscript and approving it for publication was Fahmi Khalifa.

of a lack of original examples. Finding a method to train a neural network model to classify faults with good accuracy and proper generalisation.

To understand this problem, it is necessary to know that faults in distributed lines [6], [7] depend on a physical phenomenon which, as mentioned above, produces a catastrophic event in the electrical network (short circuit of one or several phases to earth). This phenomenon has a chaotic and random nature (falling trees, lightning, fire, etc.). Therefore, it is a major handicap to obtain easily available real signals. By contrast, the training of a neural network [8] requires a large number of examples (typically tens of thousands). Neural networks learn to discover a particular pattern within a set of examples through a training process. In this process, the weights of the network were adjusted. Each time a new example is taught, the output of the network tries to ''adjust'' a little bit more and even closer to the real output (label). This fact makes it necessary to have a large number of examples that allow the network to generalise the desired pattern well. The objective is avoiding to ''learn'' just some few examples, which is known as *overfitting* [9].

On the other hand, the technique frequently used to deal with this phenomenon is to model mathematically the electrical network [10]. Using this model, we can produce a database of fault signals for certain scenarios and locations. However, even so, it is always a very complex task to obtain a database with typically tens of thousands of fault signals that will allow us to train a neural network with sufficient reliability; for instance, there may be a wide range of cases that produces each ToF. This implies that the electrical network may be in a very diverse state, even for the same ToF. Therefore, it is difficult to simulate all possible random conditions that would give rise to the same ToF.

However, a more plausible solution is to start from an existing database which includes several simulated faults. This database, although insufficient (hundreds of examples), is representative of the problem that needs to be solved. More details of this database are provided in subsequent sections.

It is at this point that our work starts by solving the problem of the limited amount of training data using a generative adversarial network (GAN) [11].

A GAN consists of two neural networks that are trained simultaneously. One of them, called the *Generator*, can generate an example from a random input (noise) of a certain dimension. The generated example is used as an input for another network, called the *Discriminator*. The *Discriminator*, on the other hand, receives these so-called *Fake* examples, along with others, from the original database. The latter, therefore, will be correctly labelled *Real* examples. The *Generator* attempts to generate more realistic examples, and the *Discriminator* attempts to identify whether an example is *Real* or *Fake*. With this ''zero-sum'' game, both networks are trained, and this process ends when the *Discriminator* is unable to tell whether the example generated by the *Generator* is *Real* or *Fake*.

From that point on, the *Generator* can be used to generate examples of this type. These have the particularity of having the main information that characterises them as belonging to that type. However, each example is different from the others because it is generated from a random signal (noise).

A final problem we will face is that although these fake images are very similar to the originals, they will not have the same distribution in common. This leads to the fact that a ''standard'' network, even if it is sufficiently powerful, will not be able to generalise well between different distributions.

This fact has generally been addressed in other studies by mixing the data from both distributions to enable the network to learn both distributions. In our case, on the contrary, we will tackle the problem using Siamese networks [12], [13], thus exploiting their best feature: adapting well to different distributions.

II. ENVIRONMENT

The new challenges facing modern society have resulted in an increasingly important electrification of the energy system with a growing role in distribution networks. It is therefore necessary to prepare these infrastructures so that new challenges will be faced in the future, including the installation of multiple distributed generation resources.

The detection and classification of faults in electricity grids [14], as well as their localisation, are considered essential requirements to achieve the objective of implementing the smart grid concept in electricity grids. Unfortunately, the locating task is a truly complex challenge, but it is also often an arduous task that involves the movement of specialised personnel with ground or aerial means across the entire affected section. This is the main reason because the automatic location of fault systems is very worthwhile and is the essence of this article.

Currently, a widely used option is to minimise the impact of outages by introducing self-healing mechanisms [15]. In any case, the use of this type of mechanism implies that they are strongly meshed (radial and redundant topology) and are able to isolate a faulty section until the problem is solved without the need for the entire network to be out of service. These faults are usually due to short circuits between one of the phases and the earth or between different phases. It should be borne in mind that as all the sections of a network are connected in parallel, a short circuit is transferred to the entire network that is ''connected'' to that section. Once the protections of the corresponding section closest to the fault are opened, leaving that section isolated, it must be possible to detect the fault and its type as well as to locate the distance to it as accurately and quickly as possible.

Alternatively, in some lines (high-voltage and medium-voltage distribution lines), there are fault passage detectors [16]. These detectors continuously monitor the voltage and current of the network. When a fault occurs, the device detects it and can supply this signal as an input for the fault locator system. However, these types of detectors are not usually deployed in low-voltage lines because of their high

cost; therefore, the detection and classification of faults is undoubtedly very useful information as a preliminary step to locating them.

In this article, our main objective is to address the task of automatically detecting/classifying faults, which is a preliminary work to solve the bigger problem of localisation, while being aware that both are parts of the same solution and have to work together.

We use neural networks to obtain promising results from the time series obtained from certain captured signals. The physical principle used to obtain these signals is time-domain reflectometry (TDR) [17], [18]. It consists of performing periodic pulse injections on the line in each of the phases of the network (R-S-T) so that the electrical response of the network is updated frequently (which will be explained in detail below). When a fault occurs, the returned signal carries implicit information regarding the ToF that has occurred. This information is used by a trained neural network to classify faults that have occurred and classify them properly.

When TDR is employed, the pulses injected into each of the phases travel throughout the network and, at each impedance change (node, junction, etc.), part of the pulse continues its journey, and another part is reflected. This reflection of the pulses makes it possible to record at the injection point all the signals that ''return'' after ''bouncing'' through the different bifurcations of the network. These pulses carry embedded information regarding the network status. When the network is operating normally, the information from the signals is different from the information they carry when a fault has occurred, and this is precisely the information that the neural network is able to extract to determine the ToF that has occurred.

III. STATE OF THE ART

As discussed in the previous section, the detection/classification process and the localisation process are part of a more global process which would be the localisation and interpretation of faults in electricity distribution networks. In other words, they represent two different phases of the same process.

Having said that, we wanted to give a more general approach to our state of the art, and in the following, we will not only review the state-of-the-art classification methods, but also provide a summary of the localisation methods (outside the scope of this publication).

A. METHODS FOR FAULT CLASSIFICATION

In this section, we show state-of-the-art fault detection/classification. According to [19] and, [20] it comprises three major groups.

- Prominent techniques
- Hybrid techniques
- Modern techniques

Prominent techniques are most commonly used for fault classification and are further divided into three subgroups. One of the techniques that falls under this group is numerical tools based on wavelet transform (WT).

In this technique, the key is to choose a ''*mother wavelet*'' and then perform checks using versions of this WT. The WT can separate the signal into frequencies that can then be analysed with the help of multi resolution analysis (MRA). For example, it is possible to use discrete wavelet transform (DWT) to classify faults once the fault currents are known at a given location [21].

On the other hand, but also in the same group, artificial neural networks (ANN) are usually used to tackle with this problem. These types of systems can be trained by showing labelled examples to learn the features common to that class. These trained systems can then classify the new example shown to them.

There are some experiences of this technique implemented on MATLAB software to notice the fault on transmission lines. The output of the Simulink model was used to train the ANN to identify faults in transmission systems [22].

Also, under this group, efforts have been made to address this problem by means of Fuzzy Logic. The fuzzy-logic technique uses an easy relationship between the input and output variables. Therefore, the fuzzy logic technique performs simple control to deal with numerous issues, especially when the numerical model is not well known or is difficult to solve.

There are strategies for investigating overhead line failures based on a fuzzy system. For example, by comparing the s-transform and wavelet transform [23], it can be concluded that the fuzzy decision tree (DT) based on the s-transform provides accurate fault classification.

Hybrid techniques attempt to compensate for the shortcomings of separate methods. Neuro-fuzzy techniques have also been found in this group. These neural systems have attempted to adapt to changing situations. The combination of fuzzy inference systems that link human learning and performance approaches with certain improvement strategies has led to this technique.

One type of combination is the Stockwell transform (ST) and multilayer perceptron neural network (MLP-NN) / FFNN [24], [25] tested in a simulated IEEE 13-node test feeder. IEEE 13-node is a very small circuit model used to test common features of distribution analysis software. In the proposed technique, the three-phase current waveforms are measured from different points and then processed using ST to extract statistical features. The features are later fed into the MLP-NN / FFNN system to detect and classify the faults.

Another type of system that combines techniques is wavelet and ANN techniques. Wavelet and ANN techniques combine the features of a wavelet approach and an artificial neural network to obtain better results in fault classification. Some work has been carried out on fault classification using current signals used for thyristor-controlled series-compensated transmission systems by integrating the DWT and ANN algorithms [26].

On the other hand, the combination of wavelet and fuzzy logic is used to decompose the output signals of the simulated power grid. These output signals were then used as inputs to the fuzzy-logic block. The fuzzy logic block has the particular rules used for this example that result in the type of fault.

In [27], a method that uses the mother wavelet Daubechies4 (db4) and a combination of DWT and fuzzy logic to classify faults was developed.

Finally, wavelet and neuro-fuzzy techniques [28] can be mixed for fault detection and classification using wavelet MRA coefficients only. The fault location for a series-compensated transmission system using WT and ANFIS was developed in [29].

Modern techniques include support vector machines. This is a technique for learning separation functions in classification tasks (pattern recognition). This technique was based on statistical learning. Therefore, the input vectors were mapped nonlinearly into a high-dimensional feature space. This has been effectively applied to many classification problems, for example, by combining the SVM and wavelet techniques used to detect and classify fault types [30].

Another group is the genetic algorithm. Genetic algorithms (GA) work with variable encoding. (GA) uses a population of points at a time, in contrast to the single-point approach of traditional optimisation methods. It has been proposed that some methods contain a pre-processing unit that depends on both the DWT and GA, in which the DWT has been used to extract characteristic features from the input current signal [31].

In addition, we find Euclidean distance-based methods for this group. The Euclidean distance between successive current samples can be used for power-line fault detection and to identify the faulty phase [32].

Focusing on neural networks, which is the technique used by us, we have found some additional articles that have special relevance for the work developed in this paper:

Some studies have used neural networks to process power line voltage and current signals to classify faults [33], [34], [35], [36], [37]. The voltages and currents were digitised to form the input to the neural network. Also, there are some works to making detection and location of aged cable sections in underground lines [38]. In this case, the transfer function of the cable is used as the input of the CNN.

Some studies have also been conducted on fault detection, attempting to extrapolate the voltage values from several simulated power grids. These values were used to train a neural network to detect faults in a real electrical network [39].

We have found some studies in which convolutional neural networks (CNN) were used for processing time series. The fault signals are time-series signals, so this kind of work is very relevant for us. In particular, EEGNet, a compact CNN for the classification and interpretation of EEG-based signals (electroencephalography EEG)), has been used to classify this type of signal [40].

Another interesting work is the processing of the time signals of partial discharge phenomena in power grids using image transformations (scalogram) [41]), in which the nature of the signals is very similar to our own. The transformation of this type of signal into images allows it to be processed by convolutional neural networks (CNN).

This type of neural network provides excellent results in image processing.

Another type of transform of time signals to images presented in the literature is the Gramian angular fields (GAF) transform [42].

We studied this transformation in the present study to use them with our signals.

The state of the art of deep learning includes publications that discuss the use of a special type of network called a generative adversarial network (GAN). Using these GAN, synthesised examples can be generated from a limited database. In our case, we have the problem of the scarcity of examples, so we can probably use this type of neural network to expand our database of signals of the transients produced in the electrical grid in fault [43], [44].

As has been shown, in the literature, there are several publications proposing the use of Neural Networks for the detection of faults and other phenomena of a similar nature in electrical distribution networks.

The possibility of being able to detect and classify the ToF by injecting periodic pulses into the network is currently state-of-the-art and can be a great help as a preliminary step in locating faults in automatic systems.

B. METHODS FOR FAULT LOCATION

Two state-of-the-art techniques are available for locating faults in power lines.

- Impedance measurement
- Methods based on travelling waves

1) IMPEDANCE MEASUREMENT

The first technique involves measuring the impedance of the line at the fundamental frequency from a point on the network. The point at which it occurs can be calculated by observing how it varies when a failure occurs.

Fault location in double circuit power networks is presented in [45]. In this paper, the new method considers the mutual effect of double circuit lines It has been tested over IEEE 13-node test feeder.

However, although this method works well for transport grids because it is generally simple with no bifurcations [46], it does not yield good results in distribution lines. In these lines, there are numerous bifurcations, and it is not possible to equip each section with a detector because of the high cost.

However, the measurement of these networks from a single point results in a large error because of the lack of proportionality between the impedance value and the distance caused by the multiple bifurcations of the network.

2) METHODS BASED ON TRAVELLING WAVES

Methods based on travelling waves are based on the propagation of waves through conductors. These methods are based

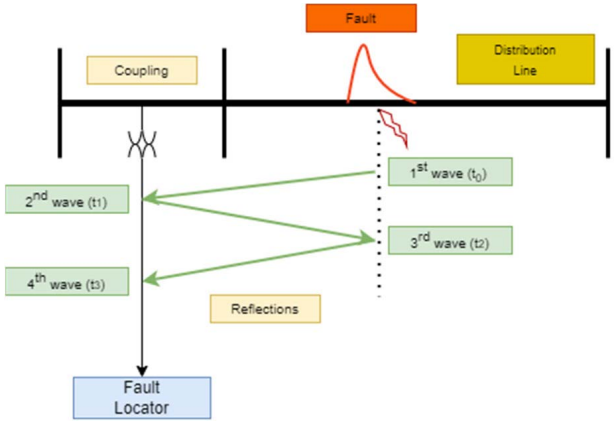

FIGURE 1. Fault location using the travelling wave of the spike event principle.

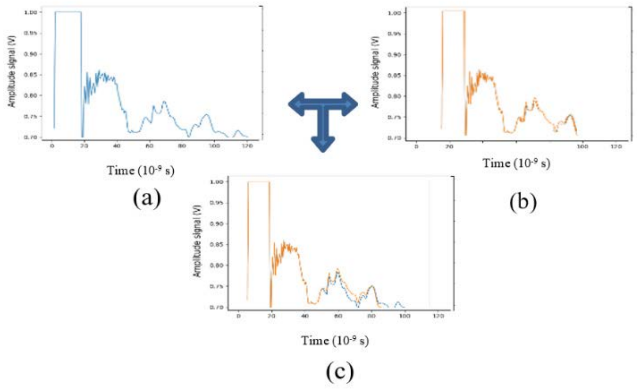

FIGURE 2. Pre-fault signal (a), Fault signal (b), comparison of both signals (c).

on the well-known telegrapher equations. One of the techniques within this group consists of measuring the bounce of a high-frequency signal that appears when a failure event occurs [47]. Short circuits caused by faults produces a high frequency transient that travels through the network (Fig 1).

This technique has provided good results in transportation lines where the use of two devices, one at each end of the section to be monitored, is widespread.

However, in distribution lines with many bifurcations, it is not possible to instal a device at each node because of the high cost.

Another difficulty lies in the time synchronisation that must exist between the equipment for the calculation of the distance and the prior knowledge of each section of the lines.

Other travelling wave methods are based on the injection of a signal and the analysis of the electrical response of the system. Following the telegrapher's equations, these signals undergo reflections at each location impedance change, as well as attenuations and distortions, until they return to the starting point. The occurrence of a fault implies a change in the characteristic impedance such that localisation is possible, at least in theory.

This technique is known as time-domain reflectometry (TDR). In distribution lines, the biggest challenge that TDR must overcome is resolving the multiple reflections caused by shunts, which complicates the analysis of the electrical response of the system. Thus, [48] it is proposed to inject through a healthy and faulted phase, and then perform a modal transformation to decouple the three-phase signals (using the Karrenbauer transformation matrix). The problem with this methodology is that it requires a healthy phase, which is not always available (three-phase faults), and that the injected pulse must have too high the amplitude (high voltage), which requires the network to be de-energised.

Techniques have also been proposed to measure the travel time of transients generated by the fault itself and by an injected signal. Later, the comparison of both allows the localisation of the fault to be calculated [49]. The method is accurate at the simulation level; however, it requires a high sampling rate (the use of the wavelet transform is proposed). In addition, it is not possible to locate all the faults because it is required that the occurrence of the fault temporally coincides with the high part of the sine wave cycle in order to have the detection capability.

Another proposed technique based on TDR consists of performing a periodic injection on the line in a pre-fault state so that the electrical response of the network is updated frequently. When a fault occurred, the injection was repeated, and the responses were compared (Fig. 2). Thus, an attempt can be made to locate the fault from the first point of divergence between the two signals [17], [47], [50], [51]. In the figure, it can be observed that the signals begin to diverge at approximately 50×10^{-9}s.

The pre-f ault signal (line response to pulse injection when the fault has not yet occurred) and the fault signal (line response to pulse injection when the fault has already occurred) are almost the same until the pulse reaches the point where the fault is located. It is this phenomenon the one that is exploited in the TDR technique to locate the fault and, in our case, to detect and classify the fault.

Regardless of the type of fault, the pre-fault and fault signals begin to differ from the moment they reach the point where the fault has occurred

3) USE OF FAULT PASSAGE RELAYS TO DETECT THE FAULT

In medium-voltage lines (distribution lines/15 kV to 20 kV), there are devices in transformer substations called fault passage relays. These devices monitor the voltage and current in each phase and detect when a fault occurs in any phase. Once the fault passage relays warning that a fault has occurred, the locating system can operate with certainty that the line is indeed faulted. Protection systems are alerted, and they can open the section of the line where the fault is located until the problem is resolved (fault-cleared).

However, in low-voltage distribution lines (230 V ac), these devices usually do not exist, and as there are large numbers of bifurcations, the installation of many devices would be unfeasible.

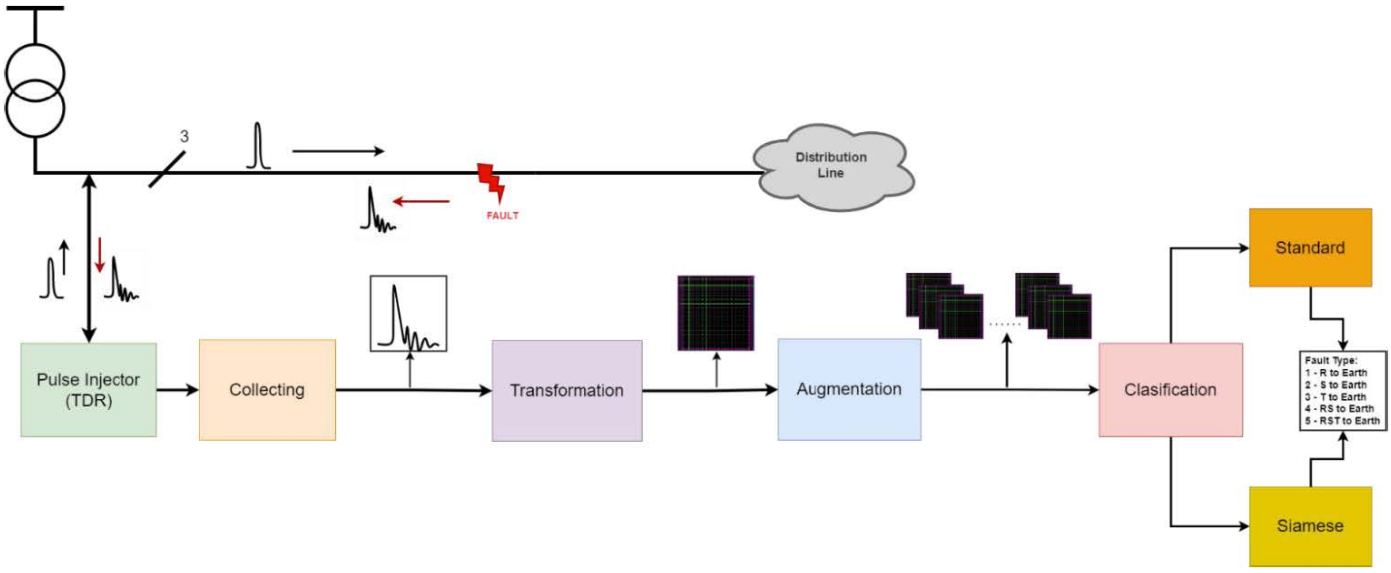

FIGURE 3. Methodology block diagram.

C. STRUCTURE OF THE PAPER

This paper aims to demonstrate the use of the pulse injection technique (TDR) for fault detection and classification as a preliminary step in fault localisation.

For this purpose, neural networks are used, which are trained to classify the signals obtained as a response of the electrical grids to the injected signals.

IV. METHODOLOGY

This section describes the proposed methodology based on the injection of signals into the distribution line and the analysis and classification of the received bounces. The methodology, including the pulse injection and subsequent transformations, is illustrated in Fig. 3. The following subsections explain the different steps of the methodology in detail.

To obtain a set of examples with which the neural network can be trained, the electrical grid of interest is modelled, as well as the injector with which the pulses are produced in each of the phases.

In this study, a real electrical grid was modelled using PSCAD^{TM}software. Faults at different locations as well as the responses to the injected signals were simulated. Despite being able to simulate a large number of examples (tens or hundreds), obtaining a large database to train a neural network typically requires tens of thousands of examples. A large number of examples allow the generalisation of the problem and prevent the network from learning examples (known as overfitting).

Based on the above, the contribution of the present paper is threefold:

1) To demonstrate that there is sufficient information embedded in the signals reflected by the network by injected pulses (TDR), and that it can be extracted to detect and classify them by type.
2) To demonstrate that with the applied methodology of GAN, it is possible to generate high-quality examples of synthesized signals and solve the problem of the scarcity of original examples of this type of signal.
3) To propose a methodology for the union of GAN and Siamese networks (a type of neural network that is explained in detail below). With this methodology, the accuracy improves dramatically when training with only synthetic examples.

A. COLLECTING PHASE: TDR SIGNALS

The first process consists of creating a database with signals obtained using the software (PSCAD^{TM}). To do this, a real electrical network was modelled beforehand, and a series of five fault types was simulated at different points in the distribution line:

- Fault type 1: Short circuit between R to Earth.
- Fault type 2: Short circuit between S to Earth.
- Fault type 3: Short circuit between T to Earth.
- Fault type 4: Short circuit between R-S to Earth.
- Fault type 5: Short circuit between R-S-T to Earth.

The procedure followed, based on the time-domain reflectometry (TDR) technique, consists of injecting short-period pulses (∼10 ns) separated every few seconds (e.g. every 5 s). It should be noted that these pulses were injected into each of the three phases (R-S-T in a three-phase system).

According to the physics of transmission lines, these pulses travel through the network and are reflected at every bifurcation; therefore, some of them are bounced back. The magnitude of these reflections depended on the impedance of the line at each bifurcation.

As shown in Fig. 4, the pulses were injected into each phase with a time lag to allow the signal to be extinguished and therefore, to prevent the induction of the pulses into other phases.

Injection and reading of the response signal were performed at the same physical point on the line. In such a way that as soon as the pulse is injected, the response signal

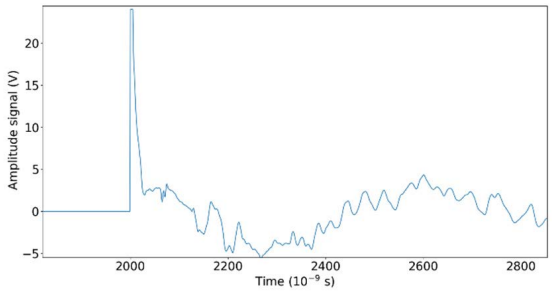

FIGURE 4. Detail of the injected pulse and the grid response during the very first moments in one phase.

received by the line starts to be digitised. When the pulse encounters a point on the line at fault (short circuit), the impedance value at that point changes. The returning signal carries information about the impedance change at that point.

This technique is suitable for high-, medium-, and low-voltage distribution lines. However, its use is most relevant for low-voltage lines, as fault passage relays are not normally **installed** because of high installation costs.

In this study, the injected signals were sampled in a simulator at 100 Msps (Mega samples per second). For each of the three injected signals (R-S-T), approximately 40 μs were digitised, after which the signal was practically extinguished. Thus, the total sampling time for the three phases was 40 μs $\times$ 3 = 120 μs. At the indicated sampling rate, 12,000 digitised values (parameters) were obtained, which could be used as input to the neural network.

B. TRANSFORMATION PHASE: FROM TIME SIGNALS TO IMAGES

Currently, in the state of the art, there are several examples of time-series problems that are treated very satisfactorily by Convolutional Neural Networks through their prior transformation from time series to images [41], [42], [52].

Therefore, a standard technique is to convert a time series into images for better and easier data processing. For instance, in [52], the Gramian Angular field (GAF) transform was used to transform the time series into images.

In the GAF technique, we represent the time series in a polar co-ordinate system instead of typical Cartesian coordinates. Here, the amplitude of the signal is encoded as the angular cosine, and the timestamp is the radius, as shown in Equation (1). This information is gathered in the form of a matrix in which the relationships between different time instants can be identified. In this matrix, each element is the cosine of the summation of angles (GASF) (2) or the sine of the difference of the angles (GADF) (3).

$$\begin{cases} \varphi = arccos(\tilde{x}_i), & -1 \leq \tilde{x}_i \leq 1, \tilde{x}_i \in \tilde{X} \\ r = \dfrac{t_i}{N}, & t_i \in \mathbb{N} \end{cases} \tag{1}$$

$$GASF = \left[cos\left(\varphi_i + \varphi_j\right)\right] \tag{2}$$

$$GADF = \left[sin\left(\varphi_i - \varphi_j\right)\right] \tag{3}$$

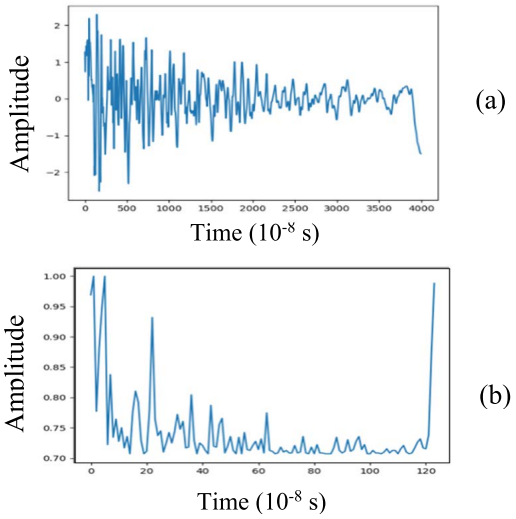

FIGURE 5. Comparison of (a) an original time-series signal with (b) a 128-dimension GASF matrix recovered as time-series signal.

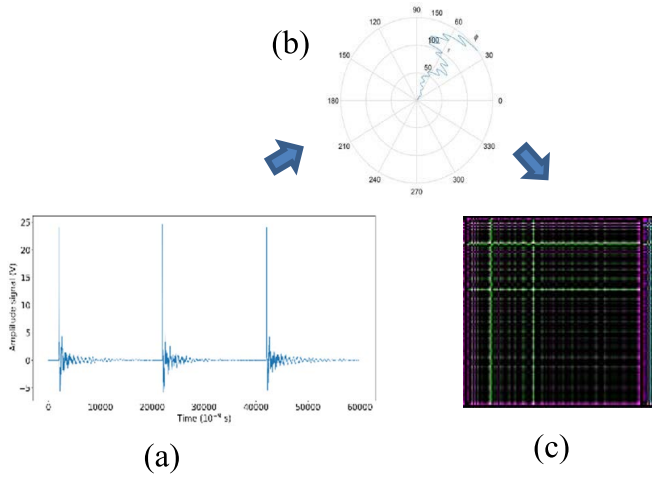

FIGURE 6. Encoding of the fault temporal signal (a) by transform into a polar coordinate system (b) by (1) and finally calculate its GASF image (c) with (2) and (3). (Numbers in brackets refer to equations).

Applying this technique to each phase (R-S-T), we digitised 4,000 samples. In total, we have 12,000 samples (4,000 $\times$ 3), which leads to high dimensionality in the output matrix of the GAF transformation. To reduce this dimensionality, [17] an algorithm called *Piecewise Aggregate Approximation* (PAA) was proposed in [38]. First, we use the PAA algorithm to reduce the dimensionality to 128 (the choice of this parameter is justified below in the "Results" section). After applying PAA, GASF is applied to obtain a 128 $\times$ 128 $\times$ 3 channel matrix, where each channel corresponds to the signal of each of the three phases of the distribution line (R-S-T). As demonstrated in [52], the GASF transformation has an advantage over the GADF transformation in that the temporal signal can be reconstructed from the image (Fig. 5). This property will allow us to compare the original signals with the "reduced" ones (Fig. 6).

Once the signals have been adapted in such a way, the new format can be used in subsequent processing phases.

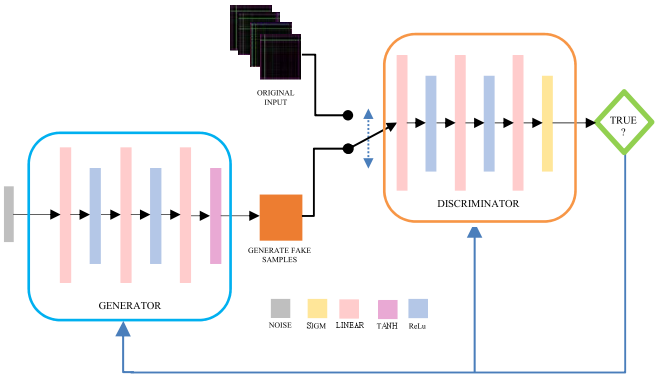

FIGURE 7. GAN generator and discriminator layers structure.

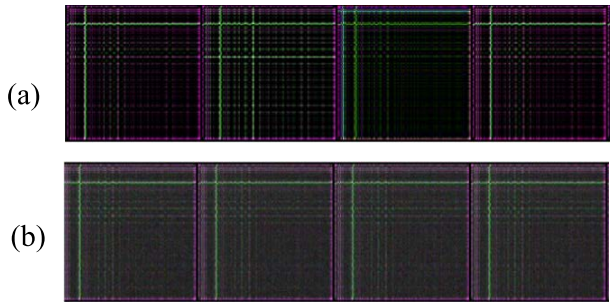

FIGURE 8. Appearance of the original GASF signals (a) and synthesized by the GAN (b) once the GAN has been trained. It can be seen that they are very similar even to the naked eye.

C. DATASET AUGMENTATION PHASE: GAN

At this stage, our database was converted to a GASF image database. However, owing to the problem discussed above and the difficulty of obtaining more examples quickly and easily, the sample set had a limited size of 200 signals/images that included five types of faults. Thus, only 40 samples were available for each class.

Because our next phase will be automatic classification, a very small number of samples will be a real handicap, and it is well known that any learning algorithm highly depends on a large training dataset.

This issue is common in many cases where data extraction is extremely difficult, and in some cases, becomes impossible. As previously mentioned, simulating tens of thousands of examples is unfeasible because of the simulation time required. Another related problem is the need to manually adjust the parameters to generate diverse fault types. A wide range of cases can occur due to the stochastic nature of the phenomenon for each ToF. Therefore, we used GAN to generate synthetic examples, thereby increasing the initial database.

As we have seen, dimensionality reduction leads to a substantial reduction in training time and allows for easier implementation of GAN. We have tested different types of GAN: Convolutional GAN (CGAN) [53], Conditional GAN (cGAN) [54], even Conditional Deep Convolutional GAN (cDCGAN) [55]. We did not obtain satisfactory results due to the well-known problem of convergence of this type of Neural Networks known as "*mode collapse*." This problem causes the GAN to generate examples of a limited number of types.

Finally, we generated examples with a simpler GAN of linear layers, training each type separately with an independent GAN. By simplifying the GAN, we achieved convergence and obtained a database of 10,000 examples (2,000 examples for each ToF). Although we have achieved this at the cost of having a large number of parameters (104,306,000), we have prioritized the ease of training over the GAN optimization.

The GAN consists of a generator (D) and discriminator (D), as shown in Fig. 7. The generator has a random signal (noise) as input, which is used by the generator to produce new output images of the required dimension (*Generated sample*) ($128 \times 128 \times 3$).

TABLE 1. % examples used.

TRAINING	VALIDATION	TESTING
100%	100%	100%
SYNTHETICS	SYNTHETICS	ORIGINAL

On the other hand, the Discriminator is presented with original images (*Real samples*) and images generated by the Generator (*Generated samples*).

The Discriminator has to try to label them as "*True*" or "*False*". The successive training of the generator and discriminator ends once the discriminator is not able to distinguish the generated examples from the real ones. At this point, the generator can be used to produce as many examples as necessary (Fig. 8).

D. CLASSIFICATION PHASE: FAULT TYPES

Finally, at this stage, we have a database of "synthetic" GASF data (*Generated samples*) produced with the help of GAN, and a set of "original" data (*Real samples*) obtained from the simulation.

Usually, the training, validation, and testing data are split into a mixture of *Generated* and *Real samples* to achieve measurable results and improvements. For example, in, [44] the authors proposed using mixtures of no more than 50% of *Generated samples*.

However, we have a database of very few examples (200), and we cannot train the neural network with 200 original examples + 200 synthetic examples (400 total), as they are still too few examples to train a neural network.

To avoid this situation, we have proposed a different training solution, in which the distribution of training, validation, and testing data is made up as shown in Table 1. The training and validation sets are composed only of *Generated* data, and the test set is built only with *Real samples*.

As a first check, we verified the results obtained using the well-tested networks. From the simplest to the most complex, LeNet, AlexNet, and ResNet18 were used in this work. With these classifiers, the results were very poor, as expected and as previously reported.

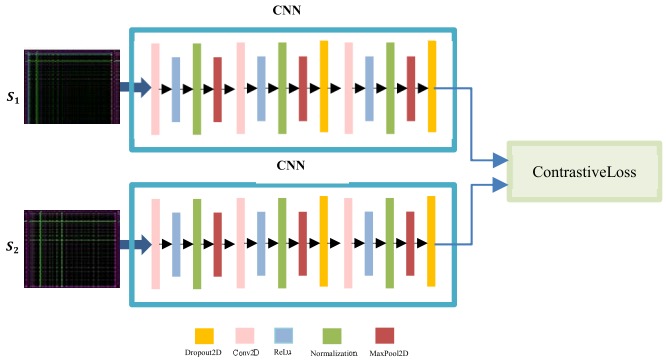

FIGURE 9. Architecture of siamese convolutional networks which are joined by the loss function in (4).

All these tests lead to the conclusion that the model cannot be generalized. The model only learns the distribution of the training examples (*Generated*) but fails to work with *Real samples.*

Then, as a suitable alternative to try to obtain better results, we aimed to verify whether we could use another approach based on neural networks that could be trained only with synthetic data and had a good performance when tested with original data. For this purpose, we used Siamese Convolutional Networks [13]

As shown in Fig. 9, the Siamese are twin nets that share the same weights. In this case, it can be seen that even if there are two convolutional networks, overall, we have half the parameters with respect to the GAN (46,854,530). The main feature is that they can be trained to learn a space in which the features of different classes are very close to each other. This is also our scenario, in which the different fault GASF images appear similar to each other. This was achieved by exposing the network to a pair of similar and dissimilar observations.

The network minimizes the Euclidean distance between similar pairs and maximizes the distance between dissimilar pairs ($L = contrastive\ loss$).

In (4), we can see that s_1 and s_2 are two samples (GASF images), y is a Boolean denoting whether the two samples belong to the same class, α and β are two constants, and m is the margin.

$$L(s_1, s_2, y) = \alpha(1-y)D^2w + \beta y max(0, m - D_w)^2 \quad (4)$$

$$D_w = \|f\ (s_1; w_1) - f\ (s_2; w_2)\ \|_2 \quad (5)$$

where (5) is the Euclidean distance computed in the embedded feature space. It can be seen that if y is 1 (different classes), the left-hand term disappears, and we attempt to maximize the distance between examples. On the other hand, if y is 0 (same class), the right-hand term disappears, and we attempt to minimize the distance between examples.

V. RESULTS

This section describes the methodology used in our experiments. An introduction is made to the configuration of the examples in the database, specifically how they have been selected for the different phases of the training (training, validation, and testing). Then, the results obtained for each case are presented.

A. STRUCTURE OF THE EXPERIMENTS

To carry out the experiments in this work, we relied on a database of 200 examples of *Real samples* (Fig. 6 (a)), converted to images using the GASF transformation (Fig. 6 (b)), and 10.000 GASF *Generated samples* (2.000 for each of the five types under study).

In the first group of experiments, we focused on demonstrating the potential losses due to the GASF transformation and the subsequent suitability of GAN images. This will provide us with significant conclusions to determine whether these steps affect the quality of our results.

In the second group of experiments, where existing state-of-the-art neural networks (LeNet, AlexNet, and ResNet18) were trained, the database of synthetic examples was split into training (80%) and validation (20%). We then tested the database of original examples (200 examples, 40 examples of each ToF: $40 \times 5 = 200$).

Finally, when dealing with the Siamese network in the last experiment, a set of pairs randomly selected from the *Generated samples* were used to train the network. Two important facts should be mentioned at this point:1. This set was chosen to prevent imbalance among the types. 2. The validation and training phases were achieved with synthetic data (*Generated*), and tests were carried out with the original data (*Real*).

B. STUDY OF THE GASF TRANSFORMATION AND ITS RELATED LOSSES

As previously mentioned, the first step in processing is to transform the time signals into images using the GASF transform. In this step, it is necessary to decide which dimensionality reduction should be applied when performing this transformation. As explained in [56], this dimensionality reduction is obtained by applying *Piecewise Aggregate Approximation* (PAA).

Therefore, PAA is a source of potential loss and distortion. Therefore, a study in the frequency domain can demonstrate how this reduction distorted the original signals. Therefore, to proceed, we compute the FFT of the recovered signals already reduced according to the following procedure:

- A *Real sample* is initially transformed into GASF images of different dimensionalities (4000, 1000, 512, and 128, respectively).
- Each GASF *Generated sample* was back processed to obtain new versions of the same signal.
- Finally, we computed the FFT for the last signals (see Fig. 10).

From the study of these FFTs, it can be deduced that this dimensionality reduction is equivalent to a low-pass filter, as it is observed that as the reduction increases, the higher frequencies disappear and the lower frequencies are preserved.

For other types of studies, where the objective is to extract other types of more complex information (distance to the

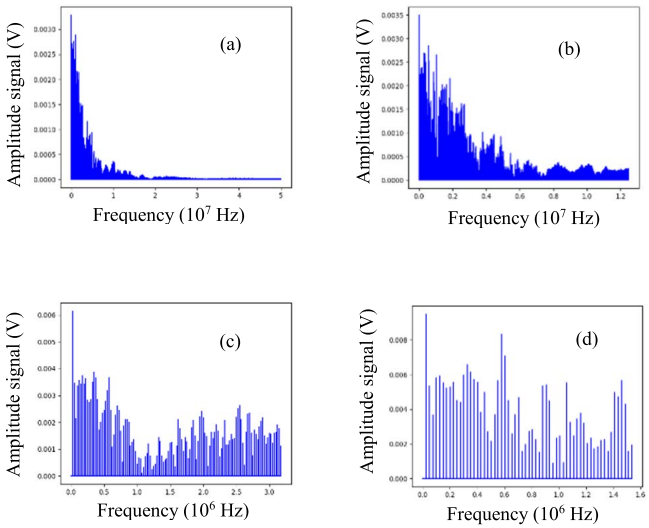

FIGURE 10. FFT of GASF images recovered of the same signal. (a) Dimensionality = 4,000 (Original) / (b) Dimensionality = 1,000 / (c) Dimensionality = 512 / (d) Dimensionality = 128. It can be observed that the higher frequencies disappear, while the lower frequencies are preserved when the dimensionality reduction increases.

fault, for instance), these high frequencies can become relevant. In our case and in view of the subsequent results, the assumed reduction (128 × 128) is adequate and allows us to save time in the training/validation phase.

C. ANALYSIS OF POTENTIAL MEASUREMENT ERRORS

Simulations based on real power distribution networks can lead to many difficulties in obtaining an adequate amount of data. This is why the central motif of this article is to obtain valuable fake data (generated samples) that can be used to train a neural network and obtain optimal results.

But at the same time, simulations can give us some uncertainty about the performance of the classifier in the face of possible failures of the measurement devices that can occur in a real environment. Indeed, this is a significant factor that distinguishes a simulated network from a real one. That is why this aspect has a specific section in this article.

In this sense, we are going to focus our interest on the study of three types of measurement errors:

1) RANDOM ERROR

Configured as a white noise signal, which has the next properties a) the signal is not statistically correlated between two different times, and b) its power spectral density (PSD) is constant throughout its spectrum. This type of error provides us with information on the behavior of the classifier over the entire frequency spectrum.

The results of the tests with this type of error are presented in Fig. 11, where errors of different signal-to-noise ratios have been used.

Several training epochs with different accuracy rates have been chosen, and each of them has been processed with noisy signals of 1 dB, 10 dB, 20 dB, 30 dB and 40 dB.

FIGURE 11. Impact of measurement error (white noise) on results.

FIGURE 12. Impact of measurement error (bias) on results.

The conclusions that can be drawn from the figure are, on the one hand, the stability of the network with similar accuracy rates when the performance of the network in the corresponding epoch is partial or different from 100%. Except for epoch 3, where there is a generalized drop in network performance in the presence of noise. On the other hand, in epochs with a 100% hit rate, similar 100% accuracy rates are obtained from the network regardless of the level of noise.

2) BIAS ERROR

It provides an estimation of the accuracy of the measurement system and represents the systematic error that can occur in the system.

Fig. 12 shows the results with respect to this type of error. The experiment is set up identically to the random error case, and the results are also very similar. A drop in performance at epoch 2, and identical behavior when 100% accuracy is obtained in the validation can be observed.

3) AMPLIFICATION ERROR

In the latter case, we consider the error that may be introduced by the instrumentation, due to its limited bandwidth.

The classifier's tolerance to this type of error has a much simpler justification, as this would be a subset of the errors considered in the first two cases.

TABLE 2. Original vs synthetic data correlation.

Correlation	Type 1	Type 2	Type 3	Type 4	Type 5
max	0.93	0.97	0.95	0.95	0.93
min	0.53	0.72	0.54	0.35	0.41

TABLE 3. Original vs original data correlation.

Correlation	Type 1	Type 2	Type 3	Type 4	Type 5
max	1	1	1	1	1
min	0.31	0.61	0.38	0.24	0.46

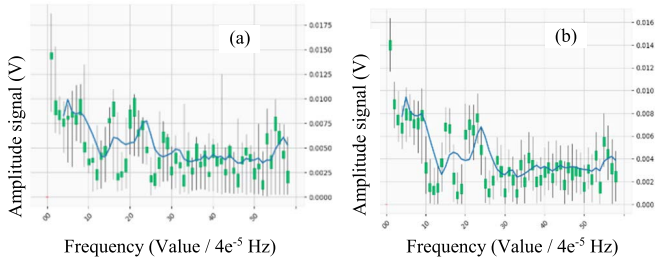

FIGURE 13. Original samples fault type 3 FFT statistics (a) and synthetics samples fault type 3 FFT statistics (b). Blue line is the moving average using 5 samples.

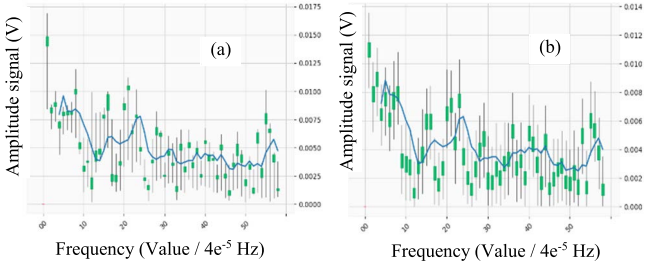

FIGURE 14. Original samples fault type 5 FFT statistics (a) and synthetics samples fault type 5 FFT statistics (b). Blue line is the moving average using 5 samples.

D. CHECKING THE SUITABILITY OF THE IMAGES OBTAINED WITH THE GAN

As mentioned above, we trained a GAN to synthesize examples and increase the database size after transforming the temporal signals into images. This would be useless if those images were not of sufficient quality and did not appear to be very similar. To do this, we select the *Real* signals and compare them with the *Generated* signals, converted back from GASF images, to check whether they are suitable. Therefore, a comparison will be made with signals and not with GASF images for a better understanding of the negative effects.

In Fig. 11 and 12, we can see the comparison between each harmonic of all the signals, both the *Real* and *Generated* signals for each ToF. In these figures, the amplitude variation of each harmonic is represented by the black lines. Similarly, the green flag represents the 50^{th} percentile.

Looking at the graphs and moving average (blue line), it can be seen that both types of signals have a very similar frequency distribution pattern, which means that the GAN has consistently synthesized in terms of frequency spectrum vs. amplitudes.

Another aspect to highlight, in case of *Generated* signals, the percentile variation remains constant throughout the frequency spectrum. Meanwhile, the *Real* ones show different variabilities in each of the harmonics.

Table 2 lists the maximum and minimum values shown in Figure 13. It can be stated that, in general, both signals are strongly correlated.

However, there are some *Real* signals that show a low correlation (blue color) with the rest of the Generated signals.

Fig. 15 (a) shows them with a frequency distribution pattern that is different from the rest. In these cases, the GAN has not learned to generalize this type of signal, which may be a limitation of GAN. Moreover, the rest of the examples with similar patterns were well synthesized by GAN and showed strong correlations.

Finally, the reader can appreciate the degree of correlation between the *Real* signals (see Fig. 14 and Table 3). The signals have a different pattern, since they are originally poorly correlated with all the others.

E. TRAINING STANDARD NEURAL NETWORKS MODELS

Our first attempt to classify was to train the standard models LeNet [57], AlexNet [58], and ResNet18 [59] with our new extended database to verify the results. Fig. 16 shows the progression of the complete training, validation, and testing processes for the AlexNet model. We continue applying the same strategy to ensure a fair comparison (training and validation phase using newly *Generated* data and testing results with the *Real* dataset).

The model can obtain values close to 100% after a few epochs, both in training and validation (with *Generated* data).

However, in the test stage, with *Real* examples, the accuracy is poor, which means that the model cannot be generalized well. This is in line with what exists in the literature regarding the need to train using a limited number of syn-

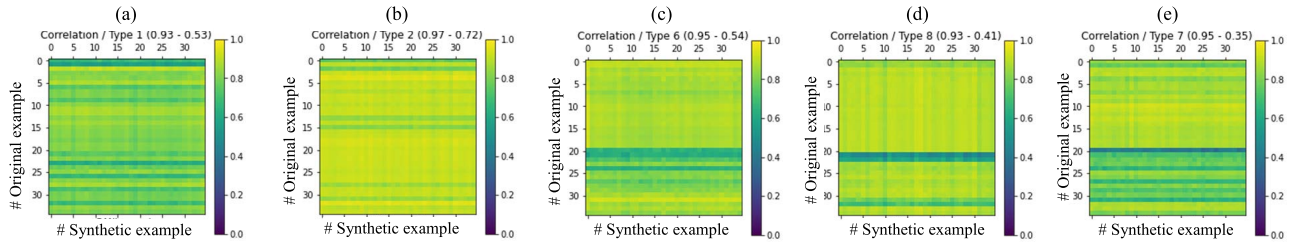

FIGURE 15. FFT correlation synthetic vs original examples for each ToF: type 1 (a), type 2 (b), type 3 (c), type 4 (d), type 5 (e).

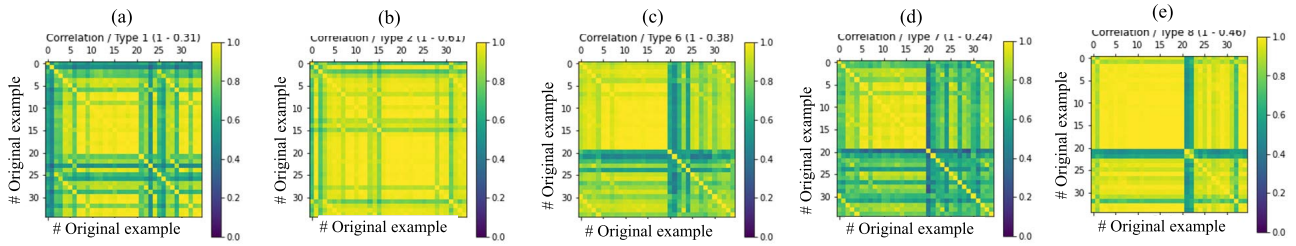

FIGURE 16. FFT correlation original vs original examples for each ToF: type 1 (a), type 2 (b), type 3 (c), type 4 (d), type 5 (e).

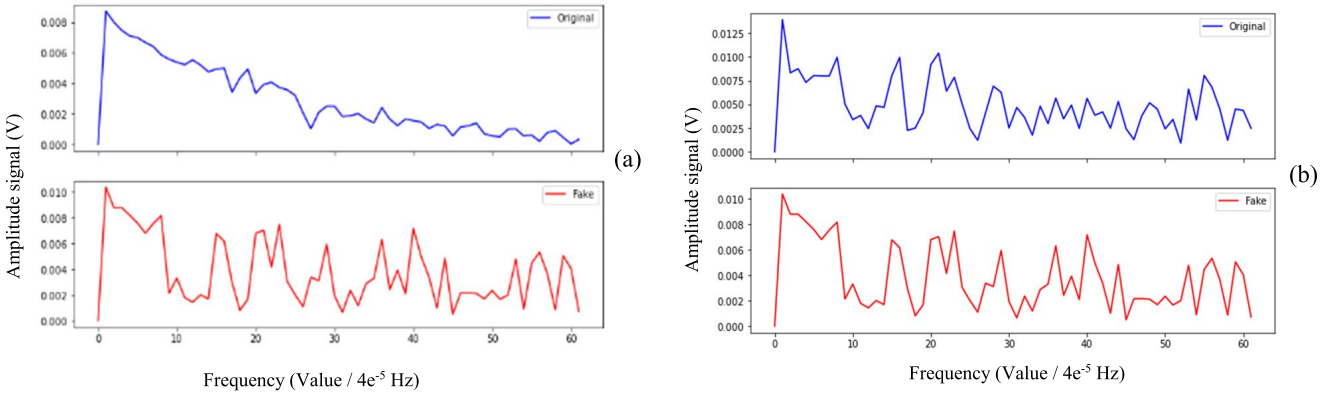

FIGURE 17. Comparison of FFT between original and synthetic signals: Comparison between original signal number 22 (blue) and synthetic signal number 34 (red), both belonging to fault type 5 (a). Comparison between the original signal number 10 (blue) and synthetic signal number 34 (red), both belonging to fault type 5 (b).

TABLE 4. Accuracy (%).

	TRAINING	VALIDATION	TESTING
LeNet	99.98%	100%	27.36%
AlexNet	99.98%	100%	33.83%
ResNet18	99.98%	100%	35.82%

thetic examples [44]. Table 4 lists the training results of the LeNet, AlexNet, and ResNet18 models. Similar results were obtained for the three models.

F. TRAINING THE SIAMESE NEURAL NETWORK

Siamese networks are well known for their effectiveness in *one-shot* or *few-shots* learning strategies [28], being able to adapt to new distributions quickly.

Applying the same learning strategy as in the previous sections, in Fig. 17 we can observe the evolution of the training loss for each epoch, as well as the loss and accuracy in training and validation phase for different learning rates. For smaller values of the latter parameter, less aggressive curves are achieved.

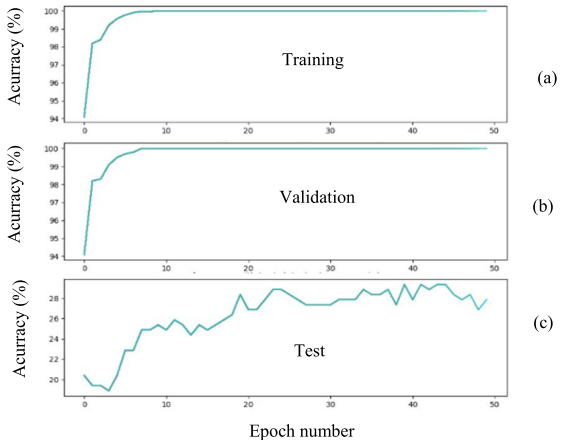

FIGURE 18. Accuracy of the training phase (a) with known synthetic data, validation phase (b) with unknown synthetic data, and test phase (c) with unknown original data of the AlexNet model. The training and validation phases were performed using 100% synthetic examples, and the test phase was performed using 100% original examples.

We would also like to highlight the performance with the test data. The Siamese network (SN) is able to generalize between both distributions (synthetic and original), and the

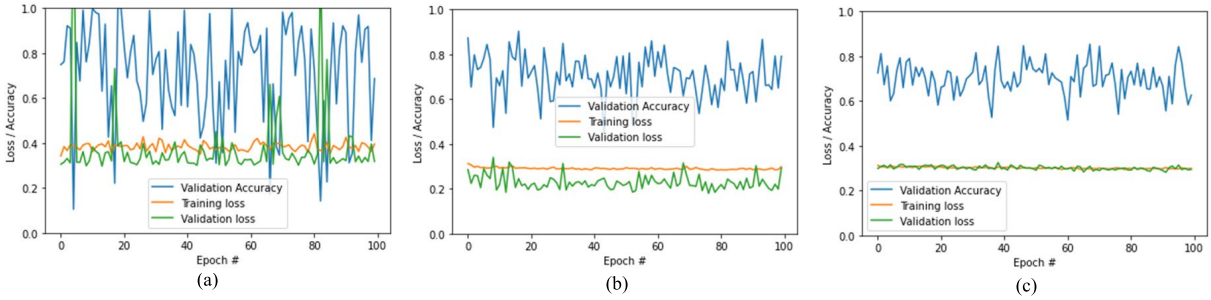

FIGURE 19. Validation accuracy and Training / Validation Loss phases for different learning rates, 1e-4 (a), 1e-5 (b), 1e-6 (c), and for each Epoch.

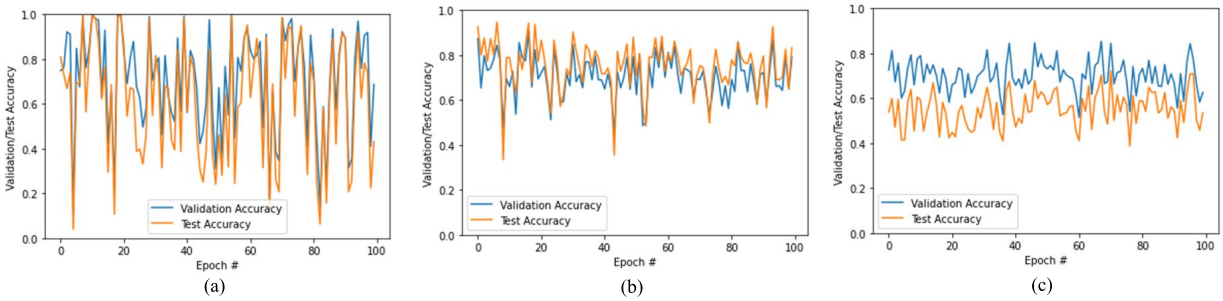

FIGURE 20. Validation and Test accuracy phases for different learning rates, 1e-4 (a), 1e-5 (b), 1e-6 (c), and for each Epoch.

results are even better if the correct learning rate is finally chosen (in this case, $1e^{-5}$). In Fig. 18, we can see this comparison between the validation and test accuracies for each epoch as a function of the learning rate.

In conclusion, it can be said that the network converges to validation accuracy values of approximately 70% and test accuracy values of approximately 80% for the correct learning rate. This represents an improvement of more than two times with respect to the standard networks trained in Section D. This result shows that contrastive learning helped us to effectively classify original signals. In this way, the SN has been able to classify original examples that it has never seen before, but also belongs to a different distribution.

Apart from this result, it can be seen that with high learning rates ($1e^{-4}$) as shown in Fig.17 (a), it is worth noting that even with this high variability, and owing to the ability of Siamese networks, it is able to return 100% accuracy rates both in the validation and test phases.

As mentioned before, this behavior can be explained because this type of network can be used for *one-shot-learning*, so the network does not require much training.

Thus, the model can correctly classify never-seen examples belonging to another distribution. With a sufficient number of synthetic examples, it took a few epochs to correctly learn to separate and classify unseen originals.

VI. CONCLUSION

We propose a solution to the problem of fault detection and classification with a few examples: the generation of synthetic examples by means of GAN networks, combined with the application of contrastive loss (Siamese networks).

In relation to the expected objectives set in this study:

1. It has been demonstrated that fault-type information is present in the signals reflected by the network as a result of injected pulses (TDR). Very good results were achieved by performing dimensionality reduction by applying the *Piecewise Aggregate Approximation* (PAA) technique. This reveals that the information of the ToF is in the low frequencies of the signal and can be dispensed with, at least in this study, higher frequencies.
2. It has been possible synthesized examples of each of the five types of faults used in this study were generated. We went from having a database of 200 examples (original examples) to a database of 10,000 synthesized examples (2,000 of each type).
3. It has been possible to train a network (Siamese with *Contrastive Loss* output) only with synthesized examples and test it with the original examples, yielding very high accuracy.

These synthesized examples have been divided into two groups, one for training and one for validation.

These two groups will belong to the same data distribution, so the generalization could not be tested yet. To certify that the system does not only generalize to the training distribution a test has been performed on the original 200 data, which belong to a different distribution.

This new method facilitates the training of neural networks with this type of signal, for which few examples are available owing to their nature.

VII. FUTURE WORK

Our work is directly linked to a research institution that is strongly committed to TDR technology, which leads us to continue advancing in this field. First, we are trying to understand the limits to which we can take neural networks in the understanding of this type of phenomenon; second, we are excited by the results obtained, and we are encouraged to discover new particularities that can help solve different problems in this area.

However, our short-term points of interest are as follows:

1. To explore whether our method is valid also for high impedances and for simultaneous fault detection.
2. To explore whether our method may be affected by the presence of distributed generations in the distribution networks
3. To explore whether the neural network can generalize the learned fault types to other real distribution lines, without retraining or at least with a minimal learning phase. The versatility of the process must be such that it is functional in diverse environment
4. To explore the possibility of extracting more complex information, such as fault location, by adapting the technique described in this paper. The challenge here is to move from a classification problem to a linear regression problem by generating synthetic examples.
5. Finally, we believe that we have kept open the door that others have opened with one-short learning methods. This philosophy has a huge potential to be pursued, and new contributions can generate the common know-how that the research community needs.

REFERENCES

[1] D. P. Mishra and P. Ray, "Fault detection, location and classification of a transmission line," *Neural Comput. Appl.*, vol. 30, no. 5, pp. 1377–1424, Sep. 2018, doi: 10.1007/s00521-017-3295-y.

[2] M. Mirzaei, M. Z. A. A. Kadir, E. Moazami, and H. Hizam, "Review of fault location methods for distribution power system," *Austral. J. Basic Appl. Sci.*, vol. 3, no. 3, pp. 2670–2676, 2009.

[3] R. J. Hamidi and H. Livani, "Traveling-wave-based fault-location algorithm for hybrid multiterminal circuits," *IEEE Trans. Power Del.*, vol. 32, no. 1, pp. 135–144, Feb. 2017, doi: 10.1109/TPWRD.2016.2589265.

[4] S. Wei, G. Yanfeng, and L. Yan, "Traveling-wave-based fault location algorithm for star-connected hybrid multi-terminal HVDC system," in *Proc. IEEE Conf. Energy Internet Energy Syst. Integr.*, Nov. 2017, pp. 1–5, doi: 10.1109/EI2.2017.8245645.

[5] J. Teng, X. Zhan, L. Xie, X. Zeng, Y. Liu, and L. Huang, "A novel location method for distribution hybrid lines," in *Proc. IEEE Conf. Energy Internet Energy Syst. Integr. (EI2)*, Nov. 2017, pp. 1–5, doi: 10.1109/EI2.2017.8245425.

[6] L. Wang, "The fault causes of overhead lines in distribution network," in *Proc. MATEC Web Conf.*, vol. 61, Jun. 2016, p. 02017, doi: 10.1051/MATECCONF/20166102017.

[7] S. Das, S. Santoso, and S. N. Ananthan, "Fault location on transmission and distribution lines," in *Fault Location on Transmission and Distribution Lines*, Jan. 2022, doi: 10.1002/9781119121480.

[8] S.-C. Huang and T.-H. Le, "Training neural network," in *Principles and Labs for Deep Learning*. New York, NY, USA: Academic, Jun. 2021, pp. 117–146, doi: 10.1016/B978-0-323-90198-7.00007-0.

[9] O. A. M. López, A. M. López, and J. Crossa, "Overfitting, model tuning, and evaluation of prediction performance," in *Multivariate Statistical Machine Learning Methods for Genomic Prediction*. Cham, Switzerland: Springer, 2022, pp. 109–139, doi: 10.1007/978-3-030-89010-0.

[10] K. Berns, A. Köpper, and B. Schürmann, "Electrical networks," in *Technical Foundations of Embedded Systems* (Lecture Notes in Electrical Engineering), vol. 732, pp. 19–43, 2021, doi: 10.1007/978-3-030-65157-2_3.

[11] D. Zhang, M. Ma, and L. Xia, "A comprehensive review on GANs for time-series signals," *Neural Comput. Appl.*, vol. 34, no. 5, pp. 3551–3571, Mar. 2022, doi: 10.1007/S00521-022-06888-0.

[12] G. Koch, R. Zemel, and R. Salakhutdinov, "Siamese neural networks for one-shot image recognition," in *Proc. ICML Deep Learn. Workshop*, 2015, pp. 1–30.

[13] S. Dey, A. Dutta, J. Ignacio Toledo, S. K. Ghosh, J. Llados, and U. Pal, "SigNet: Convolutional Siamese network for writer independent offline signature verification," 2017, *arXiv:1707.02131*.

[14] H. Ungrad, W. Winkler, and A. Wiszniewski, "The main criteria for detecting faults," in *Protection Techniques in Electrical Energy Systems*. Boca Raton, FL, USA: CRC Press, Aug. 2020, pp. 28–38, doi: 10.1201/9781003067504.

[15] J. Jiao, G. Lai, L. Zhao, J. Lu, Q. Li, X. Xu, Y. Jiang, Y. He, C. Ouyang, F. Pan, H. Li, and J. Zheng, "Self-healing mechanism of lithium in lithium metal," *Adv. Sci.*, vol. 9, no. 12, Apr. 2022, Art. no. 2105574, doi: 10.1002/ADVS.202105574.

[16] M. Brehm, L. Trigo, and D. Slomovitz, "Semiautomatic testing system for high voltage detectors," in *Proc. IEEE 9th Power, Instrum. Meas. Meeting (EPIM)*, Nov. 2018, pp. 1–3, doi: 10.1109/EPIM.2018.8756432.

[17] J. Oasa, M. Yamanaka, S. Higashiyama, Y. Inaoka, T. Hisakado, O. Wada, T. Matsushima, T. Hirayama, and K. Yamaoka, "Verification of fault location by TDR measurement on an actual line including multiple ground-mounted equipment," in *Proc. 26th Int. Conf. Exhib. Electr. Distrib.*, Sep. 2021, pp. 1274–1278.

[18] R. Lacoste, "The darker side: Time domain reflectometry," in *Circuit Cellar*, no. 225. Apr. 2009, ch. 3, pp. 33–47, doi: 10.1016/B978-1-85617-762-7.00003-4.

[19] A. Prasad, J. B. Edward, and K. Ravi, "A review on fault classification methodologies in power transmission systems: Part—I," *J. Electr. Syst. Inf. Technol.*, vol. 5, no. 1, pp. 48–60, May 2018, doi: 10.1016/J.JESIT.2017.01.004.

[20] A. Prasad, J. Belwin Edward, and K. Ravi, "A review on fault classification methodologies in power transmission systems: Part—II," *J. Electr. Syst. Inf. Technol.*, vol. 5, no. 1, pp. 61–67, May 2018, doi: 10.1016/J.JESIT.2016.10.003.

[21] B. Nayak. (2014). *Impact Factor: 1.852 Classification of Transmission Line Faults Using Wavelet Transformer*. Accessed: Jun. 1, 2022. [Online]. Available: https://www.ijesrt.com

[22] S. Kesharwani, D. Kumar, and M. Scholar, "Detection of power quality disturbances using wavelet transform," *Int. J. Sci., Eng. Technol. Res.*, vol. 3, no. 5, pp. 1–6, 2014. Accessed: Jun. 2, 2022. [Online]. Available: https://www.researchgate.net/publication/301695115

[23] S. R. Samantaray, "A systematic fuzzy rule based approach for fault classification in transmission lines," *Appl. Soft Comput.*, vol. 13, no. 2, pp. 928–938, Feb. 2013, doi: 10.1016/J.ASOC.2012.09.010.

[24] A. Aljohani, A. Aljurbua, M. Shafiullah, and M. A. Abido, "Smart fault detection and classification for distribution grid hybridizing ST and MLP-NN," in *Proc. 15th Int. Multi-Conf. Syst., Signals Devices (SSD)*, Mar. 2018, pp. 94–98, doi: 10.1109/SSD.2018.8570582.

[25] M. Shafiullah and M. A. Abido, "S-transform based FFNN approach for distribution grids fault detection and classification," *IEEE Access*, vol. 6, pp. 8080–8088, 2018, doi: 10.1109/ACCESS.2018.2809045.

[26] W. J. Cheong, "A novel fault location technique based on current signals only for thyristor controlled series compensated transmission lines using wavelet analysis and self organising map neural networks," in *Proc. 8th IEE Int. Conf. Develop. Power Syst. Protection*, 2004, pp. 224–227, doi: 10.1049/CP:20040104.

[27] A. Ngaopitakkul, C. Apisit, S. Bunjongjit, and C. Pothisarn, "Identifying types of simultaneous fault in transmission line using discrete wavelet transform and fuzzy logic algorithm," *Int. J. Innov. Comput. Inf. Control*, vol. 9, no. 7, pp. 2701–2712, 2013.

[28] N. Hooda and M. Malik, "Review on neuro-fuzzy system," *SSRN Electron. J.*, vol. 2022, pp. 1–11, Mar. 2022, doi: 10.2139/SSRN.4033495.

[29] E. S. M. T. Eldin, "Fault location for a series compensated transmission line based on wavelet transform and an adaptive neuro-fuzzy inference system," in *Proc. Electr. Power Quality Supply Rel. Conf.*, Jun. 2010, pp. 229–235, doi: 10.1109/PQ.2010.5549994.

[30] M. Singh, B. K. Panigrahi, and R. P. Maheshwari, "Transmission line fault detection and classification," in *Proc. Int. Conf. Emerg. Trends Electr. Comput. Technol.*, Mar. 2011, pp. 15–22, doi: 10.1109/ICETECT.2011.5760084.

[31] J. Upendar, C. P. Gupta, and G. K. Singh, "Discrete wavelet transform and probabilistic neural network based algorithm for classification of fault on transmission systems," in *Proc. IEEE Conf. Exhib. Control, Commun. Autom.*, vol. 1, Dec. 2008, pp. 206–211, doi: 10.1109/INDCON.2008.4768827.

[32] C. D. Prasad and D. J. V. Prasad, "Fault detection and phase selection using Euclidean distance based function for transmission line protection," in *Proc. Int. Conf. Adv. Electr. Eng. (ICAEE)*, Jan. 2014, pp. 1–4, doi: 10.1109/ICAEE.2014.6838516.

[33] P. Sharma, D. Saini, and A. Saxena, "Fault detection and classification in transmission line using wavelet transform and ANN," *Bull. Electr. Eng. Informat.*, vol. 5, no. 3, pp. 284–295, Sep. 2016, doi: 10.11591/eei.v5i3.537.

[34] D. Mnyanghwalo, H. Kundaeli, E. Kalinga, and N. Hamisi, "Deep learning approaches for fault detection and classifications in the electrical secondary distribution network: Methods comparison and recurrent neural network accuracy comparison," *Cogent Eng.*, vol. 7, no. 1, Jan. 2020, Art. no. 1857500, doi: 10.1080/23311916.2020.1857500.

[35] J. J. Q. Yu, Y. Hou, A. Y. S. Lam, and V. O. K. Li, "Intelligent fault detection scheme for microgrids with wavelet-based deep neural networks," *IEEE Trans. Smart Grid*, vol. 10, no. 2, pp. 1694–1703, Mar. 2019, doi: 10.1109/TSG.2017.2776310.

[36] D. Baskar and P. Selvam, "Machine learning framework for power system fault detection and classification," *Int. J. Sci. Technol. Res.*, vol. 9, p. 2, Jan. 2020. [Online]. Available: https://www.ijstr.org

[37] F. Rudin, G.-J. Li, and K. Wang, "An algorithm for power system fault analysis based on convolutional deep learning neural networks," *Int. J. Res. Educ. Sci. Methods.*, vol. 5, no. 9, pp. 11–18, 2017.

[38] Y. Wu, P. Zhang, and G. Lu, "Detection and location of aged cable segment in underground power distribution system using deep learning approach," *IEEE Trans. Ind. Informat.*, vol. 17, no. 11, pp. 7379–7389, Nov. 2021, doi: 10.1109/TII.2021.3056993.

[39] N. Sapountzoglou, J. Lago, B. De Schutter, and B. Raison, "A generalizable and sensor-independent deep learning method for fault detection and location in low-voltage distribution grids," *Appl. Energy*, vol. 276, Oct. 2020, Art. no. 115299, doi: 10.1016/j.apenergy.2020.115299.

[40] V. J. Lawhern, A. J. Solon, N. R. Waytowich, S. M. Gordon, C. P. Hung, and B. J. Lance, "EEGNet: A compact convolutional neural network for EEG-based brain–computer interfaces," *J. Neural Eng.*, vol. 15, no. 5, Oct. 2018, Art. no. 056013, doi: 10.1088/1741-2552/aace8c.

[41] S. Barrios, D. Buldain, M. P. Comech, I. Gilbert, and I. Orue, "Partial discharge classification using deep learning methods—Survey of recent progress," *Energies*, vol. 12, no. 13, p. 2485, Jun. 2019, doi: 10.3390/en12132485.

[42] Z. Wang and T. Oates, "Encoding time series as images for visual inspection and classification using tiled convolutional neural networks," in *Proc. Workshops 29th AAAI Conf. Artif. Intell.*, 2015, pp. 1–7. [Online]. Available: https://www.aaai.org

[43] K. Yang, W. Gao, R. Fan, T. Yin, and J. Lian, "Synthetic high impedance fault data through deep convolutional generated adversarial network," in *Proc. IEEE Green Technol. Conf. (GreenTech)*, Apr. 2021, pp. 339–343, doi: 10.1109/GREENTECH48523.2021.00061.

[44] X. Wang, H. Huang, Y. Hu, and Y. Yang, "Partial discharge pattern recognition with data augmentation based on generative adversarial networks," in *Proc. Condition Monitor. Diagnosis (CMD)*, Sep. 2018, pp. 1–4, doi: 10.1109/CMD.2018.8535718.

[45] R. Dashti, S. Salehizadeh, H. Shaker, and M. Tahavori, "Fault location in double circuit medium power distribution networks using an impedance-based method," *Appl. Sci.*, vol. 8, no. 7, p. 1034, Jun. 2018, doi: 10.3390/app8071034.

[46] L. Peretto, R. Tinarelli, A. Bauer, and S. Pugliese. (2011). *Fault Location in Underground Power Networks: A Case Study*. Accessed: Mar. 30, 2022. [Online]. Available: https://ieeexplore-ieee-org.cuarzo.unizar.es:9443/document/5759198/

[47] N. E. Halabi, "Localizadores de faltas para redes de distribución eléctrica," Fundación CIRCE, Universidad de Zaragoza, Zaragoza, Spain, Tech. Rep., 2012.

[48] C.-C. Zhou, Q. Shu, and X.-Y. Han, "A single-phase earth fault location scheme for distribution feeder on the basis of the difference of zero mode traveling waves," *Int. Trans. Electr. Energy Syst.*, vol. 27, no. 5, p. e2298, May 2017, doi: 10.1002/ETEP.2298.

[49] W. Chonglin, W. Yangyang, L. Rui, and S. Gang. (2010). *Fault Location for Single-Phase-to-Earth Faults Based on Transient Traveling Wave Method and Artificial Pulse Signal Injection Method*. Accessed: Mar. 30, 2022. [Online]. Available: https://ieeexplore-ieee-org.cuarzo.unizar.es:9443/document/5629889/

[50] M. Abad, U. Zaragoza, N. El, H. Saudi, A.-S. Arabia, and M. G.-G. Circe-Spain, "New fault location method for up-todate and upcoming distribution networks," in *Proc. 23rd Int. Conf. Electr. Distrib.*, 2015, pp. 15–18.

[51] J. Ballestín-Fuertes, D. Cervero, H. Bludszuweit, R. Martínez, and J. A. S. Castro, "Fault location in low-voltage distribution networks based on reflectometry—A case study," *Renew. Energy Power Quality J.*, vol. 18, pp. 735–740, Jun. 2020, doi: 10.24084/REPQJ18.483.

[52] Z. Wang and T. Oates, "Imaging time-series to improve classification and imputation," 2015, *arXiv:1506.00327*.

[53] A. Patil and Venkatesh, "DCGAN: Deep convolutional GAN with attention module for remote view classification," in *Proc. Int. Conf. Forensics, Anal., Big Data, Secur. (FABS)*, Dec. 2021, pp. 1–10, doi: 10.1109/FABS52071.2021.9702655.

[54] M. Li, J. Lin, Y. Ding, Z. Liu, J.-Y. Zhu, and S. Han, "GAN compression: Efficient architectures for interactive conditional GANs," *IEEE Trans. Pattern Anal. Mach. Intell.*, early access, Nov. 9, 2021, doi: 10.1109/TPAMI.2021.3126742.

[55] F. Zhu, M. He, and Z. Zheng, "Data augmentation using improved cDCGAN for plant vigor rating," *Comput. Electron. Agricult.*, vol. 175, Aug. 2020, Art. no. 105603, doi: 10.1016/J.COMPAG.2020.105603.

[56] E. J. Keogh and M. J. Pazzani, "Scaling up dynamic time warping for datamining applications," in *Proc. 6th ACM SIGKDD Int. Conf. Knowl. Discovery Data Mining*, 2000, pp. 285–289.

[57] V. Verdhan, "Image classification using LeNet," in *Computer Vision Using Deep Learning*, 2021, pp. 67–101, doi: 10.1007/978-1-4842-6616-8_3.

[58] V. Verdhan, "VGGNet and AlexNet networks," in *Computer Vision Using Deep Learning*. Irvine, CA, USA: Univ. of California, Irvine, 2021, pp. 103–139, doi: 10.1007/978-1-4842-6616-8_4.

[59] K. He, X. Zhang, S. Ren, and J. Sun, "Deep residual learning for image recognition," in *Proc. IEEE Conf. Comput. Vis. Pattern Recognit. (CVPR)*, Jun. 2016, pp. 770–778, doi: 10.1109/CVPR.2016.90.

JAVIER GRANADO FORNÁS received the B.Sc. degree in industrial engineering (specialized in industrial electronics) and the M.Sc. degree in electronics engineering (intelligent environments specialization) from the University of Zaragoza, Spain, in 1994 and 2014, respectively. He is currently pursuing the Ph.D. degree in deep learning around classification and localization of faults in distributions lines. Since 2009, he has been working as a Senior Researcher with the Electronics Systems Group, CIRCE Technology Center. His main research interests include electronic designs control projects around deep learning and algorithms for fault detection.

ELÍAS HERRERO JARABA (Member, IEEE) received the Ph.D. degree in engineering from the University of Zaragoza.

In 1999, he worked in the automotive field at the Production Department, Opel Spain, for four years. Since June 2002, he has been a Professor at the University of Zaragoza. In the meantime, he was a Coordinator of the smart vehicle initiative at the Aragon Institute for Engineering Research (I3A). He currently holds a European patent and has led to more than six projects funded in public competitions, more than 20 projects with companies, 12 indexed publications, and more than 50 contributions to international conferences. It is worth mentioning the 3 million awards for his research in the CvLAB Research Group. His teaching work has focused on electronics, from its basics to power electronics, including embedded systems. Within the university, he has developed his research in the area of computer vision. Since 2012, he has focused his research interests in the field of neural networks, and more recently, in deep learning.

ANDRÉS LLOMBART ESTOPIÑAN (Member, IEEE) received the Industrial Engineering degree from the University of Zaragoza, in 1994.

From December 1994 to May 2001, he was an Associate Professor with the Department of Electrical Engineering, University of Zaragoza, where he performed the following teaching activities, such as electric circuit theory, industrial actuation, wind energy, and renewable energy integration. He was also a Lecturer at the Department of Electrical Engineering, University of Zaragoza, from June 2003 to May 2018. From March 2007 to March 2009, he was the Sub-Director of Institutional Relations at the Superior Polytechnic Centre, University of Zaragoza. In CIRCE Technology Center, he was in charge of Innovation and Promotion Unit, created by himself on May 2009. He has been the General Director of the CIRCE Technology Center, since April 2016, and the Former Executive Director, since January 2011. In November 2011, he was designated by the Science and Innovation Ministry as an Expert in Energy Area Committee of the 7th Funding Program of the European Union, being in charge of the coordination of electricity grids topics. He participated in more than 35 research and development +i projects; in 16 of them, he was the primary researcher. He has author of ten articles in indexed journals and more than 50 contributions in international congresses. His active participation in forums, associations, and platforms linked to activity lines. He has eight patents, of which seven are being exploited. He researched the impact reduction of power electronic source grids using passive filters in the kilowatt range. His research gave him a Ph.D. title (specialized in electrical engineering) with the University of Zaragoza, in 2000.

JOSE SALDANA (Senior Member, IEEE) was born in San Sebastián, Spain, in 1974. He received the B.S. and M.S. degrees in telecommunications engineering and the Ph.D. degree in information technologies from the University of Zaragoza, Spain, in 1998, 2008, and 2011, respectively. He is currently a Senior Researcher at the CIRCE Technology Center. He has participated in research projects related to the digitalization of power systems, including ICT performance and security, and the use of wireless communications in industrial environments. He has published over 60 articles in peer-reviewed journals and conferences and RFC7962 in the Internet Engineering Task Force (IETF) on alternative network deployments. His research interests include wired and wireless networks with tight delay constraints, including multimedia services and digital communications in electric substations. He serves on the Editorial Board for IEEE Access (Associate Editor) and the *KSII Transactions on Internet and Information Systems* (Area Editor). He has also served on the Steering Committee and TPC for many conferences, such as the IEEE Consumer Communications and Networking, the ACM Multimedia Systems Conference, IEEE ICC, and the IEEE Globecom.

3.4 Estudio 4: TransSiamese: A Transformer-Based Siamese Network for Anomaly Detection in Time Series as Approach for Fault Location in Distribution Grids

RESUMEN: La detección de faltas en redes de distribución es un desafío debido a la escasez de ejemplos reales y la naturaleza caótica de las señales de falta. En este estudio, se propone un enfoque novedoso utilizando la reflectrometría en el dominio del tiempo (TDR) junto con redes Transformers para extraer información de localización de faltas. Primero se entrenan el Transformer con ejemplos de señales de prefalta y de falta, y luego detectamos anomalías cuando la predicción del Transformer se desvía de la señal real suministrada. Esto ayuda a abordar la falta de ejemplos etiquetados.

IEEE Access
Multidisciplinary ⋮ Rapid Review ⋮ Open Access Journal

Date of publication xxxx 00, 0000, date of current version xxxx 00, 0000.

Digital Object Identifier 10.1109/ACCESS.2017.Doi Number

TransSiamese: A Transformer-Based Siamese Network for Anomaly Detection in Time Series as Approach for Fault Location in Distribution Grids

Javier Granado Fornás[1], Elías Herrero Jaraba[2], Andrés Llombart Estopiñan[1]

[1]CIRCE Technology Center Parque Empresarial Dinamiza, Ave. Ranillas 3D, 1st Floor 50018 Zaragoza (Spain)

[2] Department of Electronic Engineering and Communications, University of Zaragoza, 50018 Zaragoza, Spain

Corresponding author: Javier Granado (e-mail: jgranado@fcirce.es).

"This work was supported in by the FLEXIGRID project from the European Union's Horizon 2020 research and innovation programme under grant agreement No 864579"

ABSTRACT Fault localization in distribution grids represents a crucial aspect in achieving the concept of smart grids within electrical networks. Despite the existence of various approaches to address this issue, it remains an open and challenging topic in real situations and, therefore, complex grids. One of the main challenges stems from the scarcity of labelled real-world examples is due to the inherent chaotic nature of faults (short circuits between a phase and ground). Obtaining sufficient fault examples for neural network training purposes becomes extremely difficult. Efforts have been made to simulate fault signals and apply data augmentation techniques. However, for fault location specifically, classical augmentation techniques are not applicable due to the unique nature of the fault signals. In this paper, we propose a novel approach to address the problem of extracting fault location information from TDR (Time Domain Reflectometry) signals. This kind of signals, involve injecting pulses into the grid and record these pulses as a bounced signal due to the different impedance changes of the grid. Our approach relies on employing a Transformer for anomaly detection. This Transformer-based Siamese network architecture (abbreviated by TransSiamese) is inspired by TranAD model. This Transformer has been modified to be trained in a Siamese way with a few examples (pre-fault signals/normal state and fault signals/abnormal state). After training phase, we can run inference mode by feeding it signals representing faulty grid states (fault signals). The Transformer attempts to predict the evolution of the signal, however, from a certain point to the end, the predicted fault signal deviates from the True signal supplied. Thanks to the intrinsic property of the Siamese network, it dampens the differences between the learned and the current signal when it comes to pre-fault; on the contrary, it enhances these differences when we are immersed in a fault signal.

INDEX TERMS Artificial Neural Networks (ANNs), Deep Learning, Transformers, Siamese Neural Networks, Anomaly detection, Fault location, Transmission lines

I. INTRODUCTION

The current challenges faced by modern society have led to an increased electrification of the energy system with a greater emphasis on distribution networks. Therefore, it is important to prepare these infrastructures for future challenges, such as the installation of multiple distributed generation resources, or to achieve the goal of implementing the smart grid concept in electrical networks.

In this context, the automatic detection, classification, and location of faults, is an essential requirement and highly beneficial as it saves time and money compared to manual methods.

Self-repair mechanisms [1] require that this automatic methods are being incorporated to minimize the impact of power outages [2]–[4].

Faults are often due to short circuits between one or more phases to ground, which can affect the entire network. The use of time domain reflectometry (TDR) [5]–[8] is a physical principle used to obtain signals by injecting pulses into the network. This periodic injection of pulses allows the electrical response of the network to be frequently updated [9]–[11]. When a fault occurs, the returned signal carries embedded information about the status of the distribution grid [12].

The detection, classification, and localization of faults in power grids remain prominent and essential research areas within the field of electrical engineering, garnering continued attention and significance.

On the other hand, classification and linear regression are two fundamental methodologies within the field of machine learning. Classification is employed when the objective

involves assigning instances or examples to predefined classes, entailing the prediction of categorical or discrete label variables. Linear regression is utilized when the aim is to predict a continuous or numerical variable. The primary objective is to ascertain a linear relationship between the input features or variables and the target variable.

In summary, classification focuses on assigning instances to predefined classes, whereas linear regression is employed to predict numerical values. Both approaches employ specific techniques and algorithms tailored to their respective objectives and are applied in distinct contexts and problem domains within the realm of machine learning.

Detection and classification of faults falls in classification problems. Those problems involve determining the type of fault that occurred based on various types of signals, e.g., those generated by the grid response to pulse injection (TDR). One effective method for fault detection and classification is the use of neural networks, which requires a large database of labelled examples for training. However, due to the chaotic and catastrophic nature of faults, it is difficult to obtain such a database, and data augmentation techniques are often used.

In a previous study [13], the authors proposed a pulse injection solution based on the TDR technique, where a real network was modelled, and characteristic fault types were simulated. To avoid the lengthy simulation process, the authors generated a database of 200 signals examples [14] and synthesized the rest up to 10,000 using Generative Adversarial Networks (GANs). This synthetic example generation technique is useful for data augmentation in fault classification problems.

However, for fault location, which falls within the category of linear regression problems, the use of GANs cannot be applied as it is not possible to train them to generate different distances to the fault. Moreover, traditional data augmentation techniques involving transformations, or the addition of noise are also not applicable due to the temporal embedded information dependence of the signals.

Considering all these limitations, the authors propose the use of anomaly detection between pre-fault and fault signals. These signals have the characteristic that they are practically identical until the point where the fault occurs. From that point onward until the end of the signal, the signals become different, resulting in a continuous anomaly from the fault occurrence point to the end. This type of anomaly is not present usually in the datasets used for anomaly detection in the state-of-the-art (SOTA). Therefore, this characteristic necessitates a review of the different models used for anomaly detection.

In this article we are faced with a dichotomy defined by a problem of anomaly detection to locate electrical faults in a grid, and on the other hand, the need to address a problem different from the one normally considered in this field of detection.

In order to address this dual requirement, a transformer-based solution has been chosen [23][15]. A type of network

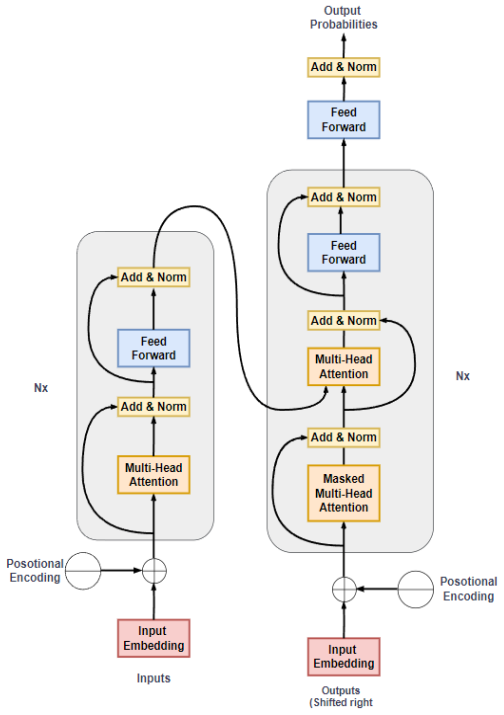

FIGURE 1. **Structure of the first Transformer (2017)**

that has demonstrated its high performance in applications with time series data, and whose inner encoder-decoder distribution is shown in Fig. 1.

Transformers learn to reconstruct signals they are trained with. The authors claim using the pre-fault and fault signals to train the Transformer. The pre-fault is the signal of the electric network's response to the injection of the pulse (TDR) when the grid is operating normally, and fault signal is the response when the grid is in fault state [7]. The propagation and reflection of TDR signals through an electrical network are very similar as long as there are no significant impedance changes in the network (faults). The transformer-type neural network is trained to model the pre-fault (normal state) signals and thus, can detect anomalies in the fault signals. After training phase, when a fault signal is presented to the trained network, the Transformer attempts to predict its evolution. Since the fault signal has an anomaly caused by the fault effect, the Transformer will fail to predict the evolution of the signal at some point and from then on.

Using this concept, we can detect this anomaly and make an approximation to the temporal zone where the anomaly occurred. Overall, the proposed method shows promise for fault location in power lines.

Having said that, our main objective is to undertake a first approach to automatic fault location using anomaly detection techniques between the pre-fault and fault signals. Specifically, a study of time series (pre-fault and fault signals) based on Transformers is conducted.

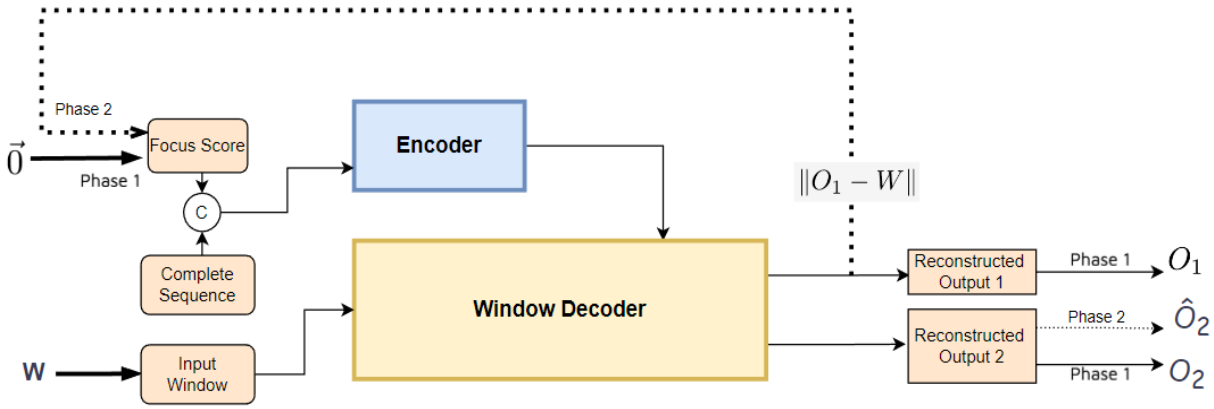

FIGURE 2. Transformer (TranAD) model with feedback used to improve the encoder response inspired by Anomaly Transformer [28]

II. RELATED WORK

Having explained the context in which this work will be situated, it is worthwhile to expand on previous work done by other researchers. It will be divided into two separate sections:

First, we will present solutions that have addressed the problem of anomaly detection using techniques other than those proposed in this article. Since they do not fall into an unique category, we will refer to them as the General case.

On the other hand, we will focus on solutions based on Transformers. In this second section, we will justify the inspirations drawn from these articles that have led us to propose the TransSiamese model developed in this article.

A. GENERAL APPROACHES

Within a generalist scope there are a multitude of solutions in the anomaly detection environment, and an adequate filter must be determined when presenting significant work in a single article that is not focused on being a literature review. This filter will be based on presenting different approaches prioritizing the date of publication and the variability of different approaches.

A first example of one of these approaches is the discord search, which aims to identify abnormal patterns within the data. LRRDS (Local Recurrence Rate based Discord Search) is a notable framework proposed to tackle this task. LRRDS leverages recurrence plots derived from the original time series data to accurately detect discords. To improve efficiency, innovative strategies such as optimizing pairwise distance comparisons between subsequences [16] or utilizing models like SES-AD [17], which project raw sequences into a lower-dimensional space, have been explored.

The challenge of detecting anomalies in large and complex systems with factors like the lack of ground truth labels, collective occurrence of anomalies, and high-dimensional data is addressed by the CSCAD model [18]. This model combines a graph convolutional network and a variational autoencoder to exploit feature space correlation and improve sample reconstruction for anomaly detection.

In the context of spacecraft anomaly detection, an unsupervised anomaly detection approach has been proposed. This method [19] employs a Gated Recurrent Unit (GRU)-based Recurrent Neural Network (RNN) with Extreme Value Theory (EVT). A two-layer ensemble learning-based predictor framework is developed to learn the normal behaviour of multiple data channels, allowing the detection of anomalies in spacecraft telemetry.

Another category of anomaly detection models is based on Long Short-Term Memory (LSTM) methods. For example, in [20] LSTMAD learns structural features from normal training data and uses a statistical strategy based on prediction errors for anomaly detection. Experimental evaluations demonstrate the superior accuracy of LSTMAD in detecting anomalies compared to existing approaches, making it particularly effective in applications like ECG datasets and real-world data analysis.

MFAD (Meta-feature-based Anomaly Detection) is an alternative approach for time series anomaly detection [21]. It utilizes meta-features to describe the local dynamics of univariate or multivariate sequences. Unlike traditional sliding window approaches, MFAD defines six meta-features to statistically describe the local dynamics of a 1-D sequence of arbitrary length, reducing computational complexity and demonstrating superior results in identifying abnormal states in various applications.

Autoencoders have also been explored for anomaly detection purposes. The article [22] presents USAD (Unsupervised Anomaly Detection for Multivariate Time Series), a fast and stable method based on adversarial trained autoencoders. The unsupervised learning capability of the autoencoder architecture, combined with the adversarial training and model structure, enables the efficient identification of anomalies.

Some of them (DAGMM [23]), utilizes a deep autoencoder to generate low-dimensional representations and reconstruction errors for each data point, feeding them into a Gaussian Mixture Model. Unlike previous methods, DAGMM

jointly optimizes the autoencoder and mixture model parameters, striking a balance between reconstruction, density estimation, and regularization. This approach avoids the need for pre-training and outperforms state-of-the-art techniques in anomaly detection.

In the State of the Art, we can find also identification of anomalies through reconstruction probabilities. Data reconstruction is based on learning robust representations using techniques like stochastic variable connection and planar normalizing flow (OmniAnomaly [24]).

The core idea of OmniAnomaly is to capture normal patterns in multivariate time series by these representations.

Furthermore, when an anomaly is detected in an entity, OmniAnomaly can provide interpretations based on the reconstruction probabilities of its constituent univariate time series.

In the Graph Neural Network-Based Anomaly Detection (GDN [25]), the authors combine structure learning with graph neural networks and utilize attention weights to provide explanations for the detected anomalies in real sensors. It is demonstrated that this method effectively captures correlations between sensors, enabling the deduction of the underlying cause of a detected anomaly.

In[26] it is shown a contrastive autoencoder (CAE) based approach for detecting anomalies in multivariate time-series data. The autoencoder is trained using a contrastive loss function that encourages the model to learn a representation that is similar for normal patterns and dissimilar for abnormal patterns. The authors also propose a new evaluation metric, the anomaly score, to measure the degree of anomalousness of a time series. The method outperforms several state-of-the-art methods for anomaly detection in multivariate time-series data, and the authors conduct extensive ablation studies to demonstrate the importance of the contrastive loss function and the anomaly score evaluation metric.

Some of the models presented here (DAGMM, OmniAnomaly, GDN, LSTM_AD) are later used in this work to perform comparisons against our TransSiamese model.

As can be seen, the field of anomaly detection in time series analysis is continuously evolving, and various approaches and models are being explored to address the challenges presented by different types of data and applications.

B. TRANSFORMERS-BASED APPROACHES

Once the state-of-the-art in anomaly detection has been presented in a general manner, in this section, we will focus our attention on those models that use Transformers and have served as inspiration for developing our TransSiamese model.

Everything started with a paper called "Attention Is All You Need," published in 2017 [27], where was introduced an encoder-decoder architecture based on attention layers, which the authors called the Transformer (Fig.1). Time-series anomaly detection has been successfully implemented using transformer-based models due to their ability to model long-term dependencies[15], [28]. Long-term dependencies occur in time-series data when past events have an influence on future events, such as in the case of financial data.

Transformers model long-term dependencies using the self-attention mechanism. That mechanism enables the model to focus on critical parts of the input sequence while generating the output sequence. The mechanism allows the model to learn which parts of the input sequence are relevant for predicting the output and thus capture long-term dependencies.

To detect anomalies in time-series data, transformers architecture is commonly used since a Transformer is a neural network that learns to reconstruct the input data. In such a way that the model is trained on normal data under standard conditions, and the reconstruction error is used to measure the anomaly. Data points or tiny temporal regions that deviate significantly from normal behavior are considered *anomalies*.

Several transformer-based models have shown promising results for anomaly detection in time-series data, and future research in this area is expected to yield even more promising results. Models such as Gated Recurrent Transformers (GRT)[29], Multi-Head Attention Networks (MHAN)[30]–[33], Deep Transformers [34], [35], Graph Convolutional Transformers (AGRU) [36]–[38].

In addition, the literature includes publications that propose different transformer-based frameworks for detecting anomalies in multivariate time-series data. For instance, in [39] authors present a novel framework utilizing the transformer encoder architecture for the purpose of learning representations of multivariate time series. (GCT) [40]–[42], and Attention-based Gated Recurrent Units. The model incorporates an unsupervised pre-training scheme, which demonstrates substantial performance benefits compared to fully supervised learning on downstream tasks. Notably, these advantages are observed even in the absence of additional unlabeled data, as it effectively leverages existing data samples. By evaluating on multiple publicly available datasets, good performance in regression and classification tasks is proven.

[36]–[38][39][26]Of all the models that we have reviewed from the state of the art, a first source of inspiration for this article appeared in [28]. The authors propose the *Anomaly Transformer*, a method that incorporates an association discrepancy term into the transformer loss function to capture both temporal and contextual dependencies in the data. The authors also propose a new evaluation metric, the anomaly detection rate (ADR), to measure the performance of their method on different types of anomalies. The method outperforms several state-of-the-art methods for anomaly detection in time-series data, and the authors conduct extensive ablation studies to demonstrate the importance of the association discrepancy term and the ADR evaluation metric.

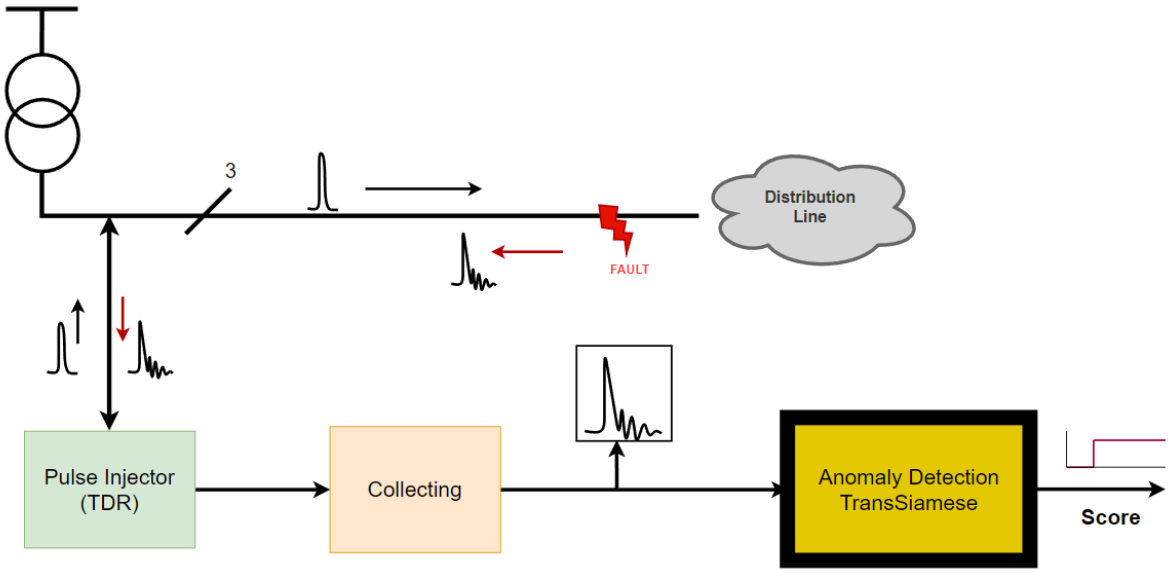

FIGURE 3. **Diagram of connection to the grid on fault state together with the transmission of the significant injection pulses.**

Here, our inspiration is based on the fact of using a new Anomaly-Attention mechanism that takes advantage of the short-term history of a few tens of samples of the signal. The encoder treats this history and passes it to the decoder to join it with the signal arriving at the current time, which improves the unsupervised detection of anomalies in time series.

Our second source of inspiration was the feedback loop the authors propose in [43] (TranAD) for focus scoring and adversarial training, specially the first one.

With this mechanism, we can highlight the small differences we have in our signals. The model, (Fig.2) uses a transformer-based encoder-decoder architecture that is designed to capture both temporal and cross-dimensional dependencies in the data. This architecture is trained to reconstruct the input data, and the reconstruction error is used as a measure of anomaly. Additionally, the authors propose a new unsupervised training algorithm that leverages the properties of the transformer architecture to learn a representation that is sensitive to anomalies in the data. They evaluate their method on several benchmark datasets and show that it outperforms several state-of-the-art methods for anomaly detection in multivariate time-series data.

The use of focus score-based auto conditioning, enable robust multimodal feature extraction and, adversarial training help gain stability. With this feature we can highlight small differences in our signals.

Furthermore, the adoption of model-agnostic meta learning (MAML) enables training the model with limited data availability.

While simple transformer models may overlook anomalies characterized by subtle deviations, the introduction of the adversarial training procedure allows for the amplification of reconstruction errors. The adversarial training process consists of two distinct phases. In the initial phase, the model aims to generate an input, known as the focus score, serves as a crucial element in guiding the attention network within the Transformer Encoder. This enables the extraction of temporal trends. Subsequently, in the second phase, the output is conditioned based on the deviations derived from the first phase.

The focus score, generated during the first phase, serves as an indicator of the discrepancies between the reconstructed output and the provided input. It operates as a prior knowledge, influencing the modification of attention weights during the subsequent self-conditioning phase. approximate reconstruction of the input window. The deviation between the inferred reconstruction and the original.

Nevertheless, although the use of the focus score is maintained in our work, the adversarial training method was not implemented due to the poor results obtained. Instead, the origin of the third inspiration is the Siamese Networks [44]–[50]. Thanks to the main characteristic, which reduce the differences between similar examples and increase the differences between different examples, we can train the Transformer to learn to model our signals better and thus improve the detection of anomalies.

In summary, all this path discussed in this section of the article has led us to a solution that works particularly well with

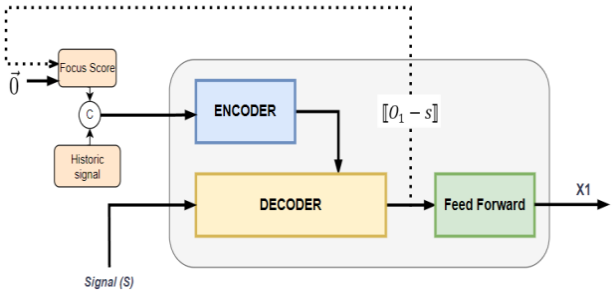

FIGURE 4. **Transformer with focus score based- self conditioning.**

the nature of the data handled in our context, that uses certain novel ideas from other authors, and that presents a novel solution in the anomaly detection environment. Thus, we can summarize our main contributions as follows:

1) We propose a novel Transformer-based approach, TransSiamese, which has demonstrated his ability to work as anomaly detector, but even as a viable and potential approach to the problem of fault localization.

2) A Siamese scheme has been used to enhance the powerful characteristics of this network to enhance the minimum differences between two signals to be compared (thanks to the Contrastive-based learning used), damping the differences between the learned and the current signal when it comes to pre-fault; and enhancing these differences when we are immersed into a fault signal.

3) Together a methodology to overcome the inherent issue of scarcity of real-world examples in such linear regression problems, where traditional Data Augmentation techniques may not be feasible due to the signal nature. And finally, in inference mode, we use an *Energy based Anomaly Score function* and propose a Weighted-energy *based Anomaly Score function*, which enhances the differences between the two-time sections of the signal and boosts the Siamese performance: the normal conditions section and the one corresponding to the time just after the failure occurs.

III. METHODOLOGY

This section outlines the proposed methodology which utilizes the injection of signals into the distribution line (TDR). These signals (pre-fault and fault signals) are then used to detect anomalies through the application of the *TransSiamese* model.

The following subsections will provide a detailed explanation of the methodology, as illustrated in Fig. 3.

A. Collecting phase: TDR signals

According to the physics of transmission lines, these pulses travel through the network and are reflected at every bifurcation. Therefore, some of them are bounced back[13]. The magnitude of these reflections depended on the impedance of the line at each bifurcation.

Therefore, the initial step involves generating a database[14] of signals using (PSCAD^{TM}) software. In order to do so, a realistic electrical network was modelled, and five types of faults were simulated at various points along the distribution line. These fault types include short circuits between R, S, and T to Earth, as well as short circuits between R-S to Earth and R-S-T to Earth.

The TDR technique, which involves injecting short-period pulses (~10 ns) into each of the three phases of an electrical grid every few seconds (e.g., every 5 s), was utilized. As per the principles of transmission lines, these pulses travel through the network and are reflected at each bifurcation, with the magnitude of the reflections being influenced by the impedance of the line at each bifurcation.

B. Anomaly Detection: Transformers

Unsupervised anomaly detection in time series remains a challenging problem, particularly when dealing with time series that exhibit complex dynamics. While some previous methods have attempted to address this challenge through pointwise representation or pairwise association learning, they do not perform well in such contexts. Recently, Transformers have emerged as a powerful approach to model anomalies in time series, owing in part to the rarity of anomalies. That makes building associations between abnormal points and the rest of the series particularly difficult.

Real-world systems often work in a continuous manner, generating successive measurements monitored by sensors in our case, the measurements come from the response of the network to injection pulses (TDR). Those signals are successive reflections caused by changes in impedance throughout the network. Detecting any anomaly between two consecutive signals (pre-fault and fault) is reduced to detecting abnormal points within the two time-series. However, anomalies are usually very rare processes and are hidden among a large number of normal points within the time series.

In the case of fault location, labelling the distance to the fault (the time at which the first anomaly occurs between both time series) is very difficult to obtain, as real examples are generally chaotic events that cannot be easily reproduced or measured in the field due to their nature. In the other side, simulating these phenomena is also complex, as simulation times make it unfeasible to have a large enough number of examples to train a supervised system. And similarly, we have problems applying data augmentation techniques due to the nature of the signals. For all the above reasons, we will focus on detecting anomalies in time series under the premise of unsupervised training.

Having said that, we use a Transformer model with focus score-based self-conditioning (Fig. 4) in this work. The Transformer requires two inputs, the first input used by the Encoder and the second by the Decoder. As used in recent work based on the Anomaly Transformer model, the Encoder oversees the short-term temporal information (Historic signal, *HS*), and the Decoder is in charge of combining the historic information with the current signal being processed. It should be noted that *HS* is constructed by joining the previous *D* signals to the current one (in our tests, the *D* parameter was set to the integer value of 10, since a variation of it did not cause significant changes in the performance of the whole system).

Therefore, in an initial state the *HS* signal history is concatenated with a zero vector and presented to the Encoder in order to obtain a first approximation of the input signal. Then, the deviation observed from this first reconstruction, termed as the focus score, serves to facilitate the attention

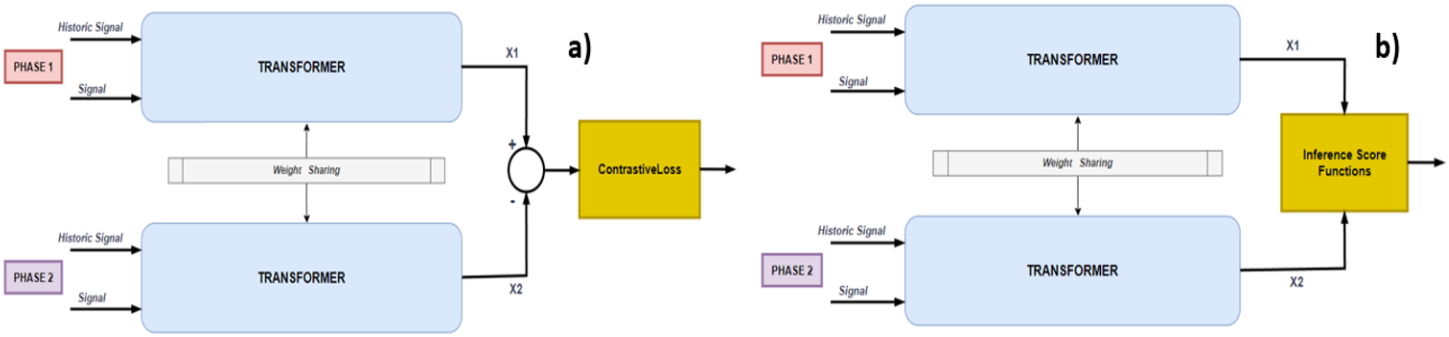

FIGURE 5. **a) Anomaly detection TransSiamese model during the Training phase, and b) Integration with the Anomaly score function for Inference**

network within the Transformer Encoder in a second iteration. In this sense, this attention network is responsible for extracting temporal trends by focusing on sequences with high deviations. Subsequently, in this new iteration known as *self-conditioning* (dashed line) in [43], the focus score derived from the first iteration indicates the disparities between the reconstructed output and the provided input.

This modification proposed in [43] aims to extract short-term temporal trends, by enabling higher neural network activation for specific input sub-sequences.

Finally, the observation O_1 returned by the Decoder in the second phase is processed by a single Feed Forward network from which the representation of the input signal S is finally obtained.

C. TransSiamese model:

The main characteristic of *TransSiamese* architecture is their ability to efficiently capture and model complex relationships between pairs of input sequences thanks to the use of Siamese structure during training. That is why two identical copies of the Transformer architecture, known as "Siamese branches" are employed. Each branch takes a different couple of inputs and processes them independently. The obtained representations from both branches are then compared to perform tasks such as similarity comparison, pair classification, or feature extraction. Furthermore, the Siamese architecture allows for joint learning and knowledge sharing between the branches, which can enhance model efficiency and generalization. This is indeed our chosen alternative, and we think it is key to the performance shown in the results section.

Fig. 5a shows the operating diagram of the Siamese model used in this article, in which the two transformers are shown, one being a copy of the other. The calculation of the loss in (1) is also shown and will be explained later.

At the end, anomalies in the tested signals do not occur in a punctual way in time. Both types of signals (pre-fault and fault) are very similar up to the point where the fault occurs, after which the signals continue to be different. Therefore, we need to think of a solution that maximises the differences in both types of signals as a whole, rather than at specific points in time.

This characteristic raise from the use of the contrastive loss function (1) during the training phase. This adaptation improves the training process of the model and contributes to its overall performance. The contrastive loss aims to minimize the Euclidean distance between pairs of similar instances (Pre-fault signals) and, at the same time, maximize the distance between pairs of dissimilar instances (pre-fault vs fault signals).

In this way, it favors the model to discriminate effectively between different classes or categories. This promotes better separation and clustering of the data and trains the Transformer more effectively to predict similar time series such as faults and pre-faults and achieve better anomaly detection. In short, we believe that the transformer is able to use the loss provided by the contrastive method to enhance the differences after each fault. In fact, it would be the fastest and most intuitive way of wanting to move away a pattern of one signal from another of a different type.

Finally, equation (1) is shown for a better understanding about all commented above in this section.

$$L = (1-y)\cdot\left\|PF - F'\right\|^2 + y\cdot\left(M - \left\|PF' - F'\right\|^2\right) \qquad (1)$$

Where, if y is 1 (when fault and non-fault signals are used), the left-hand term disappears, and we attempt to maximize the distance between examples until some threshold M. On the other hand, if y is 0 (when both signals correspond to faults), the right-hand term disappears, and we attempt to minimize the distance between examples.

D. Anomaly score functions:

On the other hand, since the results obtained from the TransSiamese network (inference mode) have to be exploited in the best possible way, we want to present a series of measures that aim to optimize and boost the output provided by the network (Fig. 5b). We have defined three Anomaly Score functions: the MAPE approximation, the Energy, and the Weighted-energy.

The simplest is the one which joins together a Euclidean distance with the MAPE function (here it is referred to as Standard). In the second one we make an estimation of the energy because it has been identified, as seen in (Fig. 6), that from the fault onwards the signals are seen with higher energy.

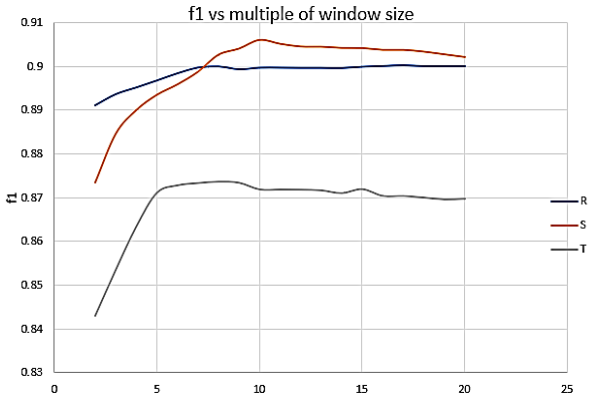

FIGURE 6. f1 vs multiple window size

And in the third point we also propose the Weighted-energy because we see that the difference in energy depends on the amplitude over the time domain of the signal.

-*Standard* function (Std) is defined as (2)

$$\text{Std} = \left\| \frac{(x_1 - x_2)}{x_1} + \sqrt{(x_1 - x_2)^2} \right\| \quad (2)$$

It is equivalent to the function MAPE (mean absolute percentage error) + RSME (root mean squared error). Where x_1 and x_2 are the outputs of the Transformer in Inference mode.

-The *Energy* function is defined as (3)-(5).

This function computes the energy over a window (w) period of each signal (x) generated by the Transformer and calculate the difference (D) between them.

$$E_{x_1} = \int_0^w |x_1(t)|^2 dt \quad (3)$$

$$E_{x_2} = \int_0^w |x_2(t)|^2 dt \quad (4)$$

$$D\ (E_{x_1}, E_{x_2}) = \left\| E_{x_1} - E_{x_2} \right\| \quad (5)$$

-The *Weighted-energy* function is defined as (6)-(9).

This function computes the energy over a window (w) period of each signal (x) generated by the Transformer and calculate the difference (D) between them.

$$E_{x_1} = \int_0^w |x_1(t)|^2 dt \quad (6)$$

$$E_{x_2} = \int_0^w |x_2(t)|^2 dt \quad (7)$$

$$Dw\ (E_{x_1}, E_{x_2}, X) = \frac{\left\| E_{x_1} - E_{x_2} \right\|}{X} \quad (8)$$

$$X = \{x_{max} : \max_{i \in W_m} x_1(i)\} \quad (9)$$

max is computed in windows of $size = s \times multiple$. For its calculation we have chosen to use the pre-fault signal (x_1). Finally, we want to show a couple of figures illustrating a couple of important characteristics to be understood. Fig.6 shows the variation of f1 as a function of a multiple (sigma), corresponding to the size of the window for calculating the maximum in relation to the window used for the energy calculation. It shows that around *multiple* =10 the f1 output stabilizes. We use this multiple to calculate the *Weighted-energy Anomaly Score*.

Fig. 7 shows the anomaly score obtained in Inference Phase. The automatic Threshold (*AT*) is marked as a red line. The output of the *Weighted-energy* function is computed by means of the Threshold to decide if this point is an anomaly.

In training mode, we use the ContrastiveLoss (1) as loss function. (Algorithm 1):

Algorithm 1 The TransSiamese train algorithm
Require:
Encoder E, Decoder D
Signals W_1 and W_2
Short-end historic signals W_{h_1} and W_{h_2}
Number of Epochs N
Evolutionary hyperparameter ϵ
Number of pairs for Siamese T
1: Initialize weights E, D
2: $n \leftarrow 0$
3: **do**
4: **for**(t = 1 to T)
5: $x_1 \leftarrow D\ (E(W_{h_1}, W_1, \vec{0}))$
6: $x_1 \leftarrow D\ (E(W_{h_1}, W_1, [\![x_1 - W_1]\!]^2))$
7: $x_2 \leftarrow D\ (E(W_{h_2}, W_2, \vec{0}))$
8: $x_2 \leftarrow D\ (E(W_{h_2}, W_2, [\![x_2 - W_2]\!]^2))$
9: $Loss \leftarrow L_{cnt}(x_i, x_j, \theta) = 1[y_i - y_j][\![f_\theta(x_i) - f_\theta(x_j)]\!]_2^2 + 1[y_i \neq y_j] max\left(0, \epsilon - [\![f_\theta(x_i) - f_\theta(x_j)]\!]_2\right)^2$
10: Update weights of E, D using $Loss$
11: $n \leftarrow n + 1$
12: **while** $n < N$

In inference mode, we use the *Anomalies Scores functions (ASF)* and *Calculate Automatic Threshold (AT)*(Algorithm 2):

Algorithm 1 The TransSiamese test algorithm

Require:

Encoder E, Decoder D

Test Dataset Signals W_1 and W_2

Short-end historic signals W_{h_1} and W_{h_2}

Number of pairs for Siamese T

1: **for**(t = 1 to T)

2: $x_1 \leftarrow \mathrm{D}\,(\mathrm{E}(W_{h_1}, W_1, \vec{0}))$

3: $x_1 \leftarrow \mathrm{D}\,(\mathrm{E}(W_{h_1}, W_1, [\![x_1 - W_1]\!]^2))$

4: $x_2 \leftarrow \mathrm{D}\,(\mathrm{E}(W_{h_2}, W_2, \vec{0}))$

5: $x_2 \leftarrow \mathrm{D}\,(\mathrm{E}(W_{h_2}, W_2, [\![x_2 - W_2]\!]^2))$

6: s $\leftarrow$ ASF (x_1, x_2)

7: $AT \leftarrow Calculate\ Automatic\ Threshold(\mathrm{s})$

8: $y_i = 1(s_i \geq AT)$

The ASF (Anomaly Score Function) could be one of the three defined in this work. *Standard*, *Energy* or *Weighted-energy*.

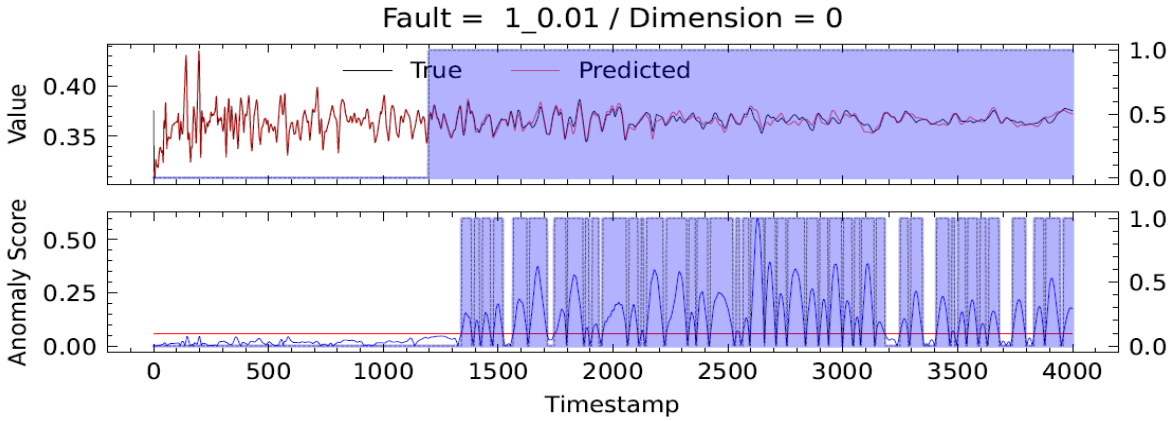

FIGURE 7. **Example de anomaly visualization between the score of the True and Predicted signal. Red line is the calculated umbral (AT)**

IV. EXPERIMENTS & RESULTS

This section describes the methodology used in our experiments. An introduction is made to comment the configuration of the examples in the database, specifically how they have been selected for the different phases of the training (training, validation, and testing). Then, the results obtained for each case are presented.

A. Structure of the experiments

In this study, we have used an existing database [14] containing 200 signals, which represent the grid's response to injected pulses using Time Domain Reflectometry (TDR)[7].

These signals were acquired using a simulator at a sampling rate of 100 Msps (Mega samples per second). Each of the three injected signals (R-S-T) was digitized for a duration of 40 µs, after which the signal essentially vanished. Consequently, the combined sampling time for all three phases amounted to 120 µs. With the given sampling rate, we obtained 12,000 digitized values (parameters).

As a result, the database consists of 200 signals, with each signal representing the grid's response to an injected pulse

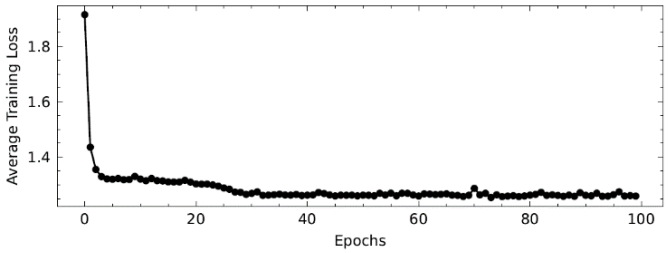

FIGURE 8. **Training graph after 100 epochs.**

under a specific fault condition (i.e., a fault between Phase R and Ground occurring 500 m away from the device used for injection/measurement). Those 200 signals are subdivided. into five groups related to the type of fault, so there are over 40 examples of each type.

Each fault group is defined according to the distance at which it is defined and the impedances specific to the corresponding fault. Thus, for each type of fault there are impedances of 0.01, 80.0, 150.0 and 1000.0 ohms. And each impedance is located at different distances from the injector: 12, 40, 283, 933, 757, 1833, 1274, 594, 968 and 649m.

On the other hand, we trained the TransSiamese model in four different experiments (B-C-D-E). All of the training process had a good training result in terms of convergency (Loss), similar to the one depicted in Fig. 8, in which the number of 100 epochs is used in all experiments commented in this paper.

Following the explanation of the experiments carried out and in operational terms, the processing is based on three necessary steps: the execution of the neural system based on the Siamese network (III-C), the calculation of the anomaly score (III-D), and finally an automatic thresholding.

Specifically, and delving deeper into the third step, the automatic threshold corresponds to the point AT (Fig. 9), and it is calculated from (10)

$$AT = argmax\left(f(\theta) \coloneqq \left\{\frac{TP(\theta)}{TP_{max}(\theta)} + \left(1 - \frac{FP(\theta)}{FP_{max}(\theta)}\right)\right\}\right) \quad (10)$$

being ϑ a considered threshold over a set of attempts evaluated over the anomaly score values. The idea behind the equation (10) is to find an optimum point in which we can minimize the False Negatives (FN) and maximize the True Positives (TP). TP are those points where the results indicate an anomaly that really exists, and FN are those points where the result indicates an anomaly, but it does not really exist. After the AT threshold has been calculated, the results above the threshold are labeled as anomalies and the results below the threshold are labeled as "normal" point.

In all experiments we will show 3 different summaries of results and provide relevant conclusions for each experiment. On the one hand, we will show a summary statistics table where we will collect the f1, precision, recall and overall ROC/AU data obtained over the total number of tests performed. On the other hand, we will show a comparison of the f1 results for the 3 scoring functions discussed in section III-D. And finally, we will show an example of processing and thresholding of a complete signal from the time the pulse appears, the fault occurs, and a sufficient time where it is diluted over time.

In general terms, we notice that different experiments achieve similar performance on all the four-evaluation metrics. The *Weighted-energy* Anomaly score function shows the best performance in all the experiments. As we said, in inference mode, the difference between the *True* and *Predicted* signal must be weighted because the difference of the two signals (absolute value) is independent of the amplitude of them, so, the *Weighted-energy* is a best way to measure the Anomaly Score more fairly.

Finally, we have conducted experiments to compare the performance of our database with other state-of-the-art (SOTA) models. It should be noted that the three processes discussed in this section, III-C, III-D and automatic thresholding have been equally well executed regardless of the approach used in the comparison. In this way the results shown will be playing on equal footing with each other.

As it can be seen later in these experiments, it is evident how our model achieves significantly higher scores due to its well-adapted behavior to the nature of our signals. Similarly, we have also conducted experiments to compare the processing time in inference and training between our model and the other selected SOTA models.

Therefore, it will be able to conclude that we have managed to train a model with a single Pre-fault signal and 200 faults and we have found that training only with that Pre-fault signal

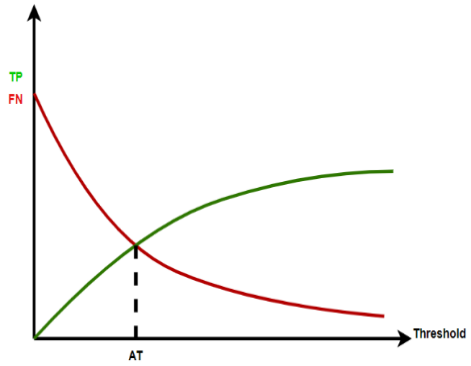

FIGURE 9. Automatic threshold calculated.

and different combinations of faults the result (f1 score) has a good performance (>0.7), testing with any ever seen example of any type of fault.

But, before starting with the explanation of the experiments, we would like to proceed to discuss the statistics used in the experiments. On the one hand, the f1 metric is a widely used performance measure in binary classification tasks, which combines precision and recall into a single value. It provides a balanced assessment of a model's ability to correctly classify positive and negative instances.

The f1 score is the mean of precision and recall. It provides a single metric that considers both precision and recall, giving equal importance to false positives and false negatives. It ranges from 0 to 1, where a value of 1 indicates perfect precision and recall, while a value of 0 indicates poor performance in correctly identifying positive instances. The f1 score is commonly used when there is an imbalance between the number of positive and negative instances in the dataset.

Precision is the ratio of true positive predictions to the sum of true positive and false positive predictions. It measures the accuracy of positive predictions, indicating how well the model identifies true positive instances.

Recall, also known as sensitivity or true positive rate, is the ratio of true positive predictions to the sum of true positive and false negative predictions. It quantifies the model's ability to identify all positive instances correctly.

On the other hand, ROC/AUC will give information on how well the classifier distinguishes between pre-fault and fault sections. Values close to 1 define a perfect classification model, and values close to 0.5 correspond to models with a random and meaningless response.

B. Anomaly Score functions comparative

In this first experiment, the idea is to test with signals from the same group (different examples for training and testing), in order to select the simplest experiment where we can clearly compare the different Anomaly Scores functions. Type 1 signals, which consist of a ground fault in phase R, have been chosen for both training and testing.

Our intention is to compare the performance of the three Anomaly Scores functions (Standard, Energy and Weighted-energy) that best fit our dataset when Pre-fault signals such as faults are known to the neural network.

Table I shows a significantly better performance of the Weighted-energy score in all four calculated statistics. On the other hand, it is worth noting in Fig. 10 the performance of the two energy-based scores on the 1T, 5T, and even on the 9T signal, corresponding to phase T signals in 3 different three-phase signals. And finally, the result of a fault corresponding to phase R, impedance 0.01 ohms, and at a distance of 1833m (12.23 sec) is shown.

C. Training with Faults type #1 / Test with all types

For this experiment we perform two different tests. First, we compare the performance of the TransSiamese model training with Faults type #1 and testing with faults type #1 (different examples from training and test). (Table II / Fig. 12 / Fig. 13). In the second test, we carried out a comparison training with examples of faults type # 1 and testing with the rest of the different examples of the Database (Table III / Fig. 14 / Fig. 15).

Performance continues to be better for the Energy weighted score. But from this data we can draw the following conclusions:

- Fig. 12 shows the first 3 signals corresponding to an impedance of 0.01 ohms, the next 3 signals correspond with an impedance of 80.0 ohms, and the final third group of three signals corresponds to an impedance of 150.0 ohms.

- Focusing on the value of f1, the first group (0.01 ohms) has a value of 68.13%, 68.36% and 77.65% respectively with each score used. The second group (150 ohms) has a value of 64.72%, 63.69%, and 69.9%. And finally, the third group (80 ohms) f1 scores are 68.21%, 65.35%, and 71.73%.

- Better performance is seen when the impedance of the fault is lower, as was logical in principle. And a worsening of the energy-based score with respect to the so-called standard. Nevertheless, the performance of the Weighted-energy remains above the other two.

D. Training with Faults type #8 / Test with all types

Now we carried out an experiment like the previous one *C*, but for the type of fault #8. For this experiment we also perform two different tests. First, we compare the performance of the TransSiamese model training with faults type #8 and testing with faults type #8 (different examples from Training and Test). (Table IV / Fig. 16 / Fig. 17). In the second test, we carried out a comparison training with examples of Faults type # 8 and testing with the rest of the different examples of the database (Table V / Fig. 18 / Fig. 19).

However, unlike the previous experiment, in this case we will focus on the larger impedances to analyze their behavior. The conclusions obtained for the first experiment are:

- The value of f1 for each of the scores for an impedance of 150 ohms is 71.54%, 72.7%, and 77.31%. For the 1000 ohms case, the value of f1 would be 69.25%, 68.08%, and 77.31%.-

The impedance value plays an important role in the performance of the proposed system; and the type of fault simulated in this case (grounding of the three phases) is easier to deal with than in the case of the previous experiment.

In a second experiment, with inference test data other than the trained faults (#8), the results are very similar, except for a couple of faults, 22 and 30, in phases R and S respectively, where the energy-based score is above the other two scores. As a detail, this is a fault with an impedance of 20 ohms and 100 ohms respectively, and the spurious result is due to an anomalous sporadic threshold behavior. Note that the colors of the graph have been changed to highlight these significant details.

E. Training with all type of Faults / Test with all types

Now we carried out an experiment similar to the previous ones but with all the types of faults to train and all the types of faults to test. (Different examples from Training and Test). (Table VI / Fig. 20 / Fig. 21).

In this last experiment, 3 faults of each impedance (0.01, 80, 150 and 1000 ohms) are used for each type of fault considered, with a total of 60 samples in the graph in Fig. 20.

It shows a greater stability in the results, and a growth in the performance of the standard and energy-based scores. But the best results for the Weighted-energy score are maintained over the first two, highlighting the best results for this score in this last experiment. It should also be noted that there were no problems related to the computation of the threshold.

F. SOTA models comparison analysis

In this experiment, we compare the performance of TransSiamese model with SOTA models for multivariate time-series anomaly detection, including TranAD [[43], LSTM_AD [51], DAGMM [23], OmniAnomaly [24], and GDN [25], training with our Dataset of 200 signals [14]. (Table VII / Fig. 22 / Fig. 23 / Fig. 24 / Fig. 25 / Fig. 26). This comparison has been done thanks to the great work done by the authors of [40] on their public GitHub (https://github.com/imperial-qore/TranAD).

We also tested some simplified versions of TranAD (with some of the features annulated), but due to its low f1 scores, do not include the results in the comparative.

Finally, we have performed tests of the average training and inference times for all models (Table VIII / Table IX).

As previously mentioned, our database consists of temporal signals that reflect the response of an electrical network to the injection of a high-frequency pulse. These temporal series

have the characteristic of continuous anomaly starting from a certain point until the end of the signal.

In contrast to typical benchmarking datasets for anomaly detection, where signals have normally punctual anomalies throughout the entire signal, our signals exhibit this continuous anomaly characteristic. This peculiarity is due to the fact that signal rebounds are almost identical until the point of the fault occurrence. From that point onward until the end of the signal, discrepancies are present throughout the signal's duration.

Training different SOTA models, as shown in Table VII, does not yield satisfactory results. While some models achieve f1 scores close to 0.5, this score does not truly reflect the essence of the f1 measure (a metric that computes how many times a model makes correct predictions across the entire dataset). The reason is the nature of the mentioned anomalies in our dataset. Since the signals have an initial zone with virtually no anomalies and from a certain time onwards, the anomaly persists until the end, a poorly-performing model will still have reasonably high correct predictions by chance alone, as they will coincidentally align with the model's erroneous predictions.

Figures (Fig 22, Fig 23, Fig 24, Fig 25, Fig 26) illustrate the response of each of the tested models, demonstrating that anomaly detection is weak in all of them due to the nature of our signals continuous anomalies. As previously mentioned, they all have a random "hit rate" within the anomaly or non-anomaly window.

This fact becomes evident when examining the ROC/AUC parameter, which reflects the relationship between the true positive rate (as a percentage of all occurring events) and the false positive rate (as a percentage of all non-occurring events). It can take values between 0 and 1, with a perfect classifier having an ROC/AUC of 1 and a random classifier having an ROC/AUC of 0.5. In our case, the models tested with our dataset have an ROC/AUC value around 0.5, revealing their poor performance (close to randomness).

The model presented in this paper combines the Siamese scheme with Contrastive learning and a score based on weighted energy computation during inference. These features result in an f1 score around 0.78 and ROC/AUC values of 0.85 when tested on our electrical signal fault database, indicating the superior performance of this model compared to other SOTA models for our specific database case.

In conclusion, we can say that our model doesn't necessarily claim superiority over other state-of-the-art (SOTA) models. Instead, we could say that it presents a new approach to anomaly detection, leveraging Transformers as a foundation.

Most SOTA models usually focus on detecting anomalies that occur sporadically within a short time frame, but our model is designed to identify anomalies that persist from a specific moment until the end of the data sequence.

Due to this reason the SOTA models are not well-suited to handle such data patterns. This approach allowed us to treat the entire signal as a whole and helped the network learn to distinguish specific temporal sections of the signal that highlight differences in the learned signal model.

Consequently, our model successfully learned to discern between the pre-fault section and the rest of the signal following the anomaly. So, it's important to note that our model's strength lies in its adaptability to a particular type of data where SOTA models might not perform well due to the inherent nature of the data.

In terms of computational cost comparison tests, the presented model "TransSiamese" (Table VIII and Table IX) ranks below only "TranAD" during training, while having lower computational cost than the rest of the models. In inference mode, it is also surpassed only by "TranAD," while having lower computational cost than the other models.

V. CONCLUSIONS

The present study becomes a new approach to the problem of anomaly detection in temporal signals using Transformers as the main component of the proposed system. The difference with respect to other authors who have used similar techniques lies in the very nature of the data that needs to be processed.

These diverge from the data normally used in anomaly detection because of their marked character of long-term changes over an oscillating signal typical of electrical systems. This means that the algorithms present so far do not provide the results offered by our proposal. Mainly because the algorithms prior to ours focus on detecting anomalies that may occur in a short period of time and sporadically.

The use of the Siamese network scheme and the corresponding training algorithm, Contrastive learning, has helped to treat the signal as a whole. Causing the network to learn to discern specific temporal sections of the signal that would enhance the differences on the learned signal model. In this way, the network has successfully learned to discern between the pre-fault section, and the rest of the signal after the fault. In short, the Siamese-Contrastive pair clearly dampens the differences in the pre-fault section and amplifies these differences during the fault period. Therefore, we dare to conclude that this is one of the differentiating features with previous anomaly detection algorithms.

On the other hand, and unlike previous proposals, during training we have used the information from the fault signals, and not only learnt the representation of the pre-fault signals (in normal conditions) to highlight the differences when a fault unfortunately appears. Also, the database used is only 200 fault signals with a single pre-fault signal. Demonstrating that the use of approximations such as the Transformer is able to obtain results using schemes such as the one presented based on the Siamese network. Finally, we have used 3 different scores to obtain the best possible thresholding. These three scores, and especially the Weighted-energy score, have given stability to the results of the Siamese network.

VI. FUTURE WORK

Future work should focus primarily on improving the results shown in this paper. Although the results presented here are good and represent an f1 value close to 80%, the expectations of the working group are to improve them in order to achieve a reliable system that will allow us to move towards the goal of fault localization.

It is this challenge, localization, which is therefore our focus of interest. And it is around this epicenter that our research will pivot from now on. In this respect, we are interested in applying other models, such as diffusion models, to the creation of a more extensive signal database.

On the other hand, the objectives of the research team in the field of electrical protection include the detection of faults in power transformers, the adjustment of protection functions based on network parameters, the development of protection algorithms for the detection of power oscillations and loss of stability, the detection of faults in DC networks, and the automatic generation of diagnostic reports.

Finally, our great challenge is to take this study to a real installation, which we are already working on and are currently carrying out field tests to obtain real faults. Here we will have the opportunity to validate our studies with simulated data and make any corrections that may be considered.

Graphics of Experiment B: Anomaly Score functions comparative

TABLE I Experiment B Statistics

	f1	Precision	Recall	ROC/AU
Standard	0.64158503	0.9387835	0.52802129	0.67264408
Energy	0.68725497	0.94739297	0.5571459	0.70070008
Energy Pond	0.77026476	0.9692443	0.6494186	0.77197252

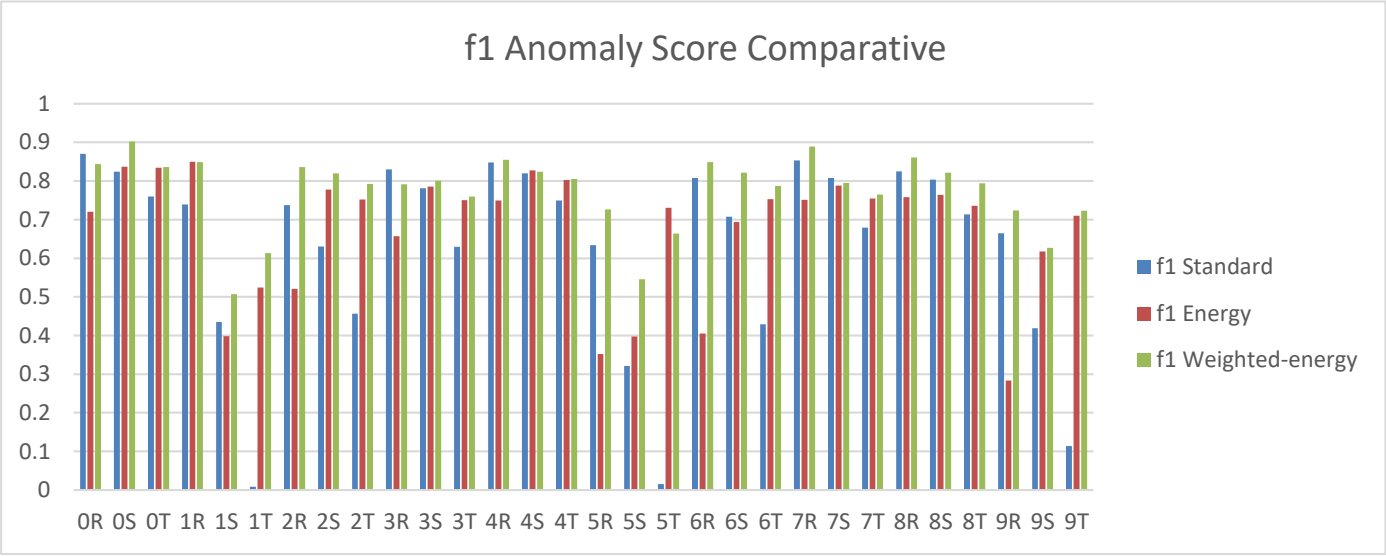

FIGURE 10. **Anomaly Score Graph for the same group of signals for training and testing**

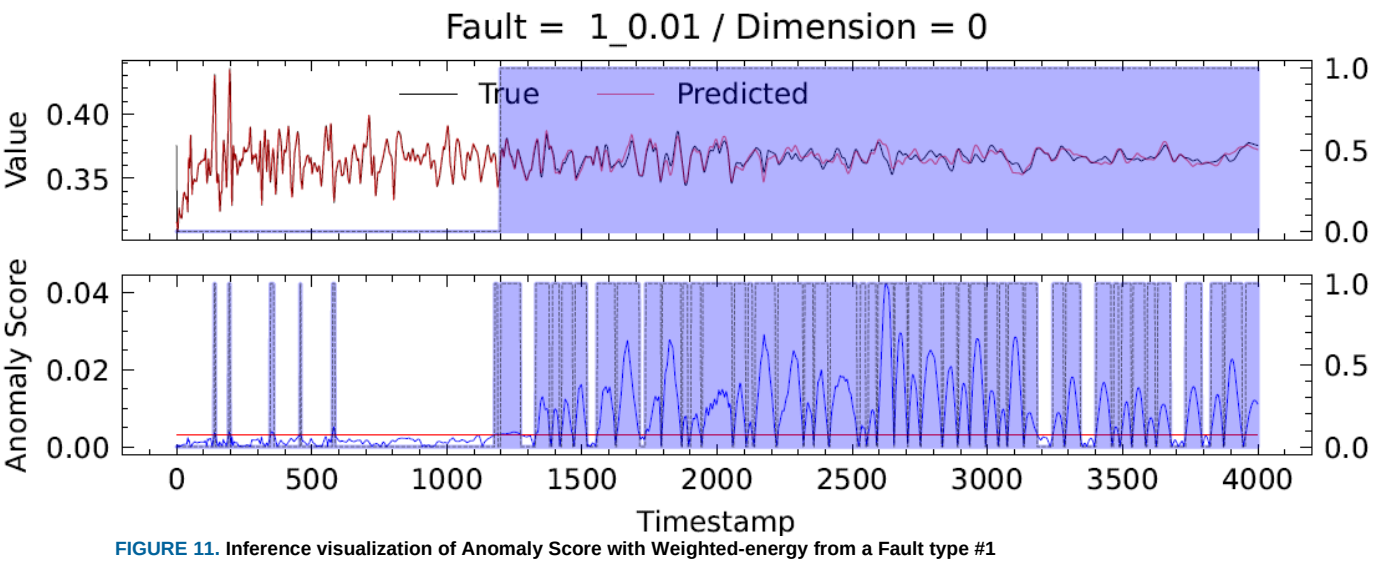

FIGURE 11. **Inference visualization of Anomaly Score with Weighted-energy from a Fault type #1**

Graphics of Experiment C-1: Training with Faults type #1 / Test with Faults type #1

TABLE II Experiment C-1 Statistics

	f1	Precision	Recall	ROC/AU
Standard	0.689699343	0.945218886	0.563306952	0.6965848
Energy	0.685920359	0.946301277	0.557836452	0.697872624
Energy Pond	0.749123135	0.966526213	0.623625054	0.757293567

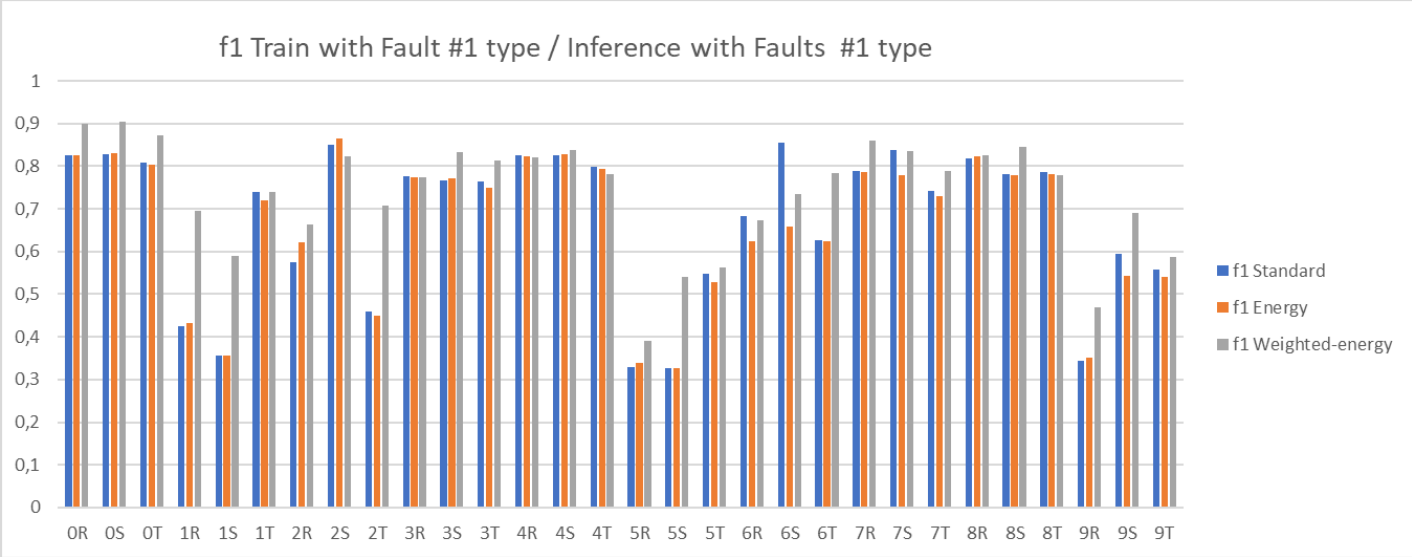

FIGURE 12. **Anomaly Score Graph for Training with Faults type #1 and Testing with Faults type #1 (different samples for training and testing)**

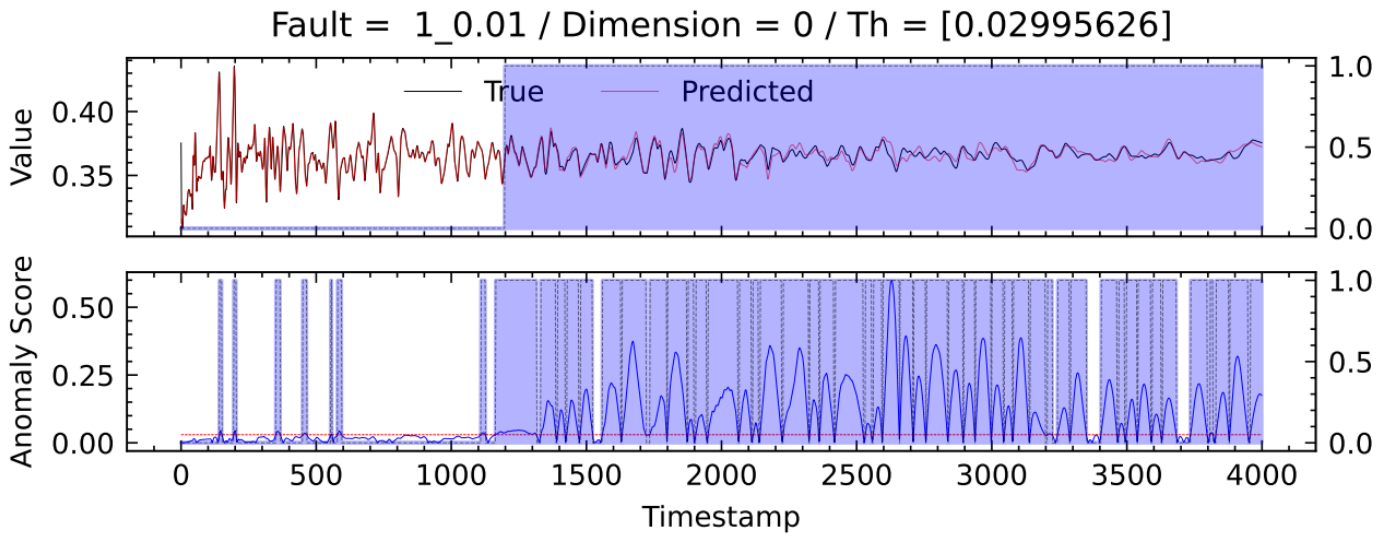

FIGURE 13. **Inference visualization of Anomaly Score with Weighted-energy from a Fault type #1**

Graphics of Experiment C-2: Training with Faults type #1 / Test with Faults different of type #1

TABLE III Experiment C-2 Statistics

	f1	Precision	Recall	ROC/AU
Standard	0.657564425	0.928790453	0.529382265	0.669702676
Energy	0.68785823	0.92747917	0.56211502	0.67521833
Energy Pond	0.750869733	0.954086755	0.626748132	0.742819733

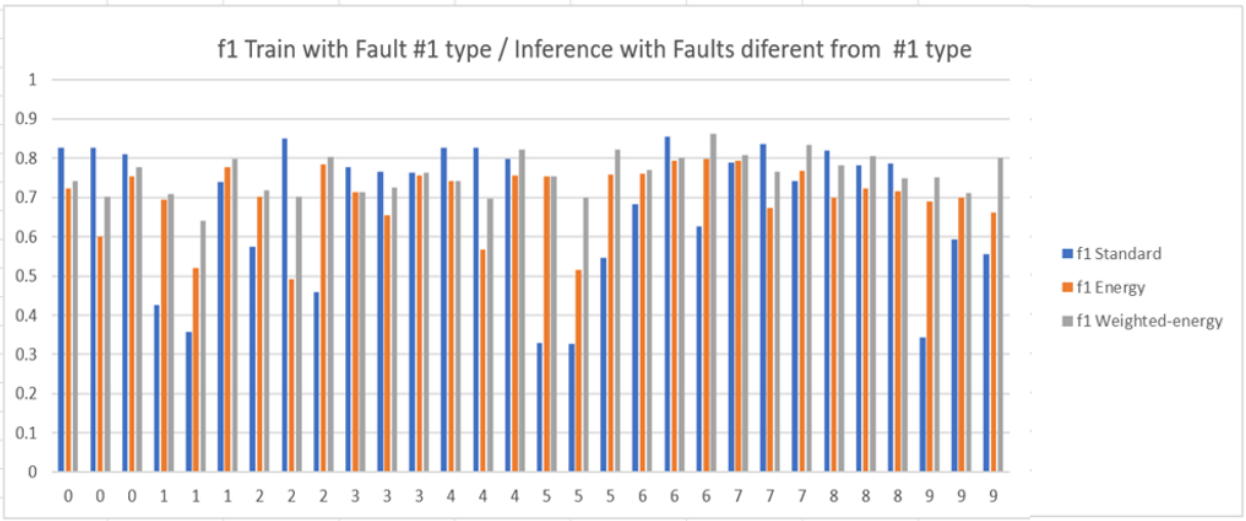

FIGURE 14. **Inference visualization of Anomaly Score with Weighted-energy from a Fault type #1**

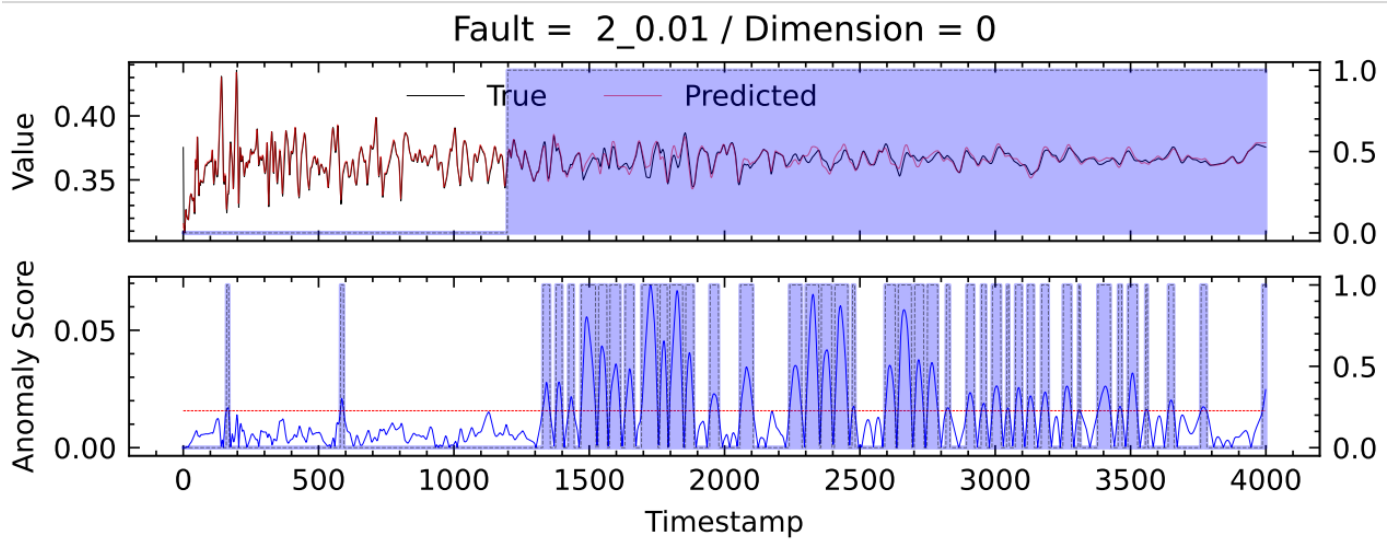

FIGURE 15. **Inference visualization of Anomaly Score with Weighted-energy from a Fault type #1 example.**

Graphics of Experiment D-1: Training with Faults type #8 / Test with Faults type #8

TABLE IV Experiment D-1 Statistics

	f1	Precision	Recall	ROC/AU
Standard	0.691373549	0.921645093	0.563082093	0.664378462
Energy	0.69564127	0.925664542	0.569371442	0.670698514
Energy Pond	0.773586772	0.951525975	0.657702626	0.750835581

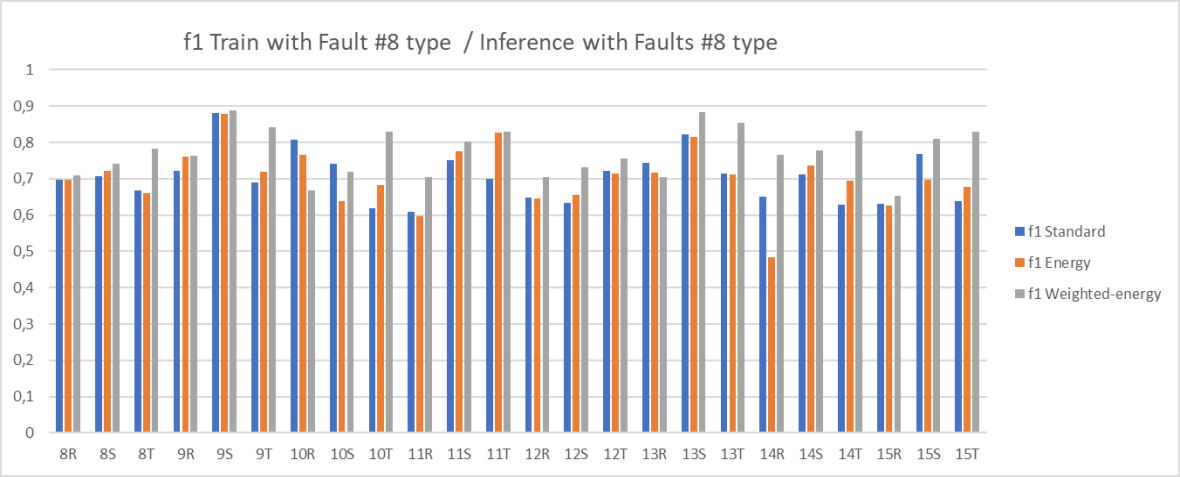

FIGURE 16. **Anomaly Score Graph for Training with Faults type #8 and Testing with Faults type #8 (similar samples for training and testing)**

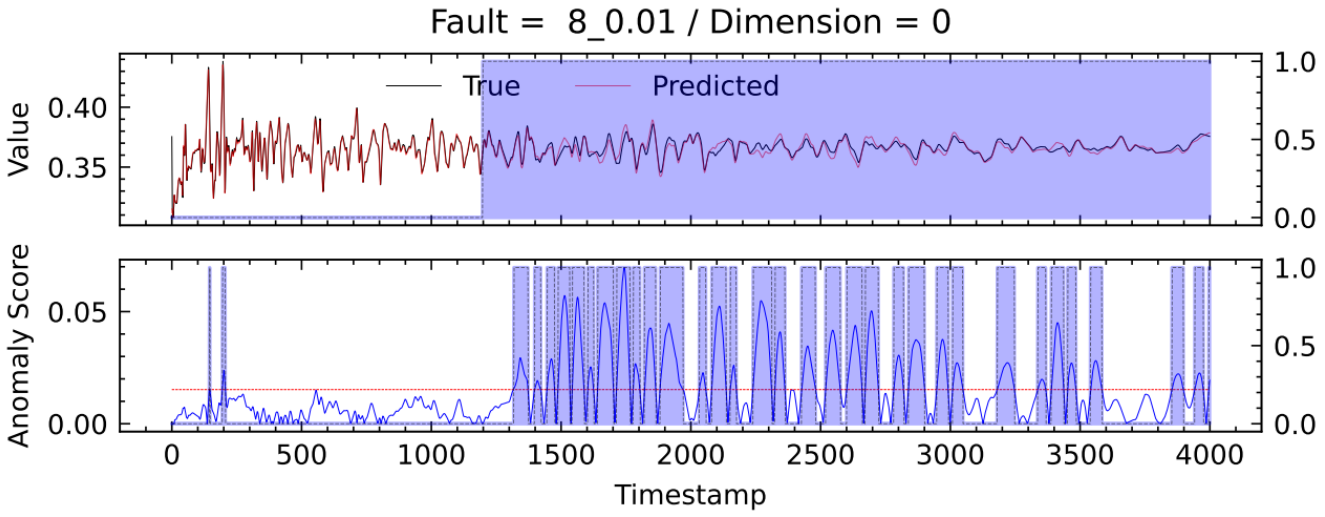

FIGURE 17. **Inference visualization of Anomaly Score with Weighted-energy from a Fault type #8**

Graphics of Experiment D-2: Training with Faults type #8 / Test with Faults other than type #8

TABLE V Experiment D-2 Statistics

	f1	precision	recall	ROC/AU
Standard	0.659910107	0.930519634	0.533532216	0.673398363
Energy	0.683029015	0.932477107	0.556738539	0.678588514
Energy Pond	0.747073327	0.956830318	0.623118222	0.745009676

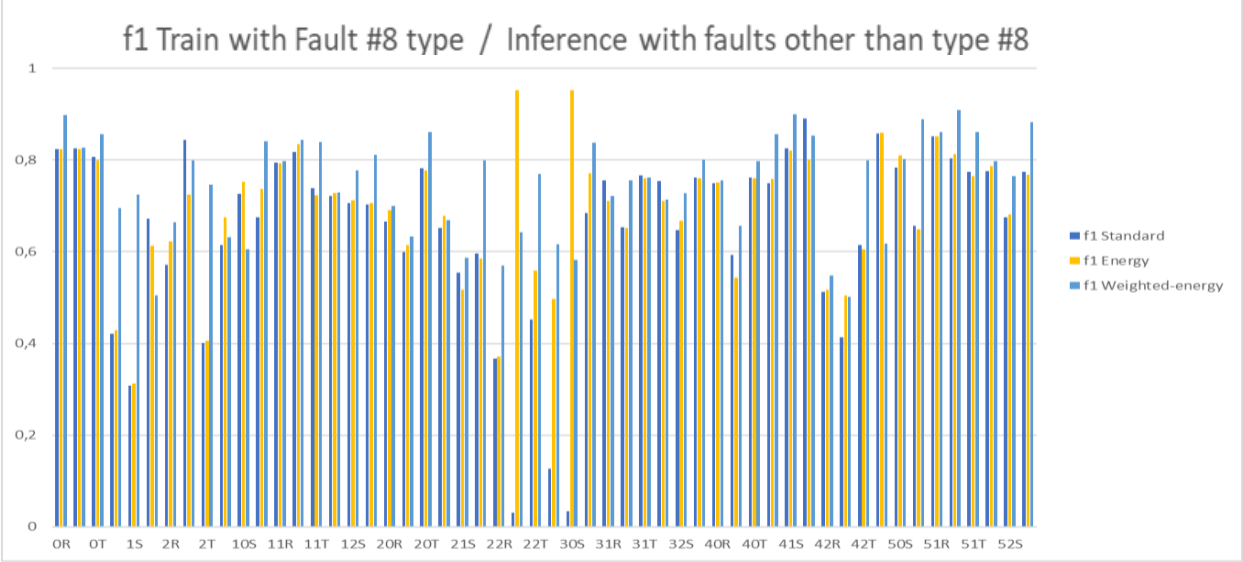

FIGURE 18. **Anomaly Score graph for Training with Faults type #8 and Testing with Faults different of type #8**

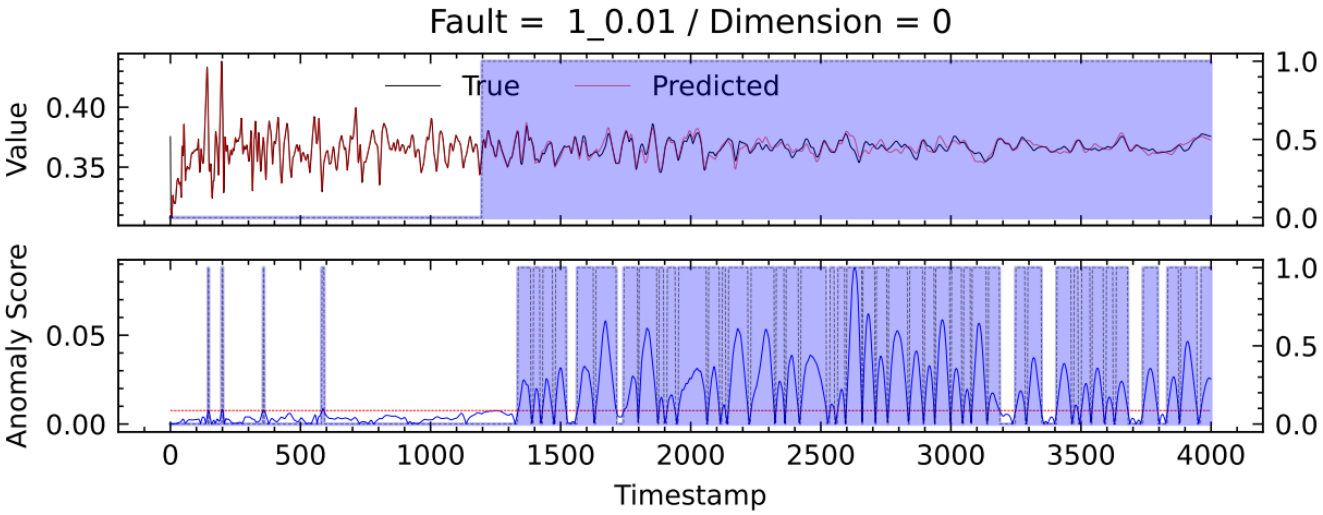

FIGURE 19. **Inference visualization of Anomaly Score with Weighted-energy from a Fault type #1**

E. Training with all type of Faults / Test with all types

TABLE VI Experiment E Statistics

	f1	precision	recall	ROC/AU
Standard	0,73399097	0,93714714	0,60816678	0,75515462
Energy	0,73356683	0,92937304	0,61009398	0,74988561
Weighted-energy	0,78584826	0,95209383	0,67382822	0,79679168

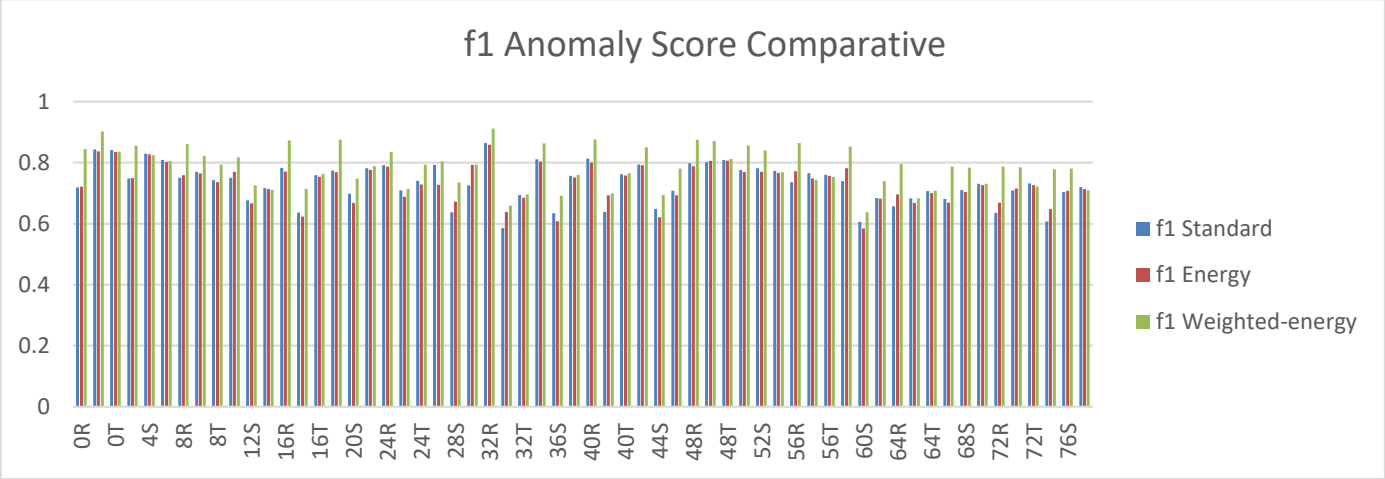

FIGURE 20. Anomaly Score graph for Training with all types of Faults and Testing with all types of Faults (different samples for training and testing)

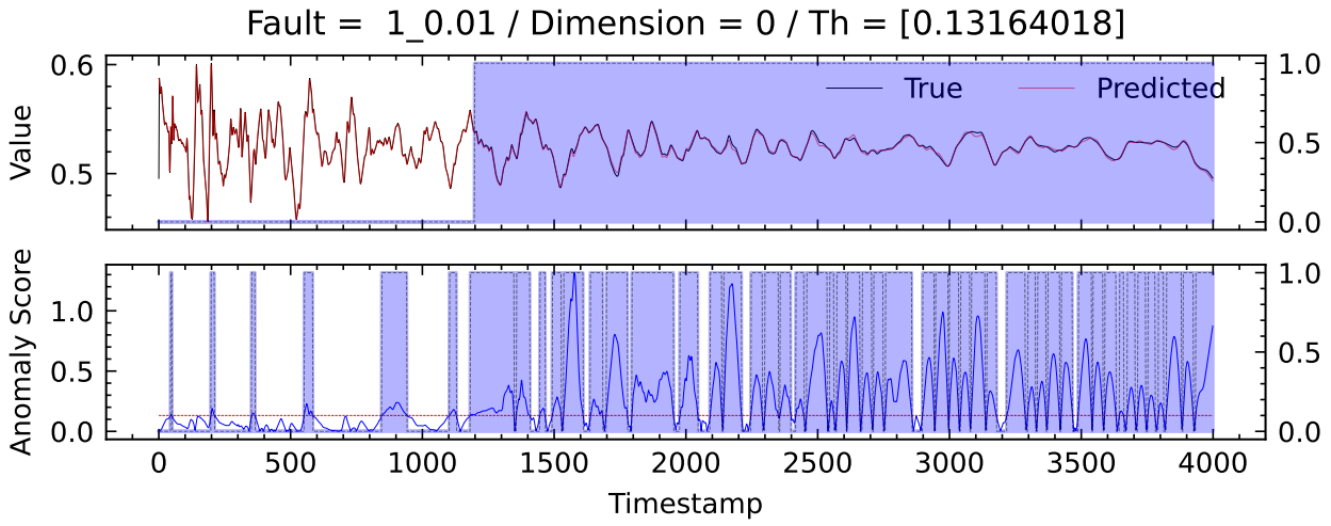

FIGURE 21. Inference visualization of Anomaly Score with Weighted-energy from a Fault type #1

F. Performance Comparison of several SOTA models

TABLE VII Performance comparison of TransSiamese with SOTA methods on the paper dataset [14]. The best scores are

	Performance comparison			
Algorithm	f1	precision	recall	ROC/AUC
DAGMM	0.0439	0.2516	0.0289	0.4296
TranAD	0.2676	0.5339	0.2918	0.4991
OmniAnomaly	0.3520	0.7076	0.2836	0.4232
GDN	0.3893	0.6508	0.3366	0.4948
LSTM_AD	0.5656	0.7957	0.5216	0.5414
TransSiamese	**0.7858**	**0.9521**	**0.6738**	**0.7968**

TABLE VIII Comparison of training times.

	Training phase			
Algorithm	Elapsed Time [seg]	Epochs	Time/epoch [seg/epoch]	% time comparative
GDN	46062.031	100	460.620	8833%
LSTM_AD	1415.840	100	14.158	272%
OmniAnomaly	1115.000	100	11.150	214%
DAGMM	798.188	100	7.982	153%
TranAD	302.844	100	3.028	58%
TransSiamese	521.465	100	5.215	100%

TABLE IX Comparison of inference times.

	Inference phase			
Algorithm	Threshold computing [seg]	Inference process [seg]	Total time consumed [seg]	% time comparative
GDN	0.07813	20.3005	20.379	10333%
OmniAnomaly	0.07813	2.4189	2.497	1266%
DAGMM	0.07813	1.7799	1.858	942%
LSTM_AD	0.07813	1.5991	1.677	850%
TranAD	0.07813	0.0791	0.157	80%
TransSiamese	0.07813	0.1191	0.197	100%

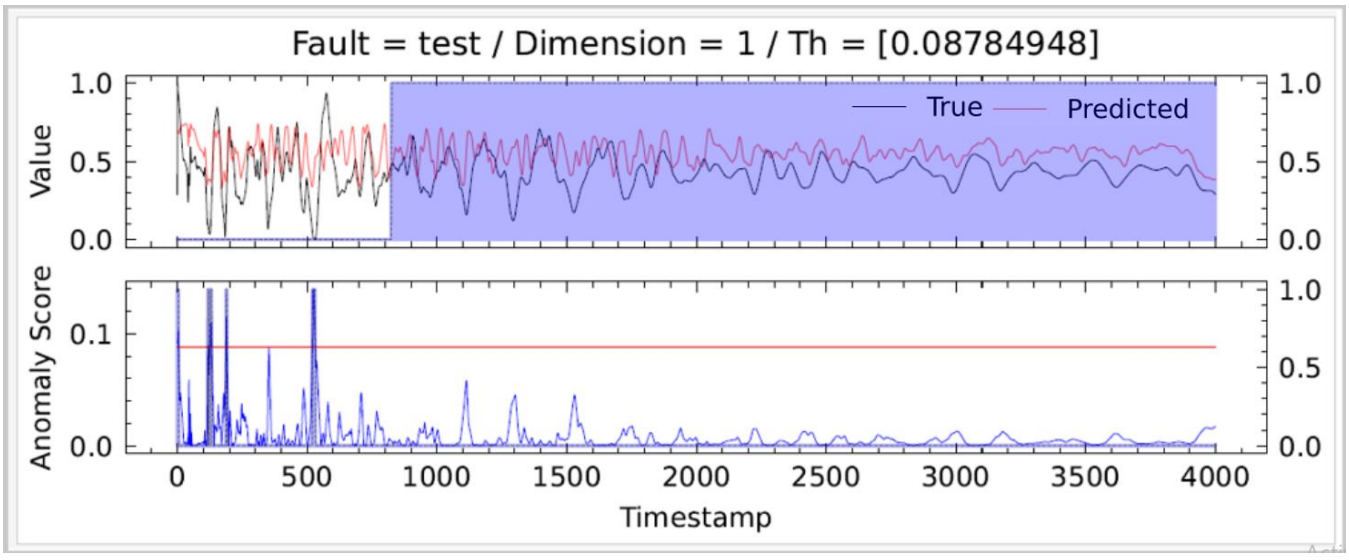

FIGURE 22. Inference visualization of Anomaly Score from LSTM-AD model

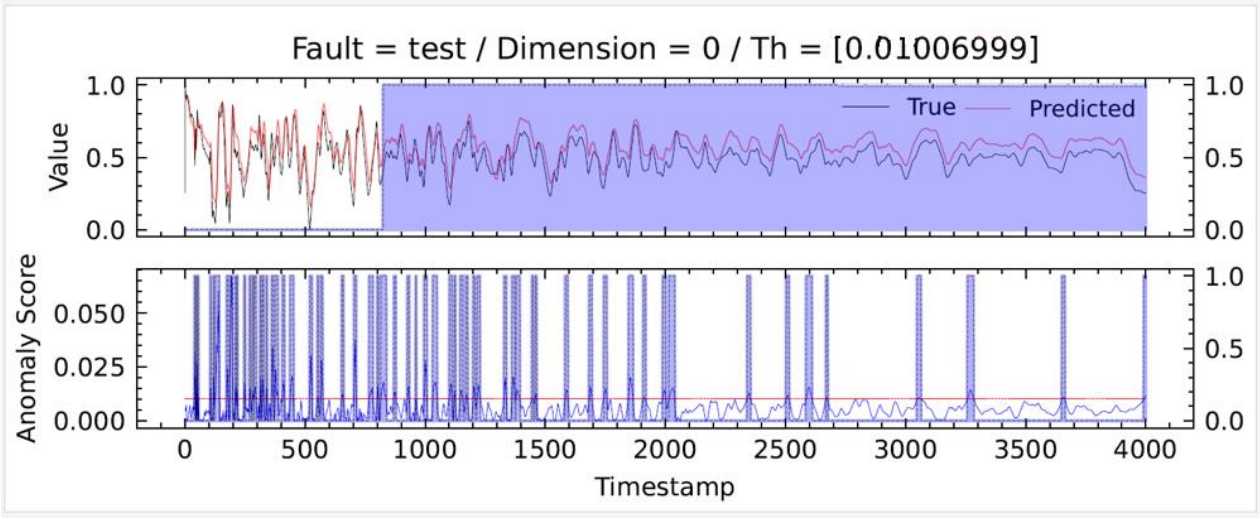

FIGURE 23. Inference visualization of Anomaly Score from GDN model

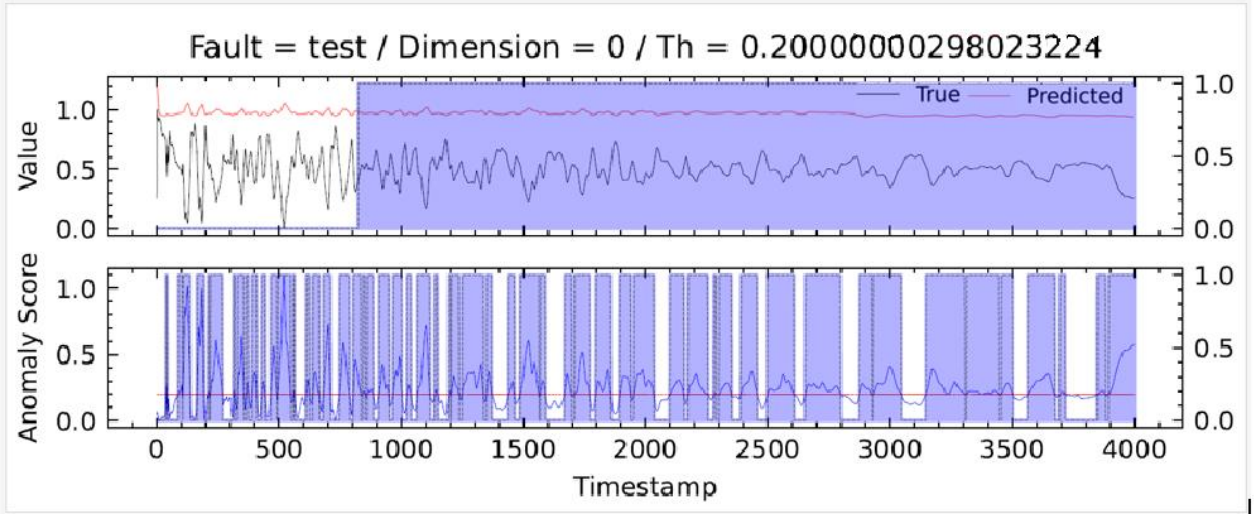

FIGURE 24. Inference visualization of Anomaly Score from LSTM-AD model

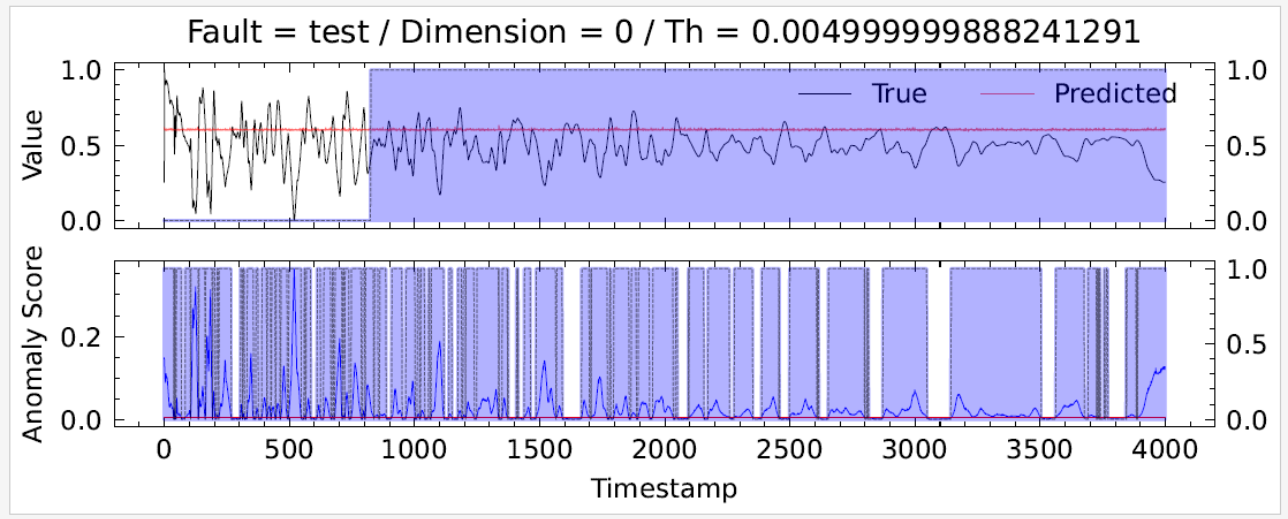

FIGURE 25. Inference visualization of Anomaly Score from Omnianomaly model

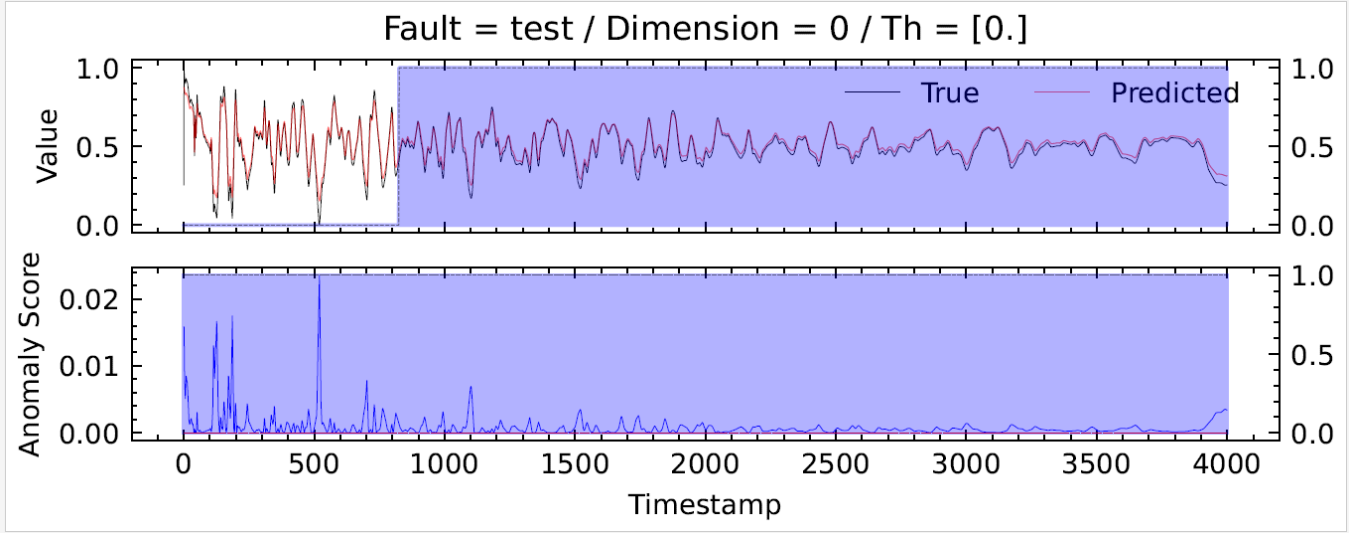

FIGURE 26. **Inference visualization of Anomaly Score from TranAD model**

REFERENCES

[1] Q. Wang, "Research on Fault Predition and Self-healing Control Technology of Distribution Network".

[2] L. Peretto, R. Tinarelli, A. Bauer, and S. Pugliese, "Fault location in underground power networks: A case study," *ISGT 2011*. pp. 1–6, 2011. doi: 10.1109/ISGT.2011.5759198.

[3] A. Bahmanyar, S. Jamali, A. Estebsari, and E. Bompard, "A comparison framework for distribution system outage and fault location methods," *Electric Power Systems Research*, vol. 145, pp. 19–34, 2017, doi: 10.1016/j.epsr.2016.12.018.

[4] J.-H. Teng, W.-H. Huang, and S.-W. Luan, "Automatic and Fast Faulted Line-Section Location Method for Distribution Systems Based on Fault Indicators," *IEEE Transactions on Power Systems*, vol. 29, no. 4, 2014, Accessed: Apr. 13, 2022. [Online]. Available: https://ieeexplore-ieee-org.cuarzo.unizar.es:9443/document/6695790/

[5] J. Oasa *et al.*, "Verification of fault location by TDR measurement on an actual line including multiple ground-mounted equipment," 2021.

[6] R. Lacoste, "Time Domain Reflectometry," *Robert Lacoste's The Darker Side*, pp. 33–47, 2010, doi: 10.1016/B978-1-85617-762-7.00003-4.

[7] J. G. Fornas, E. H. Jaraba, H. Bludszuweit, D. Cervero, and A. L. Estopinan, "Modeling and Simulation of Time Domain Reflectometry Signals on a Real Network for Use in Fault Classification and Location," *IEEE Access*, 2023, doi: 10.1109/ACCESS.2023.3253772.

[8] Y. Miyoshi and S. Saba, "Some Features and Performances of Type C Transmission-Line Fault Locators," *Transactions of the American Institute of Electrical Engineers. Part III: Power Apparatus and Systems*, vol. 76, no. 3, pp. 445–451, 1957, doi: 10.1109/AIEEPAS.1957.4499585.

[9] C. C. Zhou, Q. Shu, and X. Y. Han, "A single-phase earth fault location scheme for distribution feeder on the basis of the difference of zero mode traveling waves," *International Transactions on Electrical Energy Systems*, vol. 27, no. 5, p. e2298, May 2017, doi: 10.1002/ETEP.2298.

[10] W. Chonglin, W. Yangyang, L. Rui, and S. Gang, "Fault Location for Single-Phase-To-Earth Faults Based on Transient Traveling Wave Method and Artificial Pulse Signal Injection Method," in *2010 International Conference on Electrical and Control Engineering*, IEEE, 2010. Accessed: Mar. 30, 2022. [Online]. Available: https://ieeexplore-ieee-org.cuarzo.unizar.es:9443/document/5629889/

[11] M. Abad, U. Zaragoza, N. El, H. Saudi, A.-S. Arabia, and M. G.-G. Circe -Spain, "New fault location method for up-to-date and upcoming distribution networks," pp. 15–18, 2015.

[12] F. J. L. Padua and R. De Oliveira, "Allocation of PLC Devices in a Low-Voltage Grid," *2019 IEEE PES Conference on Innovative Smart Grid Technologies, ISGT Latin America 2019*, Sep. 2019, doi: 10.1109/ISGT-LA.2019.8895457.

[13] J. G. Fornas, E. H. Jaraba, A. L. Estopinan, and J. Saldana, "Detection and Classification of Fault Types in Distribution Lines by Applying Contrastive Learning to GAN Encoded Time-Series of Pulse Reflectometry Signals," *IEEE Access*, vol. 10, pp. 110521–110536, 2022, doi: 10.1109/ACCESS.2022.3214994.

[14] E. Herrero, J. Granado, and A. Llombart, "CVLAB-UNIZAR/CIRCE_fault_database: Initial release," Nov. 2022, doi: 10.5281/ZENODO.7316010.

[15] S. Ahmed, I. E. Nielsen, A. Tripathi, S. Siddiqui, G. Rasool, and R. P. Ramachandran, "Transformers in Time-series Analysis: A Tutorial," Apr. 2022, [Online]. Available: http://arxiv.org/abs/2205.01138

[16] M. Hu, X. Feng, Z. Ji, K. Yan, and S. Zhou, "A novel computational approach for discord search with local recurrence rates in multivariate time series," *Inf Sci (N Y)*, vol. 477, pp. 220–233, 2019, doi: 10.1016/j.ins.2018.10.047.

[17] Z. Ji, Y. Wang, K. Yan, X. Xie, Y. Xiang, and J. Huang, "A space-embedding strategy for anomaly detection in multivariate time series," *Expert Syst Appl*, vol. 206, p. 117892, Nov. 2022, doi: 10.1016/J.ESWA.2022.117892.

[18] H. Qin, X. Zhan, and Y. Zheng, "CSCAD: Correlation Structure-Based Collective Anomaly Detection in Complex System," *IEEE Trans Knowl Data Eng*, vol. 35, no. 5, pp. 4634–4645, May 2023, doi: 10.1109/TKDE.2022.3154166.

[19] G. Xiang and R. Lin, "Robust Anomaly Detection for Multivariate Data of Spacecraft through Recurrent Neural Networks and Extreme Value Theory," *IEEE Access*, vol. 9, pp. 167447–167457, 2021, doi: 10.1109/ACCESS.2021.3136505.

[20] Z. Ji, J. Gong, and J. Feng, "A Novel Deep Learning Approach for Anomaly Detection of Time Series Data," 2021, doi: 10.1155/2021/6636270.

[21] M. Hu *et al.*, "Detecting Anomalies in Time Series Data via a Meta-Feature Based Approach," *IEEE Access*, vol. 6, pp. 27760–27776, May 2018, doi: 10.1109/ACCESS.2018.2840086.

[22] J. Audibert, P. Michiardi, F. Guyard, S. Marti, and M. A. Zuluaga, "USAD : UnSupervised Anomaly Detection on Multivari-ate Time Series," vol. 20, 2020, doi: 10.1145/3394486.3403392.

[23] B. Zong *et al.*, "Deep Autoencoding Gaussian Mixture Model for Unsupervised Anomaly Detection," *31st International Conference on Machine Learning, ICML 2014*, vol. 5, pp. 3800–3809, Feb. 2018.

[24] Y. Su, R. Liu, Y. Zhao, W. Sun, C. Niu, and D. Pei, "Robust anomaly detection for multivariate time series through stochastic recurrent neural network," *Proceedings of the ACM SIGKDD International Conference on Knowledge Discovery and Data Mining*, pp. 2828–2837, Jul. 2019, doi: 10.1145/3292500.3330672.

[25] A. Deng and B. Hooi, "Graph Neural Network-Based Anomaly Detection in Multivariate Time Series," *Proceedings of the AAAI Conference on Artificial Intelligence*, vol. 35, no. 5, pp. 4027–4035, May 2021, doi: 10.1609/AAAI.V35I5.16523.

[26] H. Zhou, K. Yu, X. Zhang, G. Wu, and A. Yazidi, "Contrastive autoencoder for anomaly detection in multivariate time series," *Inf Sci (N Y)*, vol. 610, pp. 266–280, Sep. 2022, doi: 10.1016/j.ins.2022.07.179.

[27] Vaswani, A., Shazeer, N., Parmar, N., Uszkoreit, J., Jones, L., Gomez, A. N., Kaiser, Ł. & Polosukhin, I. (2017). Attention is all you need. Advances in Neural Information Processing Systems (p./pp. 5998--6008),

[28] J. Xu, H. Wu, J. Wang, and M. Long, "ANOMALY TRANSFORMER: TIME SERIES ANOMALY DETECTION WITH ASSOCIATION DISCREPANCY."

[29] J. Abulizi, Z. Chen, P. Liu, H. Sun, C. Ji, and Z. Li, "Research on Voiceprint Recognition of Power Transformer Anomalies Using Gated Recurrent Unit," *2021 Power System and Green Energy Conference (PSGEC)*, 2021, doi: 10.1109/PSGEC51302.2021.9542338.

[30] H. Wang, X. Shen, M. Tu, Y. Zhuang, and Z. Liu, "Improved Transformer With Multi-Head Dense Collaboration," *IEEE/ACM Trans Audio Speech Lang Process*, vol. 30, pp. 2754–2767, 2022, doi: 10.1109/TASLP.2022.3199648.

[31] M. Yu, D. Wu, W. Rao, L. Cheng, R. Li, and Y. Li, "Automated Road Crack Detection Method based on Visual Transformer with Multi-Head Cross-Attention," *Proceedings of 2022 IEEE International Conference on Sensing, Diagnostics, Prognostics, and Control, SDPC 2022*, pp. 328–332, 2022, doi: 10.1109/SDPC55702.2022.9915808.

[32] M. Garg, D. Ghosh, and P. M. Pradhan, "Multiscaled Multi-Head Attention-Based Video Transformer Network for Hand Gesture Recognition," *IEEE Signal Process Lett*, vol. 30, pp. 80–84, 2023, doi: 10.1109/LSP.2023.3241857.

[33] J. Zhang, Y. Chen, and J. Chen, "Join-Chain Network: A Logical Reasoning View of the Multi-head Attention in Transformer," *IEEE International Conference on Data Mining Workshops, ICDMW*, vol. 2022-November, pp. 947–957, 2022, doi: 10.1109/ICDMW58026.2022.00123.

[34] Q. Ma, M. Zhang, Y. Xu, J. Song, and T. Zhang, "Remaining Useful Life Estimation for Turbofan Engine with Transformer-based Deep Architecture," *2021 26th International Conference on Automation and Computing: System Intelligence through Automation and Computing, ICAC 2021*, 2021, doi: 10.23919/ICAC50006.2021.9594150.

[35] R. Fan, "Transformer-Based Deep Learning Method for the Prediction of Ventilator Pressure," *2022 2nd IEEE International Conference on Information Communication and Software Engineering, ICICSE 2022*, pp. 25–28, 2022, doi: 10.1109/ICICSE55337.2022.9828926.

[36] B. Padi, A. Mohan, and S. Ganapathy, "End-to-end Language Recognition Using Attention Based Hierarchical Gated Recurrent Unit Models," *ICASSP, IEEE International Conference on Acoustics, Speech and Signal Processing - Proceedings*, vol. 2019-May, pp. 5966–5970, May 2019, doi: 10.1109/ICASSP.2019.8683895.

[37] P. Awwal and S. Naval, "Optimized Attention-based Long-short-term memory and Gated Recurrent Unit for Malware Detection in Windows," pp. 217–222, Mar. 2023, doi: 10.1109/CENTCON56610.2022.10051287.

[38] S. T. Rajamani, K. T. Rajamani, A. Mallol-Ragolta, S. Liu, and B. Schuller, "A novel attention-based gated recurrent unit and its efficacy in speech emotion recognition," *ICASSP, IEEE International Conference on Acoustics, Speech and Signal Processing - Proceedings*, vol. 2021-June, pp. 6294–6298, 2021, doi: 10.1109/ICASSP39728.2021.9414489.

[39] G. Zerveas *et al.*, "Virtual Event," vol. 11, no. 21, doi: 10.1145/3447548.3467401.

[40] R. Bai *et al.*, "Hierarchical Graph Convolutional Skeleton Transformer for Action Recognition," *Proc (IEEE Int Conf Multimed Expo)*, vol. 2022-July, 2022, doi: 10.1109/ICME52920.2022.9859781.

[41] T. L. Hoang, T. D. Pham, and V. C. Ta, "Improving Graph Convolutional Networks with Transformer Layer in social-based items recommendation," *Proceedings - International Conference on Knowledge and Systems Engineering, KSE*, vol. 2021-November, 2021, doi: 10.1109/KSE53942.2021.9648823.

[42] R. Slama, W. Rabah, and H. Wannous, "STr-GCN: Dual Spatial Graph Convolutional Network and Transformer Graph Encoder for 3D Hand Gesture Recognition," *2023 IEEE 17th International Conference on Automatic Face and Gesture Recognition, FG 2023*, 2023, doi: 10.1109/FG57933.2023.10042643.

[43] S. Tuli, G. Casale, and N. R. Jennings, "TranAD," *Proceedings of the VLDB Endowment*, vol. 15, no. 6, pp. 1201–1214, Feb. 2022, doi: 10.14778/3514061.3514067.

[44] H. Takimoto, J. Seki, S. F. Situju, and A. Kanagawa, "Applied Artificial Intelligence Anomaly Detection Using Siamese Network with Attention Mechanism for Few-Shot Learning," 2022, doi: 10.1080/08839514.2022.2094885.

[45] "SIAMESE ATTENTION NETWORKS."

[46] W. Gedara, C. Bandara, and V. M. Patel, "A Transformer-Based Siamese Network for Change Detection; A Transformer-Based Siamese Network for Change Detection," 2022, doi: 10.1109/IGARSS46834.2022.9883686.

[47] W. G. C. Bandara and V. M. Patel, "A Transformer-Based Siamese Network for Change Detection," *International Geoscience and Remote Sensing Symposium (IGARSS)*, vol. 2022-July, pp. 207–210, 2022, doi: 10.1109/IGARSS46834.2022.9883686.

[48] B. Ramachandra, M. J. Jones, and R. R. Vatsavai, "Learning a distance function with a Siamese network to localize anomalies in videos."

[49] C. Ye and Q. Ma, "TS2V: A Transformer-Based Siamese Network for Representation Learning of Univariate Time-Series Data; TS2V: A Transformer-Based Siamese Network for Representation Learning of Univariate Time-Series Data," 2022, doi: 10.1109/CSCWD54268.2022.9776300.

[50] "A Transformer-Based Siamese Network for Change Detection | IEEE Conference Publication | IEEE Xplore." https://ieeexplore-ieee-org.cuarzo.unizar.es:9443/document/9883686 (accessed May 14, 2023).

[51] P. Malhotra, A. Ramakrishnan, G. Anand, L. Vig, P. Agarwal, and G. Shroff, "LSTM-based Encoder-Decoder for Multi-sensor Anomaly Detection".

JAVIER GRANADO FORNÁS received the B.Sc. in industrial engineering (specialized in industrial electronics) and M.Sc. degrees in electronics engineering (intelligent environments specialization) from the University of Zaragoza, Spain, in 1994 and 2014, respectively. He is currently pursuing the Ph.D. degree in Deep Learning around classification and localization of faults in distributions lines. Since 2009, he has been working as a Senior Researcher with the Electronics Systems Group at CIRCE Technology Center. His main research interests include electronic designs control projects around Deep Learning and algorithms for fault detection.

ELÍAS HERRERO JARABA has a PhD in Engineering from the University of Zaragoza since June 2005, and has been a professor at the University of Zaragoza since 2002. In 1999, and for 4 years, he worked in the automotive field at Opel Spain, in the production department.
Within the university he has developed his research in the area of computer vision, and since 2012 he has focused his interest in the field of neural networks, and more recently, in Deep Learning. In the meantime, he held the position of coordinator of the Smart Vehicle initiative of the Aragon Institute for Engineering Research (I3A).
He currently holds a European patent and has led to more than six projects funded in public competitions, more than 20 projects with companies, 12 indexed publications, and more than 50 contributions to international conferences. It is worth mentioning the 3M award for his research in the CvLAB research group. His teaching work has focused on electronics, from its basics to power electronics, including embedded systems.

ANDRÉS LLOMBART ESTOPIÑAN is the General Director of CIRCE since April 2016 and former Executive Director since January 2011. He was also a lecturer of the Electrical Department at University of Zaragoza since June
2003 to May 2018. In November 2011 was designated by the Science and innovation Ministry as the expert in Energy Area Committee of the7th Funding Program of the European Union, being in charge of the coordination of electricity grids topics. In CIRCE, he is in charge of Innovation and Promotion Unit, created by himself on May 2009. From March 2007 until March 2009, he was Subdirector of Institutional Relations of the Superior Polytechnic Centre of the University of Zaragoza. In 1994, he received an Industrial Engineer degree at the University of Zaragoza. Later, he researched the impact reduction of power electronic source grids using passive filters in the kilowatt range. This research gave him a PhD title (specialised in electrical engineering) by the University of Zaragoza in 2000. From December 1994 to May 2001, he was an associate professor in the Electrical Engineering Department at the University of Zaragoza, where he performed the following teaching activities: electric circuit theory, industrial actuation, wind energy, and renewable energy integration. He participated in more than 35 R&D+i projects; in 16 of them, he was the primary researcher. Authors of 10 articles in indexed journals and more than 50 contributions in international congresses. Active participation in forums, associations, and platforms linked to activity lines.
Eight patents, of which seven are being exploited.

3.5 Estudio 5:Experiencia Piloto de Localización de Faltas en Red de Media Tensión Mediante la Técnica de la Reflectrometría en el Dominio del Tiempo (TDR) en el Proyecto H2020 - Flexigrid

RESUMEN: En este artículo se presenta la experiencia piloto llevada a cabo en la instalación real modelada utilizada en esta tesis de un prototipo basado en la técnica TDR y que contiene los mismos elementos que se presentaron en el Estudio 1.

EXPERIENCIA PILOTO DE LOCALIZACIÓN DE FALTAS EN RED DE MEDIA TENSIÓN MEDIANTE LA TÉCNICA DE LA REFLECTOMETRÍA EN EL DOMINIO DEL TIEMPO (TDR) EN EL PROYECTO H2020 - FLEXIGRID

Javier Granado Fornás, Grupo de sistemas electrónicos, Centro Tecnológico CIRCE
David Cervero García, Grupo de sistemas electrónicos, Fundación CIRCE
Mario Mañana Canteli, Departamento de Ingeniería Eléctrica y Energética, Universidad de Cantabria
Roberto Cimadevilla González, ZIV Automation
Carlos Gil Martín, ZIV Automation
Jose Ivan Rodriguez Alonso, EDP Redes España
Antonio González Diego, EDP Redes España

Resumen: Actualmente, los operadores de sistemas de distribución (DSO) están especialmente preocupados por reducir los tiempos de interrupción ante una falta. Las técnicas de localización automática de faltas son un método eficaz para reducir los tiempos de interrupción que se producen durante una avería en la red de distribución. Debido a que las redes de distribución suelen tener una topología radial, de anillo o de malla, con muchos nodos y ramas, los métodos de localización necesitan supervisar toda la red o una sección importante de la misma. Además, la presencia de cargas desequilibradas es una característica de los sistemas de distribución. Las dos casuísticas anteriores pueden afectar a los métodos de localización, reduciendo su rendimiento. Por ejemplo, los métodos clásicos basados en la impedancia pueden tener errores sustanciales en este tipo de redes. Sin embargo, la técnica de localización de faltas TDR, se presenta como una solución con gran potencial para permitir la localización automática de faltas en redes de media y baja tensión. En este trabajo presentado en el proyecto FLEXIGRID, financiado por la comisión europea, se muestra como se ha desarrollado un prototipo funcional que se ha instalado en una red real de media tensión. Se presenta la arquitectura del prototipo, así como el modelo de la red real, la simulación de las faltas, y el diseño y fabricación del prototipo del inyector de señal (TDR), así como la instalación y funcionamiento de este y los resultados obtenidos y esperados en el proyecto.

Palabras clave: Redes de distribución, Localización de Faltas, Reflectometría en el dominio del tiempo (TDR).

1) INTRODUCCIÓN

Cuando se produce una falta, un número indeterminado de clientes se queda sin suministro durante el tiempo necesario para solucionar el problema y restaurar el servicio y, algunas centrales eléctricas pueden verse afectadas por ello. Las centrales de generación convencionales suelen ser muy grandes y están conectadas típicamente a la red de transporte, por tanto las faltas en las redes de distribución no suelen afectarles *per se* porque pueden seguir dando servicio a otros puntos de la red, pero la GD (Generación Distribuida) está instalada en la red de distribución y por tanto una falta en esa red no solo afecta a los usuarios de esa red sino que imposibilita a la GD para verter energía a esa red. Las técnicas de localización automática de averías pueden ayudar a minimizar este tiempo de interrupción, teniendo en cuenta que la mayoría de las interrupciones se producen durante una avería en la red de distribución [1]-[3]. Cuando los equipos de mantenimiento son capaces de encontrar el problema más rápidamente gracias a las técnicas de localización de averías, éstas pueden repararse antes.

Las técnicas de localización de averías se utilizan mucho en las líneas de transporte, donde cada línea se supervisa por separado. Pero las redes de distribución suelen tener una topología radial, de anillo o de malla, con muchos nodos y ramas [4]-[8]. Por lo tanto, los métodos de localización necesitan un enfoque diferente para obtener un sistema rentable que pueda supervisar toda la red o una sección importante de la misma. La presencia de cargas desequilibradas, laterales y diferentes tipos de cables/conductores son características específicas de los sistemas de distribución. Estas características afectan a varios supuestos de los métodos de localización, reduciendo su rendimiento. Además, las redes IT (*Isolé-Terre*) son habituales en los sistemas de distribución. La localización es más difícil en estas redes [9]. En este tipo de redes, los métodos clásicos basados en la impedancia presentan errores considerables. Existen otras técnicas, como las basadas en "onda viajera". Dentro de estas, existe fundamentalmente dos métodos:

- Medición de la señal transitoria producida por la avería. Este enfoque se utiliza ampliamente en los sistemas de transmisión [10], en los que las líneas se supervisan por separado. Sin embargo, en las redes de distribución, esas

ondas transitorias experimentan múltiples reflexiones debido a la topología. Por lo tanto, la intensidad de la señal puede ser demasiado débil cuando llega al localizador, lo que dificulta la localización del origen de la avería.

- Inyectar una señal de alta frecuencia y medir los frentes de onda reflejados. Esta técnica se denomina comúnmente reflectometría en el dominio del tiempo (TDR). En este piloto instalado para el proyecto FLEXIGRID, se ha utilizado esta técnica. En ella se inyectan pulsos en la red continuamente y se va registrando la respuesta de la red a esos pulsos. De este modo, se tiene siempre una "foto" del estado de la red antes de ocurrir la falta. Esto es necesario porque la topología de la red, así como sus impedancias conectadas pueden variar con el tiempo. Una vez que se ha producido la falta, se vuelve a realizar una nueva inyección de pulsos y su respuesta se procesa junto con la última respuesta de la red guardada antes de la falta. De este modo se obtienen mejores resultados, ya que esta técnica es más robusta frente a cambios de la topología de la red (bifurcaciones) que otras técnicas antes mencionadas.

2) EL PROYECTO H2020 FLEXIGRID

Dentro del proyecto FLEXIGRID, la localización de faltas pretende desarrollar el primer demostrador en una instalación real de un localizador de faltas basado en la técnica ya mencionada de la Inyección de pulsos de alta frecuencia (TDR).

En el proyecto se pretende colocar el prototipo (en una primera fase), en una red de Viesgo en la que se producirán faltas con un generador de faltas que se dispondrá a tal efecto. Una vez verificado el funcionamiento correcto y reajustado el algoritmo de localización, se instalará en otra red de Viesgo donde se producen faltas "naturales" con relativa frecuencia. De este modo se pretende comprobar la precisión en la localización del prototipo desarrollado. Con toda la información recopilada durante el proyecto y los datos de campo se podrá seguir mejorando el sistema de cara a conseguir diseñar un equipo que pueda ser industrializado al menor coste posible.

Esquemáticamente, el sistema se puede representar tal como se aprecia en la Figura 1.

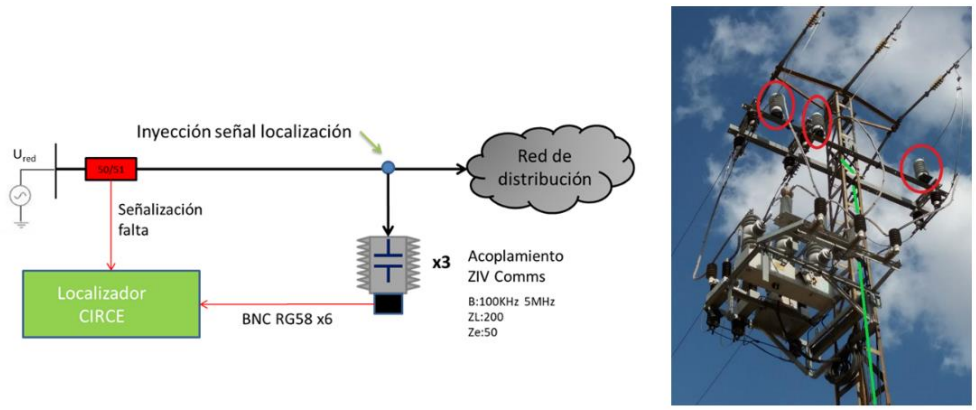

Figura 1. Esquema del localizador (TDR)

El sistema consta del localizador propiamente dicho, el cual genera los pulsos de alta frecuencia que se inyectan en la red y también digitaliza la señal de respuesta de la red para poder ser almacenada y procesada posteriormente. El Localizador se conecta a la red de MT a través de un acoplamiento desarrollado por la empresa ZIV. Este acoplamiento es en esencia una capacidad y una inductancia que sirve para aislar el localizador de la tensión de red (12kV) al bloquear las bajas frecuencias (50 Hz) de la misma. Asimismo, permite que los pulsos de alta frecuencia generados por el localizador atraviesen el acoplamiento y se inyecten en la red. También se cuenta con un relé de señalización de falta que avisa al localizador cuando se produce una falta. De este modo el localizador sabe cuándo realizar la inyección en falta.

Para alcanzar este hito se han realizado varias etapas dentro del proyecto que se detallan a continuación:

2.1) Modelado de una red real de VIESGO

La red en la que inicialmente se ha colocado el equipo es una línea de MT (12 kV) en Cantabria, (Figura 2).

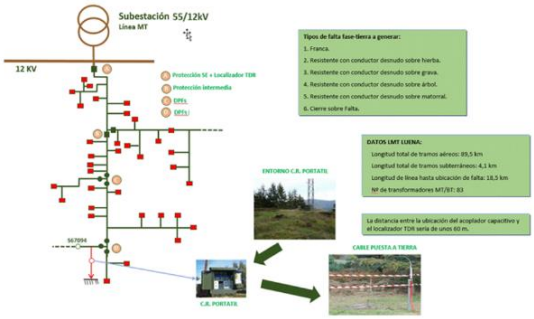

Figura 2. Detalle de la línea de MT

Tal como se ha mencionado, como primer paso se ha procedido a modelar la red, el acoplamiento y el inyector en DigSilent™ (Figura 3) para posteriormente, realizar simulaciones y determinar cuál es la mejor localización para colocar el prototipo.

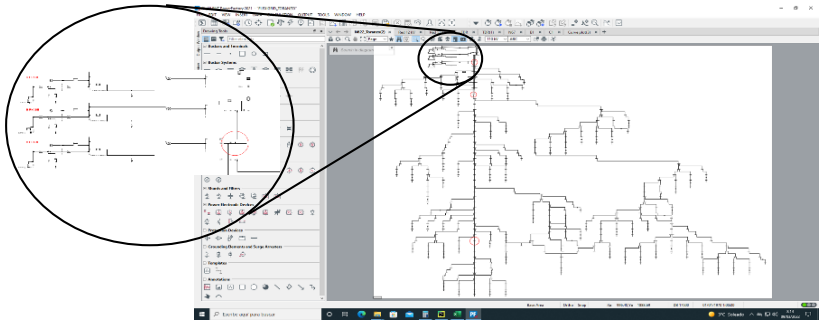

Figura 3. Detalle de la simulación de la red, acoplamineto e inyector en DigSilent

2.2) Simulación de DigSilent™

Tras el modelado se han realizado simulaciones de distintas faltas en distintas localizaciones para estudiar el resultado y verificar con un primer algoritmo básico, si las distancias reales se pueden inferir de las señales recibidas.

A continuación se muestra un ejemplo del resultado obtenido de una simulación de falta:

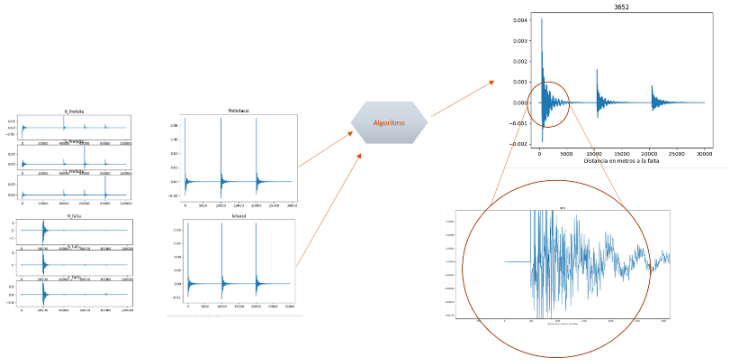

Figura 4. Señales simuladas en DigSilent™ sobre la red modelada y distancia calculada por el algoritmo

En la Figura 4 se muestra a la izquierda arriba las señales de respuesta de la red a la inyección de los pulsos (uno por cada fase R-S-T) en el estado de pre-falta (red en estado normal) y abajo la respuesta de la red en el estado de falta (se aprecian los *spikes* producidos por la falta simulada). Posteriormente se cogen los pulsos y se concatenan para conformar una única señal de pre-falta y otra de falta. Se introducen las dos señales en el algoritmo de localización para determinar el grado de precisión que se puede obtener a nivel de simulación. En este caso la distancia real era de 3650 m y la distancia calculada por el algoritmo fue de 3652 m.

2.3) Desarrollo del Hardware/Firmware del prototipo

Para el desarrollo del prototipo se ha partido de una plataforma comercial robusta y de alta capacidad de cómputo. Se ha elegido un equipo de National Instruments™. A continuación se muestra un detalle del sistema desarrollado:

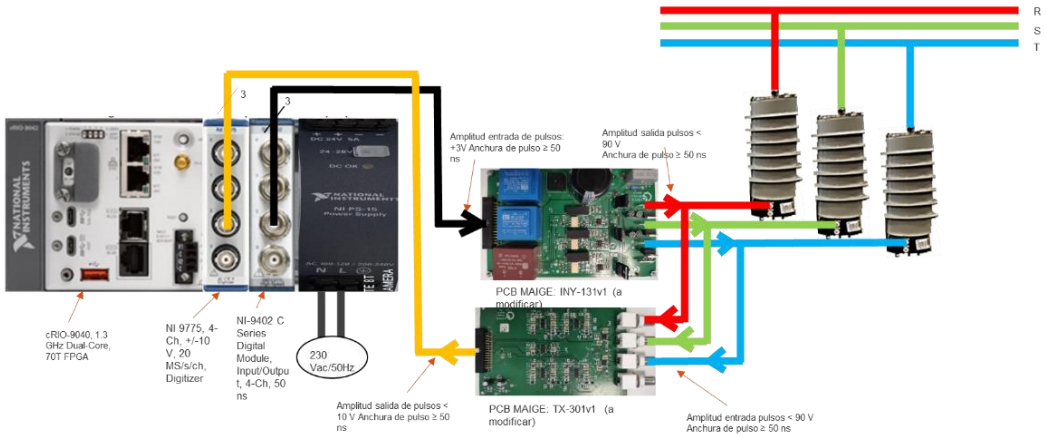

Figura 5. *Detalle del desarrollo del Hardware del localizador.*

En la Figura 5 se aprecia como el sistema comercial utilizado es un CompactRIO™ de National Instruments™, que dispone además de 4 conversores A/D para digitalizar las señales de respuesta de la red, así como 4 canales I/O con el que se generan los pulsos de alta frecuencia para inyectar en la red. Las señales de salida (pulsos) se adaptan en tensión y corriente para poder inyectar la energía necesaria a la red. Esto se consigue mediante una tarjeta electrónica desarrollada *ad-hoc* por CIRCE. Asimismo CIRCE ha desarrollado una tarjeta de adaptación de las señales de respuesta para adaptarlas en nivel de tensión a los requisitos de entrada del conversor A/D. En la Figura 5 se puede apreciar también los acoplamientos aportados por ZIV (uno por cada fase R-S-T-) para conectar el localizador a la red.

2.4) Verificación del prototipo en laboratorio

Una vez montado el prototipo, se procedió a verificar en laboratorio (Figura 6) si su funcionalidad era adecuada. Para ello se conectó a un carrete de cable de unos 2.550 m y se puso a funcionar inyectando pulsos y digitalizando la respuesta. En la Figura 7 se puede observar una señal obtenida durante las pruebas:

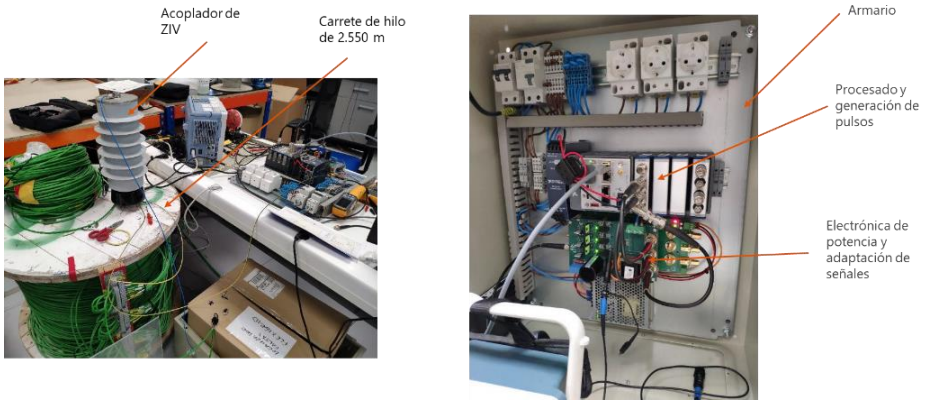

Figura 6. *Detalle del las pruebas del localizador en el laboratorio*

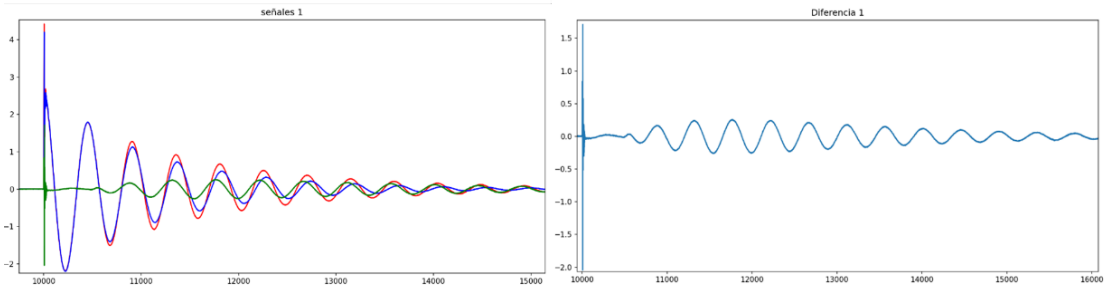

Figura 7. Izquierda: Señales inyectada en pre-falta (azul) y en falta (roja). Derecha: Señal diferencia entre pre-falta y falta.

$$d = \frac{(500) \times \left(\frac{3 \times 10^8}{1{,}5}\right) \times (50 \times 10^{-9})}{2} = 2.500\,m \quad (1)$$

En la ecuación (1) se calcula la distancia d. Las señales de pre-falta y falta empiezan a diferir en torno a las 500 muestras. Por lo tanto, teniendo en cuenta que se muestrea a 50 ns (50×10^{-9}) y que la velocidad de la señal por ese tipo de cable es aproximadamente la de la luz partido por 1,5 → $\left(\frac{3 \times 10^8}{1{,}5}\right)$ y que hay que dividir por 2 porque el pulso va hasta la falta y tiene que volver al localizador, se obtiene una distancia de la falta realizada en el carrete de prueba del laboratorio de aproximadamente 2.500 m. Calculamos el error cometido:

$$e = |Valor\ real - Valor\ obtenido| = |2.550 - 2.500| = 50\,m \quad (2) \qquad \varepsilon(\%) = \frac{e}{Valor\ real} = \frac{50}{2.550} \times 100 = 1{,}9\% \quad (3)$$

Con el cálculo del error absoluto de (2) y el error relativo de (3) se comprueba que a nivel de laboratorio, el sistema tiene una precisión suficiente como para poder instalarlo en campo.

2.5) Instalación en campo

En la primera fase de instalación en campo, se instala el prototipo en la línea de MT (Figura 8) y se recogen las señales de respuesta de la red (Figura 9):

Figura 8. Imágenes de la instalación. De izquierda a derecha, poste al lado del C.T. donde instalar el localizador/Trabajos previos para instalación bajo tensión / Instalación de los acopladores / Armario del localizador instalado dentro del C.T.

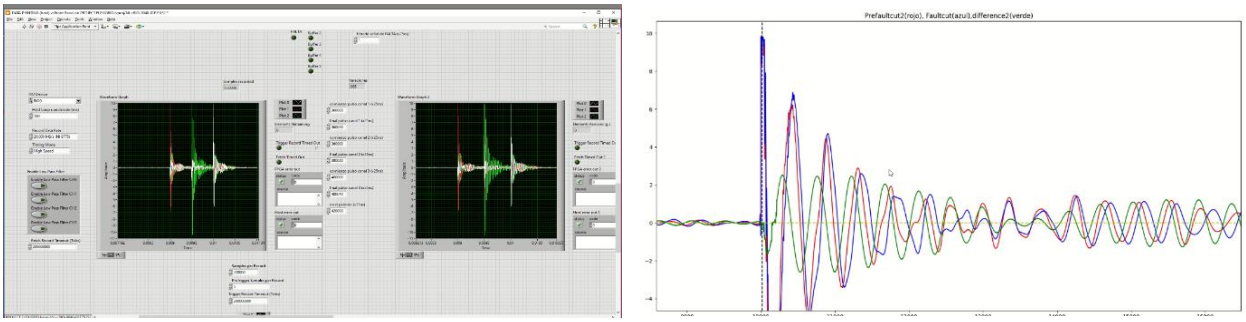

Figura 9. Imágenes de las señales del piloto instalado. Izquierda, señales digitalizadas por el Localizador con el software desarrollado bajo LabView™. Derecha, Señales procesadas off-line mediante algoritmo desarrollado en Python.

3) CONCLUSIONES

Tras su instalación, el prototipo ha estado durante 2 meses funcionando de manera ininterrumpida cumpliendo así uno de los requisitos del proyecto en cuanto a robustez del sistema. Por otro lado, las señales de respuesta de la red real tienen unas características muy similares a las simuladas y sobre todo a las inyectadas en el carrete del laboratorio. La siguiente fase del piloto es la de generar unas faltas provocadas con el generador de faltas que VIESGO tiene a tal efecto y con el que se comprobará el grado de precisión alcanzado con esta primera versión de algoritmo implementado. En función de estos resultados, se espera poder mejorar el algoritmo para, posteriormente trasladar el prototipo de localizador a otra red, donde se podrá verificar contra faltas naturales que se producen en la línea.

AGRADECIMIENTOS

Esta investigación ha recibido financiación del programa de investigación e innovación Horizon 2020 de la unión Europea bajo el marco del proyecto FLEXIGRID con Nº de acuerdo 864579.

REFERENCIAS

- [1] L. Peretto, R. Tinarelli, A. Bauer, and S. Pugliese, “Fault location in underground power networks: A case study,” ISGT 2011. pp. 1–6, 2011. doi: 10.1109/ISGT.2011.5759198.
- [2] A. Bahmanyar, S. Jamali, A. Estebsari, and E. Bompard, “A comparison framework for distribution system outage and fault location methods,” Electric Power Systems Research, vol. 145, pp. 19–34, Apr. 2017, doi: 10.1016/j.epsr.2016.12.018.
- [3] J. H. Teng, W. H. Huang, and S. W. Luan, “Automatic and Fast Faulted Line-Section Location Method for Distribution Systems Based on Fault Indicators,” IEEE Transactions on Power Systems, vol. 29, no. 4. pp. 1653–1662, 2014. doi: 10.1109/TPWRS.2013.2294338.
- [4] M. Abad López, “Algoritmos de localización de faltas en redes eléctricas,” Zaragoza, 2016.
- [5] S. Robson, A. Haddad, and H. Griffiths, “Fault Location on Branched Networks Using a Multiended Approach,” IEEE Transactions on Power Delivery, vol. 29, no. 4. pp. 1955–1963, 2014. doi: 10.1109/TPWRD.2014.2302137.
- [6] K. Sun, Q. Chen, and Z. Gao, “An Automatic Faulted Line Section Location Method for Electric Power Distribution Systems Based on Multisource Information,” IEEE Transactions on Power Delivery, vol. 31, no. 4. pp. 1542–1551, 2016. doi: 10.1109/TPWRD.2015.2473681.
- [7] S. Lotfifard, M. Kezunovic, and M. J. Mousavi, “A Systematic Approach for Ranking Distribution Systems Fault Location Algorithms and Eliminating False Estimates,” IEEE Transactions on Power Delivery, vol. 28, no. 1. pp. 285–293, 2013. doi: 10.1109/TPWRD.2012.2213616.
- [8] R. J. Hamidi and H. Livani, “Traveling-Wave-Based Fault-Location Algorithm for Hybrid Multiterminal Circuits,” IEEE Transactions on Power Delivery, vol. 32, no. 1. pp. 135–144, 2017. doi: 10.1109/TPWRD.2016.2589265.
- [9] A. Farughian, L. Kumpulainen, and K. Kauhaniemi, “Review of methodologies for earth fault indication and location in compensated and unearthed MV distribution networks,” Electric Power Systems Research, vol. 154, no. Supplement C, pp. 373–380, 2018, doi: https://doi.org/10.1016/j.epsr.2017.09.006.
- [10] X. Lin, F. Zhao, G. Wu, Z. Li, and H. Weng, “Universal Wavefront Positioning Correction Method on Traveling-Wave-Based Fault-Location Algorithms,” IEEE Transactions on Power Delivery, vol. 27, no. 3, pp. 1601–1610, 2012, doi: 10.1109/TPWRD.2012.2190108.

Capítulo 4

Conclusiones

RESUMEN: En este capítulo se presentan las principales conclusiones de los estudios expuestos, así como las principales líneas para la continuación del trabajo realizado en el presente documento.

4.1 Conclusiones del estudio

De los resultados de las cinco publicaciones que componen esta investigación se derivan tres bloques de conclusiones. El primero de estos bloques se relaciona con el **Estudio 1**, donde se ha establecido la técnica TDR como herramienta para la obtención de la base de datos de señales que han servido para elaborar las investigaciones de esta tesis. Usando esta técnica, se ha modelado una red real (además del inyector y del acoplador) y se han simulado faltas de distintos tipos y a distintas distancias del inyector.

- La técnica del TDR tiene como principal ventaja el hecho de no necesitar más que un solo equipo, ya que las señales inyectadas rebotan en la red y vuelven al punto de inyección, donde se registran y procesan.
- Además, la técnica del TDR es agnóstica con respecto de la red donde se coloca, es decir, no necesita tener un conocimiento previo de la red, ya que se inyectan pulsos en el estado de prefalta y en el de falta, con lo que se puede procesar la diferencia relativa entre los dos estados independientemente del tipo de red o de su topología.
- A diferencia de las técnicas basadas en el registro de la perturbación producida en la corriente o tensión de la propia red mientras ocurre la falta, con la técnica TDR, se pueden registrar las señales de faltas ocurridas en la red incluso aunque la red esté des-energizada al haber actuado las protecciones como respuesta a la falta.

El segundo bloque está compuesto por los **Estudios 2 y 3**, y recoge la detección y clasificación de las faltas, así como la aplicación de DA mediante el uso de GAN.

- Se ha propuesto la ampliación de la base de datos inicial obtenida mediante modelado y simulación de una red real. La escasez de ejemplos reales debido a la naturaleza de las señales, así como la imposibilidad de generar decenas de miles de ejemplos mediante simulación, imposibilitan la aplicación de NN a una red real. Con este estudio, se aporta una metodología de ampliación de la base de datos de señales de falta mediante la síntesis de ejemplos utilizando redes GAN.

- Además, se ha utilizado esta base de datos de ejemplos sintéticos para entrenar una SNN con función de perdida Contrastiva. Este tipo de red hace que los ejemplos etiquetados como diferentes se separen aún más mientras que junta los que tienen la etiqueta de ejemplos iguales. Con este tipo de red, hemos conseguido clasificar de manera satisfactoria los distintos tipos de falta, teniendo en cuenta que las señales de distinto tipo presentan diferencias muy pequeñas entre si.
- Se ha comprobado que entrenando este tipo de red Siamesa solo con la base de ejemplos sintéticos ha sido capaz de tener una precisión cercana al 100 % cuando se le muestran ejemplos originales (nunca vistos)
- Además, se ha comprobado que se puede bajar la dimensionalidad de las señales mediante la función Piecewise Aggregate Approximation (PAA por sus siglas en Inglés), pasando de 4000x3 a 128x3. Con esto se ha conseguido entrenar la SNN con menor tiempo de procesado.

El tercer bloque está formado por el **Estudio 4**, y se centra en la aplicación de Transformers a la detección de anomalias en series temporales para la detección del tiempo hasta la falta (TtoF)

- En la aproximación a la detección del TtoF, nos encontramos con el mismo problema de la escasez de ejemplos que teníamos en la clasificación. Sin embargo, aquí no podemos utilizar las redes GAN para generar ejemplos sintéticos con distintas distancias de falta. Este es un problema de regresión lineal a diferencia del problema de clasificación anterior.
- En este caso hemos utilizado las propiedades de un tipo de redes llamadas Transformers. Estas redes, al entrenarse (aún con muy pocos ejemplos), tienen la capacidad de aprender a predecir la evolución de la señal al aprender sus características.
- Una vez entrenada, si se le muestra un ejemplo en el que hay una anomalía (falta), no es capaz de predecir correctamente la evolución de esa señal a partir de ese punto. Este hecho se aprovecha para determinar el punto temporal de aparición de la falta.

– El uso del esquema de red SNN y el algoritmo de entrenamiento correspondiente, aprendizaje contrastivo, junto a una función de puntuación de anomalía basada en la energía ponderada (en inferencia), ha ayudado a tratar la señal en su totalidad. Esto ha permitido que la red aprenda a distinguir secciones temporales específicas de la señal que realzan las diferencias en el modelo de señal aprendido. De esta manera, la red ha aprendido exitosamente a discernir entre la sección previa a la falta y el resto de la señal después de la falta.

4.2 Líneas de trabajo futuro

Las líneas de trabajos futuros se pueden clasificar en dos grupos. En primer lugar están los relativos a la temática de la clasificación de faltas:

- Explorar si el método utilizado es válido también para impedancias altas y para la detección simultánea de faltas.
- También sería interesante investigar si nuestro método puede verse afectado por la presencia de generación renovable en las redes de distribución, así como su comportamiento en redes de corriente continua (DC).
- Explorar si la red neuronal puede generalizar los tipos de faltas aprendidos a otras líneas de distribución reales, sin necesidad de volver a entrenarla o al menos con una fase de aprendizaje mínima. La versatilidad del proceso debe ser tal que funcione en diversos entornos.

En segundo lugar, se encuentran los relativos a la temática de la localización de faltas:

- El trabajo futuro debería centrarse principalmente en mejorar los resultados presentados en este artículo. Aunque los resultados presentados aquí son buenos y representan un valor de f1 superior al 70 %, las expectativas del grupo de trabajo son mejorarlos para lograr un sistema confiable que nos permita mejorar en este primer paso que hemos dado en la detección del tiempo hasta la falta (TtoF).
- En el objetivo final de la localización de faltas, en esta tesis se ha conseguido llegar a extraer la información acerca de la distancia desde el inyector hasta el punto donde se ha producido la falta (DtoF). Esta distancia es una medida indirecta que se puede obtener de la determinación que se hace del tiempo que tarda el pulso inyectado en llegar al punto donde se ha producido la falta y volver "rebotado" de nuevo al inyector (TtoF). Sin embargo, esta distancia, puede "cortar" distintas bifurcaciones de la misma red, haciendo necesaria la información adicional de cual ha sido el tramo en el que se ha producido la falta.

  Esta información, a día de hoy, tiene que llegar de la propia empresa distribuidora (mediante la detección del relé de paso de falta), pero sería una línea

de mejora el hecho de poder extraer esa información también de las señales de nuestra base de datos de faltas.

– También sería interesante en el sentido del punto anterior, explorar la posibilidad de instalar varios inyectores en la misma red de manera que se pudiera extraer la localización de la falta mediante la detección de la distancia a cada inyector y el procesado de esta información.
– Finalmente, nuestro gran desafío es llevar este estudio a una instalación real, en el cual ya estamos trabajando y llevando a cabo pruebas de campo para obtener faltas reales. Aquí tendremos la oportunidad de validar nuestros estudios con datos reales y realizar mejoras para continuar avanzando en este campo.

Bibliografía

[1] L. Peretto, R. Tinarelli, A. Bauer, and S. Pugliese, "Fault location in underground power networks: A case study," in *ISGT 2011*. IEEE, 2011, pp. 1–6. [Online]. Available: https://ieeexplore-ieee-org.cuarzo.unizar.es:9443/document/5759198/

[2] A. Bahmanyar, S. Jamali, A. Estebsari, and E. Bompard, "A comparison framework for distribution system outage and fault location methods," *Electric Power Systems Research*, vol. 145, pp. 19–34, 2017.

[3] J.-H. H. Teng, W.-H. H. Huang, and S.-W. W. Luan, "Automatic and Fast Faulted Line-Section Location Method for Distribution Systems Based on Fault Indicators," pp. 1653–1662, 2014. [Online]. Available: https://ieeexplore-ieee-org.cuarzo.unizar.es:9443/document/6695790/

[4] N. E. Halabi, "Localizadores de faltas para redes de distribución eléctrica," Tech. Rep.

[5] J. G. Fornas, E. H. Jaraba, H. Bludszuweit, D. Cervero, and A. L. Estopinan, "Modeling and Simulation of Time Domain Reflectometry Signals on a Real Network for Use in Fault Classification and Location," *IEEE Access*, 2023.

[6] J. G. Fornas, E. H. Jaraba, A. L. Estopinan, and J. Saldana, "Detection and Classification of Fault Types in Distribution Lines by Applying Contrastive Learning to GAN Encoded Time-series of Pulse Reflectometry Signals." *IEEE Access*, vol. 10, pp. 110 521–110 536, 2022.

[7] J. G. Fornas, E. H. Jaraba, and A. L. Estopinan, "Generation of Synthetic Examples Using Generative Adversarial Networks (GAN) to Extend the Database of Fault Signals on Power Distribution Lines," *CIRED - international conference on electricity distribution / Rome (2023)*, 2023.

[8] J. Granado, D. Cervero, M. Mañana, R. Cimadevilla, J. Ivan Rodriguez, and A. Gonzalez, "Experiencia Piloto de Localización de Faltas en Red de Media Tensión Mediante la Técnica de la Reflectometría en el Dominio del Tiempo (TDR) en el Proyecto H2020 -FLEXIGRID," *Futured / Congreso de redes Inteligentes*, 2022.

[9] J. G. Fornas, E. H. Jaraba, and A. L. Estopinan, "A Transformer-Based Siamese Network for Anomaly Detection in Time Series as Approach for Fault Location in Distribution Grids," *IEEE Access*, 2023.

[10] S. Robson, A. Haddad, and H. Griffiths, "Fault Location on Branched Networks Using a Multiended Approach," pp. 1955–1963, 2014.

[11] S. Lotfifard, M. Kezunovic, and M. J. Mousavi, "A Systematic Approach for Ranking Distribution Systems Fault Location Algorithms and Eliminating False Estimates," pp. 285–293, 2013.

[12] R. J. Hamidi, H. Livani, and R. Rezaiesarlak, "Traveling-Wave Detection Technique using Short-Time Matrix Pencil Method," p. 1, 2017.

[13] A. Farughian, L. Kumpulainen, and K. Kauhaniemi, "Review of methodologies for earth fault indication and location in compensated and unearthed MV distribution networks," *Electric Power Systems Research*, vol. 154, no. Supplement C, pp. 373–380, jan 2018. [Online]. Available: http://www.sciencedirect.com/science/article/pii/S0378779617303735

[14] P. Stefanidou-Voziki, N. Sapountzoglou, B. Raison, and J. L. Dominguez-Garcia, "A review of fault location and classification methods in distribution grids," *Electric Power Systems Research*, vol. 209, no. May, 2022.

[15] K. Yang, R. Zhang, J. Yang, Y. Chen, and S. Chen, "Research on low-voltage series arc fault detection method based on least squares support vector machine," *Open Electrical and Electronic Engineering Journal*, vol. 9, no. 1, pp. 408–421, 2015. [Online]. Available: https://www.researchgate.net/publication/283661329_Research_on_Low-voltage_Series_Arc_Fault_Detection_Method_Based_on_Least_Squares_Support_Vector_Machine

[16] Y. Q. Chen, O. Fink, and G. Sansavini, "Combined Fault Location and Classification for Power Transmission Lines Fault Diagnosis With Integrated Feature Extraction," *IEEE Transactions on Industrial Electronics*, vol. 65, no. 1, pp. 561–569, 2018.

[17] X. Lin, F. Zhao, G. Wu, Z. Li, and H. Weng, "Universal Wavefront Positioning Correction Method on Traveling-Wave-Based Fault-Location Algorithms," *IEEE Transactions on Power Delivery*, vol. 27, no. 3, pp. 1601–1610, 2012. [Online]. Available: http://ieeexplore.ieee.org.

[18] M. Abad, S. Borroy, D. López, M. García-gracia, U. Zaragoza, N. El, H. Saudi, A. S. Arabia, and M. G.-G. Circe -Spain, "New fault location method for up-to-date and upcoming distribution networks," *CIRED 23 rd International Conference on Electricity Distribution*, no. 1290, pp. 15–18, 2015.

[19] W. Chonglin, W. Yangyang, L. Rui, and S. Gang, "Fault Location for Single-Phase-To-Earth Faults Based on Transient Traveling Wave Method and Artificial Pulse Signal Injection Method," in *2010 International Conference on Electrical and Control Engineering*. IEEE, 2010. [Online]. Available: https://ieeexplore-ieee-org.cuarzo.unizar.es:9443/document/5629889/

[20] S. Gururajapathy, H. Mokhlis, and H. Illias, "Fault location and detection techniques in power distribution systems with distributed generation: A review," *Renewable and Sustainable Energy Reviews*, vol. 74, pp. 949–958, jul 2017. [Online]. Available: http://linkinghub.elsevier.com/retrieve/pii/S1364032117303386

[21] M. A. Aftab, S. M. Hussain, I. Ali, and T. S. Ustun, "Dynamic protection of power systems with high penetration of renewables: A review of the

traveling wave based fault location techniques," *International Journal of Electrical Power and Energy Systems*, vol. 114, no. May 2019, p. 105410, 2020. [Online]. Available: https://doi.org/10.1016/j.ijepes.2019.105410

[22] A. Aljohani, A. Aljurbua, M. Shafiullah, and M. A. Abido, "Smart fault detection and classification for distribution grid hybridizing ST and MLP-NN," in *2018 15th International Multi-Conference on Systems, Signals and Devices, SSD 2018*, 2018.

[23] R. Dashti, S. M. Salehizadeh, H. R. Shaker, and M. Tahavori, "Fault location in double circuit medium power distribution networks using an impedance-based method," *Applied Sciences (Switzerland)*, vol. 8, no. 7, 2018.

[24] M. Shafiullah and M. A. Abido, "S-Transform Based FFNN Approach for Distribution Grids Fault Detection and Classification," *IEEE Access*, vol. 6, 2018.

[25] A. Ekka and A. Yadav, "Fault Identification Using Fuzzy In Renewable Energy Interfaced IEEE 13 Bus System; Fault Identification Using Fuzzy In Renewable Energy Interfaced IEEE 13 Bus System," 2022.

[26] M. Scarpetta, M. Spadavecchia, G. Andria, M. A. Ragolia, and N. Giaquinto, "Analysis of TDR Signals with Convolutional Neural Networks," *Conference Record - IEEE Instrumentation and Measurement Technology Conference*, vol. 2021-May, may 2021.

[27] D. Nagata, S. Fujioka, T. Matshushima, H. Kawano, and Y. Fukumoto, "Detection of fault location in branching power distribution network using deep learning algorithm," *IEEE International Symposium on Electromagnetic Compatibility*, vol. 2022-Septe, pp. 655–660, 2022.

[28] A. Tengg and P. Hank, "Reflectrometry based fault localization in automotive bus systems," *2012 IEEE I2MTC - International Instrumentation and Measurement Technology Conference, Proceedings*, pp. 397–402, 2012.

[29] X. Gu, "On-line Test and Fault Location of Aviation General-purpose cables based on TDR," *2022 3rd International Conference on Computer Vision, Image and Deep Learning and International Conference on Computer Engineering and Applications, CVIDL and ICCEA 2022*, pp. 294–297, 2022.

[30] M. Ziwei and W. Xueye, "A Portable Railway Signal Cable Fault Detector," *Proceedings - 2020 5th International Conference on Information Science, Computer Technology and Transportation, ISCTT 2020*, pp. 69–72, nov 2020.

[31] M. Hampe, M. Tetzlaff, and T. Muller, "Analytical Method to Check and Correct the TDR Impedance Profile of Low-Loss Transmission Lines," *IEEE International Symposium on Electromagnetic Compatibility*, vol. 2022-Septe, pp. 740–743, 2022.

[32] E. Personal, A. García, A. Parejo, D. F. Larios, F. Biscarri, and C. León, "A comparison of impedance-based fault location methods for power underground distribution systems," *Energies*, vol. 9, no. 12, 2016.

[33] C. C. Zhou, Q. Shu, X. Y. Han, and C. Qin Shu, "A single-phase earth fault location scheme for distribution feeder on the basis of the difference of zero mode traveling waves," *International Transactions on Electrical Energy Systems*, vol. 27, no. August 2016, pp. 1–9, may 2017. [Online]. Available: https://onlinelibrary.wiley.com/doi/full/10.1002/etep.2298https://onlinelibrary.wiley.com/doi/abs/10.1002/etep.2298https://onlinelibrary.wiley.com/doi/10.1002/etep.2298

[34] J. Livie, P. Gale, and A.-n. A. Wang, "Experience With On-Line Low Voltage Cable Fault Location Techniques in Scottish Power," *CIRED 19th International Conference on Electricity Distribution*, no. 0696, 2007.

[35] S. Wei, G. Yanfeng, and L. Yan, "Traveling-wave-based fault location algorithm for star-connected hybrid multi-terminal HVDC system," *2017 IEEE Conference on Energy Internet and Energy System Integration, EI2 2017 - Proceedings*, vol. 2018-Janua, pp. 1–5, jun 2017.

[36] J. Teng, X. Zhan, L. Xie, X. Zeng, Y. Liu, and L. Huang, "A novel location method for distribution hybrid lines," *2017 IEEE Conference on Energy Internet and Energy System Integration, EI2 2017 - Proceedings*, vol. 2018-Janua, pp. 1–5, jun 2017.

[37] Z. Wang and T. Oates, *Z. Wang and T. Oates, "Imaging Time-Series to Improve Classification and Imputation," May 2015, [Online]. Available: http://arxiv.org/abs/1506.00327*.

[38] D. M. De Silva and G. Poravi, "A Review on Generative Adversarial Networks," *2021 6th International Conference for Convergence in Technology, I2CT 2021*, apr 2021.

[39] C. Ledig, L. Theis, F. Huszár, J. Caballero, A. Cunningham, A. Acosta, A. Aitken, A. Tejani, J. Totz, Z. Wang, and W. Shi, "Photo-Realistic Single Image Super-Resolution Using a Generative Adversarial Network," *Proceedings - 30th IEEE Conference on Computer Vision and Pattern Recognition, CVPR 2017*, vol. 2017-Janua, pp. 105–114, sep 2016. [Online]. Available: https://arxiv.org/abs/1609.04802v5

[40] J. Y. Zhu, T. Park, P. Isola, and A. A. Efros, "Unpaired Image-to-Image Translation using Cycle-Consistent Adversarial Networks," *Proceedings of the IEEE International Conference on Computer Vision*, vol. 2017-Octob, pp. 2242–2251, mar 2017. [Online]. Available: https://arxiv.org/abs/1703.10593v7

[41] W. Chen and J. Hays, "SketchyGAN: Towards Diverse and Realistic Sketch to Image Synthesis," *Proceedings of the IEEE Computer Society Conference on Computer Vision and Pattern Recognition*, pp. 9416–9425, jan 2018. [Online]. Available: https://arxiv.org/abs/1801.02753v2

[42] F. H. Kiyoiti, S. Tanaka, C. Aranha, W. S. Lee, and T. Suzuki, "Data Augmentation Using GANs," *Proceedings of Machine Learning Research*, vol. XXX, pp. 1–16, apr 2019. [Online]. Available: https://arxiv.org/abs/1904.09135v1

[43] E. Mansfield, J. Wang, J. Russell, J. Li, and C. Adams, "Data Augmentation Generative Adversarial Networks," nov 2017. [Online]. Available: https://arxiv.org/abs/1711.04340v3

[44] F. Zhu, M. He, and Z. Zheng, "Data augmentation using improved cDCGAN for plant vigor rating," *Computers and Electronics in Agriculture*, vol. 175, p. 105603, aug 2020.

[45] T. Salimans, I. Goodfellow, W. Zaremba, V. Cheung, A. Radford, X. Chen, and X. Chen, "Improved Techniques for Training GANs," *Advances in Neural Information Processing Systems*, vol. 29, 2016. [Online]. Available: https://github.com/openai/improved-gan.

[46] A. Srivastava, L. Valkov, C. Russell, M. U. Gutmann, and C. Sutton, "VEEGAN: Reducing Mode Collapse in GANs using Implicit Variational Learning," *Advances in Neural Information Processing Systems*, vol. 2017-Decem, pp. 3309–3319, may 2017. [Online]. Available: https://arxiv.org/abs/1705.07761v3

[47] A. Prasad, J. Belwin Edward, and K. Ravi, "A review on fault classification methodologies in power transmission systems: Part—I," *Journal of Electrical Systems and Information Technology*, vol. 5, no. 1, pp. 48–60, may 2018.

[48] B. Lakshmana Nayak MTECH and A. Professor, "Impact Factor: 1.852 Classification of Transmission Line Faults Using Wavelet Transformer," *Nayak*, vol. 3, no. 2, 2014. [Online]. Available: www.ijesrt.com

[49] S. Kesharwani, D. Kumar, S. 2, and M. Scholar, "Detection of Power Quality Disturbances using Wavelet Transform SIMULATION OF FAULT DETECTION FOR PROTECTION OF TRANSMISSION LINE USING NEURAL NETWORK," *International Journal of Science, Engineering and Technology Research (IJSETR)*, vol. 3, no. 5, 2014. [Online]. Available: https://www.researchgate.net/publication/301695115

[50] S. R. Samantaray, "A systematic fuzzy rule based approach for fault classification in transmission lines," *Applied Soft Computing*, vol. 13, no. 2, pp. 928–938, feb 2013.

[51] W. J. Cheong and R. K. Aggarwal, "A novel fault location technique based on current signals only for thyristor controlled series compensated transmission lines using wavelet analysis and self organising Map neural networks," *IEE Conference Publication*, vol. 1, pp. 224–227, 2004.

[52] M. Singh, B. K. Panigrahi, and R. P. Maheshwari, "Transmission line fault detection and classification," *2011 International Conference on Emerging Trends in Electrical and Computer Technology, ICETECT 2011*, pp. 15–22, 2011.

[53] J. Upendar, C. P. Gupta, and G. K. Singh, "Discrete wavelet transform and probabilistic neural network based algorithm for classification of fault on transmission systems," *Proceedings of the INDICON 2008 IEEE Conference and Exhibition on Control, Communications and Automation*, vol. 1, pp. 206–211, 2008.

[54] P. Sharma, D. Saini, and A. Saxena, "Fault Detection and Classification in Transmission Line Using Wavelet Transform and ANN," *Bulletin of Electrical Engineering and Informatics*, vol. 5, no. 3, pp. 284–295, sep 2016.

[55] D. Mnyanghwalo, H. Kundaeli, E. Kalinga, and N. Hamisi, "Deep learning approaches for fault detection and classifications in the electrical secondary distribution network: Methods comparison and recurrent neural network accuracy comparison," *Cogent Engineering*, vol. 7, no. 1, 2020.

[56] J. J. Yu, Y. Hou, A. Y. Lam, and V. O. Li, "Intelligent fault detection scheme for microgrids with wavelet-based deep neural networks," *IEEE Transactions on Smart Grid*, vol. 10, no. 2, pp. 1694–1703, mar 2019.

[57] Baskar D and Selvam P, "Machine Learning Framework For Power System Fault Detection And Classification," *INTERNATIONAL JOURNAL OF SCIENTIFIC and TECHNOLOGY RESEARCH*, vol. 9, p. 2, 2020. [Online]. Available: www.ijstr.org

[58] F. Rudin, G.-J. Li, and K. Wang, "An Algorithm for Power System Fault Analysis based on Convolutional Deep Learning Neural Networks," Tech. Rep. 9, 2017.

[59] Z. Wu and Lu, "Detection and Location of Aged Cable Segment in Underground Power Distribution System Using Deep Learning Approach," 2021.

[60] B. d. S. N. Sapountzoglou, J. Lago and B. Raison, "A generalizable and sensor-independent deep learning method for fault detection and location in low-voltage distribution grids," 2020.

[61] V. J. Lawhern, A. J. Solon, N. R. Waytowich, S. M. Gordon, C. P. Hung, and B. J. Lance, "EEGNet: A Compact Convolutional Network for EEG-based Brain-Computer Interfaces," nov 2016. [Online]. Available: http://arxiv.org/abs/1611.08024http://dx.doi.org/10.1088/1741-2552/aace8c

[62] M. C. S. Barrios, D. Buldain and I. Orue, "Partial discharge classification using deep learning methods - Survey of recent progress," 2019.

[63] A. Vaswani, G. Brain, N. Shazeer, N. Parmar, J. Uszkoreit, L. Jones, A. N. Gomez, Ł. Kaiser, and I. Polosukhin, "Attention Is All You Need."

[64] S. Ahmed, I. E. Nielsen, A. Tripathi, S. Siddiqui, G. Rasool, and R. P. Ramachandran, "Transformers in Time-series Analysis: A Tutorial," apr 2022. [Online]. Available: http://arxiv.org/abs/2205.01138

[65] J. Xu, H. Wu, J. Wang, and M. Long, "ANOMALY TRANSFORMER: TIME SERIES ANOMALY DETECTION WITH ASSOCIATION DISCREPANCY," Tech. Rep.

[66] J. Abulizi, Z. Chen, P. Liu, H. Sun, C. Ji, and Z. Li, "Research on Voiceprint Recognition of Power Transformer Anomalies Using Gated Recurrent Unit," *2021 Power System and Green Energy Conference (PSGEC)*, 2021.

[67] H. Wang, X. Shen, M. Tu, Y. Zhuang, and Z. Liu, "Improved Transformer With Multi-Head Dense Collaboration," *IEEE/ACM Transactions on Audio Speech and Language Processing*, vol. 30, pp. 2754–2767, 2022.

[68] M. Yu, D. Wu, W. Rao, L. Cheng, R. Li, and Y. Li, "Automated Road Crack Detection Method based on Visual Transformer with Multi-Head Cross-Attention," *Proceedings of 2022 IEEE International Conference on Sensing, Diagnostics, Prognostics, and Control, SDPC 2022*, pp. 328–332, 2022.

[69] M. Garg, D. Ghosh, and P. M. Pradhan, "Multiscaled Multi-Head Attention-Based Video Transformer Network for Hand Gesture Recognition," *IEEE Signal Processing Letters*, vol. 30, pp. 80–84, 2023.

[70] J. Zhang, Y. Chen, and J. Chen, "Join-Chain Network: A Logical Reasoning View of the Multi-head Attention in Transformer," *IEEE International Conference on Data Mining Workshops, ICDMW*, vol. 2022-Novem, pp. 947–957, 2022.

[71] Q. Ma, M. Zhang, Y. Xu, J. Song, and T. Zhang, "Remaining Useful Life Estimation for Turbofan Engine with Transformer-based Deep Architecture," *2021 26th International Conference on Automation and Computing: System Intelligence through Automation and Computing, ICAC 2021*, 2021.

[72] R. Fan, "Transformer-Based Deep Learning Method for the Prediction of Ventilator Pressure," *2022 2nd IEEE International Conference on Information Communication and Software Engineering, ICICSE 2022*, pp. 25–28, 2022.

[73] R. Bai, M. Li, B. Meng, F. Li, M. Jiang, J. Ren, and D. Sun, "Hierarchical Graph Convolutional Skeleton Transformer for Action Recognition," *Proceedings - IEEE International Conference on Multimedia and Expo*, vol. 2022-July, 2022.

[74] T. L. Hoang, T. D. Pham, and V. C. Ta, "Improving Graph Convolutional Networks with Transformer Layer in social-based items recommendation," *Proceedings - International Conference on Knowledge and Systems Engineering, KSE*, vol. 2021-Novem, 2021.

[75] R. Slama, W. Rabah, and H. Wannous, "STr-GCN: Dual Spatial Graph Convolutional Network and Transformer Graph Encoder for 3D Hand Gesture Recognition," *2023 IEEE 17th International Conference on Automatic Face and Gesture Recognition, FG 2023*, 2023.

[76] B. Padi, A. Mohan, and S. Ganapathy, "End-to-end Language Recognition Using Attention Based Hierarchical Gated Recurrent Unit Models," *ICASSP, IEEE International Conference on Acoustics, Speech and Signal Processing - Proceedings*, vol. 2019-May, pp. 5966–5970, may 2019.

[77] P. Awwal and S. Naval, "Optimized Attention-based Long-short-term memory and Gated Recurrent Unit for Malware Detection in Windows," pp. 217–222, mar 2023.

[78] S. T. Rajamani, K. T. Rajamani, A. Mallol-Ragolta, S. Liu, and B. Schuller, "A novel attention-based gated recurrent unit and its efficacy in speech emotion recognition," *ICASSP, IEEE International Conference on Acoustics, Speech and Signal Processing - Proceedings*, vol. 2021-June, pp. 6294–6298, 2021.

[79] S. Tuli, G. Casale, and N. R. Jennings, "TranAD: Deep Transformer Networks for Anomaly Detection in Multivariate Time Series Data," jan 2022. [Online]. Available: https://arxiv.org/abs/2201.07284v6http://arxiv.org/abs/2201.07284

[80] H. Takimoto, J. Seki, S. F. Situju, and A. Kanagawa, "Applied Artificial Intelligence Anomaly Detection Using Siamese Network with Attention Mechanism for Few-Shot Learning," 2022. [Online]. Available: https://www.tandfonline.com/action/journalInformation?journalCode=uaai20

[81] W. Gedara, C. Bandara, and V. M. Patel, "A Transformer-Based Siamese Network for Change Detection; A Transformer-Based Siamese Network for Change Detection," 2022.

[82] B. Ramachandra, M. J. Jones, and R. R. Vatsavai, "Learning a distance function with a Siamese network to localize anomalies in videos," Tech. Rep.

[83] C. Ye and Q. Ma, "TS2V: A Transformer-Based Siamese Network for Representation Learning of Univariate Time-Series Data; TS2V: A Transformer-Based Siamese Network for Representation Learning of Univariate Time-Series Data," 2022.

Anexo A

Lista de publicaciones

A.1 Publicaciones en revistas científicas

1. J. G. Fornás, E. H. Jaraba, H. Bludszuweit, D. C. García and A. L. Estopiñan, ”Modeling and Simulation of Time Domain Reflectometry Signals on a Real Network for Use in Fault Classification and Location,ïn IEEE Access, vol. 11, pp. 23596-23619, 2023, doi: 10.1109/ACCESS.2023.3253772/Impact Factor: 3,9/JCR Ranking: Q2
2. J. G. Fornás, E. H. Jaraba, A. L. Estopiñan and J. Saldana, ”Detection and Classification of Fault Types in Distribution Lines by Applying Contrastive Learning to GAN Encoded Time-Series of Pulse Reflectometry Signals,ïn IEEE Access, vol. 10, pp. 110521-110536, 2022, doi: 10.1109/ACCESS.2022.3214994/Impact Factor: 3,367/JCR Ranking: Q2
3. J. G. Fornas, E. H. Jaraba and A. L. Estopinan TransSiamese: “A Transformer-Based Siamese Network for Anomaly Detection in Time Series as Approach for Fault Location in Distribution Grids” IEEE Access, pp. 1–1, 2023, doi: 10.1109/ACCESS.2023.3316600/Impact Factor: 3,9/JCR Ranking: Q2

A.2 Publicaciones en congresos

1. J. G. Fornas, E. H. Jaraba and A. L. Estopinan “Generation of Synthetic Examples Using Generative Adversarial Networks (GAN) to Extend the Database of Fault Signals on Power Distribution Lines” CIRED - international conference on electricity distribution / Rome (2023)/Impact Factor: 3,9/JCR Ranking: Q2
2. J. Granado, D. Cervero, M. Mañana, R. cimadevilla, J. Ivan Rodriguez y A. Gonzalez “Experiencia Piloto de Localización de Faltas en Red de Media Tensión Mediante la Técnica de la Reflectometría en el Dominio del Tiempo (TDR)e en el Proyecto H2020 -FLEXIGRID” Futured / Congreso de redes Inteligentes (2022)